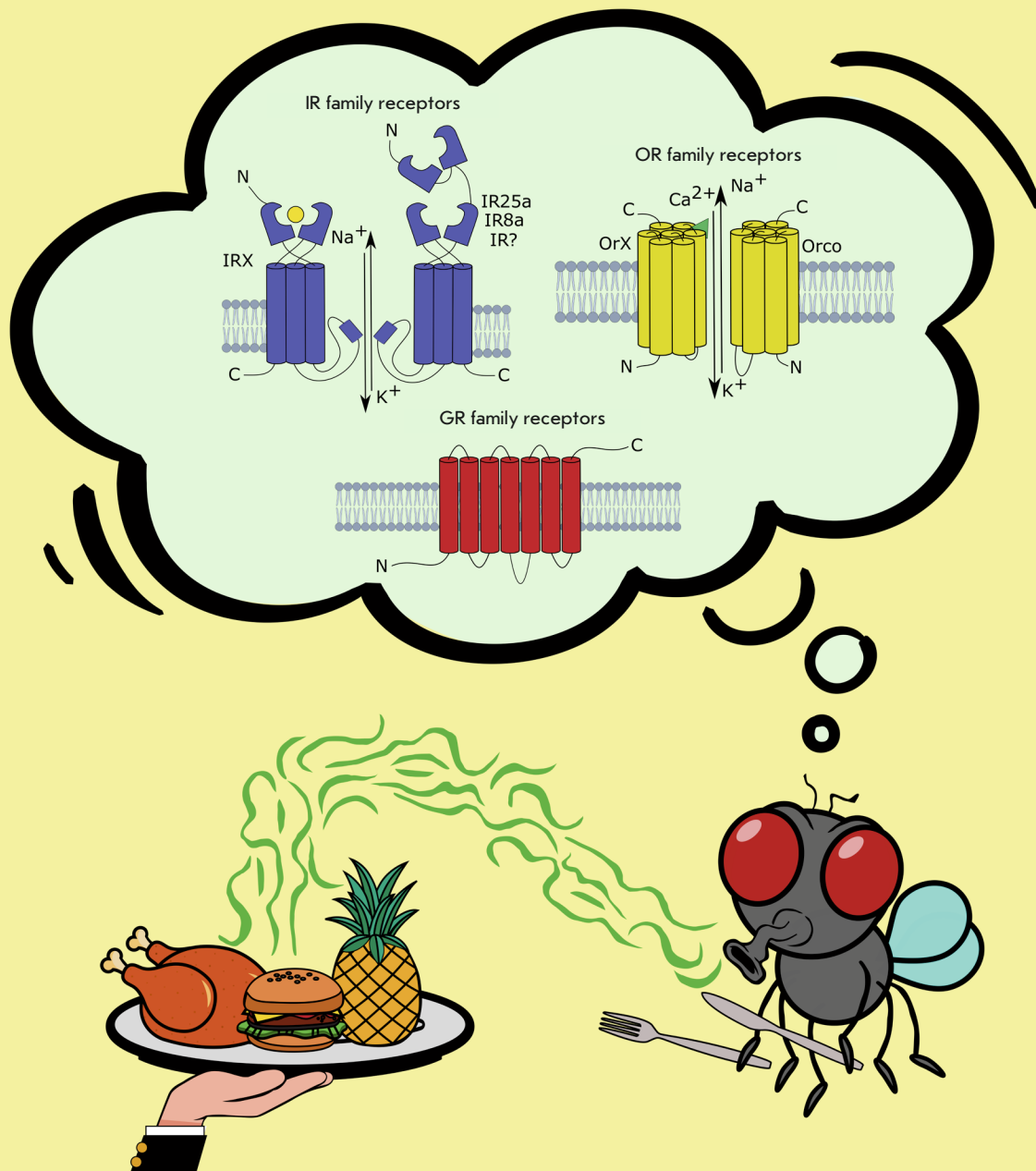


Acta Naturae

Molecular Principles of Insect Chemoreception



SUPRAMOLECULAR ORGANIZATION
AS A FACTOR OF RIBONUCLEASE
CYTOTOXICITY
P. 24

INFECTIOUS PLANT DISEASES: ETIOLOGY,
CURRENT STATUS, PROBLEMS AND
PROSPECTS IN PLANT PROTECTION
P. 46



Comprehensive solutions for cell analysis



- Cell lines and primary cells
- Traditional and specialized culture media
- Sterilizing filtration



- Biochemical reagents
- Water purification systems
- Cell counting and analysis
- Cryopreservation



An extensive range and top quality of cell lines from our partner, the European Collection of Authenticated Cell Cultures (ECACC):

- 4000 animal and human cell lines;
- Cells of 45 animal species and 50 tissue types;
- 370 B-lymphoblastoid cell lines for which human leukocyte antigen (HLA) typing data are available;
- 480 hybridoma cell lines secreting monoclonal antibodies;
- DNA, RNA, and cDNA extracted from the cell lines from our collection;

SIGMAaldrich.com/ECACC

LLC Merck

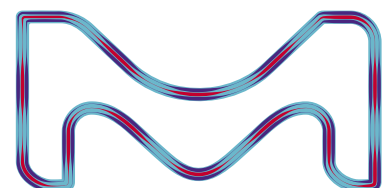
Valovaya Str., 35, Moscow, 115054, Russia;

Tel. +7 (495) 937-33-04

E-mail: mm.russia@merckgroup.com, ruorder@sial.com

SIGMAaldrich.com/cellculture

MERCKmillipore.com/cellculture

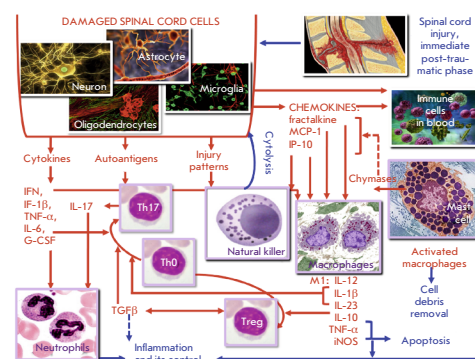


SIGMA-ALDRICH[®] is now **MERCK**

Cytokine Profile As a Marker of Cell Damage and Immune Dysfunction after Spinal Cord Injury

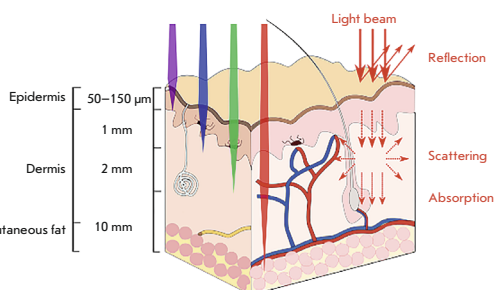
G. B. Telegin, A. S. Chernov, N. A. Konovalov, A. A. Belogurov, I. P. Balmasova, A. G. Gabibov

This study reviews the findings of recent experiments designed to investigate the cytokine profile after a spinal cord injury. The role played by key cytokines in eliciting the cellular response to trauma was assessed. The results of the specific immunopathogenetic interaction between the nervous and immune systems in the immediate and chronic post-traumatic periods are summarized. It was demonstrated that it is reasonable to use the step-by-step approach to the assessment of the cytokine profile after a spinal cord injury and take into account the combination of the pathogenetic and protective components in implementing the regulatory effects of individual cytokines and their integration into the regenerative processes in the injured spinal cord. This allows one to rationally organize treatment and develop novel drugs.



Specific characteristics of the immune response in the immediate post-traumatic phase after SCI

Near-Infrared Activated Cyanine Dyes As Agents for Photothermal Therapy and Diagnosis of Tumors



Depth of light penetration of human tissues

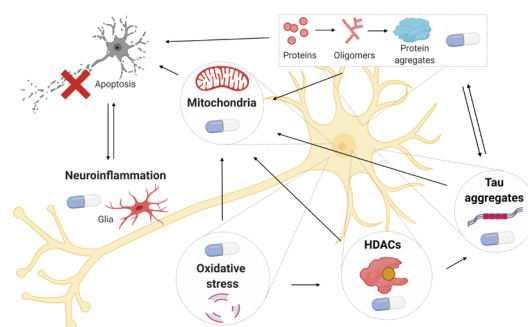
E. I. Shramova, A. B. Kotlyar, E. N. Lebedenko, S. M. Deyev, G. M. Proshkina

In this review, we focus on NIR-excited dyes and discuss prospects for their application in photothermal therapy and the diagnosis of cancer. Particular attention is focused on the consideration of new multifunctional nanoplateforms for phototheranostics, which allow one to achieve a synergistic effect in combinatorial photothermal, photodynamic, and/or chemotherapy, with simultaneous fluorescence, acoustic, and/or magnetic resonance imaging.

Promising Molecular Targets for Pharmacological Therapy of Neurodegenerative Pathologies

M. E. Neganova, Yu. R. Aleksandrova, V. O. Nebogatikov, S. G. Klochkov, A. A. Ustyugov

The review presents data on the molecular mechanisms of the key processes underlying neurodegenerative diseases such as neuroinflammation and oxidative stress, mitochondrial dysfunction, dysregulated expression of histone deacetylases, and aggregation of pathogenic protein variants. The article describes therapeutic strategies for the development of promising multi-target low-molecular-weight drugs targeting the key elements of neurodegeneration.



Molecular targets for pharmacological effects in the treatment of neurodegenerative diseases

Founders

Acta Naturae, Ltd,
National Research University
Higher School of Economics

Editorial Council

Chairman: A.I. Grigoriev
Editors-in-Chief: A.G. Gabibov, S.N. Kochetkov

V.V. Vlassov, P.G. Georgiev, M.P. Kirpichnikov,
A.A. Makarov, A.I. Miroshnikov, V.A. Tkachuk,
M.V. Ugryumov

Editorial Board

Managing Editor: V.D. Knorre

K.V. Anokhin (Moscow, Russia)
I. Bezprozvanny (Dallas, Texas, USA)
I.P. Bilenkina (Moscow, Russia)
M. Blackburn (Sheffield, England)
S.M. Deyev (Moscow, Russia)
V.M. Govorun (Moscow, Russia)
O.A. Dontsova (Moscow, Russia)
K. Drauz (Hanau-Wolfgang, Germany)
A. Friboulet (Paris, France)
M. Issagouliants (Stockholm, Sweden)
A.L. Konov (Moscow, Russia)
M. Lukic (Abu Dhabi, United Arab Emirates)
P. Masson (La Tronche, France)
V.O. Popov (Moscow, Russia)
I.A. Tikhonovich (Moscow, Russia)
A. Tramontano (Davis, California, USA)
V.K. Švedas (Moscow, Russia)
J.-R. Wu (Shanghai, China)
N.K. Yankovsky (Moscow, Russia)
M. Zouali (Paris, France)

Project Head: N.V. Soboleva

Editor: N.Yu. Deeva

Designer: K.K. Oparin

Art and Layout: K. Shnaider

Copy Chief: Daniel M. Medjo

Phone/Fax: +7 (495) 727 38 60

E-mail: vera.knorre@gmail.com, actanaturae@gmail.com

Reprinting is by permission only.

© ACTA NATURAE, 2020

Номер подписан в печать 30 сентября 2020 г.

Тираж 100 экз. Цена свободная.

Отпечатано в типографии: НИУ ВШЭ,
г. Москва, Кочновский проезд, 3

Impact Factor: 1.360

CONTENTS

REVIEWS

A. V. Gaponova, S. Rodin, A. A. Mazina,
P. V. Volchkov

**Epithelial–Mesenchymal Transition: Role
in Cancer Progression and the Perspectives
of Antitumor Treatment 4**

E. V. Dudkina, V. V. Ulyanova, O. N. Ilinskaya
**Supramolecular Organization As a Factor
of Ribonuclease Cytotoxicity 24**

O. V. Kisil, T. A. Efimenko, N. I. Gabrielyan,
O. V. Efremenkova
**Development of Antimicrobial Therapy
Methods to Overcome the Antibiotic
Resistance of *Acinetobacter baumannii* 34**

P. A. Nazarov, D. N. Baleev, M. I. Ivanova,
L. M. Sokolova, M. V. Karakozova
**Infectious Plant Diseases: Etiology,
Current Status, Problems and Prospects
in Plant Protection. 46**

M. E. Neganova, Yu. R. Aleksandrova,
V. O. Nebogatikov, S. G. Klochkov,
A. A. Ustyugov
**Promising Molecular Targets
for Pharmacological Therapy
of Neurodegenerative Pathologies 60**

E. L. Sokolinskaya, D. V. Kolesov,
K. A. Lukyanov, A. M. Bogdanov
**Molecular Principles of Insect
Chemoreception. 81**

CONTENTS

G. B. Telegin, A. S. Chernov, N. A. Konovalov,
A. A. Belogurov, I. P. Balmasova,
A. G. Gabibov

**Cytokine Profile As a Marker
of Cell Damage and Immune Dysfunction
after Spinal Cord Injury92**

E. I. Shramova, A. B. Kotlyar, E. N. Lebedenko,
S. M. Deyev, G. M. Proshkina

**Near-Infrared Activated Cyanine Dyes
As Agents for Photothermal Therapy
and Diagnosis of Tumors102**

M. P. Paramonova, A. L. Khandazhinskaya,
A. A. Ozerov, S. N. Kochetkov, R. Snoeck,
G. Andrei, M. S. Novikov

**Synthesis and Antiviral Properties of
1-Substituted 3-[ω -(4-Oxoquinazolin-4(3H)-yl)
alkyl]uracil Derivatives.....134**

T. T. Dunston, M. A. Khomutov, S. B. Gabelli,
T. M. Stewart, J. R. Foley, S. N. Kochetkov,
A. R. Khomutov, R. A. Casero Jr.

**Identification of a Novel Substrate-Derived
Spermine Oxidase Inhibitor.....140**

RESEARCH ARTICLES

I. V. Dolzhikova, D. M. Grousova,
O. V. Zubkova, A. I. Tuhvatulin,
A. V. Kovyrshina, N. L. Lubenets,
T. A. Ozharovskaia, O. Popova,
I. B. Esmagambetov, D. V. Shcheblyakov,
I. M. Evgrafova, A. A. Nedorubov,
I. V. Gordeichuk, S. A. Gulyaev,
A. G. Botikov, L. V. Panina,
D. V. Mishin, S. Y. Loginova,
S. V. Borisevich, **P. G. Deryabin**,
B. S. Naroditsky, D. Y. Logunov,
A. L. Gintsburg

**Preclinical Studies of Immunogenicity,
Protectivity, and Safety of the Combined
Vector Vaccine for Prevention of the Middle
East Respiratory Syndrome114**

B. S. Malyshev, N. A. Netesova,
N. A. Smetannikova, M. A. Abdurashitov,
A. G. Akishev, E. V. Dubinin,
A. Z. Azanov, I. V. Vihlyanov,
M. K. Nikitin, A. B. Karpov,
S. Kh. Degtyarev

**GLAD-PCR Assay of R(5mC)GY Sites
in the Regulatory Region
of Tumor-Suppressor Genes Associated
with Gastric Cancer124**

Guidelines for Authors..... 145

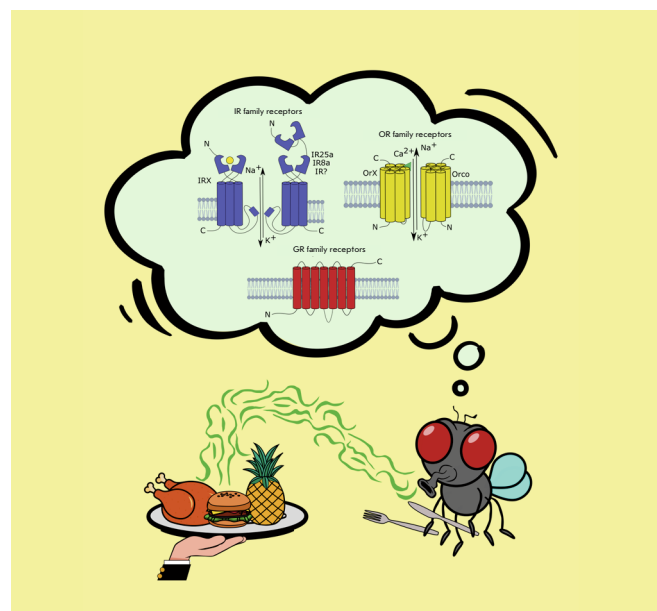


IMAGE ON THE COVER PAGE
(see the article by *E. L. Sokolinskaya et al.*)

Epithelial–Mesenchymal Transition: Role in Cancer Progression and the Perspectives of Antitumor Treatment

A. V. Gaponova^{1*}, S. Rodin², A. A. Mazina¹, P. V. Volchkov¹

¹Moscow Institute of Physics and Technology, Dolgoprudny, Moscow Region, 141701 Russia

²Department of Medical Biochemistry and Biophysics, Karolinska Institute, Stockholm, 17177 Sweden

*E-mail: annagaponova28@gmail.com

Received April 07, 2020; in final form, May 20, 2020

DOI: 10.32607/actanaturae.11010

Copyright © 2020 National Research University Higher School of Economics. This is an open access article distributed under the Creative Commons Attribution License, which permits unrestricted use, distribution, and reproduction in any medium, provided the original work is properly cited.

ABSTRACT About 90% of all malignant tumors are of epithelial nature. The epithelial tissue is characterized by a close interconnection between cells through cell–cell interactions, as well as a tight connection with the basement membrane, which is responsible for cell polarity. These interactions strictly determine the location of epithelial cells within the body and are seemingly in conflict with the metastatic potential that many cancers possess (the main criteria for highly malignant tumors). Tumor dissemination into vital organs is one of the primary causes of death in patients with cancer. Tumor dissemination is based on the so-called epithelial–mesenchymal transition (EMT), a process when epithelial cells are transformed into mesenchymal cells possessing high mobility and migration potential. More and more studies elucidating the role of the EMT in metastasis and other aspects of tumor progression are published each year, thus forming a promising field of cancer research. In this review, we examine the most recent data on the intracellular and extracellular molecular mechanisms that activate EMT and the role they play in various aspects of tumor progression, such as metastasis, apoptotic resistance, and immune evasion, aspects that have usually been attributed exclusively to cancer stem cells (CSCs). In conclusion, we provide a detailed review of the approved and promising drugs for cancer therapy that target the components of the EMT signaling pathways.

KEYWORDS Epithelial–mesenchymal transition, cancer, metastasis, resistance to anticancer therapy, cancer stem cells, chemotherapy, immunotherapy

ABBREVIATIONS EMT – epithelial–mesenchymal transition; MET – mesenchymal–epithelial transition; iPSCs – induced pluripotent stem cells; NSCLC – non-small cell lung cancer; CSCs – cancer stem cells.

INTRODUCTION

The epithelial–mesenchymal transition is a physiological process by which epithelial cells attain the properties of mesenchymal cells, both morphologically (changes in cell shape) and physiologically (movement and invasion, global changes in expression profile and metabolism).

Epithelial cells are organized into cell layers that interconnect through cell junctions and are adhered to the basement membrane. Although epithelial cells possess some ability to restructure their shape, their migration in any significant manner is confined

to the margins of the epithelial layer. The following types of cell junctions that interconnect epithelial cells are usually differentiated: the so-called adherent junctions, tight junctions based on E-cadherins binding to the actin cytoskeleton, and gap junctions and hemidesmosomes that are linked by cytoke- ratin-based intermediate filaments.

The key components of epithelial cell junctions are the transmembrane molecules E-cadherin and β -catenin, which bind cadherins to the actin cytoskeleton. In vertebrates, over 100 types of cadherin with varied tissue specificities have been identified [1] due

to a large variety of genes synthesizing cadherins and alternative splicing. The junctions between vertebrate epithelial cells are formed by E-cadherin homodimers.

Cadherins are transmembrane proteins consisting of an extracellular, a transmembrane, and cytoplasmic domain. The extracellular calcium-binding site is formed by five domains; the transmembrane region consists of a single chain of glycoprotein repeats. The cytoplasmic region is connected to β -catenin and the p120 protein, which stabilizes cadherin on the cell surface. β -Catenin interconnects the cytoplasmic region of cadherin to α -catenin [2, 3]. The latter is connected to actin of the cytoplasmic skeleton and regulates the assembly of actin filaments by repressing Arp2/3-mediated actin polymerization [4]. Proper functioning of this protein complex ensures intercellular adhesion, as well as coordination of the cytoskeletal dynamics, control over cell layer movement during embryogenesis, and tissue morphogenesis and homeostasis [5, 6].

Unlike epithelial cells, mesenchymal cells and fibroblasts do not have an apical-basal polarity and are fusiform in shape. Although they have regions of focal adhesion to the extracellular matrix, these cells can freely move in three dimensions, passing along and through the collagen networks of the extracellular matrix [7, 8].

The phenomenon of epithelial–mesenchymal transition was first described in the early 1980s in Elizabeth Hay's laboratory [9, 10], in both embryonic notochord and lens epithelial cells isolated from chicken embryos, and in differentiated chicken lens epithelial cells. Epithelial cells placed in a 3D collagen matrix *in vitro* exhibited morphological changes: they acquired a bipolar fusiform shape with long cellular processes, pseudopodia and filopodia, and they also penetrated the matrix [9].

During EMT, epithelial cells undergo a suppression of E-cadherin and the other genes responsible for the synthesis of the components that create firm adherens junctions. This leads to the loss of cell adhesion and apical-basal polarity, cytoskeleton reorganization, and an increase in cell motility. Suppression of epithelial cell expression occurs in combination with increased expression of transcription factors and the associated mesenchymal genes, such as N-cadherin, vimentin, fibronectin and extracellular matrix metalloproteinases [11–13]. Changes in the expression profiles of the genes responsible for the formation of the epithelial and mesenchymal phenotypes are considered key characteristics of EMT.

EMT TYPES

The earliest experiments at Elizabeth Hay's laboratory that demonstrated the existence of EMT showed

that this process is typical of both embryonic and differentiated cells [9]. Despite the similarity of the molecular mechanisms underlying EMT, as well as the overarching result of the process (the formation of motile cells with a mesenchymal phenotype in embryonic and differentiated cells), they play fundamentally different functional roles in the body.

Depending on the biological context, three EMT subtypes are typically distinguished: type I EMT occurs during the embryogenesis [14–16] and morphogenesis of organs [17–19], type II EMT is related to the regeneration of injured tissues [20, 21] and pathological fibrosis [22–26], and type III EMT is associated with cancer metastasis.

Type I EMT is the earliest EMT type that initially occurs during implantation, when extragerminal cells of the trophoblast undergo epithelial–mesenchymal transformation and migrate from the blastocyst body to the uterine endometrium, thus contributing to the formation of the attached placenta [27, 28].

The next EMT-related event to occur after implantation is the formation of the primary mesoderm from the primary ectoderm during gastrulation [29–31]. EMT is one of the mechanisms of ingression (eviction) of cells inside the blastula wall (the blastoderm or the primitive ectoderm), which is histologically an epithelial layer located inside the blastocoel. The cells migrate to a specific area of the embryo, the so-called primitive streak. During invagination, cells from the primitive streak form the mesoderm and endoderm through EMT [15]. The Wnt/ β -catenin signaling pathway underlies the regulation of these processes.

Another important EMT-mediated event during embryogenesis is the formation of the neural crest. The neural crest is a collection of cells secreted from the edges of the neuroectoderm during neural tube closure [32]. The population of precursor neural crest cells possesses a high migration potential over the entire embryo and is involved in the formation of various structures in the body, such as the vegetative ganglia of the nervous system, skin melanocytes, facial skeleton cartilage, adrenal chromaffin cells, and heart valves. Similar to the cells undergoing EMT during gastrulation, future neural crest cells lose their N-cadherin-mediated cell adhesion ability and detach from the neuroepithelium. Basement membrane fragmentation then takes place, causing increased expression of the genes responsible for the formation of the mesenchymal phenotype, increased motility, and subsequent active invasion [33]. The migration of neural crest cells is primarily induced by the bone morphogenetic protein (BMP) pathway and its inhibitor. Furthermore, components of the extracellular matrix (high levels of fibronectin and hyaluronic acid

are typical of the areas to which the cells of the future neural crest migrate) are among the most important EMT inducers and regulators during neural crest formation [34].

Type I EMT is involved in the morphogenesis of heart valves and the secondary palate. The anlagen of the mitral and tricuspid valves, as well as the interventricular septum of the heart, forms during TGF- β -mediated epithelial–mesenchymal transition of germinal endothelial cells [35]. Furthermore, recent research has shown the importance of the Wnt signaling pathway and hyaluronic acid to EMT during heart morphogenesis [36]. TGF- β 3-regulated EMT in the palatine suture underlies accurate morphogenesis of the facial skeleton, and the formation of the secondary palate in particular. The activated TGF- β 3 factors Snail and SIP1 bind to the E-cadherin promoter in conjunction with Smad4, thus repressing its transcription [37].

Unlike type I or III EMT, type II EMT is triggered exclusively by tissue damage and inflammation [38]. Type II EMT is part of the complex process of tissue repair and regeneration, playing an important role in tissue re-epithelization and granulation tissue formation. Re-epithelization is a process in which epidermal keratinocytes become motile, gain a mesenchymal phenotype, and migrate to the wound edges. Proliferation and replenishment of the damaged area then starts and continues until the epithelial cells on the opposite edge of the wound are met. From that point on, further cell migration ceases due to the phenomenon of contact inhibition [39].

Wound healing occurs via two parallel processes: re-epithelialization, and the ongoing remodeling (the formation of granulation tissue performed primarily by myofibroblasts that produce large amounts of extracellular matrix proteins) [40]. Many pathways of myofibroblast formation [41, 42], including those formed during EMT, have been reported [43].

Typically, after the re-epithelization is completed, myofibroblasts undergo apoptosis [44]. Disruption of EMT regulation or pathologically prolonged myofibroblast activity caused by chronic or inflammatory damage leads to fibrosis, impaired function, and, ultimately, destruction of the affected organs.

In addition to TGF β , growth factors such as FGF, HGF, and EGF are the known EMT inducers involved in wound healing [47]. Slug, a crucial transcription factor for EMT, is also part of re-epithelialization: Slug knockout mice have a lower potential for wound healing [20], being that they are related to the impaired migration of epidermal keratinocytes [48].

Cancer-specific type III EMT has been studied the least. Epithelial cancer cells are highly divergent from

normal epithelial cells in terms of their infinite replicative potential and resistance to cell signaling that would otherwise suppress their growth and proliferation, as well as their apoptotic resistance, genomic instability, metabolic deregulation, immune avoidance, and intense angiogenesis [49].

One of the key features of cancer cells is their potential for invasion, migration, and formation of metastatic foci in internal organs [49]. Many studies have focused on the role played by EMT activation in the invasion and metastasis of various cancer types, both *in vivo* and *in vitro* [50–53]. Both the mesenchymal phenotype and EMT marker expression in cancer cells are associated with chemo- [54], radio- [55], and immunotherapy [56] resistance, as well as reduced susceptibility to apoptosis and aging signaling [57,58]. Furthermore, elevated expressions of N-cadherin and vimentin are EMT markers that have been found to assist cancer cells in immune avoidance [59].

Many molecular mechanisms found to be responsible for type III EMT are conservative to the previously described type I and II ones. However, there are some unique features of EMT that are used by cancer for dissemination. The mechanisms inducing EMT in cancer cells remain poorly understood, and their role in cancer progression remains unclear and is subject to dispute. A hypothesis has been put forward that alterations in the expression of EMT markers are simply a consequence of the genomic instability of cancer cells and do not indicate that the cells are preparing to undergo embryogenesis-like EMT [60].

Next, we delve into the features of the intracellular and extracellular molecular mechanisms (the effects of the tumor microenvironment) of EMT, which underlie various aspects of tumor progression. We also discuss in detail their potential as molecular targets for antitumor therapy and markers for early cancer diagnosis.

MOLECULAR MECHANISMS OF EMT IN THE CONTEXT OF CANCER PROGRESSION (INTRA- AND EXTRACELLULAR SIGNALING)

Intracellular signaling

The coordination of intracellular signaling that is crucial to the normal functioning of EMT can be disrupted by deregulatory stimuli originating from an altered cell microenvironment, which enables fibrosis development and cancer progression.

The intracellular signals that regulate EMT are diverse and fairly well understood (*Fig. 1*). The roles played by the following signaling pathways have been described most thoroughly: (TGF)- β /BMP (SMAD-dependent and SMAD-independent variants of this

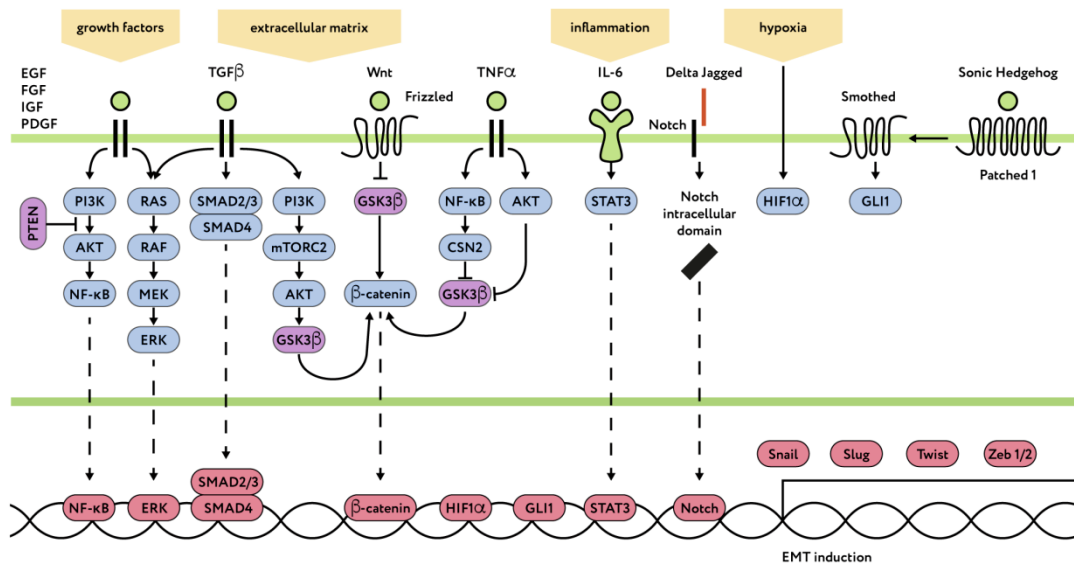


Fig. 1. The key signaling pathways that regulate EMT. The components of signal transduction inducing EMT are shown in blue; the components that suppress EMT are shown in violet; transcription factors activating the EMT processes are shown in red

signaling pathway are distinguished in the context of EMT) and Wnt (β -catenin, Notch, and Hedgehog). Additionally, receptor tyrosine kinases such as EGF, FGF, IGF, and PDGF, as well as the key transcription factors (regulated by the previously mentioned pathways and receptors) Snail1, Snail2 (also known as Slug), ZEB1, ZEB2, and Twist, which act as repressors of the E-cadherin expression and other genes responsible for the formation of the epithelial phenotype [61] (Fig. 1), have also been described in the literature.

Furthermore, SNAIL and ZEB2 activate the expression of metalloproteinases, which contribute to the degradation of the basement membrane and cancer cell invasion [62].

The epigenetic mechanisms of EMT regulation associated with methylation and acetylation of histones and miRNAs are also significant. Activation of the aforementioned molecular mechanisms enables the expression of EMT markers; namely, increased expression of N-cadherin, vimentin, type 1 fibrillar collagen, β -catenin and repression of E-cadherin, claudins, protein zonula occludens 1, occludins, cytokeratins, and matrix activation metalloproteinases (Fig. 2).

In pancreatic cancer cells, the transcription factor ZEB1 plays a key role in the regulation of EMT and the metastatic process by suppressing the E-cadherin expression via the recruitment of HDAC1 and HDAC2

deacetylases to the promoter region of the *CDH1* gene [63, 64]. Suppression of the TGF- β signaling pathway using miR-202 micro-RNA inhibits EMT in pancreatic cancer cells [65].

The transcription factor ETS1, which is characteristically elevated in prostate cancers, activates EMT through the induction of the TGF- β signaling pathway, followed by the activation of ZEB1 and SNAIL1 [66]. Recently, the role of the TRPM4 calcium ion channel in EMT regulation and invasion in prostate cancer cells has been shown to be mediated by the induction of SNAIL expression [67].

The role of the c-Myc proto-oncogene in the induction of EMT and cancer stem cells through the Wnt signaling pathway and activation of ZEB1 in triple-negative breast cancer cells was demonstrated earlier [68]. Additionally, overexpression of miR-93 micro-RNA in breast cancer cells, which suppresses the tumor suppressor PTEN (Fig. 1), is associated with EMT and tumor resistance to the cytotoxic activity of doxorubicin [69].

Inhibin B (INHBB), a membrane glycoprotein belonging to the TGF- β superfamily, and the Smad-dependent TGF- β signaling pathway regulate EMT and anoikis in the cells of head and neck squamous cell carcinomas [70]. The TGF- β /Snail and TNF- α /NF κ B signaling pathways determine the course of EMT in colorectal cancer [71, 72] (Fig. 1). Recently published

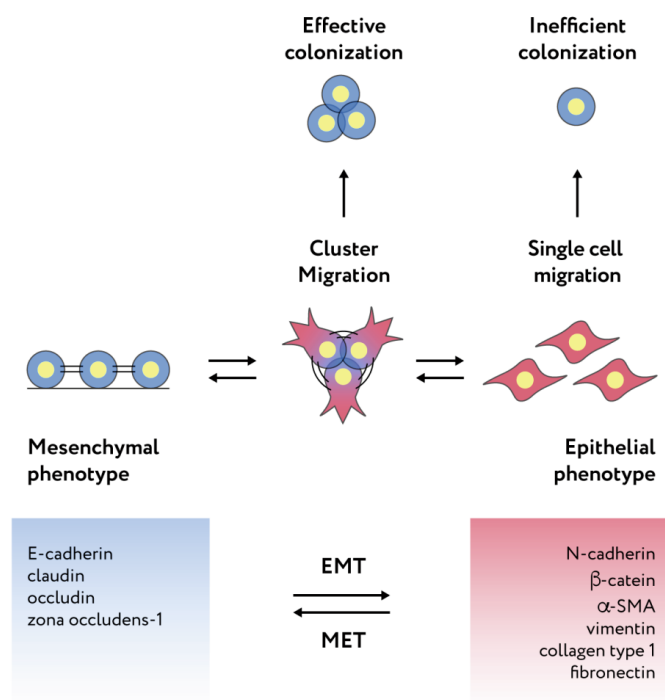


Fig. 2. Cell plasticity and the role of the intermediate epithelial–mesenchymal phenotype in the formation of secondary tumor foci (see detailed explanation in the text)

studies describe the new molecular regulators of EMT involved in the metastasis of lung cancer [73–75].

Extracellular Signaling

Activation of intracellular signaling pathways occurs due to various stimuli from the local microenvironment, such as growth factors, cytokines, hypoxia, and contact with the surrounding extracellular matrix (the tumor-associated stroma) (Fig. 1). Tumor microenvironment factors influence the survival, proliferation, and progression of cancer: that is why they are actively studied.

Inflammation is a critical component of tumor development. Chronic inflammation is associated with an increased risk of cancer. In fact, about 20% of cancers are associated with the chronic inflammation caused by infections, autoimmune reactions, and injury. In addition, the oncogenic signaling pathways in cells susceptible to malignant transformation induce the activation of inflammatory signaling pathways. Thus, tumor tissue infiltration by immune cells and

increased expression of proinflammatory cytokines are found in most tumor types regardless of whether an external inflammation is involved in their development or not [76]. A large body of evidence for the role played by various cellular and humoral components of inflammation in the induction of EMT and metastasis has been obtained [77] (Fig. 1).

Rapid tumor growth is also associated with a disruption of vascularization, causing the formation of areas of temporary or chronic hypoxia. Hypoxia and activation of hypoxia-inducible factors (HIFs) are observed in many tumors. HIFs regulate the expression of the genes responsible for the survival, proliferation, motility, metabolism, pH regulation, recruitment of inflammatory factors, and angiogenesis processes. Thus, HIF induction promotes cancer progression (as is in the case of fibrosis) and activates EMT and metastasis in many types of cancer [78–81] (Fig. 1).

Laminins are extracellular matrix proteins (to be more specific, heterotrimeric glycoproteins) that constitute the bulk of the basement membrane, which is in direct contact with epithelial cells and ensures proper signal transduction to the cells [82]. Laminins regulate polarization and migration, thereby affecting the epithelial and mesenchymal characteristics of cells during normal ontogenesis and wound healing.

The laminin-111 fragment cleaved by matrix metalloproteinase MMP2 enhances the expression of E-cadherin by suppressing SNAIL 1 and SNAIL2 expression in mouse embryonic stem cells [83].

Mouse mammary epithelial cells are usually subjected to Rac1b-mediated EMT. When treated with matrix metalloproteinase-3 (MMP3), laminin-111 inhibits the transition to a mesenchymal phenotype [84]. Activation of Rac1b (a splice variant of the small GTPase Rac1) mediated by the interaction between laminin-111 and its receptor, $\alpha 6$ integrin, is associated with an increased expression of the keratin-14 epithelial marker and suppression of the mesenchymal markers Snail1, α -smooth, muscle actin, and vimentin. In contrast, fibronectin, another extracellular matrix protein, stimulates EMT in mammary cells through binding to its $\alpha 5$ -integrin receptor [84].

The laminin-111 fragment cleaved by the matrix metalloproteinase MMP2 also inhibits tissue fibrosis *in vivo* [85]. *In vitro*, the interaction between this fragment and $\alpha 3 \beta 1$ integrin weakens TGF- $\beta 1$ -induced Smad3 phosphorylation and Snail activation in mouse peritoneal cells and inhibits the mesothelial–mesenchymal transition [85], which is a subtype of EMT.

In addition, it has been demonstrated that tumor progression is largely determined by laminins [86]; some isoforms of laminin promote tumor cell migration [87–89].

Laminins (and laminins within the basement membrane in particular) are the key factor responsible for the attachment and polarity of epithelial cells. Loss of binding and attachment to the basement membrane through laminins is associated with a loss of polarity (one of the first stages of EMT) and also correlates with an unfavorable prognosis of tumor progression [90]. EMT is typically associated with a loss of expression of the basement membrane components [91]: so, certain laminin chains can be regarded as EMT markers.

EMT transcription factors directly affect laminin expression. Snail1 suppresses the $\alpha 5$ and enhances the $\alpha 4$ chain expression of laminin in oral squamous cell carcinoma [92]. ZEB1 inhibits the expression of the $\alpha 3$ chain of laminin and type IV collagen (which also is the primary component of the basement membrane) in colorectal cancer cell lines but increases the expression of laminin $\gamma 2$ -chain [91]. The laminin $\gamma 2$ -chains are known to accumulate in the frontal area of invasive malignant tumors [93] in the form of monomers, rather than as a component of mature laminin trimers or the basement membrane [94].

It was also shown that laminins can directly affect EMT in tumor cells. In hepatocellular carcinoma cells, laminin-332 signaling via integrin- $\alpha 3$ enhances the expression of SNAIL1 and SNAIL2 and inhibits E-cadherin expression [95]. Nevertheless, the involvement of co-stimulatory signals through TGF- $\beta 1$ is required for EMT completion and transition to the invasive phenotype [95].

Other components of the extracellular matrix, namely fibronectin and collagen, also play an important role in tumor progression. Many studies have indicated that type 1 collagen is related to EMT and invasion. Its isoform, collagen 1A1, is crucial to the progression of non-small cell lung cancer (NSCLC) and is associated with EMT [96]. Progression of gastric cancer also correlates with the expression of type 1 collagen [97]. In addition, collagen fibrils in metastatic lung tumors are characterized by a higher organization as a result of collagen cross-linking with lysyl oxidase (LOX) enzymes. The expression of LOX and LOXL2 lysyl oxidase isoforms is directly regulated by miR-200 and ZEB1, the key regulators of EMT. Stabilization of collagen fibrils due to the activation of lysyl oxidase increases the rigidity of the extracellular matrix and activates the $\beta 1$ /FAK/Src integrin signaling pathway through type 1 collagen, thus triggering invasion and metastasis in lung cancer [96]. In a similar way, TGF- $\beta 1$ induces LOXL2 expression and type 1 collagen stabilization in hepatocellular carcinoma cells, thus promoting invadosome formation and tumor invasion [98].

The increased extracellular matrix stiffness that is due to collagen stabilization induces TWIST-dependent EMT and is a poor prognostic marker for breast cancer [99]. Thus, changes in the physical characteristics of the extracellular matrix, such as stiffness, can initiate EMT processes by mechanical signal transduction to tumor cells, thus promoting invasion and metastasis [99].

Fibronectin, an extracellular matrix component that ensures the connection between collagen fibers and integrin molecules on the cell surface, is also an EMT marker [100]. Fibronectin splicing isoforms containing the ED-B domain are not expressed in normal adult tissue, being present only in the tumor stroma or during embryonic development, which makes them a promising tumor-specific marker of EMT [101].

CELL PLASTICITY AND CANCER PROGRESSION

As previously discussed, EMT is crucial to a wide variety of body functions at different stages of development in various organs and tissues because of the complex variety of molecular regulatory mechanisms. In a broad sense, EMT ensures one common feature: the so-called cellular plasticity, which is the ability of cells to change their phenotype and function under certain conditions. In addition, cellular plasticity also manifests itself in that cells undergo EMT only partially (*Fig. 2*). Moreover, EMT processes can be reversible. All these processes are required for normal development; the oncogenic mechanisms use the plasticity of the original cell to transform it into a tumor cell in a completely different (pathological) context. Today, there is evidence indicating that partial EMT and the reverse process, mesenchymal-epithelial transition (MET), play a critical role in invasion and metastasis (*Fig. 2*).

In contrast to the complete EMT occurring during embryogenesis, tumor cells usually rarely undergo complete transformation into mesenchymal cells [64, 67, 102–106] but rather form a hybrid epithelial/mesenchymal phenotype, which manifests itself in the coexpression of both epithelial and mesenchymal markers. Moreover, different cancer types are characterized by different sets of coexpressing markers, which is likely due to variations in the primary pathways involved in progression (see discussion above) (*Fig. 2*).

Surprisingly, certain tumor cell populations retain a high level of expression of E-cadherin, which is crucial in maintaining the epithelial phenotype but interferes with neither the formation of a partial epithelial/mesenchymal phenotype nor its invasive or migratory potential [103, 107–112].

It has been called into question whether metastasis initiation occurs through the EMT mechanism, in experimental studies with transgenic *in vivo* models of breast [113] and pancreatic cancers [114]. However, problems related to the experimental model used by Fischer et al. [113] to study EMT were found later, including the erroneous selection of the *Fspl* and *Vim* genes as mesenchymal markers (low expression in breast cancer cells susceptible to EMT) [115]. Several independent studies have demonstrated the key role played by Snail in the regulation of EMT and metastasis in breast cancer [116, 117]. The conclusions on the non-involvement of EMT in the metastasis of pancreatic cancer drawn based on the significance of Snail and Twist expression in EMT have also been scrutinized [118]. In addition, it has been shown that ZEB1 knockdown in the same transgenic *in vivo* model is associated with a loss of cell plasticity (fixation of the epithelial phenotype by tumor cells), as well as a reduction in the invasive and metastatic abilities [64]. Moreover, it was found in a recent study using a variety of transgenic *in vivo* models that E-cadherin and the p120-catenin expression determine the organotropism of metastatic lesions in pancreatic cancer. Their expression leads to the formation of liver metastases, while not being necessary for lung metastasis formation [112].

A study of tumor material obtained from patients with metastatic breast cancer revealed the important clinical significance of the co-expression of E-cadherin and vimentin: high E-cadherin/positive staining for vimentin, as well as low E-cadherin/positive staining for vimentin, was associated with the most aggressive triple negative form of the disease. However, the worst prognosis, associated with 10-year non-relapse survival, was associated with a high level of E-cadherin/positive staining vimentin. In addition, a comparison of the expression levels of E-cadherin in primary tumors and the corresponding metastases in the lymph nodes showed that the E-cadherin level is most often unchanged (46% of cases) or increased (43% of cases) in metastases, compared to the primary tumor, being reduced in only 11% of cases [119].

The molecular mechanisms underlying the hybrid epithelial/mesenchymal phenotype are unclear [120] and often difficult to explain solely by the established concept of suppression/activation of transcription of the corresponding “epithelial” and “mesenchymal” genes. In some cases, E-cadherin dysfunction may occur, caused by mutations in the *CDH1* gene or associated with aberrant signals of the tumor microenvironment [121], and the dysfunction is not necessarily associated with a decrease in adhesion, but is

frequently associated with its increase and constitutive activation, which in some cases is important for metastasis [110].

In a recent study that used a mouse reporter line as an *in vivo* model of pancreatic cancer, Aiello et al. [107] confirmed the possibility that two EMT types are utilized during tumor invasion: complete EMT characterized by reduced E-cadherin transcription and increased vimentin transcription, and partial EMT characterized by the preserved expression of E-cadherin mRNAs and increased vimentin transcription (partial EMT is also characterized by a lower expression of the transcriptional factors *Etv1*, *Prrx1*, *Zeb1*, *Twist1*, *Snai1*, *Snai2*, and *Zeb2*, compared with complete EMT). Moreover, partial EMT was characteristic of a predominant number of tumors of the mouse model. The predominance of this EMT type was also shown in human breast and colorectal cancer cells. Tumor cells undergoing partial EMT showed no surface staining for E-cadherin during immunocytochemical studies. The authors demonstrated that the mechanisms of partial EMT are associated with recirculation of surface proteins and relocalization of surface E-cadherin to late endosomes [107].

Different EMT programs are associated with different methods of invasion. Tumor cells using partial EMT migrate as multicellular clusters with the preservation of intercellular contacts but can also migrate as single cells; in contrast, during complete EMT invasion and migration they proceed only in the form of single cells [107] (*Fig. 2*). Many studies have confirmed collective migration of tumor cell clusters [64, 109, 110, 122, 123] that undergo partial EMT [106, 123, 124] during invasion.

Although most of the cells forming these clusters express E-cadherin and maintain intercellular contacts, tumor cells at the cluster edges do not express E-cadherin and have a more mesenchymal phenotype. Thus, the “leading” cluster cells undergo completion of EMT to enhance mobility, accompanied by an increased production of the metalloproteinases that destroy the extracellular matrix associated with a renewed expression of E-cadherin, thus contributing to an active invasion of the entire cluster, including its more epithelial cells [105, 107, 110, 111, 125].

It is important to note that metastasis is an ineffective process: only a small fraction of circulating tumor cells avoid elimination and give rise to secondary tumors [126]. Despite the smaller number of circulating clusters of tumor cells compared to single tumor cells, metastases are much more often a result of the colonization of tumor cell clusters [127–129]. Moreover, these clusters cause the polyclonality of secondary tumor sites [110, 130–132].

The circulation of tumor cell clusters with partial EMT was discovered in the blood of patients with breast, lung, prostate, and colorectal cancer [124, 133–135]. It is associated with a poor prognosis: low survival rate, high risk of relapse, and resistance to chemotherapy [130, 136–139].

Tumor metastasis formation is a multi-stage process and, in addition to invasion, migration, and extravasation (penetration of tumor cells through the blood vessel wall into tissue), includes colonization (proliferation of tumor cells in the secondary tumor site), which is associated with an opposite process, the mesenchymal–epithelial transition, which once again emphasizes the importance of cell plasticity to tumor progression. Metastases are formed by epithelial cells whose morphology is identical to that of primary tumor cells, which is characterized by a re-expression of epithelial markers and repression of EMT factors [51, 106, 140–143].

Meanwhile, the molecular mechanisms underlying MET have been less studied and are usually associated with the suppression of EMT (*Fig. 2*). MicroRNAs (miRNAs), small non-coding RNAs that regulate target gene expression at the post-transcriptional level, play a significant role in suppressing EMT in various types of cancer [144–151].

However, there are mechanisms that directly stimulate the formation of an epithelial phenotype. Growth differentiation factor-10 (GDF10), also known as bone morphogenetic protein 3B (BMP-3B), inhibits vimentin expression and the migration and invasion of squamous cell carcinoma of the head and neck and increases E-cadherin expression and the sensitivity of tumor cells to cytotoxic therapy through apoptosis induction. The reduced GDF10 expression characteristic of this type of cancer is associated with a decrease in the overall survival rate. Interestingly, GDF10 expression is mediated by SMAD 2/3-dependent activating signals from the type III TGF- β receptor (TGFB3), whose expression is also reduced in this type of cancer. In addition, GDF10 repression is mediated by signals from ERK, rather than by the classical TGF- β EMT signaling [152].

A component of gap junctions, connexin (namely, its isoform Cx32), stimulates MET in hepatocellular carcinoma cells [153]. Cx32 is a suppressor of hepatocarcinogenesis and metastasis in liver cells, and its expression is reduced in hepatobiliary carcinoma cells compared to normal liver tissue [153]. The mesenchymal phenotype of tumor cells is associated with resistance to apoptosis and cytotoxic chemotherapy, and EMT is considered to be one of the resistance mechanisms. Interestingly, in an article by Yu et al. [153], an obtained line of hepatocellular cancer resis-

tant to the DNA-damaging drug doxorubicin shows signs of EMT; thus, the authors postulated the existence of chemotherapy-induced EMT associated with a reduced expression of E-cadherin and Cx32, as well as increased vimentin expression. Overexpression of Cx32 in doxorubicin-resistant cells induces MET associated with a re-expression of E-cadherin and reduced vimentin expression. However, it is worth noting that the authors somewhat self-confidently declared that there is a role for Cx32 in regulating the sensitivity of tumor cells to chemotherapy and the possibility of using it as a target for therapy based only on the potential relationship between the phenotype and sensitivity, while there were no relevant experiments confirming the sensitization of doxorubicin to cells with Cx32 overexpression [153]. A role for various connexin isoforms in metastasis has also been shown in kidney cancer [154] and melanoma [155].

Another important MET inducer is the GRHL2 transcription factor, which activates the expression of various epithelial adhesion molecules and inhibits the expression of EMT factors, such as ZEB1 [156]. The mechanisms of regulation of tumor progression controlled by GRHL2 are very diverse and obviously depend on tissue type. Moreover, this transcription factor has conflicting effects: it can contribute to tumor progression [157, 158] or suppress tumor growth [159, 160]. A large-scale study of various types of cancer compared to normal tissue samples revealed the complex expression patterns of GRHL2, being indicative of both a reduced and increased expression in various tumors. Interestingly, increased expression was observed in proliferating epithelial cells with stem cell characteristics. This was also confirmed in a study focused on the role of GRHL2 in pancreatic cancer [157] and squamous cell carcinoma of the head and neck [161]), as well as in non-invasive types of cancer [159]. In addition, increased expression of GRHL2 is associated with increased proliferative activity, large tumor sizes, and late clinical stages of colorectal cancer. GRHL2 negative breast cancer is quite rare but is commonly associated with metastasis of the lymph nodes. Meanwhile, overexpression in breast cancer cells stimulates proliferation and is associated with the lowest rate of disease-free survival [162, 163]. A similar dual effect of GRHL2 is observed in prostate cancer [164]. Kidney and stomach cancers are characterized by a high frequency of GRHL2-negative tumors [159]. In these types of cancer, it acts as a cancer suppressor and inhibits invasion and metastasis [165, 166].

The role of reprogramming factors in the induction of MET and their impact on tumor progression is poorly understood. It was shown that during the

production of induced pluripotent stem cells (iPSCs) from murine fibroblasts by induction of the overexpression of the reprogramming factors Oct3/4, Klf4, c-Myc, and Sox2 (OKMS), the epithelial program associated with the induction of the expression of miR-205/miR-200 and suppression of Snail1 and TGF- β 1/TGF- β 2 is activated, while the cells undergo MET [167, 168].

Tumor cell reprogramming experiments exert rather conflicting effects on malignant progression. On the one hand, reprogramming leads to a loss of oncogenicity [169, 170] and the suppression of metastasis [171–173], which is associated with MET, while, on the other hand, the expression of reprogramming factors is associated with a poor disease prognosis [172, 174–176]. Thus, induction of EMT using reprogramming factors and the potential of this approach as potential antitumor therapy requires further studies and a deeper understanding of the molecular mechanisms underlying the relationship between pluripotency and cell plasticity.

The initiation of MET at the stage of tumor cell colonization of foreign tissues during metastasis is associated with changes in the microenvironment, the absence of external EMT-inducing stimuli from the tumor-associated stroma, and changes in the level of oxygenation of the surrounding tissue [177–180].

EMT AND RESISTANCE TO ANTITUMOR THERAPY: ROLE IN THE FORMATION OF TUMOR STEM CELLS

Chemotherapy

For many cancer types, epithelial–mesenchymal transition is associated with a poor prognosis not only in relation to metastasis. EMT is one of the mechanisms underlying the development of resistance to the cytotoxic effect of antitumor drugs, which is the main challenge in modern oncology. Moreover, while the need for EMT for metastasis was called into question for pancreatic and breast cancer as discussed previously, its role in the development of resistance to chemotherapeutic drugs is not controversial [113, 114].

Overexpression of miR-93 micro RNA induces EMT and reduces sensitivity to the cytotoxic effects of doxorubicin in breast cancer cells. In addition, the gene expression levels associated with multidrug resistance were significantly increased in MCF-7 cells, with miR-93 overexpressed compared to the control. It had been previously shown that miR-93 interacts with PTEN mRNA, a known regulator of EMT in breast cancer cells [69]. Another micro RNA suppressing PTEN expression, miR-21, is also involved in EMT induction and the development of gemcitabine resistance in breast cancer cells [181].

The transcription regulator induces eIF4E Snail expression and triggers the EMT associated with invasion and resistance to cisplatin in nasopharyngeal carcinoma cells [182]. In glioblastoma cells, STAT3 activates the expression of Snail1, causing tumor resistance to another cytostatic drug, temozolomide. The use of antibodies blocking IL-6 prevents STAT3 activation and Snail expression, thus increasing the sensitivity of glioblastoma cells to temozolomide in combination therapy [183].

STAT3 activation due to Y705 phosphorylation in ovarian cancer leads to EMT induction and the development of tolerance to cisplatin. This activation of EMT is associated not with Snail, but rather with another transcription factor important for the formation of the mesenchymal phenotype Slug [184]. In addition, the authors attributed the development of cisplatin resistance directly to a decrease in autophagy caused by STAT3 activation; however, it is worth noting that the direct role of Slug activation in this study was not evaluated [184]. Meanwhile, many research groups have confirmed the direct role of Snail and Slug in the development of resistance to chemotherapy and radiotherapy in ovarian cancer [55, 185–188]. Increased Slug activation is associated with resistance to radiotherapy and temozolomide treatment in patients with malignant glioma. Patients with lower levels of Slug expression demonstrate longer progression-free survival [189]. A role for Slug in the development of multidrug resistance in the MCF-7 breast cancer cell line has also been shown. Slug induces the expression of MMP1 metalloproteinase by directly binding to the promoter region of the gene. A high level of MMP1 is associated with rapid progression and metastasis, as well as poor prognosis in patients with breast cancer [190].

Tumor suppressor FBXW7 triggering ubiquitin-dependent degradation of many oncogenic factors such as Myc, c-Jun, Cyclin E, and Notch1 is responsible for the degradation of Snail in non-small cell lung cancer cells. FBXW7 overexpression suppresses NSCLC tumor progression by arresting the cell cycle, inhibiting EMT, and increasing the sensitivity to chemotherapy. Tumor samples obtained from patients with NSCLC are characterized by reduced FBXW7 expression in most NSCLC tissues; the reduced expression level correlates with a later stage of the disease according to TNM staging and worse 5-year survival rate [191].

The use of chemotherapeutic drugs is well studied, being one of the most common approaches to cancer therapy. The cytotoxic effect of these drugs (as well as radiotherapy) extends mainly to rapidly dividing cells, since their mechanism of action involves various types of DNA damage and disrupt-

tion of mitotic spindle formation. Thus, cells with a mesenchymal phenotype characterized by a lower proliferation index are less sensitive to the cytotoxic effect of chemotherapy compared to those with an epithelial phenotype [75, 106, 192, 193]. In addition, several recent studies have demonstrated the direct effect of EMT on the well-known mechanisms of tumor cell tolerance to massive DNA damage associated with DNA repair [194–196], cell-cycle control [197–199], inactivation of reactive oxygen species [200, 201], and autophagy [202]. Thus, the molecular mechanisms behind the development of resistance to chemotherapy are diverse and, for many types of cancer, mediated by the launch of EMT; however, their relationship remains poorly understood.

Targeted antitumor therapy

Understanding of the contribution made by EMT to malignant progression has changed significantly since its discovery. Today, it is obvious that EMT plays roles other than those of the formation of a mesenchymal phenotype for tumor cells capable of invasion and migration. The EMT mechanisms can directly affect the triggering oncogenic mechanisms. Unlike cytotoxic chemotherapy, targeted antitumor therapy is aimed at specific molecular targets: proteins specific to a particular cancer type that trigger and promote tumor growth. EMT underlies the development of resistance to targeted drugs in some types of cancer. The role of EMT in the development of resistance to targeted therapy in lung cancer has been described in the greatest detail.

According to the American Institute for Cancer Research (AICR), lung cancer was the most common cancer in the world among all cases documented in 2018. Non-small cell lung cancer (NSCLC) accounts for most (about 85%) lung cancers. Activating mutations in the epidermal growth factor receptor (EGFR) gene are found in 40–89% of NSCLCs. These mutations increase the activity of the intracellular signaling pathways through autophosphorylation of the cytoplasmic section of EGFR receptor tyrosine kinase, leading to the induction of a proliferation of lung tissue epithelial cells, increased angiogenesis, invasion, and metastasis [203]. Targeted therapy aimed at inhibiting the activity of EGFR by drugs such as gefitinib, erlotinib, and afatinib is the basis for treating patients with activating mutations in the EGFR gene. However, as for cancer chemotherapy, the main challenge standing in the way of long-term effectiveness is the initial and acquired tumor resistance to the mechanism of action of an inhibitor. Various attempts have been made to solve this issue, including those related to the suppression of the EMT mechanisms.

Overexpression of TWIST1, one of the key transcription factors in EMT, has been shown to cause EGFR mutant NSCLC cells to become resistant to the EGFR inhibitors erlotinib and osimertinib [204]. Osimertinib is a third-generation EGFR inhibitor approved in 2017 for the treatment of NSCLC in patients with a specific EGFR T790M mutation that either exists *de novo* or is acquired during treatment with first-line drugs (gefitinib, erlotinib or afatinib) and is associated with resistance to these drugs. However, resistance to the antitumor effect of osimertinib occurs within approximately 10 months after treatment and is associated with the onset of the C797S mutation in EGFR exon 20. It is important to note that there is currently no approved pharmacological treatment for EGFR mutant NSCLC that progresses after the development of resistance to osimertinib. Inhibition of TWIST1 activity using an inhibitor in erlotinib- and osimertinib-resistant NSCLC cells increases their sensitivity to the cytotoxic effect of EGFR inhibitors in a dose-dependent manner. Moreover, the sensitization mechanism is associated with TWIST1 suppressing the transcription of proapoptotic BCL2L11 (BIM) by binding to the promoter region of the gene [204].

In addition, erlotinib-resistant NSCLC cell lines exhibit a mesenchymal phenotype (decreased E-cadherin expression and induction of vimentin and N-cadherin) and are characterized by the activation of not only TWIST1, but also Snail, Slug, and ZEB1. Moreover, overcoming of resistance to erlotinib with furamidine, a PRMT-1 inhibitor, was associated with EMT suppression and restoration of epithelial characteristics [205]. A number of studies have also confirmed the role played by EMT in the development of gefitinib resistance and the reversibility of resistance as a result of MET [206, 207].

In 3–7% of cases, NSCLC is associated with various translocations in the ALK gene, leading to the formation of more than 19 chimeric proteins, including EML4, KIF5B, KLC1, and TPR. However, regardless of the genes involved in the translocation, all chimeric products retain the ALK kinase domain, which is responsible for constitutive oncogenic activation of the ALK signaling pathways (including Ras/Raf/MEK/ERK1/2, JAK/STAT, PI3K/Akt, PLC- γ signaling pathways) that regulate migration, proliferation, and cell survival [208]. Most chimeric ALKs are susceptible to the inhibitor crizotinib, which has been shown to be highly effective in the treatment of similar forms of NSCLC. However, resistance to crizotinib treatment develops in most patients within a few years.

It has been found that some NSCLC lines (H2228 and DFCI032, but not H3122) with oncogenic activa-

tion of ALK express low E-cadherin levels and high levels of vimentin and other mesenchymal markers. Additionally, ALK inhibition changes the cell phenotype to an epithelial one [209]. In a recent paper by Nakamichi et al. [210], H2228 lines resistant to three different ALK inhibitors (crizotinib, alectinib, and ceritinib) were created. The obtained stable line was characterized by a reduced ALK expression and overexpression of another oncogenic protein, AXL, which is associated with EMT and stem cells. Moreover, the artificial induction of EMT using TGF- β 1 was also associated with increased AXL expression. The AXL inhibitor was of assistance in the detection of cells resistant to ALK inhibitors [210]. Hence, AXL activation can be regarded as the mechanism underlying tumor resistance to ALK inhibitors. It also induces EMT when ALK expression is low. It is EMT that is responsible for the development of the resistance. Blocking it at the AXL level, in conjunction with HDAC inhibitors, overcomes the resistance of NSCLCs with mutant ALK [211]. Long-term administration of sunitinib to treat kidney cancer also causes the activation of AXL and EMT [212].

Recent studies have also shown that EMT associated with methylation of the E-cadherin gene underlies the development of resistance to hormone therapy with tamoxifen in estrogen-positive breast cancer [213]. In HER2 positive cancer, EMT plays a key role in the development of resistance to the targeted drug trastuzumab [214, 215].

Immunotherapy

Antitumor immunotherapy aims to activate immune cells to recognize and induce cytotoxicity in tumor cells. Inhibitors of immune checkpoints (namely, CTLA4, PD-1, and PD-L1 inhibitors) are currently among the main and most successful forms of cancer immunotherapy. In 2018, the researchers James P. Allison and Tasuku Honjo were awarded the Nobel Prize in medicine and physiology for discovering this therapeutic approach and the molecular mechanisms underlying it.

CTLA4 is expressed on the surface of activated T cells (as well as on the surface of regulatory T cells (Tregs)) and interacts with the CD80 and CD86 molecules on the surface of antigen-presenting cells. Unlike the homologous co-stimulatory molecule CD28 (which also binds to CD80 and CD86), CTLA4 is a co-inhibitor of the T-cell receptor signal response and suppresses the immune response, thus maintaining the balance and preventing the development of auto-immune processes [216]. James P. Allison et al. were the first to show that the use of antibodies blocking CTLA4 enhances the immune response against tu-

mors and causes their rejection *in vivo* [217]. Identically to CTLA4, the PD-1 membrane protein suppresses the immune response. PD-1 expressed on the surface of T lymphocytes interacts with PD-L1 and PD-L2 molecules, which are normally expressed on the surface of antigen-presenting cells. In addition, tumor cells use the expression of PD-L1 on their surface to dodge the immune response [218, 219]. Honjo et al. demonstrated that inhibition of PD-1 activates the antitumor immune response regardless of the PD-L1/PD-L2 status of the tumor, while causing a milder autoimmune effect compared to the inhibition of CTLA-4 [220].

Various inhibitors of CTLA4, PD-1, PD-L1, and combinations thereof are now approved for the treatment of melanoma, renal carcinoma, non-small cell lung cancer, squamous cell carcinoma of the head and neck, urothelial carcinoma, colorectal cancer, and Hodgkin's lymphoma. Moreover, these inhibitors are used both as adjuvant therapy and as second- and third-line therapy when chemotherapy and targeted anticancer drugs fail due to the emergence of resistance. An exception is the metastatic form of non-small cell lung carcinoma with a high level of PD-L1 expression and wild-type EGFR and ALK, which require a combination therapy with ipilimumab and nivolumab (CTLA-4 and PD-1 inhibitors, respectively) as first-line treatment [221]. Today, immunotherapy is the last therapeutic option for many cancer patients in the case when chemo- and targeted therapy are ineffective.

It was discovered that EMT is associated with an increased expression of PD-L1 [222–227], as well as CD47, an inhibitory surface protein blocking phagocytosis [228] in tumor cells and hiding them from immunological surveillance (in particular during invasion and migration to secondary organs, resulting in metastasis formation). Moreover, in NSCLC, EMT is associated with reduced CD4/CD8 infiltration by T lymphocytes, which play a key role in the antitumor immune response [229] and increase the immune response. Additionally, the EMT is associated with suppression of CD4/Foxp3 T-regulatory lymphocytes [230]. Expression of EMT markers in NSCLC tissues is associated with an increased expression of the immune checkpoints PD-L1, PD-L2, PD-1, TIM-3, B7-H3, BTLA, and CTLA-4 [230] and the expression of immunosuppressive cytokines such as IL-10 and TGF- β ; however, the underlying molecular mechanisms remain unclear [229].

Tumors characterized by a high level of T-lymphocyte infiltration can be expected to be more sensitive to PD-1/PD-L1 inhibitors. However, a large number of patients with this type of tumors do not respond to

such therapy. Using data from the tumor expression profile database (The Cancer Genome Atlas (TCGA)), Wang et al. found a positive correlation between the expression of EMT markers and the level of T-lymphocyte infiltration in urothelial tumors. However, in a study of a group of patients with urothelial cancer treated with nivolumab (PD-1 inhibitor), it was shown that the high level of expression of EMT markers in tumors with a high level of T-lymphocyte infiltration was associated with a poor response to therapy and lower survival rate. Interestingly, tumor stromal cells act as a source of increased expression of EMT markers [231].

The development of tumor resistance to therapy with immune checkpoint inhibitors has been little studied thus far. Some studies indicate that EMT may be involved in this process; however, further research is needed to understand the exact molecular mechanisms.

Cancer stem cells

Currently, the classic concept explaining the development of resistance to antitumor therapy is rooted in the presence of cancer stem cells (CSCs). CSCs express markers characteristic of normal stem cells, for example CD44, CD133, CD34, and EpCAM. Through many different mechanisms, CSCs become resistant to chemotherapy and radiotherapy (unlike most of the differentiated tumor cells that undergo apoptosis in the case of effective therapy) [232–234], migration (abundant data indicate the role of CSC in metastasis [235]), and most importantly, subsequent division and differentiation into different lines of tumor cells, thus ensuring the heterogeneity of the recurrent tumor and the emergence of clones resistant to the therapy used [236].

Although CSCs undoubtedly possess the characteristics inherent to normal stem cells, there is no clear understanding of their origin. This is due to the challenges related to identifying stem markers that may differ in various types of tumors. It is likely that the same reason is behind why CSCs have not been identified for all cancer types [237]. Furthermore, it is very likely that the CSCs in these cancers have different origins.

There are several theories regarding the possible origins of CSCs. According to the first one, CSCs form from the stem cells of mature tissue, ensuring its renewal as a result of somatic mutations. It was shown that CSCs initiating acute myeloid leukemia are not only capable of differentiating into all types of blood cells but can also retain a potential for self-renewal and restoration of hematopoiesis in a series of transplantations in irradiated mice, which is the

main characteristic of hematopoietic stem cells. This fact suggests that in the case of leukemia, CSCs arise from hematopoietic stem cells as a result of mutations, which enables the tumor cell to utilize stem regulatory signaling pathways to advance tumor progression [238].

The second theory involves the formation of CSCs from differentiated cells by dedifferentiation and gain of stem cell characteristics. This assumption is rooted in an understanding of cell plasticity and the possibility of reprogramming somatic cells into pluripotent stem cells [239]. Moreover, a recent study on prostate cancer lines has shown that such reprogramming is possible and can be induced by the development of resistance to therapy [240].

To date, the specific molecular mechanisms underlying the reprogramming of tumor cells into CSCs remain poorly studied; however, there is reason to believe that these mechanisms are associated with EMT. EMT activation by ectopic expression of Snail or Twist, as well as by activation of TGF- β 1 in an epithelial cell line of breast cancer, is associated with the induction of stem marker expression (the appearance of CD44+/CD24- cells) and their increased ability to form “mammospheres” (tumor-like structures, each being a clone of a single CSC) [241]. Moreover, EMT activation via the Ras-MAPK signaling pathway in normal breast CD44-/CD24+ cells leads to their transformation into CD44+/CD24- stem tumor cells; additional activation of TGF- β 1 enhances the effect [242]. A recent study on transgenic mouse models of breast cancer, MMTV-PyMT, showed that although CSCs and normal breast stem cells are phenotypically similar, they form in different parts of the breast epithelium (luminal and basal epithelial regions, respectively) and also differ in terms of the molecular mechanisms of EMT activation (using the transcription factors Snail and Slug, respectively). This study supports the theory according to which CSCs originate from differentiated cells by being reprogrammed during EMT [125]. A role for EMT in the formation of CSCs and resistance to antitumor therapy and the metastatic progression associated with these processes has also been shown in pancreatic cancer [243, 244], prostate cancer [245], squamous cell carcinoma of the head and neck [158, 246, 247], stomach cancer [248, 249], melanoma [250], glioblastoma [251], and colorectal cancer [252, 253].

CONCLUSION: EMT PATHWAYS ARE MOLECULAR TARGETS FOR ANTITUMOR THERAPY

In this review, we have examined the role of EMT mechanisms in tumor progression, as well as the latest experimental and clinical data confirming the

Antitumor drugs suppressing various components of the EMF signaling pathways (see detailed explanation in the text)

Drug	Target	Clinical trials	Disease
Vismodegib	Smoothened (Shh signaling pathway)	Approved	Metastatic, inoperable, radiotherapy-resistant form of basal cell carcinoma
Temsirolimus and everolimus	mTOR (PI3K/AKT/mTOR signaling pathway)	Approved	Renal carcinoma, relapse of lymphoma resistant to other types of therapy, chronic lymphocytic leukemia
Galunisertib	TGFβRI	Phase 1 Phase 2 and 3	metastatic form of pancreatic cancer, myelodysplastic syndrome
Fresolimumab	TGFβ	Phase 2	Metastatic breast cancer, melanoma, kidney carcinoma, malignant pleural mesothelioma, non-small cell lung carcinoma
Tarextumab	Notch	Phase 1b/2	Stage IV pancreatic cancer
Vantictumab	Frizzled	Phase 1	Stage IV pancreatic cancer, NSCLC, metastatic breast cancer
Harmine	TWIST1	Preclinical evaluation	NSCLC

involvement of EMT in almost all of its aspects: tumor invasion and metastasis, resistance to cytotoxic and targeted therapy, and avoidance of immune surveillance. In our opinion, the most crucial aspect is the potential contribution of EMT to the emergence of CSCs, which is the basis of tumor heterogeneity according to modern theories. It is one of the primary roadblocks to cancer treatment and also a key factor in relapse. Thus, the genes within the signaling pathways and direct transcription factors that activate EMT become promising molecular targets for antitumor therapy. These are usually inhibitors of the key components of oncogenic signaling pathways that regulate not only EMT, but also proliferation, growth, survival, and angiogenesis. Moreover, the therapeutic efficacy associated with inhibiting a specific protein associated with EMT depends on the tumor type, since, as has been discussed above, different signaling pathways in EMT regulation can be utilized during tumor progression depending on the tissue type.

There are already approved drugs for combination therapy (used in combination with tyrosine kinase inhibitors or other chemo- and radiotherapy agents) and even some that can be used as monotherapy if there are no other therapeutic options, as well as second- and third-line therapy in patients who have developed drug resistance (*Table*).

An inhibitor of the canonical Shh signaling pathway, the smoothened receptor inhibitor vismodegib, has been approved for the treatment of the most common form of skin cancer, basal cell carcinoma (metastatic and inoperable disease forms), or in cases of relapse after surgical treatment and radiotherapy [254]. Inhibitors of the PI3K/AKT/mTOR components of the EMT signaling pathway, cell cycle, and VEGF signaling have been approved for the treatment of kidney carcinoma (mTOR inhibitors temsirolimus and everolimus) [255], relapses of lymphoma resistant to other types of therapy, and chronic lymphocytic leukemia, in combination with rituximab (idelalisib, a PI3K inhibitor) [256]. Furthermore, a number of inhibitors are currently undergoing clinical trials, mainly in combination therapies. Clinical trials (phase 1) of the TGFβRI inhibitor galunisertib in combination with the PD-L inhibitor durvalumab in patients with metastatic pancreatic cancer (NCT02734160) and as monotherapy in patients with advanced cancer that has spread to other body parts (NCT01373164) have been completed; clinical trials to evaluate its combination with gemcitabine in patients with an unresectable metastatic disease form are currently in phases 1 and 2 (NCT02154646). The data from the latest study have been published and have confirmed the benefits of combination therapy compared to chemotherapy

with gemcitabine. In addition, potential predictive markers of sensitivity to the therapy were determined by analyzing tumor samples derived from the patients [257]. Galunisertib was tested in phase 2 and 3 trials in patients with myelodysplastic syndrome of varying severity (NCT02008318). This treatment had an acceptable safety profile and was associated with hematological improvements in patients with low and medium risks of transformation into acute leukemia, and a positive response in patients with signs of an early stem cell differentiation blockage [258]. Many clinical trials seeking to evaluate galunisertib for the treatment of various types of tumors have been initiated in various therapeutic regimens (clinicaltrials.gov).

Fresolimumab, a monoclonal antibody that binds all isoforms of the transforming growth factor TGF- β , in combination with radiotherapy, has completed phase 2 clinical trials in the treatment of patients with metastatic breast cancer (NCT01401062). Molecular markers of sensitivity to fresolimumab therapy have been identified [259], and the potential for using it in combination therapy with PD-1 blockade in order to enhance effectiveness was assessed [260]. In addition, the drug is being tested in patients with melanoma and renal carcinoma (NCT00356460), malignant pleural mesothelioma (NCT01112293), and non-small cell lung carcinoma, in combination with radiotherapy (NCT02581787).

The Notch inhibitor tarextumab, which has been shown to be effective in preclinical trials, failed in phase 1b/2 of a randomized clinical trial set to evaluate a combination therapy (in combination with etoposide and platinum drugs) for small cell lung carcinoma (NCT01859741). The drug has also been tested in combination with nab-paclitaxel and gemcitabine for the treatment of patients with treatment-naïve stage 4

pancreatic cancer (NCT01647828). The Frizzled inhibitor vanticumab (NCT02005315) has also been used in a study with a similar design. In addition, vanticumab has successfully concluded phase 1 trials in the treatment of patients with NSCLC (NCT01957007) and metastatic breast cancer (NCT01973309).

A TWIST1 inhibitor, alkaloid harmine, causing the degradation of TWIST1 homodimers and TWIST1-E2A heterodimers is currently in the preclinical stage of trials. Harmine per se was shown to have a cytotoxic effect on a NSCLC line with mutated EGFR, Kras, and c-Met. It also proved effective in *in vivo* models, both in transgenic mice with a KRAS mutation and in xenograft models derived from patient tumor tissue (PDX – patient-derived xenograft) [261]. Thus, harmine is a promising targeted antitumor drug to be used both in NSCLC monotherapy and as a third-line drug for patients resistant to EGFR inhibitors, which is the regimen that will most likely be tested during the clinical trials.

The molecular mechanisms of EMT regulation are a promising research field in antitumor therapeutics. It is important to use our scientific knowledge about EMT both in our efforts to create new therapies and in order to improve the existing ones. Pharmacological suppression of EMT can help not only to limit metastasis development and overcome resistance to existing therapies, but also to suppress CSCs, the culprit in tumor recurrence. In some cases, drugs that inhibit the EMT are the only available therapeutic option when other types of therapy are ineffective. ●

This review was written with support from the Russian Science Foundation (project No. 18-75-10054 “The role of AMH and AMHR2 in the development and malignant progression of NSCLC.”)

REFERENCES

- Nollet F., Kools P., van Roy F. // *J. Mol. Biol.* 2000. V. 299. № 3. P. 551–572.
- Yamada S., Pokutta S., Drees F., Weis W.I., Nelson W.J. // *Cell.* 2005. V. 123. № 5. P. 889–901.
- Ishiyama N., Lee S.H., Liu S., Li G.Y., Smith M.J., Reichardt L.F., Ikura M. // *Cell.* 2010. V. 141. № 1. P. 117–128.
- Drees F., Pokutta S., Yamada S., Nelson W.J., Weis W.I. // *Cell.* 2005. V. 123. № 5. P. 903–915.
- Perez-Moreno M., Fuchs E. // *Dev. Cell.* 2006. V. 11. № 5. P. 601–612.
- Shamir E.R., Ewald A.J. // *Curr. Top. Dev. Biol.* 2015. V. 112. P. 353–382.
- Cukierman E., Pankov R., Stevens D.R., Yamada K.M. // *Science.* 2001. V. 294. № 5547. P. 1708–1712.
- Pankov R., Cukierman E., Katz B.Z., Matsumoto K., Lin D.C., Lin S., Hahn C., Yamada K.M. // *J. Cell. Biol.* 2000. V. 148. № 5. P. 1075–1090.
- Greenburg G., Hay E.D. // *J. Cell. Biol.* 1982. V. 95. № 1. P. 333–339.
- Hay E.D. // *Acta Anat. (Basel).* 1995. V. 154. № 1. P. 8–20.
- Thiery J.P., Sleeman J.P. // *Nat. Rev. Mol. Cell. Biol.* 2006. V. 7. № 2. P. 131–142.
- Maschler S., Wirl G., Spring H., Bredow D.V., Sordat I., Beug H., Reichmann E. // *Oncogene.* 2005. V. 24. № 12. P. 2032–2041.

13. Takenawa T., Suetsugu S. // *Nat. Rev. Mol. Cell. Biol.* 2007. V. 8. № 1. P. 37–48.
14. Kimelman D. // *Nat. Rev. Genet.* 2006. V. 7. № 5. P. 360–372.
15. Viebahn C. // *Acta Anat. (Basel)*. 1995. V. 154. № 1. P. 79–97.
16. Correia A.C., Costa M., Moraes F., Bom J., Novoa A., Mallo M. // *Dev. Dyn.* 2007. V. 236. № 9. P. 2493–2501.
17. Markwald R.R., Fitzharris T.P., Manasek F.J. // *Am. J. Anat.* 1977. V. 148. № 1. P. 85–119.
18. Person A.D., Klewer S.E., Runyan R.B. // *Int. Rev. Cytol.* 2005. V. 243. № 1. P. 287–335.
19. Fitchett J.E., Hay E.D. // *Dev. Biol.* 1989. V. 131. № 2. P. 455–474.
20. Hudson L.G., Newkirk K.M., Chandler H.L., Choi C., Fossey S.L., Parent A.E., Kusewitt D.F. // *J. Dermatol. Sci.* 2009. V. 56. № 1. P. 19–26.
21. Eming S.A., Martin P., Tomic-Canic M. // *Sci. Transl. Med.* 2014. V. 6. № 265. P. 265sr6.
22. Liu Y. // *Nat. Rev. Nephrol.* 2011. V. 7. № 12. P. 684–696.
23. Higgins D.F., Kimura K., Bernhardt W.M., Shrimanker N., Akai Y., Hohenstein B., Saito Y., Johnson R.S., Kretzler M., Cohen C.D., et al. // *J. Clin. Invest.* 2007. V. 117. № 12. P. 3810–3820.
24. Zeisberg M., Hanai J., Sugimoto H., Mammoto T., Char-tyan D., Strutz F., Kalluri R. // *Nat. Med.* 2003. V. 9. № 7. P. 964–968.
25. Zhou G., Dada L.A., Wu M., Kelly A., Trejo H., Zhou Q., Varga J., Sznajder J.I. // *Am. J. Physiol. Lung Cell Mol. Physiol.* 2009. V. 297. № 6. P. L1120–L1130.
26. Gressner A.M., Weiskirchen R. // *J. Cell. Mol. Med.* 2006. V. 10. № 1. P. 76–99.
27. Yamakoshi S., Bai R., Chaen T., Ideta A., Aoyagi Y., Sakurai T., Konno T., Imakawa K. // *Reproduction*. 2012. V. 143. № 3. P. 377–387.
28. Uchida H., Maruyama T., Nishikawa-Uchida S., Oda H., Miyazaki K., Yamasaki A., Yoshimura Y. // *J. Biol. Chem.* 2012. V. 287. № 7. P. 4441–4450.
29. Saunders L.R., McClay D.R. // *Development*. 2014. V. 141. № 7. P. 1503–1513.
30. Carver E.A., Jiang R., Lan Y., Oram K.F., Gridley T. // *Mol. Cell. Biol.* 2001. V. 21. № 23. P. 8184–8188.
31. Lim J., Thiery J.P. // *Development*. 2012. V. 139. № 19. P. 3471–3486.
32. Duband J.L., Monier F., Delannet M., Newgreen D. // *Acta Anat. (Basel)*. 1995. V. 154. № 1. P. 63–78.
33. Duband J.L., Dady A., Fleury V. // *Curr. Top Dev. Biol.* 2015. V. 111. P. 27–67.
34. Poelmann R.E., Gittenberger-de Groot A.C., Mentink M.M., Delpech B., Girard N., Christ B. // *Anat. Embryol (Berl.)*. 1990. V. 182. № 1. P. 29–39.
35. Azhar M., Schultz J., Grupp I., Dorn G.W., 2nd., Meneton P., Molin D.G., Gittenberger-de Groot A.C., Doetschman T. // *Cytokine Growth Factor Rev.* 2003. V. 14. № 5. P. 391–407.
36. Hernandez L., Ryckebusch L., Wang C., Ling R., Yelon D. // *Dev. Dyn.* 2019. V. 248. № 12. P. 1195–1210.
37. Jalali A., Zhu X., Liu C., Nawshad A. // *Dev. Growth Differ.* 2012. V. 54. № 6. P. 633–648.
38. Volk S.W., Iqbal S.A., Bayat A. // *Adv. Wound Care (New Rochelle)*. 2013. V. 2. № 6. P. 261–272.
39. Yan C., Grimm W.A., Garner W.L., Qin L., Travis T., Tan N., Han Y.P. // *Am. J. Pathol.* 2010. V. 176. № 5. P. 2247–2258.
40. Hinz B., Gabbiani G. // *Thromb. Haemost.* 2003. V. 90. № 6. P. 993–1002.
41. Abe R., Donnelly S.C., Peng T., Bucala R., Metz C.N. // *J. Immunol.* 2001. V. 166. № 12. P. 7556–7562.
42. Higashiyama R., Nakao S., Shibusawa Y., Ishikawa O., Moro T., Mikami K., Fukumitsu H., Ueda Y., Minakawa K., Tabata Y., et al. // *J. Invest. Dermatol.* 2011. V. 131. № 2. P. 529–536.
43. Frid M.G., Kale V.A., Stenmark K.R. // *Circ. Res.* 2002. V. 90. № 11. P. 1189–1196.
44. Gabbiani G. // *J. Pathol.* 2003. V. 200. № 4. P. 500–503.
45. Border W.A., Noble N.A. // *N. Engl. J. Med.* 1994. V. 331. № 19. P. 1286–1292.
46. Hong K.M., Belperio J.A., Keane M.P., Burdick M.D., Strieter R.M. // *J. Biol. Chem.* 2007. V. 282. № 31. P. 22910–22920.
47. Barrientos S., Stojadinovic O., Golinko M.S., Brem H., Tomic-Canic M. // *Wound Repair Regen.* 2008. V. 16. № 5. P. 585–601.
48. Savagner P., Kusewitt D.F., Carver E.A., Magnino F., Choi C., Gridley T., Hudson L.G. // *J. Cell Physiol.* 2005. V. 202. № 3. P. 858–866.
49. Hanahan D., Weinberg R.A. // *Cell*. 2011. V. 144. № 5. P. 646–674.
50. Vincent-Salomon A., Thiery J.P. // *Breast Cancer Res.* 2003. V. 5. № 2. P. 101–106.
51. Brabletz T., Jung A., Reu S., Porzner M., Hlubek F., Kunz-Schughart L.A., Knuechel R., Kirchner T. // *Proc. Natl. Acad. Sci. USA*. 2001. V. 98. № 18. P. 10356–10361.
52. Milano A., Mazzetta F., Valente S., Ranieri D., Leone L., Botticelli A., Onesti C.E., Lauro S., Raffa S., Torrisi M.R., et al. // *Anal. Cell. Pathol. (Amst.)*. 2018. V. 2018. P. 3506874.
53. Giannoni E., Bianchini F., Masieri L., Serni S., Torre E., Calorini L., Chiarugi P. // *Cancer Res.* 2010. V. 70. № 17. P. 6945–6956.
54. Li Q.Q., Xu J.D., Wang W.J., Cao X.X., Chen Q., Tang F., Chen Z.Q., Liu X.P., Xu Z.D. // *Clin. Cancer Res.* 2009. V. 15. № 8. P. 2657–2665.
55. Kurrey N.K., Jalgaonkar S.P., Joglekar A.V., Ghanate A.D., Chaskar P.D., Doiphode R.Y., Bapat S.A. // *Stem Cells*. 2009. V. 27. № 9. P. 2059–2068.
56. Kudo-Saito C., Shirako H., Takeuchi T., Kawakami Y. // *Cancer Cell*. 2009. V. 15. № 3. P. 195–206.
57. Ansieau S., Bastid J., Doreau A., Morel A.P., Bouchet B.P., Thomas C., Fauvet F., Puisieux I., Doglioni C., Piccinin S., et al. // *Cancer Cell*. 2008. V. 14. № 1. P. 79–89.
58. Vega S., Morales A.V., Ocana O.H., Valdes F., Fabregat I., Nieto M.A. // *Genes Dev.* 2004. V. 18. № 10. P. 1131–1143.
59. Terry S., Savagner P., Ortiz-Cuaran S., Mahjoubi L., Saintigny P., Thiery J.P., Chouaib S. // *Mol. Oncol.* 2017. V. 11. № 7. P. 824–846.
60. Tarin D., Thompson E.W., Newgreen D.F. // *Cancer Res.* 2005. V. 65. № 14. P. 5996–6000.
61. Goossens S., Vandamme N., van Vlierberghe P., Berx G. // *Biochim. Biophys. Acta Rev. Cancer*. 2017. V. 1868. № 2. P. 584–591.
62. Wu W.S., You R.I., Cheng C.C., Lee M.C., Lin T.Y., Hu C.T. // *Sci. Rep.* 2017. V. 7. № 1. P. 17753.
63. Aghdassi A., Sender M., Guenther A., Mayerle J., Behn C.O., Heidecke C.D., Friess H., Buchler M., Evert M., Lerch M.M., et al. // *Gut*. 2012. V. 61. № 3. P. 439–448.
64. Krebs A.M., Mitschke J., Lasierra Losada M., Schmalhofer O., Boerries M., Busch H., Boettcher M., Mougiakakos D., Reichardt W., Bronsert P., et al. // *Nat. Cell Biol.* 2017. V. 19. № 5. P. 518–529.
65. Mody H.R., Hung S.W., Pathak R.K., Griffin J., Cruz-Monserate Z., Govindarajan R. // *Mol. Cancer Res.* 2017. V. 15. № 8. P. 1029–1039.

66. Rodgers J.J., McClure R., Epis M.R., Cohen R.J., Leedman P.J., Harvey J.M., Australian Prostate Cancer B., Thomas M.A., Bentel J.M. // *J. Cell Biochem.* 2019. V. 120. № 1. P. 848–860.
67. Sagredo A.I., Sagredo E.A., Pola V., Echeverria C., Andaur R., Michea L., Stutzin A., Simon F., Marcelain K., Armisen R. // *J. Cell. Physiol.* 2019. V. 234. № 3. P. 2037–2050.
68. Yin S., Cheryan V.T., Xu L., Rishi A.K., Reddy K.B. // *PLoS One.* 2017. V. 12. № 8. P. e0183578.
69. Chu S., Liu G., Xia P., Chen G., Shi F., Yi T., Zhou H. // *Oncol. Rep.* 2017. V. 38. № 4. P. 2401–2407.
70. Zou G., Ren B., Liu Y., Fu Y., Chen P., Li X., Luo S., He J., Gao G., Zeng Z., et al. // *Cancer Sci.* 2018. V. 109. № 11. P. 3416–3427.
71. Li H., Zhong A., Li S., Meng X., Wang X., Xu F., Lai M. // *Sci. Rep.* 2017. V. 7. № 1. P. 4915.
72. Wu Y., Zhou B.P. // *Br. J. Cancer.* 2010. V. 102. № 4. P. 639–644.
73. Wang D., Shi W., Tang Y., Liu Y., He K., Hu Y., Li J., Yang Y., Song J. // *Oncogene.* 2017. V. 36. № 7. P. 885–898.
74. Yang S., Liu Y., Li M.Y., Ng C.S.H., Yang S.L., Wang S., Zou C., Dong Y., Du J., Long X., et al. // *Mol. Cancer.* 2017. V. 16. № 1. P. 124.
75. Beck T.N., Korobeynikov V.A., Kudinov A.E., Georgopoulos R., Solanki N.R., Andrews-Hoke M., Kistner T.M., Pepin D., Donahoe P.K., Nicolas E., et al. // *Cell. Rep.* 2016. V. 16. № 3. P. 657–671.
76. Crusz S.M., Balkwill F.R. // *Nat. Rev. Clin. Oncol.* 2015. V. 12. № 10. P. 584–596.
77. Suarez-Carmona M., Lesage J., Cataldo D., Gilles C. // *Mol. Oncol.* 2017. V. 11. № 7. P. 805–823.
78. Daly C.S., Flemban A., Shafei M., Conway M.E., Qualtrough D., Dean S.J. // *Oncol. Rep.* 2018. V. 39. № 2. P. 483–490.
79. Xu F., Zhang J., Hu G., Liu L., Liang W. // *Cancer Cell Int.* 2017. V. 17. P. 54.
80. Joseph J.P., Harishankar M.K., Pillai A.A., Devi A. // *Oral Oncol.* 2018. V. 80. P. 23–32.
81. Zuo J., Wen J., Lei M., Wen M., Li S., Lv X., Luo Z., Wen G. // *Med. Oncol.* 2016. V. 33. № 2. P. 15.
82. Domogatskaya A., Rodin S., Tryggvason K. // *Annu. Rev. Cell. Dev. Biol.* 2012. V. 28. P. 523–553.
83. Horejs C.M., Serio A., Purvis A., Gormley A.J., Bertazzo S., Poliniewicz A., Wang A.J., DiMaggio P., Hohenester E., Stevens M.M. // *Proc. Natl. Acad. Sci. USA.* 2014. V. 111. № 16. P. 5908–5913.
84. Chen Q.K., Lee K., Radisky D.C., Nelson C.M. // *Differentiation.* 2013. V. 86. № 3. P. 126–132.
85. Horejs C.M., St-Pierre J.P., Ojala J.R.M., Steele J.A.M., da Silva P.B., Rynne-Vidal A., Maynard S.A., Hansel C.S., Rodriguez-Fernandez C., Mazo M.M., et al. // *Nat. Commun.* 2017. V. 8. № 1. P. 15509.
86. Qin Y., Rodin S., Simonson O.E., Hollande F. // *Semin. Cancer Biol.* 2017. V. 45. № 1. P. 3–12.
87. Carpenter P.M., Sivasdas P., Hua S.S., Xiao C., Gutierrez A.B., Ngo T., Gershon P.D. // *Cancer Med.* 2017. V. 6. № 1. P. 220–234.
88. Ishikawa T., Wondimu Z., Oikawa Y., Gentilcore G., Kiessling R., Egyhazi Brage S., Hansson J., Patarroyo M. // *Matrix Biol.* 2014. V. 38. P. 69–83.
89. Oikawa Y., Hansson J., Sasaki T., Rousselle P., Domogatskaya A., Rodin S., Tryggvason K., Patarroyo M. // *Exp. Cell. Res.* 2011. V. 317. № 8. P. 1119–1133.
90. Akhavan A., Griffith O.L., Soroceanu L., Leonoudakis D., Luciani-Torres M.G., Daemen A., Gray J.W., Muschler J.L. // *Cancer Res.* 2012. V. 72. № 10. P. 2578–2588.
91. Spaderna S., Schmalhofer O., Hlubek F., Bex G., Eger A., Merkel S., Jung A., Kirchner T., Brabletz T. // *Gastroenterology.* 2006. V. 131. № 3. P. 830–840.
92. Takkunen M., Ainola M., Vainionpaa N., Grenman R., Patarroyo M., Garcia de Herreros A., Konttinen Y.T., Virtanen I. // *Histochem. Cell. Biol.* 2008. V. 130. № 3. P. 509–525.
93. Pyke C., Romer J., Kallunki P., Lund L.R., Ralfkiaer E., Dano K., Tryggvason K. // *Am. J. Pathol.* 1994. V. 145. № 4. P. 782–791.
94. Koshikawa N., Moriyama K., Takamura H., Mizushima H., Nagashima Y., Yanoma S., Miyazaki K. // *Cancer Res.* 1999. V. 59. № 21. P. 5596–5601.
95. Giannelli G., Bergamini C., Fransvea E., Sgarra C., Antonaci S. // *Gastroenterology.* 2005. V. 129. № 5. P. 1375–1383.
96. Peng D.H., Ungewiss C., Tong P., Byers L.A., Wang J., Canales J.R., Villalobos P.A., Uraoka N., Mino B., Behrens C., et al. // *Oncogene.* 2017. V. 36. № 14. P. 1925–1938.
97. Brooks M., Mo Q., Krasnow R., Ho P.L., Lee Y.C., Xiao J., Kurtova A., Lerner S., Godoy G., Jian W., et al. // *Oncotarget.* 2016. V. 7. № 50. P. 82609–82619.
98. Ezzoukhy Z., Henriot E., Piquet L., Boye K., Bioulac-Sage P., Balabaud C., Couchy G., Zucman-Rossi J., Moreau V., Saltel F. // *Eur. J. Cell. Biol.* 2016. V. 95. № 11. P. 503–512.
99. Wei S.C., Fattet L., Tsai J.H., Guo Y., Pai V.H., Majeski H.E., Chen A.C., Sah R.L., Taylor S.S., Engler A.J., et al. // *Nat. Cell. Biol.* 2015. V. 17. № 5. P. 678–688.
100. Jung H.Y., Fattet L., Yang J. // *Clin. Cancer Res.* 2015. V. 21. № 5. P. 962–968.
101. Petrini I., Barachini S., Carnicelli V., Galimberti S., Modeo L., Boni R., Sollini M., Erba P.A. // *Oncotarget.* 2017. V. 8. № 3. P. 4914–4921.
102. Bieri D., Pierce S.E., Kroeger C., Stover D.G., Pattabiraman D.R., Thiru P., Liu Donaher J., Reinhardt F., Chaffer C.L., Keckesova Z., et al. // *Proc. Natl. Acad. Sci. USA.* 2017. V. 114. № 12. P. E2337–E2346.
103. Xu Y., Lee D.K., Feng Z., Xu Y., Bu W., Li Y., Liao L., Xu J. // *Proc. Natl. Acad. Sci. USA.* 2017. V. 114. № 43. P. 11494–11499.
104. Tan T.Z., Miow Q.H., Miki Y., Noda T., Mori S., Huang R.Y., Thiery J.P. // *EMBO Mol. Med.* 2014. V. 6. № 10. P. 1279–1293.
105. Puram S.V., Tirosh I., Parikh A.S., Patel A.P., Yizhak K., Gillespie S., Rodman C., Luo C.L., Mroz E.A., Emerick K.S., et al. // *Cell.* 2017. V. 171. № 7. P. 1611–1624 e24.
106. Tsai J.H., Donaher J.L., Murphy D.A., Chau S., Yang J. // *Cancer Cell.* 2012. V. 22. № 6. P. 725–736.
107. Aiello N.M., Maddipati R., Norgard R.J., Balli D., Li J., Yuan S., Yamazoe T., Black T., Sahmoud A., Furth E.E., et al. // *Dev. Cell.* 2018. V. 45. № 6. P. 681–695 e4.
108. Shamir E.R., Pappalardo E., Jorgens D.M., Coutinho K., Tsai W.T., Aziz K., Auer M., Tran P.T., Bader J.S., Ewald A.J. // *J. Cell. Biol.* 2014. V. 204. № 5. P. 839–856.
109. Cheung K.J., Gabrielson E., Werb Z., Ewald A.J. // *Cell.* 2013. V. 155. № 7. P. 1639–1651.
110. Cheung K.J., Padmanaban V., Silvestri V., Schipper K., Cohen J.D., Fairchild A.N., Gorin M.A., Verdone J.E., Pienta K.J., Bader J.S., et al. // *Proc. Natl. Acad. Sci. USA.* 2016. V. 113. № 7. P. E854–863.
111. Gloushankova N.A., Rubtsova S.N., Zhitnyak I.Y. // *Tissue Barriers.* 2017. V. 5. № 3. P. e1356900.
112. Reichert M., Bakir B., Moreira L., Pitarresi J.R., Feld-

- mann K., Simon L., Suzuki K., Maddipati R., Rhim A.D., Schlitter A.M., et al. // *Dev. Cell.* 2018. V. 45. № 6. P. 696–711 e8.
113. Fischer K.R., Durrans A., Lee S., Sheng J., Li F., Wong S.T., Choi H., El Rayes T., Ryu S., Troeger J., et al. // *Nature.* 2015. V. 527. № 7579. P. 472–476.
114. Zheng X., Carstens J.L., Kim J., Scheible M., Kaye J., Sugimoto H., Wu C.C., LeBleu V.S., Kalluri R. // *Nature.* 2015. V. 527. № 7579. P. 525–530.
115. Ye X., Brabletz T., Kang Y., Longmore G.D., Nieto M.A., Stanger B.Z., Yang J., Weinberg R.A. // *Nature.* 2017. V. 547. № 7661. P. E1–E3.
116. Tran H.D., Luitel K., Kim M., Zhang K., Longmore G.D., Tran D.D. // *Cancer Res.* 2014. V. 74. № 21. P. 6330–6340.
117. Ni T., Li X.Y., Lu N., An T., Liu Z.P., Fu R., Lv W.C., Zhang Y.W., Xu X.J., Grant Rowe R., et al. // *Nat. Cell Biol.* 2016. V. 18. № 11. P. 1221–1232.
118. Aiello N.M., Brabletz T., Kang Y., Nieto M.A., Weinberg R.A., Stanger B.Z. // *Nature.* 2017. V. 547. № 7661. P. E7–E8.
119. Yamashita N., Tokunaga E., Iimori M., Inoue Y., Tanaka K., Kitao H., Saeki H., Oki E., Maehara Y. // *Clin. Breast Cancer.* 2018. V. 18. № 5. P. e1003–e1009.
120. Savagner P. // *Curr. Top. Dev. Biol.* 2015. V. 112. P. 273–300.
121. Petrova Y.I., Schecterson L., Gumbiner B.M. // *Mol. Biol. Cell.* 2016. V. 27. № 21. P. 3233–3244.
122. Labernadie A., Kato T., Brugues A., Serra-Picamal X., Derzsi S., Arwert E., Weston A., Gonzalez-Tarrago V., Elosgui-Artola A., Albertazzi L., et al. // *Nat. Cell Biol.* 2017. V. 19. № 3. P. 224–237.
123. Cheung K.J., Ewald A.J. // *Science.* 2016. V. 352. № 6282. P. 167–169.
124. Yu M., Bardia A., Wittner B.S., Stott S.L., Smas M.E., Ting D.T., Isakoff S.J., Ciciliano J.C., Wells M.N., Shah A.M., et al. // *Science.* 2013. V. 339. № 6119. P. 580–584.
125. Ye X., Tam W.L., Shibue T., Kaygusuz Y., Reinhardt F., Ng Eaton E., Weinberg R.A. // *Nature.* 2015. V. 525. № 7568. P. 256–260.
126. Talmadge J.E., Fidler I.J. // *Cancer Res.* 2010. V. 70. № 14. P. 5649–5669.
127. Jolly M.K., Boareto M., Huang B., Jia D., Lu M., Ben-Jacob E., Onuchic J.N., Levine H. // *Front. Oncol.* 2015. V. 5. № 1. P. 155.
128. Au S.H., Storey B.D., Moore J.C., Tang Q., Chen Y.L., Javaid S., Sarioglu A.F., Sullivan R., Madden M.W., O’Keefe R., et al. // *Proc. Natl. Acad. Sci. USA.* 2016. V. 113. № 18. P. 4947–4952.
129. Kusters B., Kats G., Roodink I., Verrijp K., Wesseling P., Ruiter D.J., de Waal R.M., Leenders W.P. // *Oncogene.* 2007. V. 26. № 39. P. 5808–5815.
130. Aceto N., Bardia A., Miyamoto D.T., Donaldson M.C., Wittner B.S., Spencer J.A., Yu M., Pely A., Engstrom A., Zhu H., et al. // *Cell.* 2014. V. 158. № 5. P. 1110–1122.
131. McFadden D.G., Papagiannakopoulos T., Taylor-Weiner A., Stewart C., Carter S.L., Cibulskis K., Bhutkar A., McKenna A., Dooley A., Vernon A., et al. // *Cell.* 2014. V. 156. № 6. P. 1298–1311.
132. Gundem G., Van Loo P., Kremeyer B., Alexandrov L.B., Tubio J.M.C., Papaemmanuil E., Brewer D.S., Kallio H.M.L., Hognas G., Annala M., et al. // *Nature.* 2015. V. 520. № 7547. P. 353–357.
133. Lecharpentier A., Vielh P., Perez-Moreno P., Planchard D., Soria J.C., Farace F. // *Br. J. Cancer.* 2011. V. 105. № 9. P. 1338–1341.
134. Armstrong A.J., Marengo M.S., Oltean S., Kemeny G., Bitting R.L., Turnbull J.D., Herold C.I., Marcom P.K., George D.J., Garcia-Blanco M.A. // *Mol. Cancer Res.* 2011. V. 9. № 8. P. 997–1007.
135. Burz C., Pop V.V., Buiga R., Daniel S., Samasca G., Aldea C., Lupan I. // *Oncotarget.* 2018. V. 9. № 36. P. 24561–24571.
136. Hou J.M., Krebs M.G., Lancashire L., Sloane R., Backen A., Swain R.K., Priest L.J., Greystoke A., Zhou C., Morris K., et al. // *J. Clin. Oncol.* 2012. V. 30. № 5. P. 525–532.
137. Zhang D., Zhao L., Zhou P., Ma H., Huang F., Jin M., Dai X., Zheng X., Huang S., Zhang T. // *Cancer Cell Int.* 2017. V. 17. № 1. P. 6.
138. George J.T., Jolly M.K., Xu S., Somarelli J.A., Levine H. // *Cancer Res.* 2017. V. 77. № 22. P. 6415–6428.
139. Papadaki M.A., Stoupis G., Theodoropoulos P.A., Mavroudis D., Georgoulas V., Agelaki S. // *Mol. Cancer Ther.* 2019. V. 18. № 2. P. 437–447.
140. Hong K.O., Kim J.H., Hong J.S., Yoon H.J., Lee J.I., Hong S.P., Hong S.D. // *J. Exp. Clin. Cancer Res.* 2009. V. 28. № 1. P. 28.
141. Stankic M., Pavlovic S., Chin Y., Brogi E., Padua D., Norton L., Massague J., Benezra R. // *Cell. Rep.* 2013. V. 5. № 5. P. 1228–1242.
142. Chaffer C.L., Brennan J.P., Slavin J.L., Blick T., Thompson E.W., Williams E.D. // *Cancer Res.* 2006. V. 66. № 23. P. 11271–11278.
143. Patil S., Rao R.S., Ganavi B.S. // *J. Int. Oral Hlth.* 2015. V. 7. № 9. P. i-ii.
144. Hiramoto H., Muramatsu T., Ichikawa D., Tanimoto K., Yasukawa S., Otsuji E., Inazawa J. // *Sci. Rep.* 2017. V. 7. № 1. P. 4002.
145. Lv M., Zhong Z., Huang M., Tian Q., Jiang R., Chen J. // *Biochim. Biophys. Acta Mol. Cell. Res.* 2017. V. 1864. № 10. P. 1887–1899.
146. Shi Z.M., Wang L., Shen H., Jiang C.F., Ge X., Li D.M., Wen Y.Y., Sun H.R., Pan M.H., Li W., et al. // *Oncogene.* 2017. V. 36. № 18. P. 2577–2588.
147. Li Y., Zhang H., Li Y., Zhao C., Fan Y., Liu J., Li X., Liu H., Chen J. // *Mol. Carcinog.* 2018. V. 57. № 1. P. 125–136.
148. He Z., Yu L., Luo S., Li M., Li J., Li Q., Sun Y., Wang C. // *BMC Cancer.* 2017. V. 17. № 1. P. 140.
149. Hu H., Xu Z., Li C., Xu C., Lei Z., Zhang H.T., Zhao J. // *Lung Cancer.* 2016. V. 97. P. 87–94.
150. Xu D., Liu S., Zhang L., Song L. // *Biochem. Biophys. Res. Commun.* 2017. V. 485. № 2. P. 556–562.
151. Yu W.W., Jiang H., Zhang C.T., Peng Y. // *Oncotarget.* 2017. V. 8. № 24. P. 39280–39295.
152. Cheng C.W., Hsiao J.R., Fan C.C., Lo Y.K., Tzen C.Y., Wu L.W., Fang W.Y., Cheng A.J., Chen C.H., Chang I.S., et al. // *Mol. Carcinog.* 2016. V. 55. № 5. P. 499–513.
153. Yu M., Han G., Qi B., Wu X. // *Oncol. Rep.* 2017. V. 37. № 4. P. 2121–2128.
154. Yano T., Fujimoto E., Hagiwara H., Sato H., Yamasaki H., Negishi E., Ueno K. // *Biol. Pharm. Bull.* 2006. V. 29. № 10. P. 1991–1994.
155. Alaga K.C., Crawford M., Dagnino L., Laird D.W. // *J. Cancer.* 2017. V. 8. № 7. P. 1123–1128.
156. Frisch S.M., Farris J.C., Pifer P.M. // *Oncogene.* 2017. V. 36. № 44. P. 6067–6073.
157. Nishino H., Takano S., Yoshitomi H., Suzuki K., Kagawa S., Shimazaki R., Shimizu H., Furukawa K., Miyazaki M., Ohtsuka M. // *Cancer Med.* 2017. V. 6. № 11. P. 2686–2696.
158. Chen W., Kang K.L., Alshaiikh A., Varma S., Lin Y.L., Shin K.H., Kim R., Wang C.Y., Park N.H., Walentin K., et al. // *Oncogenesis.* 2018. V. 7. № 5. P. 38.
159. Riethdorf S., Frey S., Santjer S., Stoupiet M., Otto B.,

- Riethdorf L., Koop C., Wilczak W., Simon R., Sauter G., et al. // *Int. J. Cancer*. 2016. V. 138. № 4. P. 949–963.
160. Pan X., Zhang R., Xie C., Gan M., Yao S., Yao Y., Jin J., Han T., Huang Y., Gong Y., et al. // *Am. J. Transl. Res.* 2017. V. 9. № 9. P. 4217–4226.
161. Chen W., Yi J.K., Shimane T., Mehrazarin S., Lin Y.L., Shin K.H., Kim R.H., Park N.H., Kang M.K. // *Carcinogenesis*. 2016. V. 37. № 5. P. 500–510.
162. Werner S., Frey S., Riethdorf S., Schulze C., Alawi M., Kling L., Vafaizadeh V., Sauter G., Terracciano L., Schumacher U., et al. // *J. Biol. Chem.* 2013. V. 288. № 32. P. 2993–3008.
163. Mooney S.M., Talebian V., Jolly M.K., Jia D., Gromala M., Levine H., McConkey B.J. // *J. Cell. Biochem.* 2017. V. 118. № 9. P. 2559–2570.
164. Paltoglou S., Das R., Townley S.L., Hickey T.E., Tarulli G.A., Coutinho I., Fernandes R., Hanson A.R., Denis I., Carroll J.S., et al. // *Cancer Res.* 2017. V. 77. № 13. P. 3417–3430.
165. Xiang J., Fu X., Ran W., Wang Z. // *Oncogenesis*. 2017. V. 6. № 1. P. e284.
166. Pawlak M., Kikulska A., Wrzesinski T., Rausch T., Kwias Z., Wilczynski B., Benes V., Wesoly J., Wilanowski T. // *Mol. Carcinog.* 2017. V. 56. № 11. P. 2414–2423.
167. Li R., Liang J., Ni S., Zhou T., Qing X., Li H., He W., Chen J., Li F., Zhuang Q., et al. // *Cell Stem Cell*. 2010. V. 7. № 1. P. 51–63.
168. Samavarchi-Tehrani P., Golipour A., David L., Sung H.K., Beyer T.A., Datti A., Woltjen K., Nagy A., Wrana J.L. // *Cell Stem Cell*. 2010. V. 7. № 1. P. 64–77.
169. Zhang X., Cruz F.D., Terry M., Remotti F., Matushansky I. // *Oncogene*. 2013. V. 32. № 18. P. 2249–60, 2260 e1–2221.
170. Miyoshi N., Ishii H., Nagai K., Hoshino H., Mimori K., Tanaka F., Nagano H., Sekimoto M., Doki Y., Mori M. // *Proc. Natl. Acad. Sci. USA*. 2010. V. 107. № 1. P. 40–45.
171. Takaishi M., Tarutani M., Takeda J., Sano S. // *PLoS One*. 2016. V. 11. № 6. P. e0156904.
172. Chang C.C., Hsu W.H., Wang C.C., Chou C.H., Kuo M.Y., Lin B.R., Chen S.T., Tai S.K., Kuo M.L., Yang M.H. // *Cancer Res.* 2013. V. 73. № 13. P. 4147–4157.
173. Zhang C., Zhi W.I., Lu H., Samanta D., Chen I., Gabrielson E., Semenza G.L. // *Oncotarget*. 2016. V. 7. № 40. P. 64527–64542.
174. Zhang J.M., Wei K., Jiang M. // *Breast Cancer*. 2018. V. 25. № 4. P. 447–455.
175. Rasti A., Mehrazma M., Madjd Z., Abolhasani M., Saeednejad Zanjani L., Asgari M. // *Sci. Rep.* 2018. V. 8. № 1. P. 11739.
176. You L., Guo X., Huang Y. // *Yonsei Med. J.* 2018. V. 59. № 1. P. 35–42.
177. Chen S., Chen X., Li W., Shan T., Lin W.R., Ma J., Cui X., Yang W., Cao G., Li Y., et al. // *Oncol. Lett.* 2018. V. 15. № 5. P. 7144–7152.
178. Del Pozo Martin Y., Park D., Ramachandran A., Ombra-to L., Calvo F., Chakravarty P., Spencer-Dene B., Derzsi S., Hill C.S., Sahai E., et al. // *Cell Rep.* 2015. V. 13. № 11. P. 2456–2469.
179. Yates C.C., Shepard C.R., Stolz D.B., Wells A. // *Br. J. Cancer*. 2007. V. 96. № 8. P. 1246–1252.
180. Ju J.A., Godet I., Ye I.C., Byun J., Jayatilaka H., Lee S.J., Xiang L., Samanta D., Lee M.H., Wu P.H., et al. // *Mol. Cancer Res.* 2017. V. 15. № 6. P. 723–734.
181. Wu Z.H., Tao Z.H., Zhang J., Li T., Ni C., Xie J., Zhang J.F., Hu X.C. // *Tumour Biol.* 2016. V. 37. № 6. P. 7245–7254.
182. Yao Y., Pang T., Cheng Y., Yong W., Kang H., Zhao Y., Wang S., Hu X. // *Pathol. Oncol. Res.* 2019. V. 26. № 3. P. 1639–1649.
183. Liang H., Chen G., Li J., Yang F. // *Am. J. Transl. Res.* 2019. V. 11. № 7. P. 4277–4289.
184. Liang F., Ren C., Wang J., Wang S., Yang L., Han X., Chen Y., Tong G., Yang G. // *Oncogenesis*. 2019. V. 8. № 10. P. 59.
185. Chang L., Hu Y., Fu Y., Zhou T., You J., Du J., Zheng L., Cao J., Ying M., Dai X., et al. // *Acta Pharm. Sin. B*. 2019. V. 9. № 3. P. 484–495.
186. Wang P., Chen J., Mu L.H., Du Q.H., Niu X.H., Zhang M.Y. // *Eur. Rev. Med. Pharmacol. Sci.* 2013. V. 17. № 13. P. 1722–1729.
187. Haslehurst A.M., Koti M., Dharsee M., Nuin P., Evans K., Geraci J., Childs T., Chen J., Li J., Weberpals J., et al. // *BMC Cancer*. 2012. V. 12. P. 91.
188. Gupta N., Xu Z., El-Sehemy A., Steed H., Fu Y. // *Gynecol. Oncol.* 2013. V. 130. № 1. P. 200–206.
189. Oh S.J., Ahn E.J., Kim O., Kim D., Jung T.Y., Jung S., Lee J.H., Kim K.K., Kim H., Kim E.H., et al. // *Cell. Mol. Neurobiol.* 2019. V. 39. № 6. P. 769–782.
190. Shen C.J., Kuo Y.L., Chen C.C., Chen M.J., Cheng Y.M. // *PLoS One*. 2017. V. 12. № 3. P. e0174487.
191. Xiao G., Li Y., Wang M., Li X., Qin S., Sun X., Liang R., Zhang B., Du N., Xu C., et al. // *Cell Prolif.* 2018. V. 51. № 5. P. e12473.
192. Kast R.E., Skuli N., Karpel-Massler G., Frosina G., Ryken T., Halatsch M.E. // *Oncotarget*. 2017. V. 8. № 37. P. 60727–60749.
193. Evdokimova V., Tognon C., Ng T., Sorensen P.H. // *Cell Cycle*. 2009. V. 8. № 18. P. 2901–2906.
194. Chen K.Y., Chen C.C., Chang Y.C., Chang M.C. // *PLoS One*. 2019. V. 14. № 7. P. e0219317.
195. Weyemi U., Redon C.E., Choudhuri R., Aziz T., Maeda D., Boufraquech M., Parekh P.R., Sethi T.K., Kasoji M., Abrams N., et al. // *Nat. Commun.* 2016. V. 7. № 1. P. 10711.
196. Hsu D.S., Lan H.Y., Huang C.H., Tai S.K., Chang S.Y., Tsai T.L., Chang C.C., Tzeng C.H., Wu K.J., Kao J.Y., et al. // *Clin. Cancer Res.* 2010. V. 16. № 18. P. 4561–4571.
197. Chakraborty S., Kumar A., Faheem M.M., Katoch A., Kumar A., Jamwal V.L., Nayak D., Golani A., Rasool R.U., Ahmad S.M., et al. // *Cell Death Dis.* 2019. V. 10. № 6. P. 467.
198. Zhang P., Wei Y., Wang L., Debeb B.G., Yuan Y., Zhang J., Yuan J., Wang M., Chen D., Sun Y., et al. // *Nat. Cell. Biol.* 2014. V. 16. № 9. P. 864–875.
199. Song N., Jing W., Li C., Bai M., Cheng Y., Li H., Hou K., Li Y., Wang K., Li Z., et al. // *Cell Cycle*. 2018. V. 17. № 5. P. 595–604.
200. Qian J., Shen S., Chen W., Chen N. // *Biomed. Res. Int.* 2018. V. 2018. № 1. P. 4174232.
201. Meng Q., Shi S., Liang C., Liang D., Hua J., Zhang B., Xu J., Yu X. // *Oncogene*. 2018. V. 37. № 44. P. 5843–5857.
202. Kim T.W., Lee S.Y., Kim M., Cheon C., Jang B.H., Shin Y.C., Ko S.G. // *Cell Death Dis.* 2018. V. 9. № 6. P. 649.
203. Prabhakar C.N. // *Transl. Lung Cancer Res.* 2015. V. 4. № 2. P. 110–118.
204. Yochum Z.A., Cades J., Wang H., Chatterjee S., Simons B.W., O'Brien J.P., Khetarpal S.K., Lemtiri-Chlieh G., Myers K.V., Huang E.H., et al. // *Oncogene*. 2019. V. 38. № 5. P. 656–670.
205. Iderzorig T., Kellen J., Osude C., Singh S., Woodman J.A., Garcia C., Puri N. // *Biochem. Biophys. Res. Commun.* 2018. V. 496. № 2. P. 770–777.
206. Hu F.Y., Cao X.N., Xu Q.Z., Deng Y., Lai S.Y., Ma J., Hu J.B. // *J. Huazhong Univ. Sci. Technol. Med. Sci.* 2016. V. 36. № 6. P. 839–845.

207. Lee A.F., Chen M.C., Chen C.J., Yang C.J., Huang M.S., Liu Y.P. // *PLoS One*. 2017. V. 12. № 7. P. e0180383.
208. Du X., Shao Y., Qin H.F., Tai Y.H., Gao H.J. // *Thorac. Cancer*. 2018. V. 9. № 4. P. 423–430.
209. Voena C., Varesio L.M., Zhang L., Menotti M., Poggio T., Panizza E., Wang Q., Minero V.G., Fagoonee S., Compagno M., et al. // *Oncotarget*. 2016. V. 7. № 22. P. 33316–33330.
210. Nakamichi S., Seike M., Miyanaga A., Chiba M., Zou F., Takahashi A., Ishikawa A., Kunugi S., Noro R., Kubota K., et al. // *Oncotarget*. 2018. V. 9. № 43. P. 27242–27255.
211. Fukuda K., Takeuchi S., Arai S., Katayama R., Nanjo S., Tanimoto A., Nishiyama A., Nakagawa T., Taniguchi H., Suzuki T., et al. // *Cancer Res*. 2019. V. 79. № 7. P. 1658–1670.
212. Zhou L., Liu X.D., Sun M., Zhang X., German P., Bai S., Ding Z., Tannir N., Wood C.G., Matin S.F., et al. // *Oncogene*. 2016. V. 35. № 21. P. 2687–2697.
213. Wang Q., Gun M., Hong X.Y. // *Sci. Rep*. 2019. V. 9. № 1. P. 14140.
214. Dong H., Hu J., Zou K., Ye M., Chen Y., Wu C., Chen X., Han M. // *Mol. Cancer*. 2019. V. 18. № 1. P. 3.
215. Wu Y., Ginther C., Kim J., Mosher N., Chung S., Slammon D., Vadgama J.V. // *Mol. Cancer Res*. 2012. V. 10. № 12. P. 1597–1606.
216. Krummel M.F., Allison J.P. // *J. Exp. Med*. 1995. V. 182. № 2. P. 459–465.
217. Leach D.R., Krummel M.F., Allison J.P. // *Science*. 1996. V. 271. № 5256. P. 1734–1736.
218. Dong H., Strome S.E., Salomao D.R., Tamura H., Hirano F., Flies D.B., Roche P.C., Lu J., Zhu G., Tamada K., et al. // *Nat. Med*. 2002. V. 8. № 8. P. 793–800.
219. Iwai Y., Ishida M., Tanaka Y., Okazaki T., Honjo T., Minato N. // *Proc. Natl. Acad. Sci. USA*. 2002. V. 99. № 19. P. 12293–12297.
220. Iwai Y., Terawaki S., Honjo T. // *Int. Immunol*. 2005. V. 17. № 2. P. 133–144.
221. Hargadon K.M., Johnson C.E., Williams C.J. // *Int. Immunopharmacol*. 2018. V. 62. № 1. P. 29–39.
222. Raimondi C., Carpino G., Nicolazzo C., Gradilone A., Gianni W., Gelibter A., Gaudio E., Cortesi E., Gazzaniga P. // *Oncoimmunology*. 2017. V. 6. № 12. P. e1315488.
223. Thar Min A.K., Okayama H., Saito M., Ashizawa M., Aoto K., Nakajima T., Saito K., Hayase S., Sakamoto W., Tada T., et al. // *Cancer Med*. 2018. V. 7. № 7. P. 3321–3330.
224. Noman M.Z., Janji B., Abdou A., Hasmim M., Terry S., Tan T.Z., Mami-Chouaib F., Thierry J.P., Chouaib S. // *Oncoimmunology*. 2017. V. 6. № 1. P. e1263412.
225. Asgarova A., Asgarov K., Godet Y., Peixoto P., Nadaradjane A., Boyer-Guittaut M., Galaine J., Guenat D., Mougey V., Perrard J., et al. // *Oncoimmunology*. 2018. V. 7. № 5. P. e1423170.
226. Ock C.Y., Kim S., Keam B., Kim M., Kim T.M., Kim J.H., Jeon Y.K., Lee J.S., Kwon S.K., Hah J.H., et al. // *Oncotarget*. 2016. V. 7. № 13. P. 15901–15914.
227. Funaki S., Shintani Y., Kawamura T., Kanzaki R., Minami M., Okumura M. // *Oncol. Rep*. 2017. V. 38. № 4. P. 2277–2284.
228. Noman M.Z., van Moer K., Marani V., Gemmill R.M., Tranchevent L.C., Azuaje F., Muller A., Chouaib S., Thierry J.P., Berchem G., et al. // *Oncoimmunology*. 2018. V. 7. № 4. P. e1345415.
229. Chae Y.K., Chang S., Ko T., Anker J., Agte S., Iams W., Choi W.M., Lee K., Cruz M. // *Sci. Rep*. 2018. V. 8. № 1. P. 2918.
230. Lou Y., Diao L., Cuentas E.R., Denning W.L., Chen L., Fan Y.H., Byers L.A., Wang J., Papadimitrakopoulou V.A., Behrens C., et al. // *Clin. Cancer Res*. 2016. V. 22. № 14. P. 3630–3642.
231. Wang L., Saci A., Szabo P.M., Chasalow S.D., Castillo-Martin M., Domingo-Domenech J., Siefker-Radtke A., Sharma P., Sfakianos J.P., Gong Y., et al. // *Nat. Commun*. 2018. V. 9. № 1. P. 3503.
232. Makena M.R., Ranjan A., Thirumala V., Reddy A.P. // *Biochim. Biophys. Acta Mol. Basis Dis*. 2018. V. 1866. № 4. P. 165339.
233. Cojoc M., Mabert K., Muders M.H., Dubrovskaya A. // *Semin. Cancer Biol*. 2015. V. 31. № 1. P. 16–27.
234. Phi L.T.H., Sari I.N., Yang Y.G., Lee S.H., Jun N., Kim K.S., Lee Y.K., Kwon H.Y. // *Stem Cells Int*. 2018. V. 2018. № 1. P. 5416923.
235. Li S., Li Q. // *Int. J. Oncol*. 2014. V. 44. № 6. P. 1806–1812.
236. Prasetyanti P.R., Medema J.P. // *Mol. Cancer*. 2017. V. 16. № 1. P. 41.
237. Zhou P., Li B., Liu F., Zhang M., Wang Q., Liu Y., Yao Y., Li D. // *Mol. Cancer*. 2017. V. 16. № 1. P. 52.
238. Hope K.J., Jin L., Dick J.E. // *Nat. Immunol*. 2004. V. 5. № 7. P. 738–743.
239. Takahashi K., Tanabe K., Ohnuki M., Narita M., Ichisaka T., Tomoda K., Yamanaka S. // *Cell*. 2007. V. 131. № 5. P. 861–872.
240. Nouri M., Caradec J., Lubik A.A., Li N., Hollier B.G., Takhar M., Altimirano-Dimas M., Chen M., Roshan-Moniri M., Butler M., et al. // *Oncotarget*. 2017. V. 8. № 12. P. 18949–18967.
241. Mani S.A., Guo W., Liao M.J., Eaton E.N., Ayyanan A., Zhou A.Y., Brooks M., Reinhard F., Zhang C.C., Shipitsin M., et al. // *Cell*. 2008. V. 133. № 4. P. 704–715.
242. Morel A.P., Lievre M., Thomas C., Hinkal G., Ansieau S., Puisieux A. // *PLoS One*. 2008. V. 3. № 8. P. e2888.
243. Junk D.J., Bryson B.L., Smigiel J.M., Parameswaran N., Bartel C.A., Jackson M.W. // *Oncogene*. 2017. V. 36. № 28. P. 4001–4013.
244. Smigiel J.M., Parameswaran N., Jackson M.W. // *Mol. Cancer Res*. 2017. V. 15. № 4. P. 478–488.
245. Ruan D., He J., Li C.F., Lee H.J., Liu J., Lin H.K., Chan C.H. // *Oncogene*. 2017. V. 36. № 30. P. 4299–4310.
246. Lee Y., Shin J.H., Longmire M., Wang H., Kohrt H.E., Chang H.Y., Sunwoo J.B. // *Clin. Cancer Res*. 2016. V. 22. № 14. P. 3571–3581.
247. Peitzsch C., Nathansen J., Schniewind S.I., Schwarz F., Dubrovskaya A. // *Cancers (Basel)*. 2019. V. 11. № 5. P. 616.
248. Yoon C., Cho S.J., Chang K.K., Park D.J., Ryeom S.W., Yoon S.S. // *Mol. Cancer Res*. 2017. V. 15. № 8. P. 1106–1116.
249. Ma X., Wang B., Wang X., Luo Y., Fan W. // *PLoS One*. 2018. V. 13. № 4. P. e0192436.
250. Wei C.Y., Zhu M.X., Yang Y.W., Zhang P.F., Yang X., Peng R., Gao C., Lu J.C., Wang L., Deng X.Y., et al. // *J. Hematol. Oncol*. 2019. V. 12. № 1. P. 21.
251. Lin J.C., Tsai J.T., Chao T.Y., Ma H.I., Liu W.H. // *Cancers (Basel)*. 2018. V. 10. № 12. P. 512.
252. Li N., Babaei-Jadidi R., Lorenzi F., Spencer-Dene B., Clarke P., Domingo E., Tulchinsky E., Vries R.G.J., Kerr D., Pan Y., et al. // *Oncogenesis*. 2019. V. 8. № 3. P. 13.
253. Tsoumas D., Nikou S., Giannopoulou E., Champeris Tsaniras S., Sirinian C., Maroulis I., Taraviras S., Zolota V., Kalofonos H.P., Bravou V. // *Cancer Genomics Proteomics*. 2018. V. 15. № 2. P. 127–141.
254. Melisi D., Garcia-Carbonero R., Macarulla T., Pezet D., Deplanque G., Fuchs M., Trojan J., Kozloff M., Simionato F., Cleverly A., et al. // *Cancer Chemother. Pharmacol*. 2019. V. 83. № 5. P. 975–991.

REVIEWS

255. Santini V., Valcarcel D., Platzbecker U., Komrokji R.S., Cleverly A.L., Lahn M.M., Janssen J., Zhao Y., Chiang A., Giagounidis A., et al. // *Clin. Cancer Res.* 2019. V. 25. № 23. P. 6976–6985.
256. Sato M., Kadota M., Tang B., Yang H.H., Yang Y.A., Shan M., Weng J., Welsh M.A., Flanders K.C., Nagano Y., et al. // *Breast Cancer Res.* 2014. V. 16. № 3. P. R57.
257. Formenti S.C., Hawtin R.E., Dixit N., Evensen E., Lee P., Goldberg J.D., Li X., Vanpouille-Box C., Schae D., McBride W.H., et al. // *J. Immunother. Cancer.* 2019. V. 7. № 1. P. 177.
258. Yochum Z.A., Cades J., Mazzacurati L., Neumann N.M., Khetarpal S.K., Chatterjee S., Wang H., Attar M.A., Huang E.H., Chatley S.N., et al. // *Mol. Cancer Res.* 2017. V. 15. № 12. P. 1764–1776.

Supramolecular Organization As a Factor of Ribonuclease Cytotoxicity

E. V. Dudkina*, V. V. Ulyanova, O. N. Ilinskaya

Institute of Fundamental Medicine and Biology, Kazan (Volga Region) Federal University, Kazan, 420008 Russia

*Email: lenatimonina@rambler.ru

Received May 11, 2020; in final form June 29, 2020

DOI: 10.32607/actanaturae.11000

Copyright © 2020 National Research University Higher School of Economics. This is an open access article distributed under the Creative Commons Attribution License, which permits unrestricted use, distribution, and reproduction in any medium, provided the original work is properly cited.

ABSTRACT One of the approaches used to eliminate tumor cells is directed destruction/modification of their RNA molecules. In this regard, ribonucleases (RNases) possess a therapeutic potential that remains largely unexplored. It is believed that the biological effects of secreted RNases, namely their antitumor and antiviral properties, derive from their catalytic activity. However, a number of recent studies have challenged the notion that the activity of RNases in the manifestation of selective cytotoxicity towards cancer cells is exclusively an enzymatic one. In this review, we have analyzed available data on the cytotoxic effects of secreted RNases, which are not associated with their catalytic activity, and we have provided evidence that the most important factor in the selective apoptosis-inducing action of RNases is the structural organization of these enzymes, which determines how they interact with cell components. The new idea on the preponderant role of non-catalytic interactions between RNases and cancer cells in the manifestation of selective cytotoxicity will contribute to the development of antitumor RNase-based drugs.

KEYWORDS ribonuclease, dimer, oligomerization, catalytic activity, cytotoxicity, antitumor activity.

ABBREVIATIONS dsRNA – double-stranded RNA; RI – mammalian ribonuclease inhibitor; BS-RNase – bovine seminal ribonuclease.

INTRODUCTION

Ribonucleases (RNases) catalyze the cleavage of phosphodiester bonds in various RNA substrates, playing a key role in the degradation and processing of cellular RNA [1]. Most of the known RNases are proteins; however, atypical RNase forms have also been encountered, the catalytic part of which is represented by an RNA molecule. Therefore, RNases are some of the few enzymes that have apparently retained a connection with the initial world of RNAs, an ancient system of RNA replicators and catalysts [1].

RNases are classified into exo- and endoribonucleases. Exoribonucleases catalyze the 3' → 5' hydrolysis of the phosphodiester bond situated between nucleotides located at the polynucleotide chain ends. Endoribonucleases cleave phosphodiester bonds within single-stranded or double-stranded RNAs.

The cells of living organisms contain various types of exo- and endoribonucleases, the main function of which is to control gene expression via changing the stability of various RNA types and eliminating unnecessary intracellular RNAs [2]. In addition, by cleaving foreign RNAs that have penetrated the cell [3] and participating in cellular suicide, RNases play a protective role [4].

Secreted RNases of microorganisms perform digestive, protective, and regulatory functions. They are required for RNA hydrolysis in the extracellular space. The cleavage of extracellular RNA in microorganisms is believed to occur mainly for extracting nutrients. Only a few reports have indicated involvement of the secreted RNases of microorganisms in the competition for an ecological niche [5], implementation of the pathogenic potential [6–8], and defense of their population and associated organisms from viral infection [9, 10].

In higher organisms, secreted RNases, on the contrary, are less involved in food digestion and are components of the innate system for defense and physiological homeostasis maintenance. In plants, they determine self-incompatibility [11]. In vertebrates, secreted RNases hydrolyze the extracellular RNA released from damaged, stress-induced, or malignant cells, thereby exerting anti-inflammatory and anti-coagulant effects, and possessing antimicrobial and antiviral activities, as well as immunomodulatory and regenerative properties [12].

Certain types of secreted RNases in animals are involved in tumorigenesis [13], while others suppress the proliferation of cancer cells and induce apoptosis in them [14–19], which makes RNases potential antitumor agents in the sparing therapy of malignant neoplasms. Selective cytotoxicity towards tumor cells is also exhibited by the microbial RNases [18–22] that are insensitive to the mammalian RNase inhibitor (RI), which opens up wide perspectives for bioengineering [23]. RNases can be internalized by cells via receptor-dependent endocytosis in order to regulate signaling pathways and intracellular RNAs [13]. In this case, the ribonucleolytic activity is not always of primary significance; probably, the key role is played by the physicochemical and structural properties of these proteins.

SECRETED RIBONUCLEASES OF BACILLI

Among the extracellular bacterial RNases exhibiting antitumor activity, secreted RNases of bacilli have been described in detail [19, 20, 22, 24, 25]. Bacillary RNases are represented by two types of endonucleolytic enzymes: low-molecular-weight guanyl-preferring RNases [24] and high-molecular-weight nonspecific RNases [26, 27]. High-molecular-weight bacillary RNases (binase II, RNase Bsn), members of the HNH endonuclease family (IPR003615), consist of about 240 amino acid residues (30 kDa). These proteins are stable in a pH range of 6.5–9.5, have an isoelectric point of about 5, and non-specifically cleave RNA to form 5'-phosphorylated oligonucleotides. For catalytic activity, they require Mg^{2+} ions. For RNA hydrolysis, the optimum pH is 8.5 and the optimum temperature is 37°C.

Low-molecular-weight guanyl-preferring bacillary RNases (binase, barnase), who are members of the N1/T1/U2 family (IPR000026), are small extracellular proteins consisting of approximately 110 amino acid residues (12 kDa). The enzymes are stable over a wide pH range (3–10). Guanyl-specific RNases are cationic proteins with an isoelectric point of about 9. They catalyze the cleavage of RNA, preferably at guanosine residues, in two successive reactions during

which transesterification of the 5'-phosphoether bond leads to the formation of cyclic 2', 3'-phosphodiester as intermediate hydrolysis products, which are subsequently cleaved to nucleoside 3'-phosphates [28]. For catalytic activity, these enzymes do not require metal ions or cofactors [29]. The optimal conditions for RNA hydrolysis are pH 8.5 and a temperature of 37°C.

The synthesis of extracellular RNases in bacilli is induced, with rare exceptions, under phosphate starvation conditions [30, 31], while that of low-molecular-weight RNases is also induced under nitrogen starvation conditions [32], which indicates how significant these enzymes are in providing cells with nutrients. It should be noted that the RNase activity level of low-molecular-weight RNases is 1–2 orders of magnitude higher than that of high-molecular-weight RNases. Low-molecular-weight RNases also have the specific features of the ribonucleolytic reaction mechanism: preference for guanyl residues, formation of the cyclic 2', 3'-ribonucleotides present in the reaction medium for at least 1 h [33], and a phosphate group at the 3' end of the formed nucleotides. Currently, 2', 3'-cycloderivatives of the nucleotides found in both pro- and eukaryotes are considered in eukaryotes as components of the pathway that protects tissues from infection and damage [34]. Nucleotides with a 5'-terminal phosphate can be ligated to similar nucleotides to form polymeric structures, while insertion of a nucleotide with a 3'-terminal phosphate requires additional reactions to transfer the phosphate group to the 5'-end. These features, along with the fact that high-molecular-weight RNases abound in the bacterial world, and that low-molecular-weight RNases are present only in a limited number of bacterial species [35], make low-molecular-weight RNases of bacilli unique proteins and suggest that they have special functions and biological properties.

For example, there is evidence that indirectly indicates the antagonistic properties of low-molecular-weight RNases [5, 24] and their involvement in the protection of bacterial cells from phage infection [9]. In pathogenic bacilli from the *Bacillus cereus* group, low-molecular-weight RNases are involved in surface toxins [35]. To date, various biological effects, from growth-stimulating to antiproliferative, of the low-molecular-weight RNases of bacilli have been demonstrated [19, 20, 22, 36, 37], which makes them promising for practical use. The potential of the high-molecular-weight RNases of bacilli has not yet been explored.

The low-molecular-weight RNases of bacilli have a high degree of primary structure similarity (more than 73%); the main differences occur in the regulatory regions of the genes, which results in different

production levels of these proteins, as well as in signal peptides that affect their secretion [35]. The enzymes have an almost identical tertiary structure and possess general physicochemical and catalytic properties. The amino acid residues His and Glu in the enzyme active site act as common acid-base groups during catalysis, and the Arg and Lys residues are important for phosphate binding.

The first studies on the isolation and purification of low-molecular-weight RNases were conducted in the 70s: *B. amyloliquefaciens* RNase (barnase) and *B. pumilus* RNase 7P (binase) were isolated and characterized [38, 39]. We have improved a method for the isolation of bacillary RNases which enables preparation of a homogeneous protein in three stages. This method was used to isolate, chromatographically purify, and characterize guanyl-preferring RNases from *B. pumilus* 7P (binase), *B. altitudinis* B-388 (balnase), and *B. licheniformis* (balifase) [30, 40, 41]. Among the presented species, the most active RNase producer is *B. pumilus* secreting binase. For a long time, *B. amyloliquefaciens* ribonuclease (barnase) was believed to be a close homologue of binase. The similarity of the primary structures of binase and barnase is 85%; however, the synthesis of barnase is not subject to phosphate regulation but depends on the multifunctional protein Spo0A [24].

Investigation of a new RNase, balnase, secreted by the *B. altitudinis* B-388 strain has demonstrated that it is the closest natural homologue of binase. The primary structures of the proteins differ only in one amino acid substitution: threonine at position 106 in the binase molecule is replaced by alanine in balnase [29], which does not affect the isoelectric point of the protein but somewhat reduces its thermal stability [29, 42].

The *B. licheniformis* RNase balifase has a primary structure similar to that of binase (73%) and barnase (74%). Balifase synthesis is induced under phosphate starvation conditions, which brings the enzyme closer to binase and balnase, but the physico-chemical properties of balifase are closer to those of barnase [41].

Despite the fact that secreted RNases of bacilli are similar in their physico-chemical and catalytic properties, they differ in their dimerization mode and stability of dimeric forms, which affects the cytotoxic properties of these RNases.

RNase oligomerization

Oligomerization is one of the most common phenomena, and a key factor, in the regulation of enzymes, ion channels, receptors, and transcription factors. Dimers and oligomers ensure the stability of proteins, activate signal transduction across the membrane, enhance enzymatic activity, and expand the possibilities for reg-

ulation, providing combinatorial specificity, allosteric properties, activation, and inhibition of the catalytic activity of enzymes [43].

Investigation of the structural organization of the RNases isolated by us – binase, balnase, and balifase – has revealed that all of them dimerize *in vivo* and are natural dimers [41, 44, 45]. Probably, the formation of RNase dimers is one of the key processes necessary for the enzymes to perform their functions and manifest their biological properties. Despite their high degree of structural similarity, the dimerization mode and stability of dimeric structures in homologous RNases are very different [22].

We have identified, for the first time, the natural dimeric structures of binase that had been known for a long time as a monomer incapable of oligomerization [44]. Previously, binase dimers had been found only in a protein crystal [46]. The theoretical possibility of enzyme dimerization in solution was considered an artifact that can occur only at a high protein concentration [47]. We have shown that binase *in vivo* occurs in two dimeric forms differing in their mechanism of formation and stability. Some binase dimers are highly stable, apparently due to the exchange of N- or C-terminal regions, and do not dissociate under denaturing conditions; others are incapable of exchanging domains between monomers (swapping interactions), which leads to the dissociation of these dimers into monomers during electrophoresis under denaturing conditions [44]. Balnase and balifase constitute only the second type of dimers [22, 41, 45].

Molecular modeling of the dimeric structures of binase, balnase, and balifase revealed a variety of dimers (*Figure*). It should be noted that bacillary RNase dimers are stabilized by non-covalent bonds, because the primary protein structures lack sulfur-containing amino acids [48]. Given the forces involved in the protein complex formation (electrostatic, hydrophobic, van der Waals, electrostatic, or their balance), two models in each group were selected (*Figure*). It is noted that binase is able to form four dimer types (*Fig. A*), while balnase (*Fig. B*) and balifase (*Fig. C*) form three and two types, respectively, with one of the types being a variant with a blocked enzyme active site.

An analysis of the mechanisms of bacillary RNase dimerization raises the question of active site accessibility for substrate hydrolysis in dimer molecules. The investigation of a binase crystal revealed that the RNA in the dimer is bound to only one of the two monomer molecules, because the catalytic site of the second subunit is blocked in the dimeric structure [21]. Mutant binase Glu43Ala/Phe81Ala has a higher catalytic activity and more pronounced cytotoxic properties towards Kasumi-1 leukemia cells compared to those

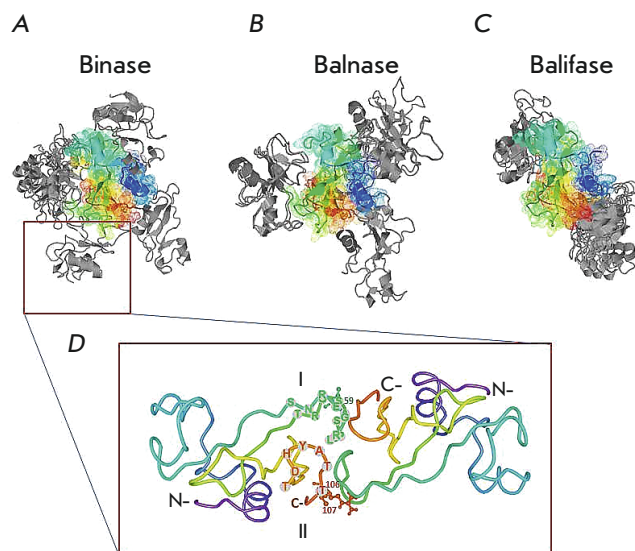


Figure. Models of bacillary RNase dimers. Modeling of the protein-protein interaction of RNase monomers was performed by the direct method through a search for structures with minimum Gibbs free energy. The models are classified into groups, based on the forces involved in the protein complex formation (electrostatic, van der Waals and electrostatic, hydrophobic, or their balance); two structures with the lowest free energy are selected from each group. One of the monomers of binase (A), balnase (B), or balifase (C) is presented as a molecule with secondary structure elements shown in rainbow colors, from the N-terminus (blue) to the C-terminus (red). The potential positions of the second monomer in RNase dimers are shown in gray. (D) The unique binase dimer that is absent in balnase and balifase. The contact surface in the dimer is formed by two flexible loops I (amino acid residues 56–69) and II (amino acid residues 99–104) [57] which enable the monomers to exchange C-terminal regions

of the wild-type enzyme, which is associated with the inability of the mutant to form self-inhibiting dimeric structures [49].

A Brownian dynamics simulation demonstrated that binase forms three dimer types, depending on the active site accessibility [50]. Dimeric structures of the first-type have two open catalytic sites that are involved in RNA hydrolysis. In dimers of the second and third types, one or both active sites are blocked. An analysis of the monomer association rate during binase dimerization showed that the rate constant of the first type dimer formation is much higher than that in models of the second and third types, and its value is comparable to the rate of binase and barstar inhibitor complex formation [50]. Given the similar levels of catalytic activity of binase, balnase, and balifase, as well as the results of the analysis of the protein emission band intensity and the area of hydrolysis zones, we can state that both active sites in the dimer molecules of the studied RNases are involved in catalysis [22] and that dimers with partial or completely closed active sites appear to be minor.

It should be noted that most of the dimers found in nature form through non-covalent bonds between

extracellular domains, transmembrane regions, and/or N, the C-termini of proteins [51]. The last mechanism can occur in two ways. The first is contact dimerization, when the loop of one of the monomers forms stabilizing contacts with another molecule; the second is terminal domain exchange or domain swapping [51]. Domain exchange is typical of proteins such as cytochrome c [52] and, in particular, some amyloidogenic proteins, such as human prion protein, cystatin C, or β_2 -microglobulin [53, 54].

The phenomenon of domain exchange partially contradicts Anfinsen's dogma that the amino acid sequence determines the unique protein tertiary structure [55]. In fact, flexible loops of the protein can occur in variable conformations, occupying more than one available energy minimum [56]. This enables domains connected to flexible protein regions to occur in different orientations and to interchange with an equivalent domain of the neighbor subunit. Therefore, the presence of more than one flexible loop enables the formation of non-covalent dimers or larger oligomers, which gives enzymes new opportunities for allosteric interactions and macromolecular signaling [57, 58]. In binase, two flexible loops are located around

the active site; the first loop is formed by the amino acid residues 56–69, and the second is formed by the amino acid residues 99–104 [59]. Both loops occur in close proximity in a binase dimer variant that is absent in other RNases (*Fig. D*). It is stabilized by Phe105, Thr106, Arg107, Glu59, and Gly60. Thr106 is the only amino acid residue changed in the balnase molecule in comparison with binase. Replacement of polar threonine with hydrophobic alanine affects the stability of balnase [22, 29, 42]. There may be an exchange of C-terminal regions during the formation of a stable binase dimer. The lack of such a mechanism in balnase and balifase leads not only to significant differences in the ways of their dimerization compared to binase, but also to a decrease in the stability of the dimers and the antitumor potential of homologous RNases [22].

To date, several RNases have been identified. Their functionality depends on the structural organization of their molecules. For example, the antiviral potential of RNase L and monocyte chemoattractant protein-1-induced protein 1 (MCP1P1) is initiated by the formation of dimeric structures [60, 61]. Among animal RNases, bovine seminal RNase (BS-RNase), which is a natural dimer, is the most fully characterized [62]. There is a correlation between the efficiency of catalysis and dimerization of microbial RNase T from *Escherichia coli* [63]. *B. subtilis* RNase J functions in a cell as a dimer or higher-order oligomer [64].

For a long time, among the diversity of RNases, only one natural dimer capable of domain exchange had been known—BS-RNase, a mixture of two dimer types [65]. Some dimeric structures form through the covalent disulfide bridges that exist between the amino acid residues Cys31 and Cys32; dimers of the second type are additionally stabilized thanks to the interchange of the N-terminal α -helices of the enzyme [66]. Only second-type dimers appear to exhibit antitumor activity. The possibility of domain exchange leads to the formation of highly stable dimeric structures that are not destroyed during the penetration of the enzyme into the cell and remain insensitive to the action of RI, exhibiting their cytotoxicity via the hydrolysis of intracellular RNA [65].

Another RNase whose dimer is capable of domain swapping is pancreatic RNase A [67]. The enzyme is able to self-associate non-covalently upon interaction with a substrate as well as oligomerize upon lyophilization in 40% acetic acid [68, 69]. Dimers and higher-order oligomers form through an exchange of the domains involving the N- and/or C-termini of the protein [70]. Swapping oligomers of RNase A increase their enzymatic activity towards double-stranded RNA (dsRNA) or DNA:RNA hybrids compared to that of the native monomer [71]. The increase in the

catalytic activity is directly proportional to the size of the oligomer; furthermore, species containing more C-swapping oligomeric structures than N-swapping ones exhibit the highest enzymatic activity because of the higher basicity of the C-oligomer charge [72]. Contradictory results were obtained in a study of the antitumor potential of RNase A oligomers, which requires further research.

Onconase, RNase of the leopard frog *Rana pipiens*, is also capable of swapping dimerization. The enzyme forms dimeric structures through the exchange of N-terminal fragments during lyophilization in 40% acetic acid [73]. In this case, the C-terminus of the enzyme is unable to proceed with the exchange because it is blocked by the disulfide bond between Cys87 and Cys104 [58]. Dimerization of onconase enhances its biological activity, as in other RNases [17, 74, 75]. For example, the onconase dimer was found to be more cytotoxic for pancreatic cancer cells than the native monomer [73]. Enhancing of cytotoxicity during dimerization is associated with an increase in the basicity of the onconase molecule, which enhances the enzyme's affinity to the negatively charged membranes of cancer cells and/or their intracellular targets [75, 76].

RNase oligomerization protects from RI and increases the molecular charge, improving the internalization of the enzyme into tumor cells; it increases the enzymatic activity of RNases and their affinity to dsRNA [62, 70]; and it provides RNases with new biological properties [65, 70] or enhances existing ones. Therefore, the ability of RNases to form oligomeric structures by means of the domain-swapping mechanism is central to their cytotoxicity.

Antitumor RNase activity

RNases exhibit selective cytotoxicity towards certain cancer cells without significantly affecting the normal cells of the body, which makes these enzymes a potential alternative to modern anticancer drugs [20, 24, 25].

The most prominent bacterial RNase, binase, exerts an antiviral effect on influenza A (H1N1), rabies, the foot and mouth disease, and several plant viruses [77]. Binase exhibits selective cytotoxicity towards tumor cells expressing certain oncogenes: *ras*, *KIT*, *AML/ETO*, *FLT3*, *E6*, and *E7* [18, 19, 21]. Despite the active investigation of RNase selectivity, the mechanism of RNase selective action still remains unclear.

The biological effects of RNases are mediated by the molecular determinants that contribute to the apoptosis-inducing effect of enzymes, which include catalytic activity, the structure and charge of the molecule, and its stability [25]. However, little attention has been paid to the contribution of supramolecular organization to RNase cytotoxicity.

For a long time, the decisive role in RNase cytotoxicity was believed to be played by their enzymatic activity [78]. However, there is increasing evidence that enzymes lacking catalytic activity are also able to induce the death of tumor cells. Mutant forms of α -sarcin and the human eosinophil cationic protein, which are incapable of RNA hydrolysis, have been shown to retain their toxicity and trigger apoptosis in cancer cells [79, 80]. The antitumor activity of the human eosinophil cationic protein is due to its interaction with the surface structures of the cell, which changes the permeability of the plasma membrane and disrupts the ionic equilibrium without internalization of the enzyme or hydrolysis of intracellular RNA [81]. RNase A and its homologues were found to be capable of binding to dsRNAs without exhibiting catalytic activity, probably affecting the regulatory functions of these molecules [20]. The high affinity of RNase A for dsRNA is due to the positively charged amino acids located near the active site [82]. Bacterial RNase III contains two separate domains, one of which binds to dsRNA, and the other deconstructs dsRNA [83]. According to the data presented, the enzyme regulates gene expression either by cleaving dsRNA or by binding to it, which leads to functional changes in the dsRNA molecule [83].

Although treatment of cells with binase leads to a decrease in the intracellular RNA level, this process is not directly associated with the induction of apoptosis [84]. A decrease in the amount of total RNA is accompanied by an increase in the expression of the pro-apoptotic genes *p53* and *hSK4* 1.5- and 4.3-fold, respectively, while the mRNA level of the anti-apoptotic gene *bcl-2* decreases 2-fold. Probably, hydrolysis of RNA substrates by binase triggers a cascade of reactions that regulate the genes that control apoptosis [84]. Also, there is no direct correlation between a decrease in the RNA level and the toxic effect of RNases. For example, in Kasumi-1 acute myeloid leukemia cells, which are extremely sensitive to binase, the total RNA level did not change even when the viability was decreased by 95% [85]. Onconase induces the apoptosis of mitogen-stimulated lymphocytes without affecting the level of intracellular RNA [86].

Today, the primary interaction between RNases and surface cell structures is considered one of the most significant processes that play an important role in the triggering of a cascade of reactions leading to the death of tumor cells. Internalization of RNases occurs either through specific interaction with cell receptors [87] or through their direct interaction with the cell membrane [76]. RNases interact with the target cell surface through the involvement of membrane lipids, ion channels, and receptors, as well as through non-

specific electrostatic binding [88]. Native and mutant dimeric RNases were shown to strongly affect aggregation, fluidity, and the fusion of cell membranes [75]. RNase A and its analogue, human pancreatic ribonuclease (RNase 1), were found to specifically interact with neutral hexasaccharide glycosphingolipid Globo H [88] located on the outer side of the epithelial cell membrane and present in large amounts in some tumor cells [89]. Onconase and BS-RNase interact with specific non-protein receptor-like molecules on the plasma membrane, which is not typical of other RNases [90].

One of the mechanisms underlying the selective cytotoxicity of binase and other cationic RNases is the ability of RNases to interact with the anionic groups on the surface of cancer cells [25]. Tumor cells are known to be more electronegative than normal cells due to a high content of acidic phospholipids [91]. Enzyme dimerization leads to an increase in the cationicity of the protein and, therefore, to the enhancement of their antitumor properties. For example, replacement of negatively charged amino acid residues on the surface of *Streptomyces aureofaciens* RNase (RNase Sa) with positively charged ones increased the cytotoxic potential of the enzyme [92, 93]. The apoptosis-inducing effect of RNase Sa on Kasumi-1 acute myeloid leukemia cells significantly correlated with an increase in the enzyme cationicity [18]. Introduction of positively charged residues into the amino acid sequence of the protein increased onconase cytotoxicity [94].

However, increasing the charge alone was found not to be enough for a successful internalization of RNases into the cell. The extremely important role of the specific orientation of the RNase molecule (onconase, BS-RNase, RNase 1, and RNase A) relative to the cell membrane was demonstrated [76]. For example, native dimeric BS-RNase adopts the most favorable orientation for its internalization when it points both of its N-termini towards the cell membrane [75]. The Gly-38Lys BS-RNase mutant with an additional cationic residue oriented towards the N-terminus interacted with the membrane more strongly and was more cytotoxic than wild-type BS-RNase [17]. The presented data once again demonstrate the importance of the three-dimensional structure of RNases, in particular the orientation of the main charges that affect the cytotoxic potential of these enzymes.

Binase causes the death of the murine-transformed lung epithelial cells MLE-12, without significantly affecting normal AT-II cells [95]. In this case, after 24-h incubation, binase reaches the nucleus of AT-II cells without exerting any cytotoxicity and causes the death of MLE-12 cells without penetrating them

[95]. How does RNase mediate its cytotoxic potential without internalization of the enzyme? This question remained unanswered for a long time.

We recently found that the selectivity of binase for tumor cells expressing the *ras* oncogene was due to the direct interaction of RNase with the endogenous protein KRAS [96]. Investigation of activated KRAS using a non-hydrolyzable analogue of GTP (GTP γ S) showed that binase prevents the exchange of GDP for GTP and reduces the interaction between RAS and the protein factors GEF and SOS1. An analysis of the phosphorylation of RAS effectors, the AKT and ERK1/2 proteins, confirmed the inhibition of the MAPK/ERK signaling pathway [96]. Therefore, the selectivity of binase for tumor cells expressing the *ras* oncogene was proven to be associated with the interaction between binase and KRAS, which leads to blockage of the MAPK/ERK signaling pathway and triggering of apoptosis in tumor cells. KRAS-bound binase is found not only in dimeric form, but also in trimeric form, which confirms the importance of enzyme aggregation into higher-order oligomers for blocking proliferative signals [96].

RNase A is also capable of affecting cellular signals, but its action is opposed to the antitumor effect of binase. The enzyme interacts with the epidermal growth factor receptor (EGFR) and activates the MAPK/ERK signaling pathway, which leads to the induction of cell proliferation and tumor growth [13]. This feature of RNase A, which was discovered relatively recently, compromises the possibility of using this enzyme as a potential antitumor agent.

Some RNases have to enter the cell to exert their cytotoxic potential. Conflicting data on the mechanism of RNase internalization have been reported. For example, onconase and RNase A are internalized in early endosomes of HeLa and K562 cells via clathrin- and caveolin-independent pathways [87], while endocytosis of onconase in Jurkat cells occurs in a dynamin-dependent way [97]. These conflicting data suggest that RNases can use different pathways to enter cells, while many aspects of RNase internalization still remain unknown. BS-RNase is internalized in the endosomes of both normal and malignant cells, but only in the latter, where the enzyme is cytotoxic, does it reach the Golgi complex that ensures its cytosolic delivery [90]. A BS-RNase variant the C-terminus of which is designed for localization in the endoplasmic reticulum lacks cytotoxicity because it cannot be released in the cytosol to exert its antitumor activity [90].

Upon reaching the cytosolic compartment, RNases encounter another obstacle; the intracellular mammalian ribonuclease inhibitor. RI is a 50-kDa protein

that is present in the cytoplasm, mitochondria, and the nucleus of animal and human cells [98]. The biological functions of RI have not yet been fully elucidated; RI is considered to be potentially involved in cell redox homeostasis [99]. RI blocks mammalian RNases by forming tight complexes with them, which inhibit their catalytic activity. The phylogenetic remoteness of bacterial RNases and amphibian RNases underlies their insensitivity to RI and makes them potential antitumor agents. BS-RNase is insensitive to RI due to natural dimerization, forming three-dimensional structures that are inaccessible for blockage by the inhibitor. Also, as mentioned earlier, only dimers stabilized by domain exchange are insensitive to RI and exhibit cytotoxicity [65], which once again emphasizes the significance of RNase oligomerization.

The use of homologous RNases to study the dimer formation mechanism allowed us to discover the contribution of dimeric structure stability to the manifestation of the antitumor potential of these enzymes. Investigation of the cytotoxic effect of balnase and balidase on the human lung adenocarcinoma cells A549 has demonstrated that binase has the most pronounced apoptogenic effect, and that its cytotoxic potential enhances as the duration of incubation with cells increases, while the activity of balnase and balifase begins to decrease after 48 h of incubation [22]. These data are an indication of the key role of the stability of dimeric structures in enzyme cytotoxicity. Balnase and balifase dimers, in contrast to binase dimers, are less stable due to their inability to domain-exchange; after 48 h, they probably dissociate into monomers, which decreases their toxic properties. Dimeric binase structures are highly stable and can induce the death of tumor cells for a long time [22].

The presented information indicates that the antitumor activity of RNases is the result of a complex interaction between the structural and functional features of the enzymes, and that RNase oligomers have a higher cytotoxic potential than monomers [62, 70].

The cytotoxic effect of RNases is known to be associated not only with the consequences of direct RNA degradation, but also with the regulatory effects of its hydrolysis products [20, 86]. The manifestation of the biological effects of RNases is related to various cellular mechanisms, including the non-catalytic interaction between RNases and cellular components, the internalization of the proteins into the cell, and the ability to avoid RI action. Each cytotoxic RNase type has its own specific set of molecular mechanisms which mediates the antitumor effect of the enzyme, but the defining one among them is the structural organization of RNase molecules, which contributes to each of the presented molecular mechanisms.

The results of our study have revealed a direct correlation between cytotoxicity and the stability of dimeric RNase structures, confirming the fundamental role played by the supramolecular organization of enzymes in their antitumor activity. ●

This study was supported by a grant from the Russian Science Foundation No. 18-74-00108 within the program for increasing the competitiveness of the Kazan (Volga Region) Federal University.

REFERENCES

1. Nucleases / Eds Linn S.M., Lloyd R.S., Roberts R.J. Cold Spring Harbor, N.Y.: Cold Spring Harbor Lab. Press, 1994.
2. Bechhofer D.H., Deutscher M.P. // *Crit. Rev. Biochem. Mol. Biol.* 2019. V. 54. P. 242–300.
3. Ezelle H.J., Malathi K., Hassel B.A. // *Int. J. Mol. Sci.* 2016. V. 17. P. 74.
4. Lee H., Lee D.G. // *J. Microbiol. Biotechnol.* 2019. V. 29. P. 1014–1021. doi:10.4014/jmb.1904.04017.
5. Ramos H.J., Souza E.M., Soares-Ramos J.R., Pedrosa F.O. // *J. Biotechnol.* 2006. V. 126. P. 291–294. doi:10.1016/j.jbiotec.2006.04.020.
6. Olombrada M., Martínez-del-Pozo A., Medina P., Budia F., Gavilanes J.G., García-Ortega L. // *Toxicol.* 2014. V. 83. P. 69–74. doi:10.1016/j.toxicol.2014.02.022.
7. Rossier O., Dao J., Cianciotto N.P. // *Microbiology.* 2009. V. 155. P. 882–890. doi:10.1099/mic.0.023218-0.
8. Agaisse H., Gominet M., Okstad O.A., Kolstø A.B., Lereclus D. // *Mol. Microbiol.* 1999. V. 32. P. 1043–1053. doi:10.1046/j.1365-2958.1999.01419.x.
9. Shah Mahmud R., Garifulina K.I., Ulyanova V.V., Evtugyn V.G., Mindubaeva L.N., Khazieva L.R., Dudkina E.V., Vershinina V.I., Kolpakov A.I., Ilinskaya O.N. // *Mol. Gen. Microbiol. Virol.* 2017. V. 32. P. 87–93. doi:10.3103/S0891416817020082
10. Maksimov I.V., Sorokan A.V., Burkhanova G.F., Veselova S.V., Alekseev V.Yu., Shein M.Yu., Avalbaev A.M., Dhaware P.D., Mehete G.T., Singh B.P., Khairullin R.M. // *Plants (Basel).* 2019. V. 8. P. 575. doi: 10.3390/plants8120575.
11. Sassa H. // *Breed Sci.* 2016. V. 66. P. 116–121. doi:10.1270/jsbbs.66.116.
12. Lee H.H., Wang Y.N., Hung M.C. // *Mol. Aspects Med.* 2019. V. 70. P. 106–116. doi:10.1016/j.mam.2019.03.003.
13. Wang Y.N., Lee H.H., Chou C.K., Yang W.H., Wei Y., Chen C.T., Yao J., Hsu J.L., Zhu C., Ying H. // *Cancer Cell.* 2018. V. 33. P. 752–769. doi:10.1016/j.ccell.2018.02.012.
14. Majchrzak A., Witkowska M., Mędra A., Zwolińska M., Bogusz J., Cebula-Obrzut B., Darzynkiewicz Z., Robak T., Smolewski P. // *Postepy Hig. Med. Dosw.* 2013. V. 67. P. 1166–1172.
15. Wang X., Guo Z. // *Oncol. Lett.* 2015. V. 9. P. 1337–1342. doi: 10.3892/ol.2014.2835.
16. Marinov I., Soucek J. // *Neoplasma.* 2000. V. 47. P. 294–298.
17. Fiorini C., Gotte G., Donnarumma F., Picone D., Donadelli M. // *Biochim. Biophys. Acta.* 2014. V. 1843. P. 976–984. doi: 10.1016/j.bbamcr.2014.01.025
18. Mitkevich V.A., Ilinskaya O.N., Makarov A.A. // *Cell Cycle.* 2015. V. 14. P. 931–932.
19. Mitkevich V.A., Burnysheva K.M., Pterushanko I.Y., Adzhubei A.A., Schulga A.A., Chumakov P.M., Makarov A.A. // *Oncotarget.* 2017. V. 8. P. 72666–72675. doi: 10.18632/oncotarget.20199.
20. Makarov A.A., Kolchinsky A., Ilinskaya O.N. // *Bioessays.* 2008. V. 8. P. 781–790.
21. Mitkevich V.A., Kretova O.V., Petrushanko I.Y., Burnysheva K.M., Sosin D.V., Simonenko O.V., Ilinskaya O.N., Tchurikov N.A., Makarov A.A. // *Biochimie.* 2013. V. 95. P. 1344–1349. doi: 10.1016/j.biochi.2013.02.016.
22. Surchenko Y., Dudkina E., Nadyrova A., Ulyanova V., Zelenikhin P., Ilinskaya O. // *BioNanoScience.* 2020. https://doi.org/10.1007/s12668-020-00720-6.
23. Sevcik J., Sanishvili R.G., Pavlovsky A.G., Polyakov K.M. // *Trends Biochem. Sci.* 1990. V. 15. P. 158–162.
24. Ulyanova V., Vershinina V., Ilinskaya O. // *FEBS J.* 2011. V. 278. P. 3633–3643.
25. Makarov A.A., Ilinskaya O.N. // *FEBS Lett.* 2003. V. 540. P. 15–20.
26. Nakamura A., Koide Y., Miyazaki H., Kitamura A., Masaki H., Beppu T., Uozumi T. // *Eur. J. Biochem.* 1992. V. 209. P. 121–127. doi:10.1111/j.1432-1033.1992.tb17268.x.
27. Skvortsova M.A., Bocharov A.L., Yakovlev G.I., Znamenetskaya L.V. // *Biochemistry (Moscow).* 2002. V. 67. P. 802–806. doi:10.1023/a:1016356926125.
28. Yoshida H. // *Methods Enzymol.* 2001. V. 341. P. 28–41.
29. Dementiev A.A., Orlov V.M., Shlyapnikov S.V. // *Russian J. Bioorg. Chem.* 1993. V. 19. P. 853–861.
30. Ulyanova V., Vershinina V., Ilinskaya O., Harwood C.R. // *Microbiol. Res.* 2015. V. 170. P. 131–138. doi:10.1016/j.micres.2014.08.005.
31. Botella E., Hübner S., Hokamp K., Hansen A., Bisicchia P., Noone D., Powell L., Salzberg L.I., Devine K.M. // *Microbiology.* 2011. V. 157. P. 2470–2484.
32. Kharitonova M.A., Vershinina V.I. // *Microbiology.* 2009. V. 78. P. 223–228. https://doi.org/10.1134/S0026261709020088.
33. Sokurenko Yu.V., Zelenikhin P.V., Ulyanova V.V., Kolpakov A.I., Muller D., Ilinskaya O.N. // *Russian Journal of Bioorg. Chem.* 2015. V. 41. P. 31–36.
34. Jackson E.K., Mi Z., Janesko-Feldman K., Jackson T.C., Kochanek P.M. // *Am. J. Physiol. Regul. Integr. Comp. Physiol.* 2019. V. 316. P. R783–R790.
35. Ulyanova V., Shah Mahmud R., Dudkina E., Vershinina V., Domann E., Ilinskaya O. // *J. Gen. Appl. Microbiol.* 2016. V. 62. P. 181–188.
36. Leshchinskaia I.B., Kupriyanova F.G., Yakovlev G.I., Kipenskaya L.V., Ilinskaya O.N. // *Karadeniz J. Med. Sci.* 1995. V. 8. P. 218–219.
37. Ilinskaya O.N., Krylova N.I. // *PriU bioWim mikrobiol.* 1993. V. 29. P. 280–285.
38. Hartley R.W., Rogerson D.L. Jr // *Prep. Biochem.* 1972. V. 2. P. 229–242.
39. Leshchinskaia I.B., Bulgakova R. Sh., Balaban N.P., Egorova G.S. // *Applied biochemistry and microbiology.* 1974. V. 10. P. 242–247.
40. Dudkina E., Ulyanova V., Shah Mahmud R., Khodzhaeva V., Dao L., Vershinina V., Kolpakov A., Ilinskaya O. // *FEBS Open Bio.* 2016. V. 6. P. 24–32.
41. Sokurenko Yu., Nadyrova A., Ulyanova V., Il-

- inskaya O. // *BioMed Res. Int.* 2016. <http://dx.doi.org/10.1155/2016/4239375>.
42. Dementiev A.A., Ryabchenko N.F., Protasevich I.I., Golyshin P.N., Stepanov A.I., Orlov V.M., Pustobaev V.N., Makarov A.A., Moiseev G.P., Karpeysky M.Y. et al. *Mol Biol.* 1992. T. 26. P. 1338–1348.
 43. Marianayagam N.J., Sunde M., Matthews J.M. // *Trends Biochem. Sci.* 2004. V. 29. P. 618–625.
 44. Dudkina E., Kayumov A., Ulyanova V., Ilinskaya O. // *PLoS One.* 2014. V. 9. P. e115818. doi:10.1371/journal.pone.0115818.
 45. Dudkina E., Ulyanova V., Ilinskaya O. // *BioNanoScience.* 2017. V. 7. P. 127–129. <https://doi.org/10.1007/s12668-016-0305-y>.
 46. Poliakov K.M., Goncharuk D.A., Trofimov A.A., Safonova T.N., Mit'kevich V.A., Tkach E.N., Makarov A.A., Shulga A.A. // *Mol. Biol.* 2010. V. 44. P. 922–928.
 47. Polyakov K.M., Lebedev A.A., Okorokov A.L., Panov K.I., Shulga A.A., Pavlovsky A.G., Karpeysky M.Y., Dodson G.G. // *Acta Cryst. D Biol. Crystallogr.* 2002. V. 58. P. 744–750.
 48. Aphanasenko G.A., Dudkin S.M., Kamirir L.B., Leshchinskaya I.B., Severin E.S. // *FEBS Lett.* 1979. V. 97. P. 77–80.
 49. Mitkevich V.A., Schulga A.A., Trofimov A.A., Dorovatovskii P.V., Goncharuk D.A., Tkach E.N., Makarov A.A., Polyakov K.M. // *Acta Cryst. D Biol. Crystallogr.* 2003. V. 69. P. 991–996.
 50. Ermakova E. // *Biophys. Chem.* 2007. V. 130. P. 26–31.
 51. Breitwieser G.E. // *Circ. Res.* 2004. V. 94. P. 17–27.
 52. Hirota S. // *J. Inorg. Biochem.* 2019. V. 194. P. 170–179. doi: 10.1016/j.jinorgbio.2019.03.002.
 53. Orlikowska M., Jankowska E., Kolodziejczyk R., Jaskolski M., Szymanska A. // *J. Struct. Biol.* 2011. V. 173. P. 406–413. doi: 10.1016/j.jsb.2010.11.009.
 54. Liu C., Sawaya M.R., Eisenberg D. // *Nat. Struct. Mol. Biol.* 2011. V. 18. P. 49–55. doi: 10.1038/nsmb.1948.
 55. Anfinsen C.B. // *Science.* 1973. V. 181. P. 223–230. doi: 10.1126/science.181.4096.223.
 56. Bennett M.J., Schlunegger M.P., Eisenberg D. // *Protein Sci.* 1995. V. 4. P. 2455–2468. doi: 10.1002/pro.5560041202.
 57. Liu Y., Eisenberg D. // *Protein Sci.* 2002. V. 11. P. 1285–1299. doi: 10.1110/ps.0201402.
 58. Wang L., Pang Y., Holder T., Brender J.R., Kurochkin A.V., Zuiderweg E.R. // *Proc. Natl. Acad. Sci. USA.* 2011. V. 98. P. 7684–7689. doi:10.1073/pnas.121069998.
 59. Bennett M.J., Sawaya M.R., Eisenberg D. // *Structure.* 2006. V. 14. P. 811–824. doi: 10.1016/j.str.2006.03.011.
 60. Garvie C.W., Vasanthavada K., Xiang Q. // *Biochim. Biophys. Acta.* 2013. V. 1834. P. 1562–1571.
 61. Lin R.J., Chien H.L., Lin S.Y., Chang B.L., Yu H.P. // *Nucl. Acids Res.* 2013. V. 41. P. 3314–3326.
 62. Gotte G., Mahmoud Helmy A., Ercole C., Spadaccini R., Laurents D.V., Donadelli M., Picone D. // *PLoS One.* 2012. doi: 10.1371/journal.pone.0046804.
 63. Zuo Y., Deutscher M.P. // *J. Biol. Chem.* 2002. V. 277. P. 50160–50164.
 64. Mathy N., Hebert A., Mervelet P., Benard L., Dorleans A., Sierra-Gallay I.L., Noirot P., Putzer H., Condon C. // *Mol. Microbiol.* 2010. V. 75. P. 489–498.
 65. Gotte G., Laurents D.V., Merlino A., Picone D., Spadaccini R. // *FEBS Lett.* 2013. V. 587. P. 3601–3608.
 66. Merlino A., Ercole C., Picone D., Pizzo E., Mazzarella L., Sica F. // *J. Mol. Biol.* 2008. V. 376. P. 427–437.
 67. Gotte G., Libonati M. // *J. Biol. Chem.* 2004. V. 279. P. 36670–36679.
 68. Crestfield A.M., Stein W.H., Moore S. // *Arch. Biochem. Biophys.* 1962. V. 1. P. 217–222.
 69. Benito A., Laurents D.V., Ribo M., Vilanova M. // *Curr. Protein Pept. Sci.* 2008. V. 9. P. 370–393. doi: 10.2174/138920308785132695.
 70. Libonati M., Gotte G. // *Biochem J.* 2004. V. 380. P. 311–327. doi: 10.1042/bj20031922.
 71. Gotte G., Laurents D.V., Libonati M. // *Biochim. Biophys. Acta.* 2006. V. 1764. P. 44–54.
 72. Gotte G., Bertoldi M., Libonati M. // *Eur. J. Biochem.* 1999. V. 265. P. 680–687. doi: 10.1046/j.1432-1327.1999.00761.x.
 73. Fagagnini A., Pica A., Fasoli S., Montioli R., Donadelli M., Cordani M., Butturini E., Acquasaliente L., Picone D., Gotte G. // *Biochem. J.* 2017. V. 474. P. 3767–3781. doi: 10.1042/BCJ20170541.
 74. Libonati M., Gotte G., Vottariello F. // *Curr. Pharm. Biotechnol.* 2008. V. 9. P. 200–209. doi: 10.2174/138920108784567308.
 75. Notomista E., Mancheno J.M., Crescenzi O., Di Donato A., Gavilanes J., D'Alessio G. // *FEBS J.* 2006. V. 273. P. 3687–3697. doi: 10.1111/j.1742-4658.2006.05373.x.
 76. Sundlass N.K., Eller C.H., Cui Q., Raines R.T. // *Biochemistry.* 2013. V. 52. P. 6304–6312. doi: 10.1021/bi400619m.
 77. Shah Mahmud R., Mostafa A., Müller C., Kanrai P., Ulyanova V., Sokurenko Y., Dzieciolowski J., Kuznetsova I., Ilinskaya O., Pleschka S. // *Virologia.* 2018. V. 15. P. 1–12. doi: 10.1186/s12985-017-0915-1.
 78. Kim J.S., Soucek J., Matousek J., Raines R.T. // *Biochem. J.* 1995. V. 308. P. 547–550.
 79. Rosenberg H.F. // *J. Biol. Chem.* 1995. V. 270. P. 7876–7881.
 80. Alford S., Pearson J., Carette A., Ingham R., Howard P. // *BMC Biochem.* 2009. doi: 10.1186/1471-2091-10-9.
 81. Navarro S., Aleu J., Jimenez M., Boix E., Cuchillo C.M., Nogues M.V. // *Cell. Mol. Life Sci: CMLS.* 2008. V. 65. P. 324–337.
 82. Sorrentino S., Libonati M. // *FEBS Lett.* 1997. V. 404. P. 1–5.
 83. Blaszczyk J., Gan J., Tropea J.E., Court D.L., Waugh D.S. // *Structure.* 2004. V. 12. P. 457–466.
 84. Mitkevich V.A., Tchurikov N.A., Zelenikhin P.V., Petrushanko I.Y., Makarov A.A., Ilinskaya O.N. // *FEBS J.* 2010. V. 277. P. 186–196.
 85. Mitkevich V.A., Petrushanko I.Y., Spirin P.V., Fedorova T.V., Kretova O.V., Tchurikov N.A., Prassolov V.S., Ilinskaya O.N., Makarov A.A. // *Cell Cycle.* 2011. V. 10. P. 4090–4097.
 86. Ardel T., Ardel W., Darzynkiewicz Z. // *Cell Cycle.* 2003. V. 2. P. 22–24.
 87. Haigis M.C., Raines R.T. // *J. Cell Sci.* 2003. V. 116. P. 313–324. doi: 10.1242/jcs.00214.
 88. Kanwar S.S., Kumar R. // *Enz. Eng.* 2017. doi: 10.4172/2329-6674.1000162.
 89. Trevino S.R., Scholtz M., Pace C.N. // *J. Mol. Biol.* 2007. V. 366. P. 449–460.
 90. Bracale A., Spalletti C.D., Mastronicola M.R. // *Biochem. J.* 2002. V. 362. P. 553–560.
 91. Ran S., Downes A., Thorpe P.E. // *Cancer Res.* 2002. V. 62. P. 6132–6140.
 92. Ilinskaya O., Decker K., Koschinski A., Dreyer F., Repp H. // *Toxicology.* 2001. V. 156. P. 101–107.
 93. Ilinskaya O.N., Koschinski A., Mitkevich V.A., Repp H., Dreyer F., Pace C.N., Makarov A.A. // *Biochem. Biophys. Res. Commun.* 2004. V. 314. P. 550–554.
 94. Futami J., Yamada H. // *Curr. Pharm. Biotechnol.* 2008. V. 9. P. 180–184. doi: 10.2174/138920108784567326.
 95. Cabrera-Fuentes H.A., Kalacheva N.V., Mukhametshina

REVIEWS

- R.T., Zelenichin P.V., Kolpakov A.I., Barreto G., Praissner K.T., Ilinskaya O.N. // *Biomed. Khim.* 2012. V. 58. P. 272–280.
96. Ilinskaya O.N., Singh I., Dudkina E.V., Ulyanova V.V., Kayumov A., Barreto G. // *Biochim. Biophys. Acta.* 2016. V. 1863. P. 1559–1567.
97. Rodriguez M., Torrent G., Bosch M., Rayne F., Dubremetz J.F., Ribó M., Benito A., Vilanova M., Beaumelle B. // *J. Cell Sci.* 2007. V. 120. P. 1405–1411. doi: 10.1242/jcs.03427.
98. Furia A., Moscato M., Cali G., Pizzo E., Confalone E., Amoroso M.R., Esposito F., Nitsch L., D'Alessio G. // *FEBS Lett.* 2011. V. 585. P. 613–617. doi: 10.1016/j.febslet.2011.01.034.
99. Monti D.M., Montesano G.N., Matousek J., Esposito F., D'Alessio G. // *FEBS Lett.* 2007. V. 581. P. 930–934. doi: 10.1016/j.febslet.2007.01.072.

Development of Antimicrobial Therapy Methods to Overcome the Antibiotic Resistance of *Acinetobacter baumannii*

O. V. Kisil¹, T. A. Efimenko^{1*}, N. I. Gabrielyan², O. V. Efremenkova¹

¹Gause Institute of New Antibiotics, Moscow, 119021 Russia

²V.I. Shumakov Federal Research Center of Transplantology and Artificial Organs, Ministry of Healthcare of the Russian Federation, Moscow, 1123182 Russia

*E-mail: efimen@inbox.ru

Received April 7, 2020; in final form, May 19, 2020

DOI: 10.32607/actanaturae.10955

Copyright © 2020 National Research University Higher School of Economics. This is an open access article distributed under the Creative Commons Attribution License, which permits unrestricted use, distribution, and reproduction in any medium, provided the original work is properly cited.

ABSTRACT The spread of antibiotic resistance among pathogens represents a threat to human health around the world. In 2017, the World Health Organization published a list of 12 top-priority antibiotic-resistant pathogenic bacteria for which new effective antibiotics or new ways of treating the infections caused by them are needed. This review focuses on *Acinetobacter baumannii*, one of these top-priority pathogens. The pathogenic bacterium *A. baumannii* is one of the most frequently encountered infectious agents in the world; its clinically significant features include resistance to UV light, drying, disinfectants, and antibiotics. This review looks at the various attempts that have been made to tackle the problem of drug resistance relating to *A. baumannii* variants without the use of antibiotics. The potential of bacteriophages and antimicrobial peptides in the treatment of infections caused by *A. baumannii* in both planktonic and biofilm form is assessed. Such topics as research into the development of vaccines based on the outer membrane proteins of *A. baumannii* and the use of silver nanoparticles, as well as photodynamic and chelate therapy, are also covered.

KEYWORDS *Acinetobacter baumannii*, multidrug resistance, biofilms, bacteriophage therapy, antimicrobial peptides.

ABBREVIATIONS WHO – World Health Organization; MDR – multidrug resistance; ESKAPE – *Enterococcus faecium*, *Staphylococcus aureus*, *Klebsiella pneumoniae*, *Acinetobacter baumannii*, *Pseudomonas aeruginosa*, *Enterobacter* spp.; MIC – minimum inhibitory concentration.

INTRODUCTION

Antimicrobial therapy is among the most consequential medical breakthroughs achieved in the 20th century. It has helped save millions of lives. However, antimicrobial therapy also has shortcomings, such as a certain degree of toxicity, microbiome disturbance, and the formation of resistant pathogen forms causing serious infectious diseases. Their rapid spread threatens to dent the effectiveness of modern medicine, including that of surgical intervention, organ transplantation, and hematologic diseases when patients have a weakened immune system and, therefore, the risk of infection increases. According to the World Health Organization (WHO), *Acinetobacter baumannii* is one amongst six particularly dangerous bacteria because it is multidrug-resistant (MDR) and does not respond to antimicrobial therapy. For these bacteria, WHO has

suggested using the abbreviation ESKAPE (to escape from the action of antibiotics): *Enterococcus faecium*, *Staphylococcus aureus*, *Klebsiella pneumoniae*, *Acinetobacter baumannii*, *Pseudomonas aeruginosa*, and *Enterobacter* spp. [1]. After eight years, the list of bacterial pathogens that do not respond to antimicrobial therapy was expanded to 12 and the bacteria were subdivided into three groups according to their level of threat to human health (critical, high or medium); new effective antibiotics or new ways to treat infections caused by these pathogens need to be developed [2].

Numerous articles published thus far have suggested various options for antimicrobial therapy that are effective on the infections caused by these pathogens [3]. Our review focuses exclusively on antibiotic-resistant strains of the Gram-negative *A. baumannii* pathogen and aims to describe alternative approaches

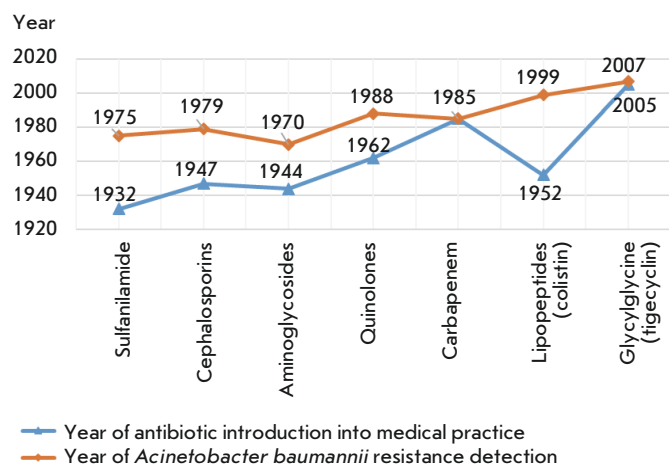


Fig. 1. Time intervals between the introduction of an antibiotic into medical practice and the first reports of *Acinetobacter baumannii* resistance [5]

to the treatment of infections caused by *A. baumannii*, including bacteriophage therapy, preventive vaccination, light therapy, silver ion therapy, and chelate therapy.

The genus *Acinetobacter* contains Gram-negative, strictly aerobic, lactose-fermenting, fixed rod-shaped bacteria. Members of the genus *Acinetobacter* are ubiquitous saprophytic microorganisms. They can be isolated from various sources: soil, surface water, and the mucous membranes of the upper respiratory tract of humans. The genus *Acinetobacter* currently includes 27 species. From a clinical point of view, three phylogenetically related *Acinetobacter* species are of the greatest interest: *A. baumannii*, *A. pittii*, and *A. nosocomialis*. They are the most significant pathogens causing nosocomial infections [4]. The important adaptive features of *A. baumannii* include its high mutation rate, which leads to rapid development of antibiotic resistance. *Figure 1* shows the time intervals separating the introduction of an antibiotic into medical practice and the detection of resistance by *A. baumannii* to it [5].

Presumably, the first infections caused by *A. baumannii* were documented at U.S. military treatment facilities during the wars in Iraq and Afghanistan [6, 7]. *Acinetobacter baumannii* was even referred to as “Iraqibacter”, since it affected thousands of American soldiers during the Iraq war [8]. The first studies of hospital-acquired infections caused by *A. baumannii* were conducted in the early 1980s [9, 10]. It is interesting to note that 30 years ago infections caused by *Acinetobacter* species were not considered a public health threat, although the mechanisms of innate resistance

by *A. baumannii* were documented and described. However, the research conducted over the past decade has shown that in addition to its own internal resistance mechanisms, *A. baumannii* can successfully acquire multiple determinants of resistance by horizontal gene transfer, becoming an MDR bacterium. Today, *A. baumannii* MDR strains are endemic and epidemic in hospitals around the world, with mortality rates ranging from 40% to 70% for diseases requiring artificial lung ventilation, 25–30% for meningitis, and 34–49% for bacteremia [11]. A study of infections spread in intensive care units conducted in 75 countries across five continents assumes that *A. baumannii* is one of the most common infectious agents in the world [12]. The WHO estimates that the spread of MDR *A. baumannii* is today a serious global threat. *Table 1* shows the main stages in recognizing *A. baumannii* as a multidrug-resistant nosocomial pathogen.

Sequencing of the genomes of 49 strains of MDR *A. baumannii* within one U.S. hospital system showed that almost every analyzed strain was unique [25]. A comparative analysis of *A. baumannii* strains revealed a transfer of mobile genetic elements, homologous recombination within the entire genome, deletions and mutations, all occurring within short periods of time. The variations in the gene composition of the strains did not have clear spatial (location in a hospital) or temporal patterns, thus proving that there was a pool of circulating strains in this hospital with significant interstrain interaction. Thus, the exchange of genetic material and rearrangements of the bacterial genome lead to multiple genetic combinations and provide an infinite source of genetic adaptability for *A. baumannii*.

A. baumannii is a successfully survivable in-hospital pathogen not only because of its ability to “switch” its genomic structure and capture resistance markers, but also because of its innate biofilm-forming ability [11]. In contrast to the planktonic state, biofilms are communities of bacteria enclosed in a self-produced exopolysaccharide matrix that serves to attach the bacteria to surfaces, including medical implants and human tissue: teeth, skin, trachea, and urethra. It is known that bacteria in the biofilm can be 10–1,000 times more resistant to antibiotics than their planktonic forms [26]. Infections associated with the formation of biofilms attached to surfaces are very difficult to treat. Therefore, preventing the early stage of biofilm formation is considered an important step in infection prevention and treatment.

Biofilm formation is a step-by-step process that includes three phases: adhesion, maturation, and detachment (*Fig. 2*). During the adhesion phase, plankton cells attach to the surface through weak interactions [27]. After initial attachment, weakly bound

Table 1. Historical reference of the *Acinetobacter baumannii* pathogen

Year	Fact	Reference
1911	The genus <i>Acinetobacter</i> was first described	[13]
1968	The modern designation of the genus <i>Acinetobacter</i> (from the Greek <i>akinetos</i> , “fixed”) proposed by Brisou and Prevot in 1954, was accepted.	[14, 15]
1974	The genus <i>Acinetobacter</i> designation is included in Bergey’s Manual of Systematic Bacteriology (described as having only one species: <i>Acinetobacter calcoaceticus</i>)	[16]
1984	First report of resistance to imipenem	[17]
1986	The <i>Acinetobacter calcoaceticus-baumannii</i> complex is divided into four species based on DNA hybridization studies: <i>A. calcoaceticus</i> ; <i>A. baumannii</i> ; <i>A. pittii</i> ; <i>A. nosocomialis</i> <i>A. baumannii</i> is described as an agent that causes a nosocomial infection	[18]
1999	First report of resistance to colistin	[19]
2001	The WHO published the first international appeal: “Global Strategy for Containment of Antimicrobial Resistance”	[20]
2007	First report of resistance to tigecycline	[21]
2009	Bacteria that are dangerous to human health are grouped in ESKAPE (including <i>Acinetobacter</i>)	[1]
	The USA (CDC) and EU (ECDC) established the Transatlantic Taskforce on Antimicrobial Resistance (TATFAR)	[22]
2015	The WHO developed a new “Global Strategy for Containment of Antimicrobial Resistance”	[23]
2017	The WHO published the “Global priority list of antibiotic-resistant bacteria to guide research, discovery, and development of new antibiotics”	[24]

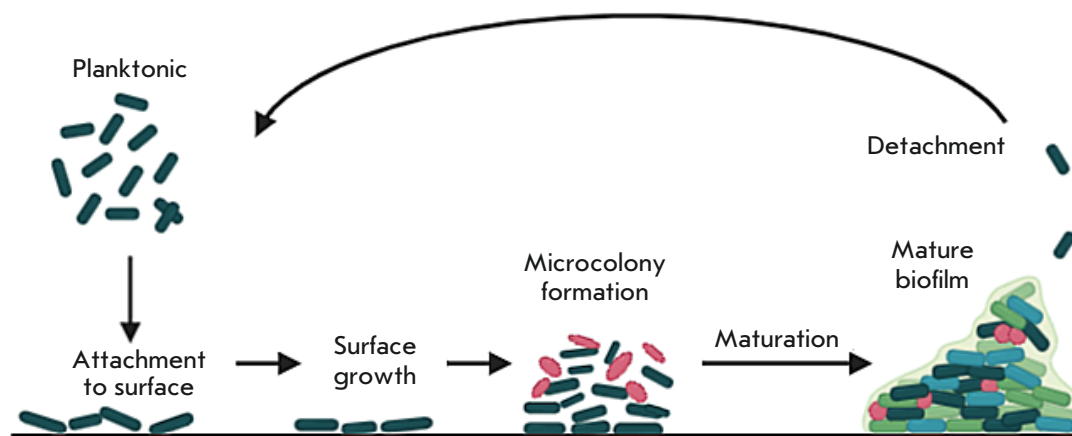


Fig. 2. Stages of biofilm formation

cells stably attach due to more specific molecular interactions between bacterial surface structures such as pili and host molecules functioning as receptors (such as fibronectin). During the biofilm maturation phase, bacteria produce large amounts of exopolysaccharides, which form most of the biofilm’s biomass. During the detachment phase, cells (single or clusters) separate and colonize neighboring sites. The biofilm is highly resistant to drugs because of the low diffusion

of antibiotics in it, the presence of persistent cells, and the slow growth rates and low metabolism of cells deep in the biofilm. Due to the proximity of the cells, the biofilm is characterized by increased horizontal transfer of resistance genes. It has been proved that *A. baumannii* can attach to tissues and form a biofilm at a surgical site, which complicates infection prevention and treatment and is especially critical when medical implants are used [28].

During outbreaks of nosocomial infections, *A. baumannii* isolates have been found on various surfaces surrounding patients, including furniture and hospital equipment, doors, electrical switches, wash basins, etc. (over 30 items) [11]. It is noteworthy that outbreaks associated with infected items have ended once the source of the infection was removed, replaced, or properly disinfected. Today, proper hygiene, and hand hygiene in particular, is an efficient and simple means for preventing a bacterial infection of whatever nature.

The mechanism of *A. baumannii* infection is associated with a number of factors, including a long hospital stay (especially in intensive care units), the disease severity, blood transfusion, the use of an intravascular catheter or endotracheal tube, intubation with artificial ventilation, inadequate initial antibacterial therapy, and contamination of patient environment with *A. baumannii*. Contaminated surfaces, medical equipment, poor hand hygiene, and violations of sanitary requirements by patients and medical staff can be the cause of infection and result in its rapid transmission; medical staff transmits microorganisms to patients or facilitates bacteria exchange between patients [29]. *A. baumannii* is transmitted from person to person through airborne droplets: so, the respiratory system is the main infection route. Kotay et al. [30] found that bacteria can also spread through wash basins. It was shown that the bacteria, in the form of a biofilm, multiply in drain pipes and gradually occupy the space higher up the pipe towards the wash basin. Water flows from a faucet lead to dispersion of droplets, which spread the bacteria.

Diseases caused by *A. baumannii* do not differ in any special clinical manifestations from other infections. However, the following specific features may help medical staff determine whether a patient is infected with *A. baumannii*: (1) late infection and (2) excessive use of broad-spectrum antibiotics in the early stages of treatment. The loose use of antibiotics is considered the main reason behind the development of a significant proportion of MDR *A. baumannii* variations [31]. It has been repeatedly shown that administration of antibiotics in concentrations below MIC increases the probability of *A. baumannii* biofilm formation [32].

The effectiveness of antimicrobial drugs against Gram-negative bacteria depends on the balance between several fundamental molecular intracellular processes that occur before the antimicrobial drug interacts with the target: (1) drug influx mediated by porins; (2) drug outflow mediated by efflux systems; (3) drug inactivation, usually by irreversible cleavage catalyzed by periplasmic and cytoplasmic enzymes; and (4) modification of the target to which the drug can bind [33]. High antimicrobial resistance of *A. baumannii* is due to an interconnection between all these

mechanisms. It is achieved by obtaining new genetic information through horizontal gene transfer and mutations. New genetic determinants are acquired by *A. baumannii* strains through the combined effect of mobile genetic elements (insertion sequences, transposons), integrons, and transferable plasmids. Changes can be a result of either spontaneous mutations leading to a modification of the drug target or insertions/deletions of the mobile elements that alter the expression of endogenous resistance mechanisms or membrane permeability. In addition to these mechanisms, *A. baumannii* can accumulate many determinants of resistance in the so-called “resistance islands” (specific genome regions containing clusters of horizontally transferred DNA that include antimicrobial resistance genes). Such clusters provide a “shelter” to mobile elements, since insertion into this site causes no damage to the host cell [34, 35]. It has been assumed that *Acinetobacter* spp. can play an important role in the transfer of resistance genes to other Gram-negative microorganisms [36].

Thirty years ago, infections caused by *A. baumannii* could be effectively treated with conventional antibiotics, but the global spread of MDR strains has dramatically reduced the number of agents that are effective on infections caused by this pathogen. To date, it has been established that *A. baumannii* is resistant to such antibiotics as penicillins, cephalosporins, chloramphenicol, aminoglycosides, fluoroquinolones, and tetracyclines [29]. Multidrug resistance of many clinical *A. baumannii* isolates severely restricts the currently available treatment options, so there is an urgent need for new therapies and methods that would be effective against MDR *A. baumannii*.

In recent years, combination therapy has been increasingly used for infections caused by MDR Gram-negative bacteria. It is obvious that the probability of resistance against a combination of two drugs is much less than that against one drug. In addition, the synergistic effect of combination antibiotics exceeds the effect of antibiotic monotherapy. However, some combinations cause an opposite effect, resulting in much more severe damage. One antibiotic can induce resistance to the second antibiotic administered within the combination, thus leading to an antagonistic effect [3].

Adjuvants show good prospects for use in clinical antibacterial practice. These substances per se have almost no antimicrobial activity, but in combination with antibiotics, adjuvants can inhibit resistance mechanisms in various ways: (1) by increasing antibiotic absorption through the bacterial membrane; (2) by inhibiting efflux pumps; and (3) by changing the physiology of resistant cells that promote biofilm spreading (in particular, by quorum quenching) [37]. It is known

that bacteria produce the chemical signals necessary for intercellular communication and adaptation to the environment. The mechanism of quorum sensing in bacteria consists in the expression of a certain phenotype when a high population density is reached [38]. The molecules inhibiting quorum sensing suppress phenotypic manifestation of the trait, such as biofilm formation. Combinations of 1-[(2,4-dichlorophenethyl) amino]-3-phenoxypropan-2-ol and combinations with various antibiotics inhibit the growth of all pathogens of the ESKAPE group in both planktonic and biofilm form [39].

The number of antibiotics effective on Gram-negative infections decreases with every year. In the 21st century, only 33 antibiotics have been introduced into medical practice, including only two new natural antibiotics, daptomycin and fidaxomicin [40]. An analysis of the list of antibiotics recommended by the Clinical and Laboratory Standards Institute (CLSI, USA) has shown that since 2010, many antibiotics proposed for the treatment of ESKAPE-related infections have been replaced by a relatively small number of antibiotic + antibiotic combinations [3]. Thus, due to the limited availability of antibiotics for treating infections caused by Gram-negative MDR bacteria, alternative strategies are needed. Among them, feature such methods as the use of bacteriophages and their enzymes, antimicrobial peptides, photodynamic and chelate therapy, and nanoparticles.

Bacteriophage therapy

One of the possible therapeutic agents against *A. baumannii* is bacteriophages, the most widely encountered organisms on the planet, whose number exceeds 10³¹ according to a number of estimates [41]. The fundamental aspect of phage–bacterium interaction is phage

specificity, i.e. the ability to infect a strictly defined host bacterium. Bacteriophages are adsorbed on the bacterial cell, inject their genome through the membrane into the cell, through which mechanism they express their own genes, replicate the genome in the host cell, and release virions after lysis of bacterial cells. The advantages of bacteriophage over antibiotic therapy include drug tolerance and the fact that bacteria develop resistance to bacteriophages at the lowest rate. In addition, bacteriophages are highly specific to their targets, unlike broad-spectrum antibiotics, which kill normal bacterial flora and disrupt the microbiome of healthy humans [42].

As the incidence and mortality rate of MDR pathogens increase, interest in bacteriophages is returning all over the world. Since 2010, scientists from different countries have discovered new bacteriophages infecting MDR *A. baumannii* [43–46]. In most cases, bacteriophages against *A. baumannii* have been studied *in vitro*, but the ability of bacteriophages to lyse *A. baumannii* has recently increasingly come to be evaluated by simulating the infectious process *in vivo*. Table 2 summarizes the results of bacteriophage therapy of infections caused by *A. baumannii* over the past five years. Thus, it was shown that two lytic bacteriophages isolated from hospital wastewater were able to infect more than 50% of carbapenem-resistant clinical strains of *A. baumannii*. Less than 20% of *Galleria mellonella* larvae survived 96 h after infection with *A. baumannii*. With the introduction of bacteriophages, larval survival increased to 75%, while treatment with polymyxin B increased survival to only 25% [47]. Improvement in wound infection healing in the phage-infected group and a significant reduction in mortality in rats, compared to infected animals treated with an antibiotic, was also observed [48].

Table 2. Summary of the data from studies on bacteriophage use

Antimicrobial agent	Infection model	Efficiency of infection inhibition	Antibiofilm activity	Reference
WCHABP1, WCHABP12	Larvae of <i>Galleria mellonella</i> infected by <i>A. baumannii</i>	The survival of larvae of <i>Galleria mellonella</i> increased to 75%	*	[47]
Phage (without definition, probably belongs to the <i>Siphoviridae</i> family)	Rat wound infection	100% inhibition of the pathogen	*	[48]
Cocktail of AB-Army1 and AB-Navy1-4	Murine wound infection	Inhibition of the pathogen	▲	[49]
Cocktail of AB-Navy1, AB-Navy4, AB-Navy71, AB-Navy97 and AbTP3Φ1	Human pancreatic pseudocyst	100% inhibition of the pathogen	*	[50]

Note: “*” – no data; “▲” – biofilm destruction.

A bacteriophage cocktail was successfully used against *A. baumannii* in the mouse model of a full-thickness dorsal infected wound: bacterial load in the wound decreased, thus preventing the spread of the infection and necrosis in surrounding tissues [49]. It was shown that the bacteriophages in the cocktail function in combination: the action of one of them is aimed at transferring the population of *A. baumannii* from the biofilm to the planktonic state, in which the cells are sensitive to other bacteriophages in the mixture. Although individual bacteriophages in that study exhibited some antibacterial properties, they were not as effective as a complex bacteriophage cocktail [49]. It should be noted that testing a phage cocktail against a collection of 92 clinical isolates of MDR *A. baumannii* revealed that only 10 strains were susceptible to therapy: this fact emphasizes that the spectrum of action of phages is very narrow, which must be taken into account when using them as therapeutic agents. So, it is optimal to use bacteriophages belonging to different families and having a wide range of hosts (different *A. baumannii* isolates) to prepare a phage cocktail.

A bacteriophage cocktail was successfully applied in the treatment of a diabetic patient with necrotizing pancreatitis complicated by a MDR *A. baumannii* infection [50]. Despite numerous courses of antibiotics (a combination of meropenem, tigecycline, and colistin), the condition of the 68-year-old patient deteriorated over a 4-month period. After the failure of antibiotic treatment, three phage cocktails with lytic activity against *A. baumannii* were prepared. Administration of these bacteriophages intravenously and percutaneously into the abscess cavities led to complete cure of the patient. It should be noted that during bacteriophage therapy, serial *A. baumannii* isolates with significantly reduced sensitivity to the introduced phages appeared; i.e., the *A. baumannii* population started to evolve in response to the selection pressure exerted by the phages. This aligns with the data [51] showing that during the use of bacteriophages some *A. baumannii* can acquire resistance and avoid lysis by bacteriophages. A bacteriophage loses its ability to effectively infect its bacterial host if receptors become unavailable, for example, due to the biofilm formation that prevents bacteriophage access to the cell membrane. Although the bacteriophage cocktail had lost its antibacterial activity, it still prevented the growth of *A. baumannii* with increased resistance to minocycline [50]. This antibiotic was added to bacteriophage therapy 4 days after the initial administration of the cocktail. The combinatorial activity existing between bacteriophages and conventional antibiotics was previously demonstrated in animal models [49]. Once the *A. baumannii* population is transferred to an encapsulated state, antibiotics can more readily

penetrate the bacterial membrane. Thus, in addition to potential therapeutic applications, bacteriophages can be used to eliminate *A. baumannii* biofilms. In this case, the combination of phages with antibiotics creates a situation in which bacteria are destroyed either by the bacteriophage, or by an antibiotic, or through their combined action.

It is assumed that bacteriophages can transfer the genetic elements that cause drug resistance and pathogenicity in bacteria. However, culturing on a bacterial isolate already present in the patient minimizes the risk of introducing exogenous genetic information that ensures increased virulence or resistance to antibiotics. In addition, the natural specificity of a bacteriophage to a bacterial type and even strain minimizes the potential for horizontal gene transfer, compared to more random plasmid conjugation or absorption of exogenous DNA in nature.

The numerous advances achieved in the treatment of MDR *A. baumannii* infections through local and systemic administration of bacteriophages, including in combination with antibiotics, highlight the potential of bacteriophages as relates to bacterial infections. However, bacteriophage therapy is difficult to standardize for mass production. In addition, the complete genomes of bacteriophages contain some genes with unknown functions: so, it is difficult to predict the long-term safety of bacteriophages [52].

Phage adsorption on a susceptible host cell is determined by a specific interaction between the phage's receptor-binding proteins located on the tail fibrils (with or without enzymatic activity) and a specific receptor on the cell surface. Exopolysaccharide depolymerases are responsible for partial destruction of the exopolysaccharides of the bacterial cell wall. These enzymes are shared components between bacteriophage spines and fibrils. Destruction of the bacterial capsule reduces biofilm formation and, as a result, antibiotic resistance: so, using bacteriophage depolymerases to eliminate the biofilm in the treatment of bacterial infections was proposed [53–55]. Various isolated phages against *A. baumannii* were shown to encode depolymerase, which successfully eliminates the capsular exopolysaccharide of the bacterium [53, 56, 57]. Thus, endolysin (LysAB3) of phage ϕ AB3 specific to *A. baumannii* effectively eliminates the biofilm associated with *A. baumannii* *in vitro* [58]. The antibacterial mechanism of LysAB3 may be associated with the ability of the structural region of amphiphilic peptide to enhance the permeability of the cytoplasmic membrane of *A. baumannii* by degradation of bacterial wall peptidoglycan.

Bacteriophages infecting *Acinetobacter* species are usually highly specific to the host strain [59]. From the

perspective of therapeutic application, the high specificity of bacteriophages can be considered as either a useful or a limiting factor. However, if the genes encoding the bacteriophage's fibril tail protein are replaced with genes from other phages, the new chimeric phage will lose its sensitivity to the original hosts and be able to lyse the new hosts. Thus, the chimeric phage ϕ AB1tf6 obtained by replacing the gene encoding the tail fiber protein of phage ϕ AB1 with the corresponding gene from ϕ AB6 has acquired the host range of the second bacteriophage [53].

The bacteriophage's tail spine proteins can be used as a bioengineering tool to obtain a glycoconjugate vaccine against *A. baumannii* [53, 60, 61]. Glycoconjugate vaccines are produced by conjugating an antibacterial exopolysaccharide to a carrier protein. The vaccine, based on oligosaccharide fragments, elicits a stronger immune response compared to that elicited by a vaccine based on whole bacterial exopolysaccharides, due to their heterogeneity. Chemical synthesis of polysaccharides is labor-intensive and has a low yield, while chemical hydrolysis of bacterial exopolysaccharides yields a mixture of heterogeneous oligosaccharide fragments. Using bacteriophage tail spine proteins that can hydrolyze the bacterial exopolysaccharide is a potential alternative to obtaining oligosaccharides of a given size. It has been shown that the tail spike protein of bacteriophage ϕ AB6 can depolymerize the exopolysaccharide of the *A. baumannii* strain 54149, with the formation of homogeneous oligosaccharide fragments that can be used as a platform for obtaining a glycoconjugate vaccine [60, 61].

Prophylactic vaccination

Prophylactic vaccination can be one of the alternative methods to combat bacterial infections [62]. A classic vaccine is a pharmaceutical product that stimulates the immune system, thus preventing pathogen development. To trigger a long-term immune response that includes both the innate and adaptive immune systems, the vaccine must resemble the pathogen but not cause the concomitant disease. In the initial developments of vaccines against *A. baumannii*, it was assumed that a lot of bacterial antigens must be included in the vaccine. It was believed that whole-cell vaccines could stimulate a response against multiple antigens, which would provide protection against a wide range of strains within a species. Thus, outer membrane vesicles of *A. baumannii* were successfully used as an antigen [63]. The inactivated whole-cell vaccine successfully protected mice against two clinical isolates of *A. baumannii*, including a resistant strain. Later, separate bacterial components were used to develop the vaccine. It was discovered using

a murine model that vaccination with a specific cell surface protein involved in the formation of a *A. baumannii* biofilm reduces the bacterial load in tissues and ensures high antibody titers [64].

The *A. baumannii* outer membrane proteins OmpA, Omp34 kDa, and OprC were shown to be effective in developing an antibacterial vaccine. A DNA vaccine consisting of plasmids encoding two proteins of the *A. baumannii* outer membrane, OmpA and Pal, was designed [65]. The OmpA protein is considered the most promising antigen for developing vaccines against *A. baumannii*, since it is a virulence factor involved in the pathogenesis of *A. baumannii* and shows high immunogenicity in animal models. In addition, OmpA is highly conserved among various strains; it is the most common protein identified in the outer membrane vesicles of *A. baumannii*. Pal is a peptidoglycan-associated cell wall lipoprotein that plays an important role in ensuring outer membrane integrity. A mouse model of pneumonia showed the significant efficacy of the DNA vaccine against an acute *A. baumannii* infection; effective cross-protection was observed when we immunized mice infected with clinical strains of *A. baumannii*.

Prophylactic vaccination and passive immunization can be very effective tools in preventing and treating the most common and serious infections caused by *A. baumannii*. However, only a few vaccines tested on animals have been included in clinical studies, and no vaccine against *A. baumannii* has yet been approved for human vaccination. In addition, the question remains: which population groups will benefit from prophylactic vaccination against *A. baumannii* and when should they be vaccinated?

Antimicrobial peptides

Antimicrobial peptides (AMPs) meet the definition of "antibiotics." They are formed by living organisms and exhibit an antibiotic effect against pathogens. One of the first antibiotics was lysozyme isolated from human tears and saliva by Alexander Fleming in the 1920s. In 1939, at the beginning of antibiotics science, gramicidins, peptide antibiotics of bacillary origin, were described. AMPs are now found in organisms belonging to all taxonomic groups. In most multicellular organisms, AMPs are the central element of the non-specific innate defense system; it is the first line of defense against an invasion by a wide range of pathogens [66–68]. This review considers a special group of antimicrobial peptides; namely, those formed in the human and animal bodies. These AMPs also meet the definition of "humoral factors of innate immunity" [69].

Natural antimicrobial peptides usually consist of 12–60 amino acid residues and contain cationic amino

Table 3. Summary of the data from studies of the use of antimicrobial peptides (AMPs)

Antimicrobial agent	Infection model	Efficiency inhibition of the infection	Antibiofilm activity	Reference
Histatin 5 (N)	<i>In vitro</i>	85–90% inhibition of the pathogen	–	[73]
LL37 (N), WLBU2 (S)	<i>In vitro</i>	Inhibition of the pathogen	Δ	[28]
1018 (N)	<i>In vitro</i>	Inhibition of the pathogen	▲, Δ	[74]
HBcARD-150-177C (M)	Mouse model of lung infection	The survival of mice increased to 62.5–80%	*	[75]
SAAP-148 (S)	<i>Ex vivo</i> mouse and <i>in vivo</i> human wound skin infection	100% inhibition of the pathogen	▲, Δ	[76]
K11 (S)	Murine wound infection	99% inhibition of the pathogen	*	[77]
N10 (S), NB2 (S)	<i>In vitro</i>	Inhibition of the pathogen	▲	[79]

Note: “N” – naturally occurring AMPs; “M” – modification of naturally occurring AMPs; “S” – synthetic AMPs; “–” – no activity; “” – no data; “▲” – biofilm destruction, “Δ” – prevention of biofilm formation.

acids, usually arginine and lysine residues. This allows AMPs to interact with negatively charged bacterial membranes and, in some cases, even penetrate them (translocate into host cells) due to a large electric potential gradient, which leads to bacterial cell lysis [70]. In addition to destroying the membranes, AMPs can interfere within intracellular processes, preventing the biosynthesis of nucleic acids, proteins, and cell walls. Furthermore, cell wall peptidoglycans, cytosolic RNAs, proteins, and cytosolic enzymes/chaperones can act as targets for AMPs [71].

Today, many of the AMPs of higher organisms are undergoing clinical trials as potential new antimicrobials, or as adjuncts to existing antibiotics in treatment regimens for infectious diseases [72]. Table 3 summarizes the results of a study of the ability of AMPs to inhibit infections caused by *A. baumannii*. Histatin 5 (Hst 5), a histidine-rich AMP isolated from human and higher primate saliva, was shown to exhibit strong bactericidal activity against ESKAPE pathogens [73]. The action of this AMP caused the death of 85–90% of *A. baumannii* cells, while Hst 5 showed no significant antibiofilm activity. Conjugation of Hst 5 with spermidine was found to increase the bactericidal activity of the peptide against *A. baumannii*. The results of testing of the natural peptide 1018 triggering the degradation of the important signaling nucleotide (p)ppGpp have been reported [74]. Treatment with peptide 1018 at concentrations having no effect on plankton cell growth fully prevented the formation of biofilms and led to the destruction

of mature biofilms in representative strains of both Gram-positive and Gram-negative pathogens, including *A. baumannii*. Low concentrations of peptide 1018 led to biofilm dispersal; higher concentrations caused the death of biofilm cells. Thus, the recognition and dispersal of bacterial membranes (without destroying the bacteria) can interfere with bacterial attachment to surfaces (such as medical implants or surgical sites) and contribute to the success of antimicrobial therapy.

In addition to natural AMPs, synthetic derivatives with improved activity have been proposed; natural AMPs were used as a reference template for their development. Chimeric AMPs created from two different AMPs were shown to improve antimicrobial activity. Other successful examples of AMPs modification include substitutions with D-amino acids, β-naphthylalanine, and α,α-dialkyl amino acids [75]. A panel of synthetic peptides was obtained based on human LL-37 AMP [76]. It was shown that peptide SAAP-148 suppresses MDR *A. baumannii* without causing resistance and prevents biofilm formation. A 4-h course of treatment with a hypromellose ointment containing SAAP-148 was shown to completely eliminate acute and biofilm-related *A. baumannii* infections in an *ex vivo* human wound infection model and an *in vivo* murine skin infection model. Synthetic peptide K11 (a hybrid of melittin, cecropin A1, and magainin 2) in subinhibitory concentrations exhibits antimicrobial activity against *A. baumannii* [77]. In addition, K11 can modulate oxidant and antioxidant levels, thereby pro-

moting wound tissue regeneration in mice. K11 mixed with carbopol hydrogel heals infected wounds thanks to the synergism of the antibacterial properties of AMP and the moisturizing properties of the gel. Thus, thanks to their dual bioactivity, AMPs can destroy an infection and simultaneously exhibit immunomodulatory properties. Therefore, AMPs are considered a promising therapeutic tool for treating skin and soft tissue infections.

The phage display technique is one of the approaches used to identify peptides with antibacterial properties [78]. This method was used to select peptides targeted to *A. baumannii* [79]. To search for antimicrobial peptides against *A. baumannii* growing either in planktonic or biofilm form, biopanning was performed using a peptide library on five XDR *A. baumannii* strains grown in a medium containing human blood (blood biopanning) and the biofilms formed by these strains (biofilm biopanning). Thus, a number of peptides specific to *A. baumannii* were detected. Among those, two peptides were selected based on the similarity of their amino acid composition to that of other known AMPs. Both peptides exhibited antibacterial activity against *A. baumannii* (MIC 500 µg/mL), as well as significant antimicrobial activity; the combination of these two peptides more effectively reduced the formation of a *A. baumannii* biofilm compared to each individual peptide [79].

However, despite the numerous successful results both *in vitro* and *in vivo*, new AMPs have not found clinical application, yet. Destruction of AMPs by tissue proteases and their cytotoxicity stands in the way of their introduction into clinical practice.

Antimicrobial photodynamic therapy

Antimicrobial photodynamic therapy, either *per se* or in combination with a photosensitizer, induces photooxidative stress, which causes microbial death. *In vitro* studies have shown that blue light is effective against both planktonic and biofilm-growth forms of all six ESKAPE pathogens, including *A. baumannii* [80]. This conclusion has also been confirmed through *in vivo* data. It was shown that the use of weakly penetrating blue light ($\lambda = 415 \pm 10$ nm) may be preferable for wound infections and the disinfection of a hospital environment. Bacterial biofilms were also highly susceptible to blue light. In general, antimicrobial photodynamic therapy is a promising approach to treating infections caused by ESKAPE pathogens, especially when applied topically.

Metal nanoparticles

Metal nanoparticles, especially silver and silver-containing compounds, have recently been of increas-

ing interest for managing bacterial infections. Silver nanoparticles (AgNPs) synthesized using physical, chemical, or biological methods release silver cations that disrupt electron transport and signal pathways or cause the formation of reactive oxygen species, which ultimately damage important biomolecules such as cell wall components, membranes, DNA, or proteins. Silver is an effective low-toxicity antimicrobial agent. A combination of AgNPs and antibiotics may be an effective solution to the problem of MDR *A. baumannii*; they can possibly be used at lower and less toxic doses compared to the drugs currently commonly used in clinical settings. In mice infected with carbapenem-resistant *A. baumannii*, synergistic antibacterial activity of AgNPs, in combination with polymyxin B, was detected; the survival rate was 60% compared to the control group receiving the antibiotic or AgNP alone [81]. Cobrado et al. [82] have recently reported that a burn unit contaminated with *A. baumannii* was successfully disinfected using an automated aerosolized hydrogen peroxide/silver cation dry-mist disinfection system.

Iron chelation therapy

Iron is an important cofactor in many processes occurring in bacterial cells; so, it is possible to view iron chelators and iron competitors as potential antibacterial agents. Chelation therapy is aimed at iron metabolism and achieving antibacterial activity by suppressing iron intake into cells. Pathogenic microorganisms have an effective mechanism for obtaining iron through using siderophores, low-molecular-weight compounds that bind iron [83]. The siderophore-iron complex binds to the corresponding receptors on the bacterial cell surface and is absorbed at places where iron is needed for intracellular metabolism. Most siderophores are high-affinity iron chelators whose affinity for Fe^{3+} is so high that they can use the host organism as a source of iron. Synthetic chelators have recently been developed to compete with the iron absorption systems of pathogenic microorganisms. The high efficiency of iron chelators (deferoxamine, deferiprone, Apo6619, and VK28) was evaluated against *A. baumannii* strains *in vitro* [84]. Synthetic iron chelators based on hydroxypyridinone ligands have been proposed as new bacteriostatic agents [83]. A number of new secondary/tertiary amine/amide chelators were obtained, and their antimicrobial properties were evaluated on the panel of microorganisms. Although it is an established fact that iron chelators can sequester iron and provide an alternative approach to treatment without the use of antibiotics, it is necessary to perform additional studies and characterize their *in vivo* effectiveness.

CONCLUSIONS

Antibiotics can be viewed as chemical weapons in the interspecific struggle between microorganisms that has unfolded over millions of years of evolution. Moreover, each time a new antibiotic has been introduced into clinical practice, bacteria have developed an appropriate complex resistance strategy. As a result of this endless tug of war, pathogens armed with multiple resistance mechanisms have emerged, such as the *A. baumannii* considered in this review. The successful survival of *A. baumannii* as an in-hospital pathogen is facilitated by its high adaptability due to mutability and its ability to “switch” its genomic structure by horizontal transfer of resistance genes, as well as its innate ability to form biofilms.

The spread of multidrug-resistant strains necessitates the development of new approaches to the

prevention and treatment of infections caused by *A. baumannii*, forcing us to search for alternative treatment methods that can be widely used in the future. The following methods have been proposed thus far: bacteriophage therapy, prophylactic vaccination, the use of antimicrobial peptides, photodynamic therapy, silver ion therapy, and chelate therapy. However, for each of these methods for preventing and treating the infections caused by MDR *A. baumannii*, there exist limitations that need to be addressed before these treatments can be applied in clinical practice.

In our review, we considered the existing research and prospects for expanding the means used to combat MDR *A. baumannii* strains. ●

This work was supported by the Russian Science Foundation (project no. 17-00-00393).

REFERENCES

1. Boucher H.W., Talbot G.H., Bradley J.S., Edwards J.E., Gilbert D., Rice L.B., Scheld M., Spellberg B., Bartlett J. // *Clin. Infect. Dis.* 2009. V. 48. № 1. P. 1–12.
2. Tacconelli E., Carrara E., Savoldi A., Harbarth S., Mendelson M., Monnet D.L., Pulcini C., Kahlmeter G., Kluytmans J., Carmeli Y., et al. // *Lancet Infect.* 2018. V. 18. P. 318–327.
3. Mulani M.S., Kamble E.E., Kumkar S.N., Tawre M.S., Pardi K.R. // *Front. Microbiol.* 2019. V. 10. № article 539. DOI: 10.3389/fmicb.2019.00539.
4. Nemeč A., Krizova L., Maixnerova M., van der Reijden T.J., Deschaght P., Passet V., Vanechoutte M., Brisse S., Dijkshoorn L. // *Res. Microbiol.* 2011. V. 162. P. 393–404.
5. Gonzalez-Villoria A.M., Valverde-Garduno V. // *J. Pathogens.* 2016. V. 2016. Article ID 7318075. P. 1–10.
6. Zapor M.J., Moran K.A. // *Curr. Opin. Infect. Dis.* 2005. V. 18. № 5. P. 395–399.
7. Turton J.F., Kaufmann M.E., Gill M.J., Pike R., Scott P.T., Fishbain J., Craft D., Deye G., Riddell S., Lindler L.E., et al. // *J. Clin. Microbiol.* 2006. V. 44. № 7. P. 2630–2634.
8. Howard A., O’Donoghue M., Feeney A., Sleator R.D. // *Virulence.* 2012. V. 3. P. 243–250.
9. Aarabi B. // *Neurosurgery.* 1987. V. 20. P. 610–616.
10. Joly-Guillou M.L., Bergogne-Berezin E., Vieu J.F. // *Presse Medicale.* 1990. V. 19. № 8. P. 357–361.
11. Petrosillo N., Drapeau C.M., Di Bella S. *Emerging Infectious Disease.* (Amsterdam). Elsevier. Acad. Press, 2014. Ch. 20. P. 255–272.
12. Vincent J.L., Rello J., Marshall J., Silva E., Anzueto A., Martin C.D., Moreno R., Lipman J., Gomersall C., Sakr Y., et al. // *J. Am. Med. Assoc.* 2009. V. 302. P. 2323–2329.
13. Beijerinck M.W. // *Proc. Royal Acad. Sci. (Amsterdam).* 1911. V. 13. P. 1066–1077.
14. Brisou J., Prevot A. // *Ann. l’Institut Pasteur.* 1954. V. 86. № 6. P. 722–728.
15. Baumann P., Doudoroff M., Stanier R.Y. // *J. Bacteriol.* 1968. V. 95. P. 1520–1541.
16. Bergey D.H., Buchanan R.E., Gibbons N.E., American Society for Microbiology. // *Bergey’s manual determinative bacteriology.* Baltimore: Williams & Wilkins Co., 1974. P. 1246.
17. Paton R., Miles R.S., Hood J., Amyes S.G., Miles R.S., Amyes S.G. // *Int. J. Antimicrob. Agents.* 1993. V. 2. № 2. P. 81–87.
18. Bouvet P.J., Grimont P.A. // *Int. J. Syst. Evol. Microbiol.* 1986. V. 36. № 2. P. 228–240.
19. Hejnar P., Kolár M., Hájek V. // *Acta Univ. Palacki. Olomuc. Fac. Med.* 1999. V. 142. P. 73–77.
20. World Health Organization (WHO). *Global Strategy for Containment of Antimicrobial Resistance.* Available online at: https://www.who.int/drugresistance/WHO_Global_Strategy.htm/ru/
21. Navon-Venezia S., Leavitt A., Carmeli Y. // *J. Antimicrob. Chemother.* 2007. V. 59. № 4. P. 772–774.
22. Transatlantic Taskforce on Antimicrobial Resistance: Progress report. Available online at: https://www.cdc.gov/drugresistance/pdf/tatfar-progress_report_2014.pdf
23. World Health Organization (WHO). *Global Strategy for Containment of Antimicrobial Resistance.* Available online at: <https://apps.who.int/iris/bitstream/handle/10665/254884/9789244509760-rus.pdf>
24. World Health Organization (WHO). *Global priority list of antibiotic-resistant bacteria to guide research, discovery, and development of new antibiotics.* Available online at: http://www.who.int/medicines/publications/WHO-PPL-Short_Summary_25Feb-ET_NM_WHO.pdf?ua=1.
25. Wright M.S., Haft D.H., Harkins D.M., Perez F., Hujer K.M., Bajaksouzian S., Benard M.F., Jacobs M.R., Bonomo R.A., Adams M.D. // *mBio.* 2014. V. 5. № 1. P. e00963–13.
26. Bjarnsholt T. // *APMIS Suppl.* 2013. V. 136. P. 1–51. DOI: 10.1111/apm.12099.
27. Batoni G., Maisetta G., Esin S. // *Biophys. Acta Biomembr.* 2016. V. 1858. P. 1044–1060.
28. Lin Q., Deslouches B., Montelaro R.C., Di Y.P. // *Int. J. Antimicrob. Agents.* 2018. V. 52. P. 667–672.
29. Nasr P. // *J. Hosp. Infect.* 2020. V. 104. № 1. P. 4–11.
30. Kotay S., Chai W., Guilford W., Barry K., Mathers A.J. // *Appl. Environ. Microbiol.* 2017. V. 83. P. e03327–16.
31. Garnacho-Montero J., Amaya-Villar R., Ferrandiz-Millon C., Diaz-Martin A., Lopez-Sanchez J.M., Gutier-

- rez-Pizarra A. // *Expert Rev. Anti. Infect. Ther.* 2015. V. 13. P. 769–777.
32. Geisinger E., Isberg R.R. // *PLoS Pathog.* 2015. V. 11. P. e1004691.
33. Tommasi R., Brown D.G., Walkup G.K., Manchester J.L., Miller A.A. // *Nat. Rev. Drug Discovery.* 2015. V. 14. P. 529–542.
34. Fournier P.E., Vallenet D., Barbe V., Audic S., Ogata H., Poirel L., Richet H., Robert C., Mangenot S., Abergel C., et al. // *PLoS Genet.* 2006. V. 2. № 1. P. e7.
35. Roca I., Espinal P., Vila-Farrés X., Vila J. // *Front. Microbiol.* 2012. V. 3. № article 148. DOI: 10.3389/fmicb.2012.00148.
36. Bonnin R.A., Poirel L., Nordmann P. // *Future Microbiol.* 2014. V. 9. P. 33–41.
37. Bernal P., Molina-Santiago C., Daddaoua A., Llamas M.A. // *Microb. Biotechnol.* 2013. V. 6. P. 445–449.
38. Whitehead N.A., Barnard A.M., Slater H., Simpson N.J., Salmond G.P. // *FEMS Microbiol. Rev.* 2001. V. 25. № 4. P. 365–404.
39. Defraigne V., Verstraete L., van Bambeke F., Anantharajah A., Townsend E.M., Ramage G., Corbau R., Marchand A., Chaltin P., Fauvart M., et al. // *Front. Microbiol.* 2017. V. 8. № article 2585. DOI: 10.3389/fmicb.2017.02585.
40. Efimenko T.A., Terekhova L.P., Efremenkova O.V. // *Antibiotiki i Khimioterapiya.* 2019. №5–6. P. 64–68. (In Russian)
41. Comeau A.M., Hatfull G.F., Krisch H.M., Lindell D., Mann N.H., Prangishvili D. // *Res. Microbiol.* 2008. V. 159. № 5. P. 306–313.
42. Pelfrene E., Willebrand E., Cavaleiro Sanches A., Sebris Z., Cavaleri M. // *J. Antimicrob. Chemother.* 2016. V. 71. P. 2071–2074.
43. Ghajavand H., Esfahani B.N., Havaei A., Fazeli H., Jafari R., Moghim S. // *Res. Pharm. Sci.* 2017. V. 12. P. 373–380.
44. Fedotova O.S., Zakharova Yu.A. // *Medical almanac.* 2018. V.1. P. 126–129. (In Russian)
45. Hua Y., Luo T., Yang Y., Dong D., Wang R., Wang Y., Xu M., Guo X., Hu F., He P. // *Front. Microbiol.* 2018. V. 8. № article 2659. DOI: 10.3389/fmicb.2017.02659.
46. Cha K., Oh H.K., Jang J.Y., Jo Y., Kim W.K., Ha G.U., Ko K.S., Myung H. // *Front. Microbiol.* 2018. V. 9. № article 696. DOI: 10.3389/fmicb.2018.00696.
47. Zhou W., Feng Y., Zong Z. // *Front. Microbiol.* 2018. V. 9. № article 850. DOI: 10.3389/fmicb.2018.00850.
48. Shivaswamy V.C., Kalasuramath S.B., Sadanand C.K., Basavaraju A.K., Ginnavaram V., Bille S., Ukken S.S., Pushparaj U.N. // *Microb. Drug Resist.* 2015. V. 21. P. 171–177.
49. Regeimbal J.M., Jacobs A.C., Corey B.W., Henry M.S., Thompson M.G., Pavlicek R.L., Quinones J., Hannah R.M., Ghebremedhin M., Crane N.J., et al. // *Antimicrob. Agents Chemother.* 2016. V. 60. P. 5806–5816.
50. Schooley R.T., Biswas B., Gill J.J., Hernandez-Morales A., Lancaster J., Lessor L., Barr J.J., Reed S.L., Rohwer F., Benler S., et al. // *Antimicrob. Agents Chemother.* 2017. V. 61. № 10. P. e00954–17.
51. Liu Y., Mi Z., Niu W., An X., Yuan X., Liu H., Wang Y., Feng Y., Huang Y., Zhang X., et al. // *Future Microbiol.* 2016. V. 11. P. 1383–1393.
52. Hatfull G.F. // *Bacteriophage Genomics. Curr. Opin. Microbiol.* 2008. V. 11. № 5. P. 447–453.
53. Lai M.J., Chang K.C., Huang S.W., Luo C.H., Chiou P.Y., Wu C.C., Lin N.T. // *PLoS One.* 2016. V. 11. № 4. № article e0153361. DOI: 10.1371/journal.pone.0153361.
54. Lin H., Paff M.L., Molineux I.J., Bull J.J. // *Front. Microbiol.* 2017. V. 8. № article 2257. DOI: 10.3389/fmicb.2017.02257.
55. Pan Y.J., Lin T.L., Chen Y.Y., Lai P.H., Tsai Y.T., Hsu C.R., Hsieh P.F., Lin Y.T., Wang J.T. // *Microb. Biotechnol.* 2019. V. 12. № 3. P. 472–486.
56. Hernandez-Morales A.C., Lessor L.L., Wood T.L., Migl D., Mijalis E.M., Cahill J., Russell W.K., Young R.F., Gill J.J. // *J. Virol.* 2018. V. 92. № 6. № article e01064–17. DOI: 10.1128/JVI.01064-17.
57. Liu Y., Leung S.S.Y., Guo Y., Zhao L., Jiang N., Mi L., Li P., Wang C., Qin Y., Mi Z., et al. // *Front. Microbiol.* 2019. V. 10. № article 545. DOI: 10.3389/fmicb.2019.00545.
58. Zhang J., Xu L.L., Gan D., Zhang X. // *Clin. Lab.* 2018. V. 64. P. 1021–1030.
59. Lin N.T., Chiou P.Y., Chang K.C., Chen L.K., Lai M.J. // *Res. Microbiol.* 2010. V. 161. P. 308–314.
60. Lee I.M., Tu I.F., Yang F.L., Ko T.P., Liao J.H., Lin N.T., Wu C.Y., Ren C.T., Wang A.H.J., Chang C.M., et al. // *Sci. Rep.* 2017. V. 7. № article 42711. DOI:10.1038/srep42711.
61. Lee I.M., Yang F.L., Chen T.L., Liao K.S., Ren C.T., Lin N.T., Chang Y.P., Wu C.Y., Wu S.H. // *J. Am. Chem. Soc.* 2018. V. 140. P. 8639–8643.
62. Shahid F., Ashraf S.T., Ali A. // *Methods Mol. Biol.* 2019. V. 1946. P. 329–336.
63. McConnell M.J., Rumbo C., Bou G., Pachón J. // *Vaccine.* 2011. V. 29. P. 5705–5710.
64. Fattahian Y., Rasooli I., Mousavi Gargari S.L., Rahbar M.R., Darvish Alipour Astaneh S., Amani J. // *Microb. Pathog.* 2011. V. 51. P. 402–406.
65. Lei L., Yang F., Zou J., Jing H., Zhang J., Xu W., Zou Q., Zhang J., Wang X. // *Mol. Biol. Rep.* 2019. V. 46. P. 5397–5408.
66. Phoenix D.A., Dennison S.R., Harris F. // *Antimicrobial Peptides: Their History, Evolution, and Functional Promiscuity / Singapore: Wiley-VCH Verlag GmbH & Co., 2013. P. 231.*
67. Kang H., Kim C., Seo C.H., Park Y. // *J. Microbiol.* 2017. V. 55. P. 1–12.
68. Musin Kh.G. // *Infektsiya i immunitet.* 2018. V. 8. № 3. P. 295–308. (In Russian)
69. Zharkova M.S., Orlov D.S., Kokryakov V.N., Shamova O.V. // *Vestnik SPbGU.* 2014. Iss. 1, P. 98–114. (In Russian)
70. Pfalzgraff A., Brandenburg K., Weindl G. // *Front. Pharmacol.* 2018. V. 9. № article 281. DOI: 10.3389/fphar.2018.00281.
71. Gaglione R., Dell’Olmo E., Bosso A., Chino M., Pane K., Ascione F., Itri F., Caserta S., Amoresano A., Lombardi A., et al. // *Biochem. Pharmacol.* 2017. V. 130. P. 34–50.
72. Ma Y.X., Wang C.Y., Li Y.Y., Li J., Wan Q.Q., Chen J.H., Tay F.R., Niu L.N. // *Adv. Sci. (Weinh).* 2019. V. 7. № 1. P. 1901872.
73. Du H., Puri S., McCall A., Norris H. L., Russo T., Edgerton M. // *Front. Cell. Infect. Microbiol.* 2017. V. 7. № article 41. DOI: 10.3389/fcimb.2017.00041.
74. de la Fuente-Nunez C., Reffuveille F., Haney E.F., Straus S.K., Hancock R.E. // *PLoS Pathog.* 2014. V. 10. № 5. P. e1004152.
75. Chen H.L., Su P.Y., Kuo S.C., Lauderdale T.L.Y., Shih C. // *Front. Microbiol.* 2018. V. 9. № article 1440. DOI: 10.3389/fmicb.2018.01440.
76. de Breij A., Riool M., Cordfunke R.A., Malanovic N., de Boer L., Koning R.I., Ravensbergen E., Franken M., van der Heijde T., Boekema B.K., et al. // *Sci. Transl. Med.* 2018. V. 10. № 423. P. eaan4044.
77. Rishi P., Vashist T., Sharma A., Kaur A., Kaur A., Kaur N., Kaur I. P., Tewari R. // *Pathog. Dis.* 2018. V. 76. № article 7. DOI: 10.1093/femspd/fty072.

REVIEWS

78. Huang J.X., Bishop-Hurley S.L., Cooper M.A. // *Antimicrob. Agents Chemother.* 2012. V. 56. P. 4569–4582.
79. Irani N., Basardeh E., Samiee F., Fateh A., Shooraj F., Rahimi A., Shahcheraghi F., Vaziri F., Masoumi M., Pazhouhandeh M., et al. // *Microb. Pathog.* 2018. V. 121. P. 310–317.
80. Halstead F.D., Thwaite J.E., Burt R., Laws T.R., Raguse M., Moeller R., Webber M.A., Oppenheim B.A. // *Appl. Environ. Microbiol.* 2016. V. 82. P. 4006–4016.
81. Wan G., Ruan L., Yin Y., Yang T., Ge M., Cheng X. // *Int. J. Nanomed.* 2016. V. 11. P. 3789–3800.
82. Cobrado L., Pinto S. A., Pina-Vaz C., Rodrigues A. // *Surg Infect (Larchmt)*. 2018. V. 19. P. 541–543.
83. Workman D.G., Hunter M., Wang S., Brandel J., Hubscher V., Dover L.G., Tétard D. // *Bioorganic Chem.* 2020. V. 95. № article 103465. DOI: 10.1016/j.bioorg.2019.103465.
84. Thompson M.G., Corey B.W., Si Yuan., Craft D.W., Zurawski D.V. // *Antimicrob. Agents Chemother.* 2012. V. 56. P. 5419–5421.

Infectious Plant Diseases: Etiology, Current Status, Problems and Prospects in Plant Protection

P. A. Nazarov^{1,2,3*}, D. N. Baleev⁴, M. I. Ivanova⁵, L. M. Sokolova⁵, M. V. Karakozova⁶

¹Belozersky Institute of Physico-Chemical Biology, Lomonosov Moscow State University, Moscow, 119991 Russia

²Moscow Institute of Physics and Technology, Dolgoprudny, Moscow region, 141701 Russia

³Federal Scientific Vegetable Center, VNISSOK, Moscow region, 143080 Russia

⁴All-Russian Scientific Research Institute of Medicinal and Aromatic Plants, Moscow, 117216 Russia

⁵All-Russian Scientific Research Institute of Vegetable Growing, Branch of the Federal Scientific Vegetable Center, Vereya, Moscow region, 140153 Russia

⁶Center of Life Sciences, Skolkovo Institute of Science and Technology, Moscow, 121205 Russia

*E-mail: nazarovpa@gmail.com

Received May 25, 2020; in final form, June 30, 2020

DOI: 10.32607/actanaturae.11026

Copyright © 2020 National Research University Higher School of Economics. This is an open access article distributed under the Creative Commons Attribution License, which permits unrestricted use, distribution, and reproduction in any medium, provided the original work is properly cited.

ABSTRACT In recent years, there has been an increase in the number of diseases caused by bacterial, fungal, and viral infections. Infections affect plants at different stages of agricultural production. Depending on weather conditions and the phytosanitary condition of crops, the prevalence of diseases can reach 70–80% of the total plant population, and the yield can decrease in some cases down to 80–98%. Plants have innate cellular immunity, but specific phytopathogens have an ability to evade that immunity. This article examined phytopathogens of viral, fungal, and bacterial nature and explored the concepts of modern plant protection, methods of chemical, biological, and agrotechnical control, as well as modern methods used for identifying phytopathogens.

KEYWORDS bacteria, fungi, viruses, pesticides, phytopathogen, selection, disease resistance, integrated pest management, biological control, agrotechnical control, plant immunity.

ABBREVIATIONS IPM – integrated pest management, RNA – ribonucleic acid, DNA – deoxyribonucleic acid.

INTRODUCTION

A plant is considered to be susceptible to infection if environmental factors alter its physiological processes thus resulting in a disrupted structure, growth, functions, or other parameters. Plant diseases are classified as infectious and non-infectious depending on the nature of a causative agent. The symptoms of the disease may depend on its cause, nature, and the location of the impact site. The factors causing plant diseases can be of biotic and abiotic nature. Non-infectious diseases are caused by unfavorable growth conditions; they are not transmitted from a diseased plant to a healthy one. Infectious diseases, on the contrary, can spread from one susceptible host to another, since the infectious agent can reproduce in the plant or on its surface.

The signs of plant diseases include wilting, spotting (necrosis), mold, pustules, rot, hypertrophy and hyperplasia (overgrowth), deformation, mummification, discoloration, and destruction of the affected tissue.

Wilting results from the loss of turgor pressure in the cells and tissues. It is caused by both abiotic and biotic factors. Spotting is mostly associated with the partial death of plant tissues due to biotic factors. Mold and pustules occur as a result of fungal damage to a plant. Rot leads to both the death of intracellular contents (bacterial wet or fungal dry rot) and destruction of the intercellular substance and cell membrane (fungal dry rot). Hypertrophy and hyperplasia represent an excessive growth and proliferation of the affected tissue caused by pathogens. Deformations (leaf wrinkling, twisting, and curling; threadlike leaves, fruit ugliness, and double-floweredness) can be caused by various biotic and abiotic factors due to an outflow of the products of photosynthesis, uneven intake of nutrients by the plant, or uneven growth of various tissue elements. In mummification, plant organs are damaged by the fungal mycelium, which leads to plant shrinkage, darkening, or compaction. Color changes usually occur due to chloroplast dysfunction and low content of chloro-

phyll in the leaves, which manifests itself in the light color of some leaf areas (mosaic discoloration) or the entire leaf (chlorosis) [1, 2].

Infectious agents can spread through the air, with water, be transmitted by animals, humans, and remain infectious for many months or years. The natural reservoirs of infectious agents are soil, water, and animals: especially insects.

Infectious plant diseases are mainly caused by pathogenic organisms such as fungi, bacteria, viruses, protozoa, as well as insects and parasitic plants [1]. With the development of agriculture, infectious plant diseases have become an increasingly significant factor affecting crop yield and economic efficiency. In the field environment, each plant cultivated as a monoculture has uniform conditions and requirements for planting, care, and harvesting, which leads to higher yields and lower production costs than in polyculture [3]. Over the past half century, the use of modern technologies, including cultivation of monocultures, has allowed us to reduce the amount of additional land needed for food production. However, growing the same crop in the same location year after year depletes the soil and renders it unable to ensure healthy plant growth. Another crucial issue is the susceptibility of monocultures to infectious diseases. Losses can amount to up to 30% even at the stage of storage, transportation, and distribution to the consumer (*Fig. 1*) [4, 5]. Therefore, it is necessary to arrest or prevent the development of infectious diseases at all stages of crop production: starting from seed handling technologies and ending with the delivery and storage of the product on store shelves and in consumers' homes. This review summarizes existing data on the causes and pathogenetic mechanisms of infectious plant diseases caused by viruses, bacteria, and fungi that affect major agricultural crops, including cereals, vegetables, and industrial crops. The article considers the current status, as well as the problems and prospects of plant protection.

PLANT IMMUNITY AND MECHANISMS FOR ITS EVASION

Plants typically are resistant to non-specific pathogens thanks to the presence of a waxy cuticle covering the epidermal cell layer and the constant synthesis of various antimicrobial compounds. Specific pathogens use a variety of strategies to penetrate plants, which often render such protection ineffective. Fungi can penetrate directly into epidermal cells or form hyphae over plant cells and between them, which does not require special structures or conditions. Meanwhile, bacterial and viral infections often require either damaged tissues, specialized structures (e.g., stomata) for entering the cell, or a specific carrier (vector). The latter is usually an insect, a fungus, or protozoa. How does plant infection

with phytopathogens occur? In order to understand this, it is important to keep in mind that, unlike animals, plants rely on the innate immunity of each cell and systemic signals emanating from the sites of the infection and not on mobile defense cells and the somatic adaptive immune system. Moreover, an infection by pathogenic microorganisms is not always successful because of the structural changes in the cell wall or programmed cell death.

Plants have so-called trichomes: outgrowths of the epidermis that prevent pathogen growth and penetration. Trichomes may contain antimicrobial compounds or exert an inhibitory effect on the microbial hydrolytic enzymes involved in cell wall damage. The role of the cell wall cannot be overestimated: it is the first obstacle that pathogenic microorganisms must evade; successful protection at this line of defense is most effective against non-specific pathogens. The cell wall consists of cellulose microfibrils and hemicellulose; it is reinforced with lignin and contains a significant amount of proteins that perform structural and enzymatic functions [6]. The heterogeneity of the structure of the plant cell wall forces pathogens to use various strategies to penetrate it.

Antimicrobial plant compounds, which contain low-molecular-weight non-protein substances, are divided into two groups: phytoanticipins and phytoalexins. Phytoanticipins, such as saponins, phenylpropanoids, alkaloids, cyanogenic glycosides, and glucosinolates, are antimicrobial compounds pre-synthesized by plants. Phytoalexins are formed in response to a pathogenic attack and include various phenylpropanoids, alkaloids, and terpenes. An overlap between these groups of antimicrobial agents is explained by the fact that the phytoalexins of some plants can act as phytoanticipins in others [7]. In addition, small RNAs regulate the expression of a wide range of genes in plants and comprise natural immunity against viruses [8]. Plants can also absorb and process exogenous hairpin double-stranded RNAs (dsRNAs) to suppress the genes responsible for the life maintenance and virulence of viruses pathogenic to plants, fungi, and insects [9]. Aspartate-specific apoptotic proteases (phytaspartases), which induce apoptosis, the process of programmed cell death, play an important role in plant defense [10].

Plants have two types of immune system. The first one uses transmembrane pattern recognition receptors that respond to slowly evolving microbial or pathogen-associated molecular patterns, while the second one acts mainly inside the cell using the polymorphic protein products encoded by most disease resistance (R) genes [11].

Plant R genes interact with the *avr* (avirulence) gene products of the corresponding pathogens. In

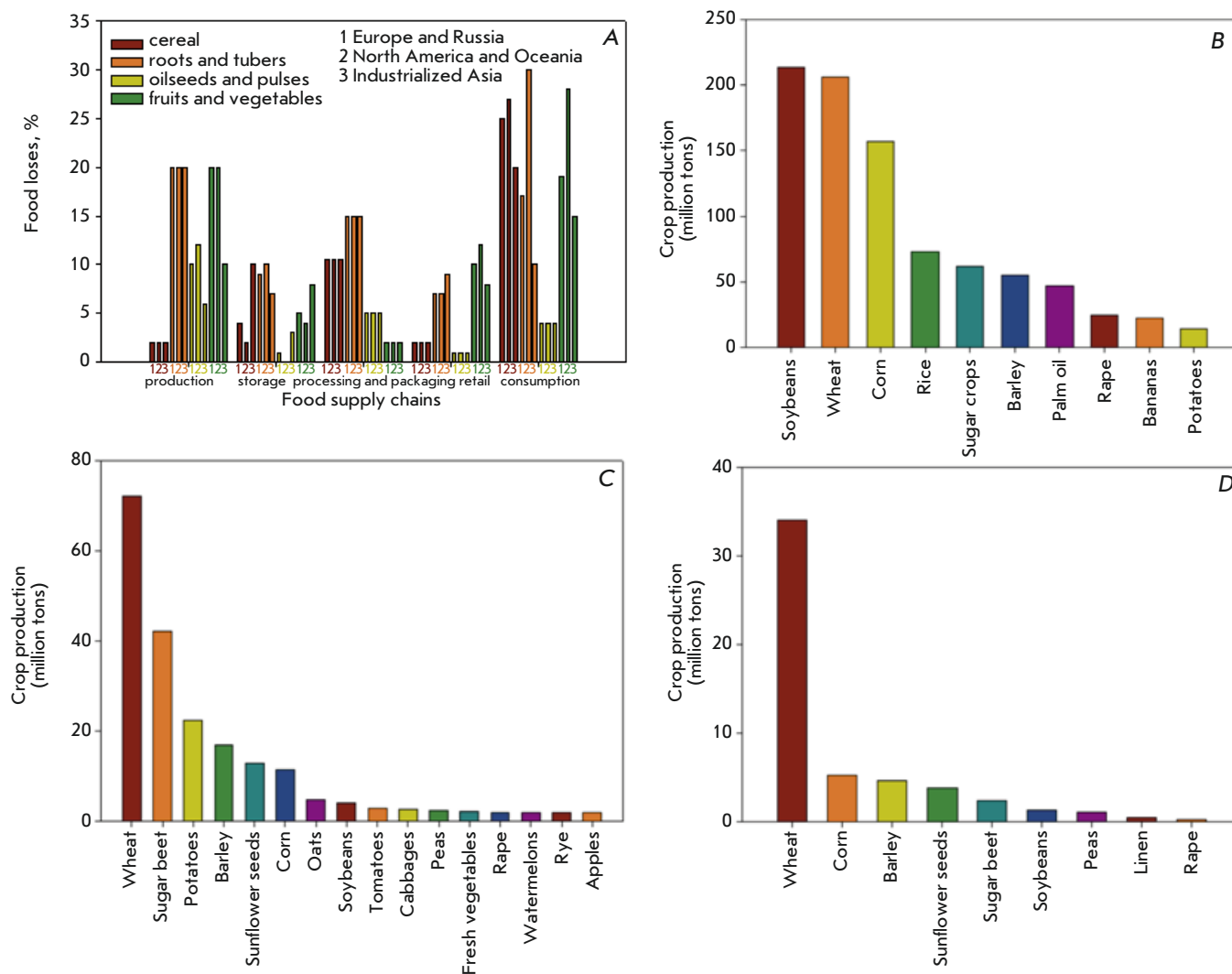


Fig. 1. A - crop losses in industrialized countries (medium and high per capita income) at each stage of the production process, starting from cultivation and ending with consumption by households. The results present data for three regions: 1 – Europe (including Russia), 2 – North America and Oceania (USA, Canada, Australia, and New Zealand) and 3 – Industrial Asia (Japan, China, South Korea). Losses are calculated by weight as a percentage of the total mass of the product at the production stage [4]. B - top 10 most grown crops in the world (by import). C - the most grown plant crops in Russia. D - the main exported plant products from Russia [5]

the presence of the corresponding R gene encoding a receptor that triggers the defense response cascade, the receptor recognizes the *avr* gene product and the plant exhibits a resistance phenotype. For protection against bacterial, viral, and fungal infections, as well as against insects, plants encode only eight classes of the R gene products [12] that trigger the downstream reaction cascade, which indicates degeneracy of the plant immune system. The number of R genes in the genome can amount to about 100, which is clearly not

enough to recognize all possible pathogens. Apparently, recognition of pathogens by the plant immune system is also of a degenerative nature [13].

The general mechanism of protection against pathogens is, apparently, as follows: during the first phase of an infection, receptors recognize pathogen-associated molecular structures (for instance, flagellin) and trigger an immune response to prevent colonization, which leads to the elimination of a non-specific infection. A specific pathogen produces effector molecules that

interfere with the molecules of the immune response, which triggers the so-called effector-mediated susceptibility in susceptible plants. In resistant plants, the R gene products recognize effectors, with further formation of effector-mediated resistance, which can trigger a hypersensitivity (programmed cell death) response in the pathogen-infected area [13]. During the course of evolution, pathogens have developed several strategies to suppress plant defense responses, such as altering the programmed cell death pathway, inhibiting protective compounds in the cell wall, as well as changing the hormonal status of plants and the expression pattern of defense genes [14]. However, the products of R defense genes against a viral infection can trigger a series of responses at once. For instance, the defense against potato virus X first starts with the inhibition of viral replication in the absence of a hypersensitivity reaction, while overexpression of the *avr* gene induces a hypersensitivity reaction, which renders the plant extremely resistant to this virus [15].

Plants can develop the so-called acquired resistance if the infection that causes resistance in one part of the plant spreads to other parts. This fact indicates that the signaling molecules can move from the affected area to other cells and enhance immunity to the previously encountered pathogen. It should be noted that acquired resistance is not a *de novo* acquired resistance but an activation of the existing resistance genes in response to a pathogenic attack. The cells accumulate salicylic acid and the various proteins associated with pathogenesis (e.g., chitinase). Such acquired resistance is of a temporary nature and can be both systemic and local [16].

Symbiotic bacteria colonizing the rhizosphere antagonize soil pathogens through various mechanisms: siderophores suppress plant pathogens by competing for iron; antibiotics suppress competing microorganisms, while chitinases and glucanases lyse microbial cells. Moreover, as a result of symbiosis with bacteria, plants can develop another, extremely peculiar type of resistance: induced systemic resistance, which is also mediated by salicylic acid, ethylene, jasmonic acid, and lipopolysaccharides. In contrast to acquired systemic resistance, induced systemic resistance provides non-specific protection, has no dose-dependent correlation with the effect, does not affect the pathogen directly, and does not depend on the proteins associated with pathogenesis [16]. Instead, it is determined by the plant genotype and can cause changes in plant metabolism, leading to a general increase in resistance [16].

Thus, understanding the mechanisms of plant defense and the pathways utilized by phytopathogens to overcome that defense allows one to devise a systematic approach to plant protection.

THE MOST SIGNIFICANT PHYTOPATHOGENS

Viruses and viroids

Viruses are non-cellular infectious agents that can only replicate in living cells. Viruses infect all types of organisms, from plants and animals to bacteria and archaea [17]. They can be integrated into the host's genome and remain there as an inactive provirus or actively replicate and regulate the host's biosynthesis processes. The suppression of viral gene transcription can lead to a latent infection [18]. Plant viruses mainly come in the form of single-stranded (ss) and double-stranded (ds) RNA viruses, as well as single-stranded and DNA-containing retroviruses [17]. Due to a wide diversity of their genetic material, the reproductive cycle and life pattern often vary from virus to virus (*Fig. 2A*). Viruses are composed of a nucleic acid molecule and a protective protein coat (capsid). Capsid can sometimes contain a combination of proteins and lipids, which form a lipoprotein membrane. The typical size of a plant virus is 30 nm [19].

The virion enters the cytoplasm of the plant cell via passive transport through wounds caused by mechanical damage to the cuticle and cell wall, since it is unable to pass through these structures on its own. Upon entering the cell, the virus uncoats. DNA-containing viruses also need to penetrate the nucleus in order to start transcription and mRNA synthesis. All viruses encode at least two types of proteins: replication proteins, which are required for the synthesis of nucleic acid, and structural proteins, which form the capsid. In some cases, there are also proteins that are responsible for virion motility; they ensure transport of virus particles between the plant cells. Viral replication proteins bind to cellular proteins to form a complex that produces multiple copies of the viral genome which interact with structural proteins to form new virions, which are then released from the cell. This is the standard viral life cycle.

Plant viruses can be transmitted vertically (from parents to offspring) and horizontally (from diseased plants to healthy ones). Viruses utilize small intercellular channels called plasmodesmata to penetrate neighboring cells (*Fig. 2B*). Viruses often express the proteins that ensure virion motility by modifying channels to facilitate the transmission of the infection to a neighboring cell [20]. This is how a local infection of a plant takes place. In order to infect an entire plant, a virus must enter its vascular system, where it then moves passively through the sieve tubes of the phloem with the flow of substances: this is how it can infect cells distant from the primary site of the infection [19, 20].

Some viruses are very stable and resistant to heat, can remain viable for a long time in plant cells and the

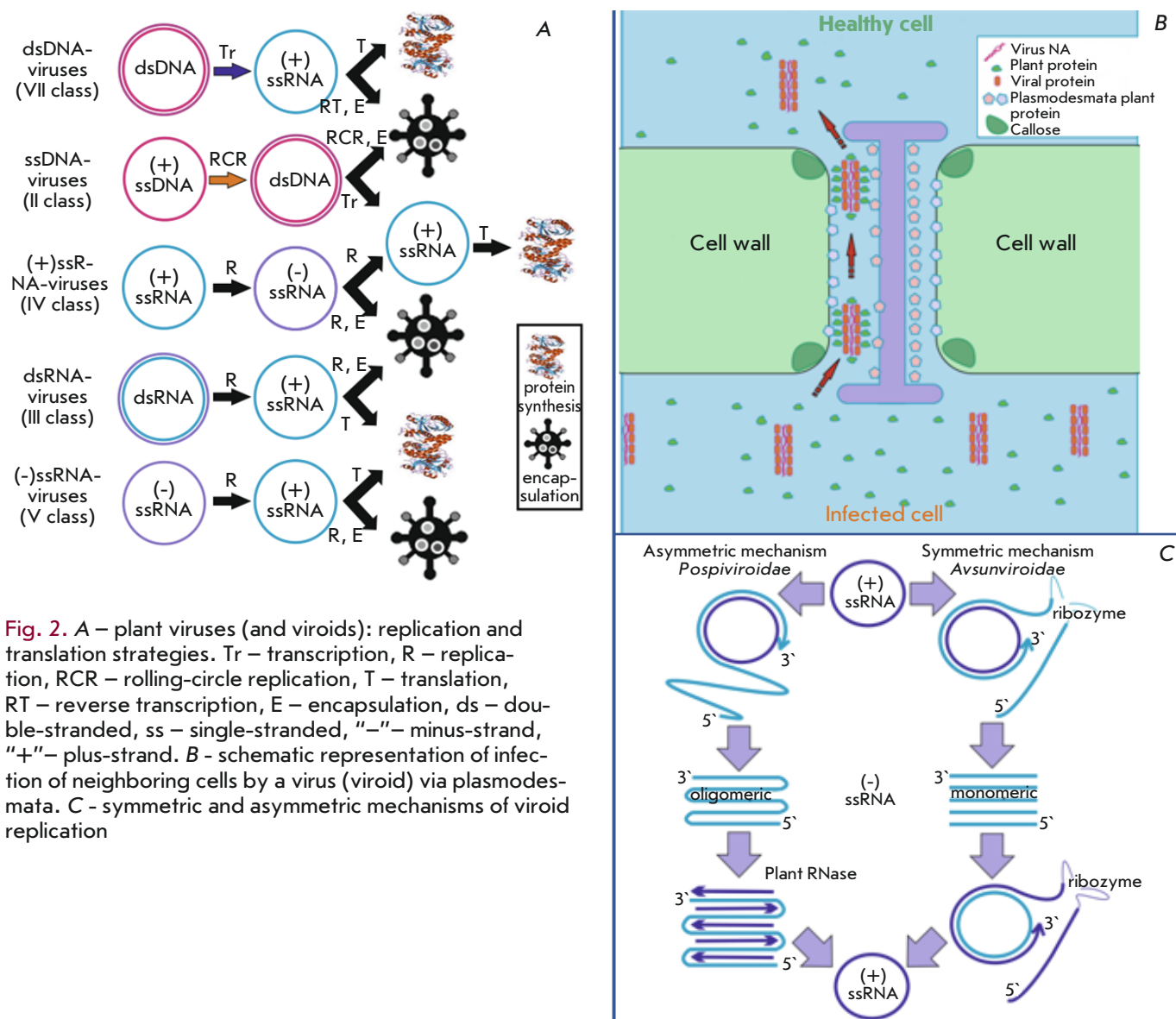


Fig. 2. A – plant viruses (and viroids): replication and translation strategies. Tr – transcription, R – replication, RCR – rolling-circle replication, T – translation, RT – reverse transcription, E – encapsulation, ds – double-stranded, ss – single-stranded, “-” – minus-strand, “+” – plus-strand. B - schematic representation of infection of neighboring cells by a virus (viroid) via plasmodesmata. C - symmetric and asymmetric mechanisms of viroid replication

products derived from them [21, 22], and can spread through passive mechanical transport from one plant to another [23]. However, most plant viruses actively spread from infected plants to healthy ones using a carrier organism (vector). Carriers are divided into a mechanical vector, in which the agent does not propagate, and a biological one, in which part of the viral life cycle takes place [24]. The main vectors of plant viruses are arthropods, nematodes, and fungi that feed on plants [25].

Plant viruses pose a serious threat to a wide range of crops, while the economic losses caused by viruses are second only to the losses caused by other pathogens [26]. Moreover, some viruses can infect more than 1,000 different plant species comprising more than 85

families [27]. In the majority of subtropical and tropical regions, a viral infection can lead to a loss of up to 98% of the crop [28]. Viruses manifest themselves in a different way depending on the stage of crop production: they can inflict colossal damage at the stage of crop growth, while at the stage of harvesting, storage, and transportation, the damage from a viral infection is minimal. It should be also noted that, in some cases, plants are found infected with viruses in the absence of any obvious symptoms [29].

The symptoms of viral diseases can be divided into five main types: growth suppression (reduced growth of the entire plant or its leading shoots); discoloration (mosaic, chlorotic rings, leaf chlorosis, variegation); deformations (leaf wrinkling, corrugation, threadlike

leaves); necrosis; and impaired reproduction (flower sterility, parthenocarpy, shedding of flowers and ovaries) [2].

There is another type of infectious agents: viroids, which are circular RNAs that cause various diseases in plants and animals. Taxonomically, they belong to viruses (families *Pospiviroidae* and *Avsunviroidae*). In contrast to viruses, viroids lack a protein envelope (capsid) and present covalently linked ssRNA molecules 200–500 nucleotides long, which is 50–80 times shorter than the viral genome. Viroids do not encode proteins and cannot replicate autonomously. It is considered that the viroid can employ the DNA-dependent RNA polymerase, endoribonuclease, and DNA ligase 1 (which is usually silent) of the host cell for its replication [30]. Viroids replicate via a rolling-circle mechanism, with members of the families *Pospiviroidae* and *Avsunviroidae* replicating through an asymmetric and symmetric pathway, respectively (*Fig. 2C*). The molecular mechanism of the pathogenic action of viroids is not fully understood. It is believed that viroids can alter the phosphorylation state of gene products via binding to cellular kinases [31], affect the expression of the genes associated with growth, stress, development, and protection [32], induce the proteins associated with pathogenesis during an infection [33], cause post-transcriptional suppression of gene expression by RNA interference, impair splicing [34], and induce demethylation of rRNA genes. It is surprising that the substitution of one nucleotide at a certain position alters the pathogenicity of the viroid significantly [35]. The RNA molecule of *Pospiviroidae* family members has five domains: a central domain (C) containing the central, conserved region, which plays an important role in viroid replication; a pathogenicity domain (P) implicated in the manifestation of disease symptoms; a variable domain (V), which is, apparently, responsible for viroid adaptation; and the transport domains T1 and T2 (in cases of co-infection with two viroids, they can exchange with these domains, which can contribute to their evolution). Viroids of the family *Avsunviroidae* lack the central conserved region but contain the sequences involved in the formation of the ribozyme structures necessary for self-cleavage of RNA strands [36].

The main symptoms of viroid diseases are reduced growth of the entire plant or its parts, discoloration (chlorosis, anthocyanosis), and deformation of various organs [2].

Thus, viruses and viroids represent a rather large group of pathogens that cause plant diseases and can result in serious damage to crops in the absence of management and preventive measures, especially when infected at early stages of plant growth.

Bacteria and phytoplasmas

Bacteria are found almost everywhere and can be pathogenic to animals, plants, and fungi [37]. Bacterial genetic information is encoded in the DNA in the form of a chromosome; more than one chromosome can be found in a cell. A bacterial cell can contain extrachromosomal mobile genetic elements: plasmids that can carry important virulence factors or, on the contrary, biological control factors. Bacteria can also contain a prophage, which represents bacteriophage DNA integrated into the genome. Most bacteria divide by binary fission, usually with simultaneous duplication of both chromosomal DNA and extrachromosomal elements. Division of a bacterial cell requires the presence of the membrane potential [38]. Bacteria can contain more than one plasmid, since some of them can be lost during division. For instance, *Pantoea stewartii* can harbor up to 13 different plasmids [39]. Although bacteria usually transfer plasmids within their population [40], horizontal transfer of genetic information remains quite common in the prokaryotic world.

Bacteria have a cell membrane which separates the cytoplasm from the external environment. Bacteria are divided into Gram-positive and Gram-negative organisms depending on the cell wall structure [41]. The cell wall of Gram-positive bacteria consists of a membrane and a thick peptidoglycan layer. The main component of the latter is multilayered murein. Peptidoglycan also contains proteins, lipids, and teichoic and teichuronic acids. The cell wall of Gram-negative bacteria has two membranes with a peptidoglycan layer between them. The outer membrane contains lipopolysaccharides and porins but lacks teichoic and lipoteichoic acids.

Due to the presence of a cell wall, bacteria need secretion systems to pump out xenobiotics, as well as release various proteins and virulence factors (*Fig. 3A*). The secretion systems are divided into several groups based on their structure. There are at least six different types of secretion systems typical of Gram-negative bacteria, four types found in Gram-positive bacteria, and two types present in both groups [42]. The secretion systems also play a key role in the virulence of phytopathogenic bacteria. It should be noted that, during the division of a bacterial cell, an asymmetry between mother and daughter cells can be observed, where the mother cell retains most of the secretion system transporters, while the daughter cell receives a smaller part of transporters and is forced to synthesize them *de novo* [43].

As a rule, phytopathogenic bacteria grow more slowly than non-pathogenic ones isolated from plants and have a temperature optimum of 20–30°C.

Bacterial pathogens contain several types of genes: virulence genes, which play a major role in infection

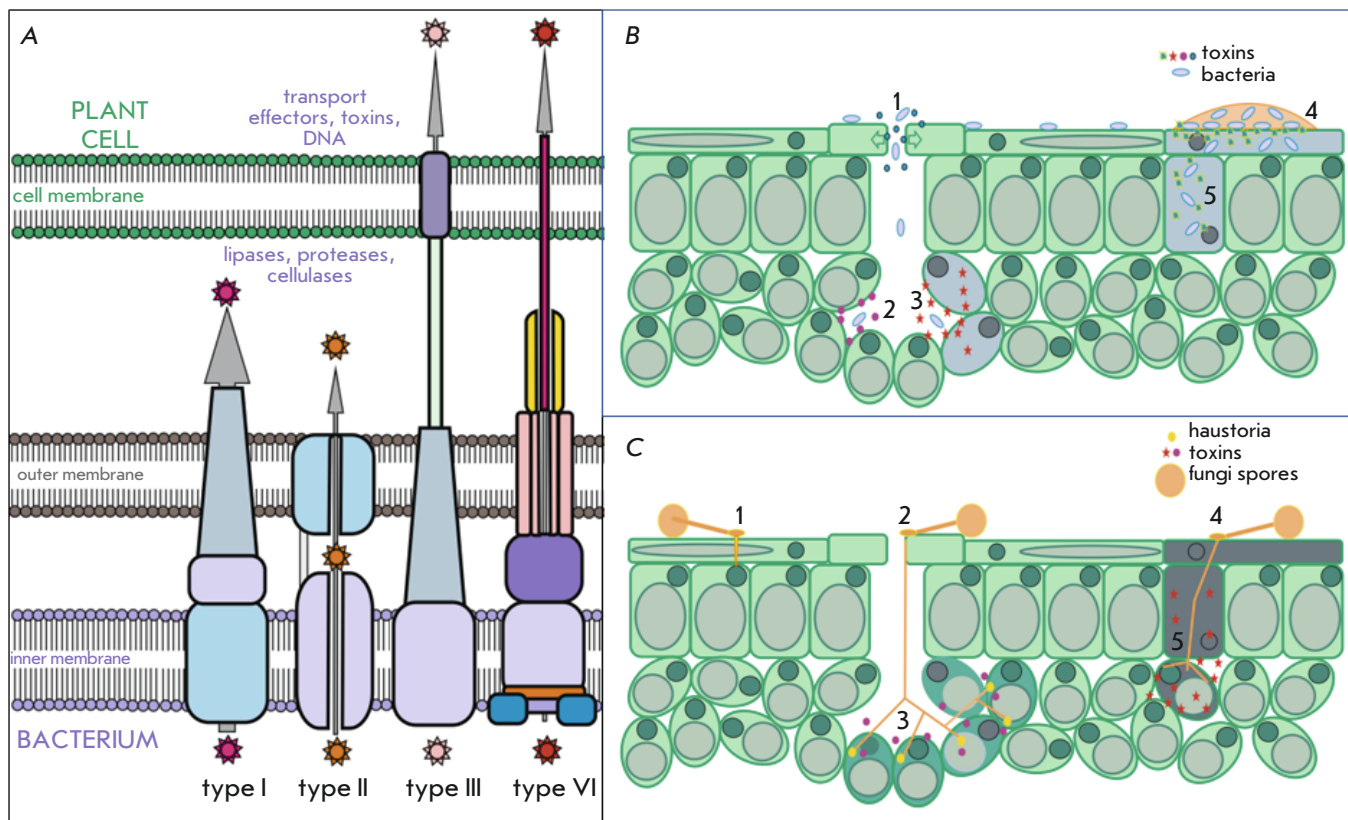


Fig. 3. A – bacterial secretory systems that are used to infect plant cells and tissues. B - development of bacterial infection: 1 – penetration through the stomata due to phytotoxins, 2 – secretion of phytotoxins to modify the physiology, immune system, and metabolism of plants, 3 – secretion of phytotoxins for degradation of the cell wall and cytotoxic effect on plant cells, 4 – surface colonization and formation of biofilms, 5 – damage to plant cells due to ice nucleation and formation of crystals. C - development of fungal infection: 1 – penetration into an intact cell at the site of appressorium attachment through the combined effect of mechanical force and enzymes that destroy the plant cell wall, 2 – penetration of the fungus through stomata, 3 – secretion of phytotoxins to modify plant physiology, immune system, and metabolism in biotrophic fungi 4 – penetration of the fungus through the wound; 5 – secretion of phytotoxins for degradation of the cell wall and cytotoxic effect on plant cells

and contribution to virulence, and disease-specific genes, which are important for disease manifestation (*Fig. 3B*). There are a series of genes that are required for host recognition, pathogen attachment to the plant surface, formation of infectious structures, as well as penetration and colonization of the host tissue. Pathogenic factors may either remain attached to the bacterial surface or can be released to the external environment. Pathogenic bacteria cause many serious plant diseases around the world, although not as many as fungi or viruses; however, the economic damage from bacterial diseases is relatively less severe than that from fungi and viruses [44]. Bacteria wreak havoc at all stages of crop production. Furthermore, due to the increase in the average annual temperature, there is reason to believe that the damage from bacterial spot and economic losses will only continue to grow in the

coming years [45]. With an annual increase in the average daily temperature in summer of 3–4°C, the prevalence of bacterial diseases increases twofold, while the prevalence of plant infection grows by 30–50% [45].

There are two types of bacterial diseases: systemic bacterial blight (penetration of the pathogen in the plant's vascular system, its further spread through the conductive bundles and adjacent tissues with disruption of the normal process of water consumption) and local bacterial blight (damage to the parenchymal tissues of individual plant organs). The main symptoms of bacterial diseases are wilting, necrosis, chlorosis, rot, overgrowth (galls), and scab.

Phytoplasmas and Spiroplasmas are two groups of very small (about 1 µm in diameter) bacteria without a cell wall (they are separated from the external environment by a cytoplasmic membrane). They cause

phytoplasmosis and growth retardation. Like mycoplasmas, a related genus of bacteria, phytoplasmas are apparently one of the most primitive and autonomously reproducing living organisms [46]. The genome of phytoplasmas is 0.5–1.3 million bp [47], while the genome of *Mycoplasma genitalium*, a model organism for studying the minimal genome, comprises 0.58 million bp [48]. Phytoplasmas exhibit gliding motility [49], while representatives of the genus *Spiroplasma* have a spiral shape and move in a twisting motion [50]. Cultivation of phytoplasmas in axenic cultures is quite difficult, which indicates their greater dependence on the host metabolism [51].

Phytoplasmosis significantly decreases both crop yield and its quality. Crop losses reach 40% for eggplants, 60% for tomatoes, 93% for pepper, 30–80% for potatoes, and 100% for cucumbers [52]. Plants with phytoplasmosis are characterized by such disorders of generative organs as virescence (greening of flowers and loss of normal pigmentation), phyllodia (transformation of part of a flower into a leaf-like formation), and proliferation (appearance of several “pseudo” flowers instead of one). In addition, phytoplasmosis can lead to the witches’ broom symptom (increased bushiness), dwarfism and wilting of plants, as well as leaf deformations. There is only one known case of positive phytoplasmosis, which leads to an economically useful effect: it is phytoplasmosis of poinsettia, a popular seasonal ornamental plant.

Fungi

Fungi are characteristic representatives of the domain Eukaryota. Unlike bacteria, they have a complex cell structure with a distinct nucleus and mitochondria. Fungal genome is much smaller than that of most eukaryotes but much larger than prokaryotic. Fungi have a cell wall, which usually consists of chitin, mannan, and chitosan, and also includes various proteins, lipids, and polyphosphates. Fungi form a mycelium: a system of thin branching hyphae, which sometimes lacks intercellular septa and forms a syncytium. Fungi are found in all ecological niches and can cause significant harm. Fungi appear to be evolutionarily much older than plants; the duration of their coexistence can be compared to the evolutionary age of higher plants [53]. About 80% of the plants present on our planet to date are symbiotic with fungi [54]. However, fungi sometimes disrupt the delicate balance of the mutually beneficial cooperation by turning into plant pathogens classified as biotrophs, hemibiotrophs, and necrotrophs. As a rule, pathogenic fungi enter plants through damaged leaves and stomata. However, in many cases, fungi secrete specific infectious structures and enzymes that destroy a plant’s cell wall (*Fig. 3C*).

In the case of necrotrophs, which have a wide range of hosts, the host cells die quickly from the combined action of enzymes destroying the plant’s cell wall, reactive oxygen species, and/or toxins [55, 56]. Biotrophs, whose life cycle is associated with a living host cell, secrete effector molecules that suppress the plant’s immune system. These fungi exhibit specificity and interact with the host via special biotrophic hyphae in the interphase region where biomolecules synthesized by the plant are absorbed [57]. Fungi can develop specific outgrowths of hyphae, so-called apressoria, which provide attachment of the fungus to the substrate, thus allowing the pathogen to penetrate the cell wall using a combination of mechanical force and enzymes that degrade the plant’s cell wall. Haustoria move from the base of the appressorium through the destroyed areas and penetrate the lumen. As a rule, haustoria contain a large number of mitochondria and ribosomes with a well-developed endoplasmic reticulum; haustorium is usually separated from the plant cell by invagination of the host plasmalemma [58]. At the same time, one can assume that an increased pressure of plant defense can cause a transition from biotrophy to necrotrophy [53].

Phytopathogenic fungi are the most dangerous plant pathogens to cause harm at all stages of crop production. The most common way to fight fungi is considered to be treatment with fungicides. The use of fungicides is associated with serious environmental and medical risks, namely the emergence of resistance and horizontal transfer of resistance genes, with the occurrence of species with multiple resistance [59]. At least 150 chemical compounds with different mechanisms of action are used as fungicides in world agriculture; however, there have been cases of resistance among various types of phytopathogens against almost all major classes of fungicides recorded to date [60].

The main symptoms of fungal diseases include wilting, spotting, mold (mycelium and sporulation of the fungus on the surface of affected organs), pustules (accumulation of fungal spores), overgrowth, deformations, mummification (shrinkage, darkening, and compaction of the infected tissue), and rot [2].

To date, more than 10,000 fungal species associated with plants have been discovered, and it is not surprising that fungal infections cause more harm than the diseases caused by other pathogenic microorganisms [61].

Complex diseases

Although it is believed that a plant disease is caused by one pathogen species or strain, microbes occur in nature mainly as part of complex multi-species consortia/communities. Most laboratory studies focus on individual strains grown in a pure culture. However,

they cannot explain the complex course of certain plant diseases. Therefore, the diseases where more than one pathogen is involved are usually termed “complex” due to their complicated diagnosis and subsequent control [62]. Synergistic interactions can occur between viruses, bacteria, fungi, and different groups of pathogens. For instance, the synergism of virus–virus type is observed when cowpea is co-infected with cowpea mosaic virus and cucumber mosaic virus, with the severity of the disease and the degree of growth retardation being greater than in the case of infection with individual viruses [63]. Synergism of the type bacterium–bacterium, which exacerbates the disease severity, can be observed when tomato is co-infected with the bacteria *Pseudomonas corrugata* and *P. mediterranea*, which cause tomato pith necrosis [64]. Synergism of the type fungus–fungus occurs quite often; it causes complex diseases such as ascochyta blight complex of pea [65], mango malformation disease [66], etc. Brown apical necrosis of walnut resulting from the interaction of numerous pathogenic fungi and bacterium *Xanthomonas arboricola* represents an example of a synergistic interaction between different groups of pathogens [67]. Synergism between different pathogens resulting in more severe disease symptoms is more common than expected and may be crucial in understanding microbial pathogenesis and evolution, as well as further developing effective strategies of disease management [62].

Thus, phytopathogens are ubiquitous and cause various plant diseases (Fig. 4).

Identification of phytopathogens

Early diagnosis of plant diseases is a key factor that determines the timely use of protective measures and, as a result, determines the yield and quality of crop products. To date, in addition to conventional visual examination and the method of indicator plants, serological methods and methods based on DNA and RNA technologies are required in order to accurately identify plant diseases. The most common methods of serological diagnosis include enzyme immunoassay, immunoblotting, dot-blot hybridization, immunochromatography [68], and serologically specific electron microscopy [69]. Methods based on DNA detection include fluorescence *in situ* hybridization [70], various polymerase chain reaction (PCR) techniques, including nested PCR, cooperative PCR, multiplex PCR, real-time PCR, and DNA fingerprinting. There are also RNA-based approaches: isothermal amplification of nucleic acids [71], the AmpliDet RNA real-time diagnostic system [72], and reverse-transcription PCR. These methods allow for quick and accurate detection of the pathogen and identification of its taxonomic rank. Novel approaches for a more accurate and sensitive detection are now being developed. These are the next-generation sequencing and metagenomic analysis, two-hybrid analysis, phage display, as well as biosensor technologies based on electrochemistry and biophotonics [73]. Thus, modern methods allow for accurate identification of a phytopathogen even in the absence of infection symptoms.



Fig. 4. Infectious plant diseases. From left to right, top row: tomato mosaic virus, downy mildew of lettuce, bacterial blight of cauliflower, rye ergot, middle row: potato spindle tuber viroid (William M. Brown Jr, amended), lettuce bacterial blight, mixed viral infection on the ramson (cucumber mosaic virus, tobacco rattle virus, tobacco mosaic virus), Septoria blight of celery; bottom row: Fusarium blight of dill, onion rust, black rot (alternariosis) of carrots, and tomato leaf curl virus

Integrated pest management (IPM)

The system of managing the phytosanitary state of ecosystems using integrated methods of pest management to ensure the phytosanitary prosperity of the territory is effectively used in many countries [74].

IPM is based on the assessment of an acceptable level of pests for determining the pest threshold. A prerequisite for this is the constant monitoring of pests, quarantine measures and seed purity, as well as the selection of resistant varieties cultivated in the area. If the level of harmfulness is reached, then methods of mechanical and biological control are mostly applied; however, if necessary, chemical-control methods can be used in a responsible and targeted manner.

The costs of IPM and chemical management are practically comparable, while IPM provides longer duration of the effect, increases yields by 10–30%, improves product quality, reduces climate risks, and has a pronounced environmental upside [75].

Seed reserves

In the IPM paradigm, healthy planting material is a prerequisite for the effective use of the system. Unfortunately, the seeds of most plants often serve as reservoirs for various phytopathogens, and the infection can be located both on the surface of the seed and inside of it. There are several strategies for regulating the seed transmission of a pathogen existing to date: the use of pathogen-free seeds and the search for methods of pre-sowing seed treatment. The most effective way to combat fungi is considered to be treatment of seeds with fungicides. Contact fungicides are used to destroy pathogens on the seed surface, while translaminar fungicides can penetrate into the seed and destroy the pathogen inside of it. These agents must act delicately to avoid damaging the fetus [76]. In recent years, there have been various strategies developed to control the pathogens on seeds, including physical treatment (mechanical and thermal treatment, ultrasonic and ultraviolet light exposure), treatment with natural compounds and biological control agents, as well as substances inducing resistance [77].

About 11 million tons of agricultural seeds are sown in Russia annually. The volume rate of domestic seeds in the world's cereal crops is 90%; it is 46% for corn, 43% for vegetables, 42% for soybeans, 32% for spring rape, and 26% for sunflower [78]. On the contrary, the volume rate of foreign seeds used in Russia varies from 30 to 90% depending on the culture, with the cost reaching 681,000 US dollars. The share of the seed business in the total sales of large agrochemical companies such as Syngenta, Bayer, DuPont, Dow, and Monsanto, is on the increase; they have acquired seed companies and comprehensively expanded their re-

search on crop protection by developing and creating resistant varieties and hybrids using modern high-end and high-performance technologies, including genome editing [79].

Plant breeding and bioengineering

Modern plant breeding for resistance to pathogens utilizes approaches and methods of conventional and cell selection. The emergence of the complete genomic sequences of some economically important crops now makes it possible to effectively search for resistance genes, as well as the corresponding DNA markers. Today, genetic markers based on DNA polymorphism (RFLP, RAPD, AFLP, CAPS) and short tandem repeats (STRs, or SSRs), as well as DNA microarray technology Diversity Arrays Technology (DArT) [80, 81], are actively used. A long-term increase in plant resistance can be achieved by using gene pyramiding [82]; namely through the development of genetically engineered varieties and distant hybridization technology.

Modern biotechnology approaches are becoming increasingly important for the production of virus-resistant plant varieties and hybrids. Introduction of an anti-sense gene in the plant for its modification allows one to disrupt viral reproduction [83]. The gene encoding the protein that has an affinity for viral RNA and inhibits its replication is also inserted into the plant's genome [84] to cause a delay in the expression of the transport protein or a modification of plasmodesma [85]. Constant expression of chitinase or lysozyme of bacteriophage T4 results in enhanced plant resistance to fungal and bacterial infections [86, 87]. Transgenic potato plants transcribing an RNA ribozyme that cleaves the RNA minus-strand of the spindle tuber viroid have been obtained [88].

New breeding methods to select varieties resistant to plant pathogens include powerful molecular tools for precise genetic modification, including the CRISPR/Cas9 system, which allows for more accurate genome editing than the use of *Agrobacterium*-mediated transformation [89].

Agrotechnical control

Agrotechnical control is a mandatory component of the IPM system. Adequate agricultural technology provides enhanced plant resistance to diseases and prevents massive infection by creating optimal conditions for plant growth and development. At the same time, crop rotation and selection of predecessors, the system of soil cultivation, fertilizers, dates of sowing and harvesting, as well as the destruction of weeds and post-harvest plant residues are of primary importance [90]. Placement of neighboring crops in the crop rotation and soil tillage are also essential [91]. Destroying

The most significant phytopathogens

Viruses	Bacteria	Fungi
The world's most significant phytopathogens		
<i>Tobacco mosaic virus</i>	<i>Pseudomonas syringae</i>	<i>Magnaporthe oryzae</i>
<i>Tomato spotted wilt virus</i>	<i>Ralstonia solanacearum</i>	<i>Botrytis cinerea</i>
<i>Tomato yellow leaf curl virus</i>	<i>Agrobacterium tumefaciens</i>	<i>Puccinia</i> spp.
<i>Cucumber mosaic virus</i>	<i>Xanthomonas oryzae</i>	<i>Fusarium graminearum</i>
<i>Potato virus Y</i>	<i>Xanthomonas campestris</i>	<i>Fusarium oxysporum</i>
<i>Cauliflower mosaic virus</i>	<i>Xanthomonas axonopodis</i>	<i>Blumeria graminis</i>
<i>African cassava mosaic virus</i>	<i>Erwinia amylovora</i>	<i>Mycosphaerella graminicola</i>
<i>Plum pox virus</i>	<i>Xylella fastidiosa</i>	<i>Colletotrichum</i> spp.
<i>Brome mosaic virus</i>	<i>Dickeya dadantii</i>	<i>Ustilago maydis</i>
<i>Potato virus X</i>	<i>Dickeya solani</i>	<i>Melampsora lini</i>
<i>Citrus tristeza virus</i>	<i>Pectobacterium carotovorum</i>	<i>Phakopsora pachyrhizi</i>
<i>Barley yellow dwarf virus</i>	<i>Pectobacterium atrosepticum</i>	<i>Rhizoctonia solani</i>
<i>Potato leafroll virus</i>	<i>Clavibacter michiganensis</i>	
<i>Tomato bushy stunt virus</i>		
The most significant phytopathogens in Russia		
<i>Barley stripe mosaic virus</i>	<i>Candidatus Phytoplasma</i> spp.	<i>Alternaria solani</i>
<i>Wheat streak mosaic virus</i>	<i>Xanthomonas translucens</i>	<i>Fusarium avenaceum</i>
<i>Winter wheat Russian mosaic virus</i>	<i>Pseudomonas cichorii</i>	<i>Plasmopara halstedii</i>
<i>Oat Siberian mosaic virus</i>	<i>Rathayibacter tritici</i>	<i>Phytophthora infestans</i>
<i>Beet necrotic yellow vein virus</i>	<i>Pseudomonas fuscovaginae</i>	<i>Tilletia caries</i>
<i>Lettuce mosaic virus</i>	<i>Acidovorax citrulli</i>	

post-harvest residues and weeds, which retain a large number of pathogens, while many weeds serve as reservoirs for them, is also of prime importance.

Chemical control

Chemical control plays a crucial role in preventing losses associated with plant diseases, especially with the advent of numerous fungicides with selective toxicity, which expands possibilities for using them in targeted fashion.

The total cost of research, development, and registration of a new crop protection product rose from USD 152 million in 1995 to USD 286 million in 2014. Worldwide sales have been increasing by about 6.5% annually since 1999 [92]. There are more than 600 different chemical control agents on the market to date (fungicides, pesticides, herbicides, nematicides, molluscicides, rodenticides, and antibiotics), and the economic sector is now valued at more than USD 50 billion [93].

There are now strict regulations on the use of chemical pesticides; and many products have been taken off the market, banned or have failed to pass re-registration. For instance, six out of the ten major chemical control products used in 1968 are currently banned as

household and agricultural pesticides in the United States.

Biological control and alternative to antibiotics

Modern agriculture is becoming an increasingly high-end and multidisciplinary industry with each passing year [94]. The uncontrolled use of herbicides leads to the appearance of populations of weeds that are resistant to them [95]. Although success in disease management mainly depends on crop resistance and the agricultural methods used, antibiotics such as gentamicin, oxolinic acid, oxytetracycline, and streptomycin are widely used in crop production [96]. The use of antibiotics in crop production is about 0.12%. However, in recent years, due to the widespread antibiotic resistance, more emphasis has been placed on alternative forms of combating phytopathogens. One such approach is the use of various methods of biological control [97]. Examples of biological control include the use of antagonist strains and antibiotic producers, bacteriophages, insects for weed control, and parasitic insects for controlling insect pests. For plant disease management, substances that are not themselves representatives of the groups of antibiotics or antimycotics, such as photo-

sensitizers, bacteriophages, phagolysins, antimicrobial peptides, and antibiofilm agents [98], are used. They are especially useful if, in addition to antibacterial activity, they have other properties, e.g., the ability to reduce the level of reactive oxygen species or inhibit bacterial multidrug efflux pumps [99].

The most significant plant pathogens

Several years ago, *Molecular Plant Pathology* conducted a series of surveys among specialists in the field of molecular plant pathology, which allowed the journal to select the ten most significant phytopathogenic fungi [100], viruses [101], and bacteria [102] (Table).

One cannot but agree with such a choice. However, the structure of agricultural products and crops grown in Russia differs from global ones and is predominantly comprised of wheat, sugar beet, potatoes, barley, oats, sunflower, and corn and, thus, requires adjustments to the list of pathogens specific to these cultures [2, 65, 79, 103, 104].

CONCLUSION

With the advent of modern diagnostic approaches, genome editing and sequencing technologies, as well as microbiome and proteomic analysis methods, the study of the mechanisms and effect of phytopathogens on plants has moved to a multidisciplinary level. In this review, we have attempted to provide a comprehensive picture of the current state of pest management. However, to our deep regret, we could not consider many aspects of the interaction between plants and phytopathogens, such as damage by ice nucleation proteins, which cause the formation of ice crystals in plant cells [105] or the conserved nature of the sequences of effector molecules in bacteria: pathogens of humans, animals, and plants [106]. ●

Acknowledgments: The reported study was funded by the Russian Foundation for Basic Research (project number 19-116-50156).

REFERENCES

- Horst R.K. Plant / In: Westcott's Plant Disease Handbook. Boston, MA: Springer, 2001. P. 65–530.
- Shkalikov V.A., Beloshapkina O.O., Bukreev D.D., Gorbachev I.V., Dzhaliilov F.S.-U., Korsak I.V., Minaev V. Yu., Stroykov Yu. M. Plant protection from disease. M.: Kolos, 2010. 404 p.
- Cardinale B.J., Matulich K.L., Hooper D.U., Byrnes J.E., Duffy E., Gamfeldt L., Balvanera P., O'Connor M.I., Gonzalez A. // *Am. J. Botany*. 2011. V. 98. № 3. P. 572–592.
- FAO. Global food losses and food waste – Extent, causes and prevention. Rome, 2011.
- FAOSTAT (http://www.fao.org/faostat/en/#rankings/commodities_by_country).
- Smirnova O.G., Kochetov A.V. // *Vavilov Journal of Genetics and Breeding* 2015. V. 19. No. 6. P. 715–723.
- Chesnokov Yu.V. // *Agricultural Biology* 2007. № 1. P. 16–35.
- Khalid A., Zhang Q., Yasir M., Li F. // *Front. Microbiol.* 2017. V. 8. P. 43.
- Morozov S.Yu., Soloviev A.G., Kalinina N.O., Talyanskiy M.E. // *Acta Naturae*. 2019. V. 11. № 4. P. 13–21.
- Chichkova N.V., Galiullina R.A., Beloshistov R.E., Balakireva A.V., Vartapetyan A.B. // *Russian Journal of Biorganic Chemistry* 2014. V. 40. P. 658–664.
- Dangl J.L., Jones J.D. // *Nature*. 2001. V. 411. № 6839. P. 826–833.
- Gururani M.A., Venkatesh J., Upadhyaya C.P., Nookaraju A., Pandey S.K., Park S.W. // *Physiol. Mol. Plant P.* 2012. V. 78. P. 51–65.
- Jones J.D., Dangl J.L. // *Nature*. 2006. V. 444. № 7117. P. 323–329.
- Abramovitch R.B., Martin G.B. // *Curr. Opin. Plant. Biol.* 2004. V. 7. № 4. P. 356–364.
- Maule A.J., Caranta C., Boulton M.I. // *Mol. Plant Pathol.* 2007. V. 8. № 2. P. 223–231.
- van Loon L.C., Bakker P.A., Pieterse C.M. // *Annu. Rev. Phytopathol.* 1998. V. 36. P. 453–483.
- Koonin E.V., Senkevich T.G., Dolja V.V. // *Biol. Direct*. 2006. V. 1. P. 29. doi: 10.1186/1745-6150-1-29.
- Richert-Pöggeler K.R., Minarovits J. // *Plant virus-host interaction: Molecular approaches and viral evolution* / Eds Gaur R.K., Hohn T., Pradeep Sharma P. Elsevier Inc., 2014. P. 263–275.
- Gergerich R.C., Dolja V.V. // *Plant Health Instructor*. 2006. doi: 10.1094/PHI-I-2006-0414-01
- Dorokhov Y.L., Ershova N.M., Sheshukova E.V., Komarova T.V. // *Plants (Basel)*. 2019. V. 8. № 12. P. 595.
- Sriwahyuni W., Hanapi M., Hartana I. // *Hayati J. Biosci.* 2008. V. 15. № 3. P. 118–122.
- Iftikhar Y., Jackson R., Neuman B.W. // *Pak. J. Agri. Sci.* 2015. V. 52. № 3. P. 667–670.
- Hull R. *Plant Virology*. Cambridge, MA: Acad. Press, 2014. 1118 p.
- Gray S.M., Banerjee N. // *Microbiol. Mol. Biol. Rev.* 1999. V. 63. № 1. P. 128–148.
- Walkey D. *Applied Plant Virology*. London: Chapman and Hall, 1991.
- Pennazio S., Roggero P., Conti M. // *Arch. Phytopathol. Plant Protect.* 1996. V. 30. № 4. P. 283–296.
- Zitter T.A., Murphy J.F. // *Plant Hlth Instructor*. 2009. <https://www.apsnet.org/edcenter/disandpath/viral/pd-lessons/Pages/Cucumbermosaic.aspx>
- Czosnek H., Laterrot H. // *Arch. Virol.* 1997. V. 142. P. 1391–1406.
- Takahashi H., Fukuhara T., Kitazawa H., Kormelink R. // *Front. Microbiol.* 2019. V. 10. P. 2764.
- Nohales M.-Á., Flores R., Daròs J.-A. // *Proc. Natl. Acad. Sci. USA*. 2012. V. 109. № 34. P. 13805–13810.
- Hiddinga H., Crum C., Hu J., Roth D. // *Science*. 1988. V. 241. № 4864. P. 451–453.
- Owens R.A., Tech K.B., Shao J.Y., Sano T., Baker C.J. //

- Mol. Plant-Microbe Interact. 2012. V. 25. № 4. P. 582–598.
33. Owens R.A., Hammond R.W. // *Viruses*. 2009. V. 1. № 2. P. 298–316.
34. Adkar-Purushothama C.R., Perreault J.P. // *Wiley Interdiscip Rev RNA*. 2020. V. 11. № 2. e1570.
35. Wassenegger M., Spieker R.L., Thalmeir S., Gast F.U., Riedel L., Sanger H.L. // *Virology*. 1996. V. 226. № 2. P. 191–197.
36. Malinovsky V.I. // *Agricultural Biology* 2009. V.5. P. 17–24.
37. Whitman W.B., Coleman D.C., Wiebe W.J. // *Proc. Natl. Acad. Sci. USA*. 1998. V. 95. № 12. P. 6578–6583.
38. Strahl H., Hamoen L.W. // *Proc. Natl. Acad. Sci. USA*. 2010. V. 107. № 27. P. 12281–12286.
39. Coplin D.L., Rowan R.G., Chisholm D.A., Whitmoyer R.E. // *Appl. Environ. Microbiol.* 1981. V. 42. № 4. P. 599–604.
40. Dimitriu T., Marchant L., Buckling A., Raymond B. // *Proc. Biol. Sci.* 2019. V. 286. № 1905. 20191110.
41. Gupta R.S. // *Crit. Rev. Microbiol.* 2000. V. 26. P. 111–131.
42. Green E.R., Meccas J. // *Microbiol. Spectr.* 2016. V. 4. № 1. 10.1128/microbiolspec.VMBF-0012-2015
43. Bergmiller T., Andersson A.M.C., Tomasek K., Balleza E., Kiviet D.J., Hauschild R., Tkacik G., Guet C.C. // *Science*. 2017. V. 356. № 6335. P. 311–315.
44. Vidhyasekaran P. *Bacterial disease resistance in plants: Molecular biology and biotechnological applications*. Binghamton, NY: Haworth Press, 2002. 464 p.
45. Ignatov A.N., Egorova M.S., Khodykina M.V. // *Plant Protection and Quarantine*. 2015. V.5. P. 6–10.
46. Maniloff J. // *Proc. Natl. Acad. Sci. USA*. 1996. V. 93. № 19. P. 10004–10006.
47. Kakizawa S., Oshima K., Namba S. // *Trends Microbiol.* 2006. V. 14. № 6. P. 254–256.
48. Fraser C.M., Gocayne J.D., White O., Adams M.D., Clayton R.A., Fleischmann R.D., Bult C.J., Kerlavage A.R., Sutton G., Kelley J.M., et al. // *Science*. 1995. V. 270. № 5235. P. 397–403.
49. Uenoyama A., Miyata M. // *Proc. Natl. Acad. Sci. USA*. 2005. V. 102. № 36. P. 12754–12758. doi: 10.1073/pnas.0506114102.
50. Shaevitz J.W., Lee J.Y., Fletcher D.A. // *Cell*. 2005. V. 122. № 6. P. 941–945.
51. Kube M., Schneider B., Kuhl H., Dandekar T., Heitmann K., Migdoll A.M., Reinhardt R., Seemuller E. // *BMC Genomics*. 2008. V. 9. P. 306. doi: 10.3389/fmicb.2019.01349
52. Kumari S., Nagendran K., Rai A.B., Singh B., Rao G.P., Bertaccini A. // *Front. Microbiol.* 2019. V. 10. P. 1349. doi: 10.3389/fmicb.2019.01349
53. Zeilinger S., Gupta V.K., Dahms T.E., Silva R.N., Singh H.B., Upadhyay R.S., Gomes E.V., Tsui C.K., Nayak S.C. // *FEMS Microbiol. Rev.* 2016. V. 40. № 2. P. 182–207.
54. Karandashov V., Nagy R., Wegmuller S., Amrhein N., Bucher M. // *Proc. Natl. Acad. Sci. USA*. 2004. V. 101. № 16. P. 6285–6290.
55. Wang X., Jiang N., Liu J., Liu W., Wang G.L. // *Virulence*. 2014. V. 5. № 7. P. 722–732.
56. Heller J., Tudzynski P. // *Annu. Rev. Phytopathol.* 2011. V. 49. P. 369–390.
57. Yi M., Valent B. // *Annu. Rev. Phytopathol.* 2013. V. 51. P. 587–611.
58. Horbach R., Navarro-Quesada A.R., Knogge W., Deising H.B. // *J. Plant Physiol.* 2011. V. 168. № 1. P. 51–62.
59. Soanes D., Richards T.A. // *Annu. Rev. Phytopathol.* 2014. V. 52. P. 583–614.
60. Scherbakova L.A. // *Agricultural Biology* 2019. V.54. № 5. P. 875–891.
61. Hussain F., Usman F. // *Abiotic and Biotic Stress in Plants*. London, UK: IntechOpen, 2019.
62. Lamichhane J.R., Venturi V. // *Front. Plant Sci.* 2015. V. 6. P. 385.
63. Pio-Ribeiro G., Wyatt S.D., Kuhn C.W. // *Phytopathology*. 1978. V. 68. P. 1260–1265.
64. Moura M.L., Jacques L.A., Brito L.M., Mourao I.M., Duclos J. // *Acta Hort.* 2005. V. 695. P. 365–372.
65. Le May C., Potage G., Andrivon D., Tivoli B., Outreman Y. // *J. Phytopathol.* 2009. V. 157. P. 715–721.
66. Freeman S., Shtienberg D., Maymon M., Levin A.G., Ploetz R.C. // *Plant Dis.* 2014. V. 98. P. 1456–1466.
67. Belisario A., Maccaroni M., Coramusi A., Corazza L., Pryor B.M., Figuli P. // *Plant Dis.* 2004. V. 88. P. 426.
68. Martinelli F., Scalenghe R., Davino S., Panno S., Scuderi G., Ruisi P., Villa P., Stroppiana D., Boschetti M., Goulart L.R., et al. // *Agron. Sustain. Dev.* 2015. V. 35. № 1. P. 1–25.
69. Derrick K.S. // *Virology*. 1973. V. 56. № 2. P. 652–653.
70. Salgado-Salazar C., Bauchan G.R., Wallace E.C., Crouch J.A. // *Plant Methods*. 2018. V. 14. P. 92. <https://doi.org/10.1186/s13007-018-0362-z>
71. Scuderi G., Golmohammadi M., Cubero J., Lopez M.M., Cirvilleri G., Llop P. // *Plant Pathology*. 2010. V. 59. P. 764–772.
72. Szemes M., Schoen C.D. // *Anal. Biochem.* 2003. V. 315. № 2. P. 189–201.
73. Goulart L.R., Vieira C.U., Freschi A.P., Capparelli F.E., Fujimura P.T., Almeida J.F., Ferreira L.F., Goulart I.M.B., Brito-Madurro A.G., Madurro J.M. // *Crit. Rev. Immunol.* 2010. V. 30. P. 201–222.
74. Maredia K.M., Dakouo D., Mota-Sanchez D. *Integrated Pest Management in the Global Arena*. Wallingford, UK: CABI Publ., 2003. 560 p.
75. Lyubovedskaya A. // *Plant protection*. 2017. V.9. P. 2–3.
76. Lamichhane J.R., You M.P., Laudinot V., Barbetti M.J., Aubertot J.-N. // *Plant Disease*. 2020. V. 104. № 3. P. 610–623.
77. Spadaro D., Herforth-Rahme J. van der Wolf J. // *Acta Hort.* 2017. V. 1164. P. 23–32.
78. Pivovarov V.F., Pyshnaya O.N., Gurkina L.K., Naumenko T.S., Soldatenko A.V. // *Vegetable crops of Russia*. 2017. V. 3. № 36. P. 3–15.
79. Nishimoto R. // *J. Pestic. Sci.* 2019. V. 44. № 3. P. 141–147.
80. Mohanta T.K., Bashir T., Hashem A., Abd Allah E.F., Bae H. // *Genes (Basel)*. 2017. V. 8. № 12. P. 399.
81. Raats D., Yaniv E., Distelfeld A., Ben-David R., Shanir J., Bocharova V., Schulman A., Fahima T. // *Cleaved amplified polymorphic sequences (CAPS) markers in plant biology* / Ed. Shavrukov Y. N.Y.: NOVA Publ., 2014.
82. Afanasenko O.S., Novozhilov K.V. // *Ecological genetics*. 2009. V. 7. № 2. P. 38–43.
83. Simon-Mateo C., Garcia J.A. // *Biochim. Biophys. Acta*. 2011. V. 1809. P. 722–731.
84. Chekalin N.M. *Genetic basis for the selection of legumes for resistance to pathogens*. Poltava: Intergraphics, 2003. 186 p.
85. Hipper C., Brault V., Ziegler-Graff V., Revers F. // *Front. Plant Sci.* 2013. V. 4. P. 154.
86. Richa K., Tiwari I.M., Devanna B.N., Botella J.R., Sharma V., Sharma T.R. // *Front. Plant Sci.* 2017. V. 8. P. 596.
87. During K., Porsch P., Fladung M., Lorz H. // *Plant J.* 1993. V. 3. P. 587–598.
88. Yang X., Yie Y., Zhu F., Liu Y., Kang L., Wang X., Tien P. // *Proc. Natl. Acad. Sci. USA*. 1997. V. 94. № 10. P. 4861–4865.
89. Borrelli V.M.G., Brambilla V., Rogowsky P., Marocco A., Lanubile A. // *Front. Plant Sci.* 2018. V. 9. P. 1245.

REVIEWS

doi:10.3389/fpls.2018.01245.

90. Leoni C., de Vries M., ter Braak C.J.F., van Bruggen A.H.C., Rossing W.A.H. // *Eur. J. Plant Pathol.* 2013. V. 137. P. 545–561.
91. Panth M., Hassler S.C., Baysal-Gurel F. // *Agriculture.* 2020. V. 10. P. 16.
92. Hirooka T., Ishii H. // *J. Gen. Plant Pathol.* 2013. V. 79. P. 390–401.
93. Phillips McDougall. Evolution of the crop protection industry since 1960. Phillips McDougall, Midlothian, UK, 2018.
94. Schut M., Rodenburg J., Klerkx L., van Ast A., Bastiaans L. // *Crop Protection.* 2014. V. 56. P. 98–100.
95. Moss S.R. // *Pesticide Outlook.* 2003. V. 14. P. 164–167.
96. Stockwell V.O., Duffu B. // *Rev. Sci. Tech. Off. Int. Epiz.* 2012. V. 31. № 1. P. 199–210.
97. Köhl J., Kolnaar R., Ravensberg W.J. // *Front. Plant Sci.* 2019. V. 10. P. 845.
98. Nazarov P.A. // *Bulletin of the Russian State Medical University.* 2018. No. 1. P. 5–15.
99. Nazarov P.A., Osterman I.A., Tokarchuk A.V., Karakozova M.V., Korshunova G.A., Lyamzaev K.G., Skulachev M.V., Kotova E.A., Skulachev V.P., Antonenko Y.N. // *Sci. Rep.* 2017. V. 7. № 1. P. 1394.
100. Dean R., van Kan J.A., Pretorius Z.A., Hammond-Kosack K.E., Di Pietro A., Spanu P.D., Rudd J.J., Dickman M., Kahmann R., Ellis J., et al. // *Mol. Plant. Pathol.* 2012. V. 13. № 4. P. 414–430.
101. Scholthof K.B., Adkins S., Czosnek H., Palukaitis P., Jacquot E., Hohn T., Hohn B., Saunders K., Candresse T., Ahlquist P., et al. // *Mol. Plant. Pathol.* 2011. V. 12. № 9. P. 938–954.
102. Mansfield J., Genin S., Magori S., Citovsky V., Sriariyanum M., Ronald P., Dow M., Verdier V., Beer S.V., Machado M.A., et al. // *Mol. Plant Pathol.* 2012. V. 13. № 6. P. 614–629.
103. Alekseeva K.L., Ivanova M.I. Diseases of green vegetables (diagnosis, prevention, protection). M.: FSINI Rosinformagroteh, 2015. 188 p.
104. Alekseeva K.L., Baleev D.N., Bukharov A.F., Bukharova A.R., Ivanova M.I. // *Kartofel' i ovoshhi.* 2015. № 12. P. 33–34.
105. Gurian-Sherman D., Lindow S.E. // *FASEB J.* 1993. V. 7. № 14. P. 1338–1343.
106. Ghosh P. // *Microbiol. Mol. Biol. Rev.* 2004. V. 68. № 4. P. 771–795.

Promising Molecular Targets for Pharmacological Therapy of Neurodegenerative Pathologies

M. E. Neganova, Yu. R. Aleksandrova, V. O. Nebogatikov, S. G. Klochkov, A. A. Ustyugov*

Institute of Physiologically Active Compounds of the Russian Academy of Sciences, Moscow region, Chernogolovka, 142432 Russia

*E-mail: alexey@ipac.ac.ru

Received March 25, 2020; in final form, April 20, 2020

DOI: 10.32607/actanaturae.10925

Copyright © 2020 National Research University Higher School of Economics. This is an open access article distributed under the Creative Commons Attribution License, which permits unrestricted use, distribution, and reproduction in any medium, provided the original work is properly cited.

ABSTRACT Drug development for the treatment of neurodegenerative diseases has to confront numerous problems occurring, in particular, because of attempts to address only one of the causes of the pathogenesis of neurological disorders. Recent advances in multitarget therapy research are gaining momentum by utilizing pharmacophores that simultaneously affect different pathological pathways in the neurodegeneration process. The application of such a therapeutic strategy not only involves the treatment of symptoms, but also mainly addresses prevention of the fundamental pathological processes of neurodegenerative diseases and the reduction of cognitive abilities. Neuroinflammation and oxidative stress, mitochondrial dysfunction, dysregulation of the expression of histone deacetylases, and aggregation of pathogenic forms of proteins are among the most common and significant pathological features of neurodegenerative diseases. In this review, we focus on the molecular mechanisms and highlight the main aspects, including reactive oxygen species, the cell endogenous antioxidant system, neuroinflammation triggers, metalloproteinases, α -synuclein, tau proteins, neuromelanin, histone deacetylases, presenilins, etc. The processes and molecular targets discussed in this review could serve as a starting point for screening leader compounds that could help prevent or slow down the development of neurodegenerative diseases.

KEYWORDS neurodegeneration, neuroinflammation, oxidative stress, histone deacetylases, proteinopathy, aggregation of pathogenic proteins.

ABBREVIATIONS DAM – disease-associated microglia; HATs – histone acetyltransferases; HDACi – histone deacetylase inhibitors; HDACs – histone deacetylases; mGluR5 – metabotropic glutamate receptor 5; MMP-3, MMP-9 – matrix metalloproteinase 3, 9; NDD – neurodegenerative diseases; NMDA – N-methyl-D-aspartate; PSEN1, PSEN2 – presenilin 1, 2; ROS – reactive oxygen species; SIRT6 – sirtuins; TIM – translocase of the inner membrane; TOM – translocase of the outer membrane; TREM2 – triggering receptors expressed on myeloid cells 2.

INTRODUCTION

The development of effective therapeutic approaches to the treatment of neurological disorders is one of the most daunting challenges of modern biomedicine. The central issue is the absence of drugs that affect the disease pathogenesis. At the same time, the number of patients with the most common neurodegenerative diseases (NDD), such as Alzheimer's disease and other forms of dementia, is estimated at approximately 30–35 million and doubles every 10

years worldwide[1]. The figure is expected to reach 70 million people in the next 10 years [2]. Total worldwide treatment expenses for patients with neurological disorders in 2015 amounted to US\$ 818 billion and could potentially jump to US\$ 2 trillion by 2030 [2]. About one hundred drugs for the treatment of Alzheimer's disease, including vaccines, undergo clinical trials every year [3]. However, despite the vast resources involved, no new drug has been brought to market since 2003. An analysis of current devel-

opments in the field of new medicinal products for NDD suggests that most of the activity is focused on a search for multi-target compounds that affect the key aspects of pathogenesis [4]. Proteinopathy processes (pathological aggregation of specific proteins in the brain), mitochondrial dysfunction, neuroinflammatory processes, and dysfunction of histone deacetylases (HDACs), which serve as regulatory elements in the expression of the genes related to neurological disorders, are among the key pathological features that need addressing.

PROBLEMS AND TARGETS IN THE TREATMENT OF NEURODEGENERATIVE DISEASES

Today, about a billion people worldwide suffer from neurodegenerative diseases. The most common are Alzheimer's disease, Parkinson's disease, and amyotrophic lateral sclerosis. They can occur as a result of a combination of genomic, epigenomic, metabolic and environmental factors. The risk of developing most neurodegenerative diseases increases with age, resulting in a progressive neurodegenerative process (in some cases due to the death of neuronal cells in various brain regions, in other cases as a result of motoneuron death), as well as neuroinflammatory processes. Currently, the available treatment methods cannot prevent or arrest the progression of neurodegenerative diseases. No basic therapy which could accrue significant benefits to patients with detrimental disorders has been developed so far. Modern treatment methods can only improve a patient's condition affecting symptom manifestation with cognitive impairments and motor body functions temporarily. However, with the improvements in our quality of life, average life expectancy has increased considerably, and so has the number of age-related diseases. Hence, the detection of new targets for drug action, the development of new synthesis methods, and target-oriented selection of potential neuroprotectors are a priority both in modern medical chemistry and healthcare in general.

In neurodegenerative diseases, the progression of pathology begins many years before the appearance of the first evident symptoms of the disease. Numerous studies have suggested that there are a number of common events among pathological conditions which can explain why an ageing brain is vulnerable to neurodegeneration. Physiological neuronal processes such as endosomal-lysosomal autophagy, neuroinflammatory reactions, mitochondrial homeostasis, and proteostasis are beyond systemic control in neurodegenerative diseases. The changes that occur in the redox cell balance and mitochondrial functioning, the impairment of the expression and activity of

epigenetic enzymes and the increased pool of aggregated proteins with an impaired tertiary structure (A β , α -synuclein, etc.) are the main indicators of the development of neurodegenerative diseases (*Fig. 1*).

Oxidative stress and, in particular, peroxidation of membrane lipids, impairment of endogenous antioxidant mechanisms (glutathione system), and mitochondrial dysfunction (suppression of the activity of complex I and complex IV of the respiratory chain – cytochrome-c-oxidase) are inter-related and reinforce each other, leading to neurodegenerative processes [5, 6, 7]. Moreover, dead cell remnants and the aggregated proteins released into the extracellular environment from the neuron provoke glial activation and the release of cytokines and free radicals, leading to neuronal death, which triggers an additional pathological process: neuroinflammation. Pharmacological treatment of the abovementioned manifestations of early neurodegeneration stages could arrest the disease's progression. This is therefore highly important for the medical treatment of neurodegeneration (*Fig. 1*).

Role of oxidative stress in the development of a neurodegenerative process

Oxidative stress, a process which occurs as a result of the impairment of the pro-oxidant-antioxidant balance that promotes oxidative species, leading to potential damage to the cell [8, 9] and is the result of excessive accumulation of reactive oxygen species (ROS), as well as a decreased activity of the antioxidant system of cell defence, has always played a pivotal role in neurodegenerative diseases (Alzheimer's disease, Parkinson's disease, and others), including ageing [10–13]. The concentration of reactive oxygen species in physiological conditions is maintained at a relatively low level thanks to the activity of endogenous antioxidant mechanisms such as the glutathione system, superoxide dismutase, catalase, etc. [14]. However, with age and due to genetic and ecological risk factors, the redox system becomes unbalanced, resulting in the production of reactive oxygen species [15, 16]. Though ROS in moderate concentrations plays an important role in physiological processes (for example, in the regulation of signalling pathways and induction of the mitogenic response), its overproduction and imbalance in the endogenous antioxidant defence system leads to oxidative damage such as post-translation modifications and the oxidation of proteins, lipids and DNA/RNA, which are the shared features of many NDDs [17, 18]. Thus, patients with various neurological disorders (in particular, Alzheimer's disease and Parkinson's disease) suffer from ROS overproduction in the brain [19, 20], leading to increased peroxidation

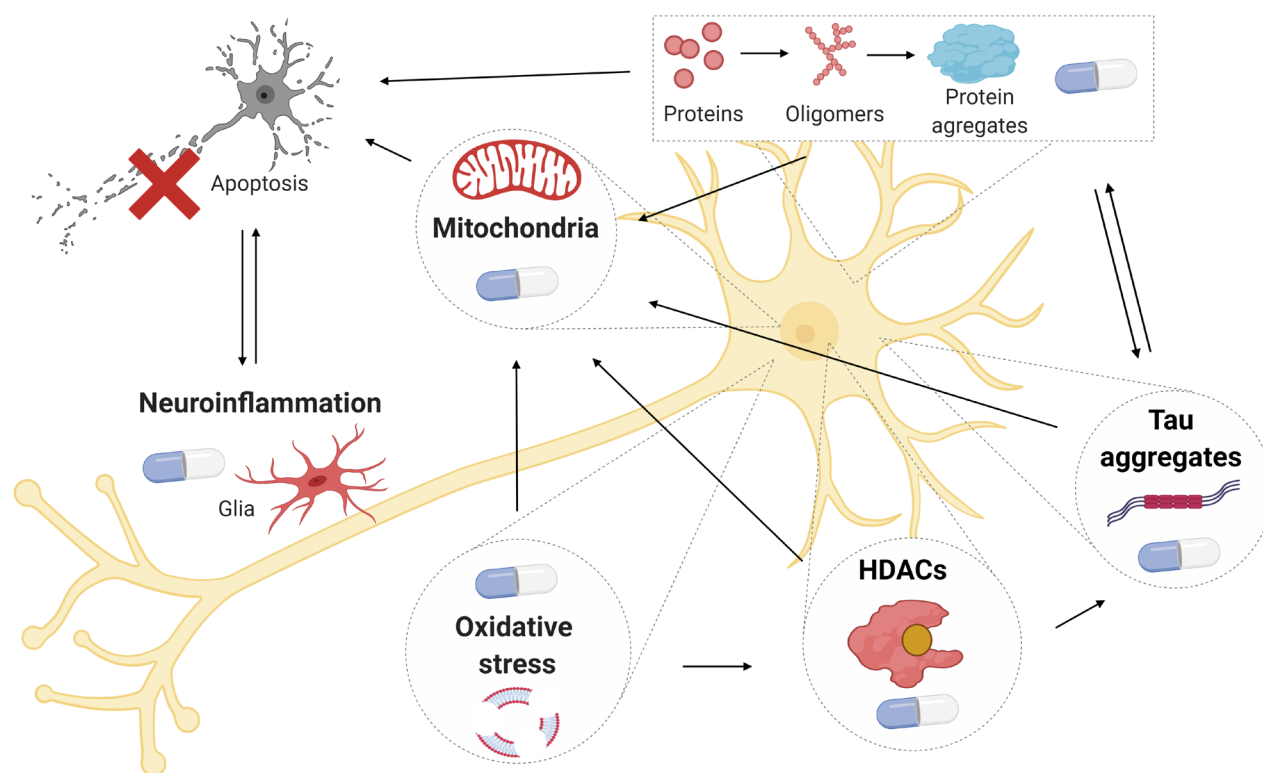


Fig. 1. Molecular targets for pharmacological effects in the treatment of neurodegenerative diseases

of membrane lipids through the action of free radicals, an elevated content of malone-dialdehyde in the system, excessive accumulation of metals with variable valency, and mitochondrial dysfunction with a subsequent release of apoptogenic factors and further neuronal apoptosis (*Fig. 2*) [21, 22].

It should be noted that such neuronal susceptibility to oxidative damage has several reasons [23, 16]. Membrane lipids in the brain contain a large amount of polyunsaturated fatty acids, which are prone to free radical attack and lipid peroxidation. In addition, active neurons also exhibit a high level of oxygen consumption, exacerbating therefore ROS production [24]. Moreover, it has also been shown that the brain contains quite a small amounts of enzymes for its own antioxidant cell protection, which play an important role in the metabolism of free radicals [25].

Malondialdehyde, 4-hydroxy-trans-2,3-nonenal, acrolein, and F2-isoprostanes are known oxidative stress markers that are routinely encountered in the brain and cerebrospinal fluid of patients with Alzheimer's. Greilberger *et al.* investigated the blood of healthy individuals and that of patients with neuro-

degenerative disorders (mild cognitive disorders and Alzheimer's), and they discovered that the significant increase in malondialdehyde, carbonylated proteins, and oxidized albumin levels found in NDD patients compared to their controls indicates a relationship between lipid peroxidation induced by oxidative stress and the development of neurodegenerative disorders [26]. 4-hydroxy-trans-2,3-nonenal has the highest reactivity and hippocampal cytotoxicity and can accumulate in significant amounts in the brain and cerebrospinal fluid of Alzheimer's and Parkinson's patients [27, 28].

Oxidative stress is considered an important cause of both forms of Parkinson's: the inherited and sporadic forms [17]. A high level of oxidized lipids, proteins, and DNA was found in the biological material of Parkinson's patients, as well as decreased levels of reduced glutathione [29–31], which leads to the generation of more reaction-capable species mediated by the Fenton's and Haber-Weiss reactions. Overproduction of reactive oxygen forms leads to the degeneration of dopaminergic neurons and, as a consequence, to the development of key symptoms of Parkinson's, includ-

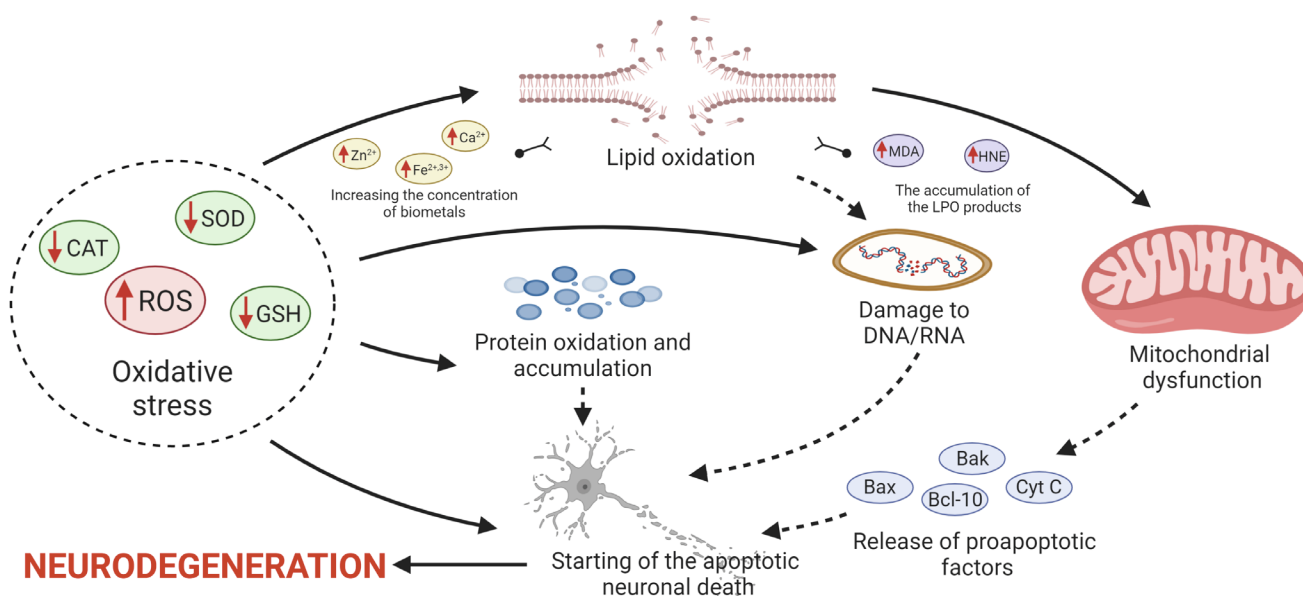


Fig. 2. Oxidative stress in the development of neurodegenerative diseases. The increase of oxidative processes is associated with hyperproduction of reactive oxygen species and a decreased activity of the endogenous antioxidant defence system of cells leading to oxidative damage to lipids, proteins, and DNA/RNA, which triggers a cascade of apoptotic neuronal cell death and promotes neurodegeneration

ing muscular rigidity, bradykinesia, resting tremor, and postural instability. Thus, patients with Parkinson's show a 80–90% loss of dopaminergic neurons in substantia nigra and a 40–50% loss of the ventral tegmental area [32].

The possibility of using antioxidants in the treatment of neurodegenerative diseases was confirmed in the end of the last century, but new neuroprotectors are now actively sought among the compounds that inhibit oxidative processes. Vitamin E utilization in the therapy of Alzheimer's patients at 2000 IU a day for 2 years attenuates the functional decrease of cognitive functions [33]; similarly, administration of this antioxidant at an early age can potentially reduce the risk of Parkinson's [34]. Another known free radical acceptor is Vitamin C, which protects membrane phospholipids from peroxidation and participates in catecholamine biosynthesis [35]. Despite the fact that ascorbic acid is not a direct scavenger of lipophilic radicals, it has a synergic effect when combined with vitamin E [36, 37]. Resveratrol is a naturally occurring phytoalexin that has the ability to capture active oxygen species, acting as a metal chelator and enzymatic activity modulator [38, 39]. Its antioxidant properties include effective inhibition of lipid peroxidation in

the hippocampus and are confirmed by an increased catalase activity [38]. It has also been shown that the extract derived from the leaves of the Chinese Ginkgo tree (*Ginkgo biloba* L.), which has some of the most potent antioxidant properties, can improve cognitive brain functions in the Alzheimer's disease by reducing the toxicity of A β -plaques [40].

The positive impact of the antioxidant compounds used as neuroprotectors was also confirmed by studies of a natural compound derivative representing the alkaloid-derived adducts securinine and tryptamine and also known as allomargaritarine. A study of the neuroprotective properties of this conjugate in various neurotoxicity models using a primary culture of the rat cortex showed that allomargaritarine has a pronounced cytoprotective effect that contributes to an increased cell survival rate after glutamate, Fe³⁺ and A β exposure. The ability of allomargaritarine to protect neurons from death correlated with its antioxidant potential: namely, there was a concentration-dependent inhibition of lipid peroxidation caused by ferric iron ions and tert-butylhydroperoxide [41, 42]. Allomargaritarine also has an anticonvulsant activity [43], which may be due to its antioxidant potential, since oxidative stress is known to be involved

in the pathogenesis of epilepsy [44, 45]. Antioxidant properties are considered one of the mechanisms of the neuroprotective action of one of the bioisosteric analogues of cinnamonic acid. Moderate inhibition of rat brain homogenate peroxidation was shown, and, importantly, there was an increased cell survival count of human neuroblastoma SH-SY5Y in ionomycin-induced neurotoxicity [46]. When assessing the effect of structural analogues of Dimebon (derivatives of tetrahydro-gamma-carboline derivatives) on the ratio of reduced and oxidized glutathione, it turned out that DF-407 effectively inhibited the accumulation rate of reactive oxygen species and increased the GSH/GSSG ratio, which indicates a possible effect on the cell defence system and correlates with a decrease of the glutamate-induced death rate of cortical neurons in the brain of new born rats [47]. Therefore, the key role that oxidative stress plays in the development of neurodegenerative diseases, as well as the positive results achieved through the use of antioxidants as potential neuroprotectors, suggests that manipulation of the levels of reactive oxygen species can be considered as a promising means for treating neuropathologies and alleviating their accompanying symptoms.

Neuroinflammatory reactions in a neurodegenerative process

Neuroinflammation is a pathological process which is typical of a number of neurodegenerative diseases such as Parkinson's, Alzheimer's, amyotrophic lateral sclerosis, and Huntington's disease. Many of these disorders are proteinopathies and are characterized by an accumulation of specific protein deposits, in particular A β in Alzheimer's [48], resulting in the activation of immunocompetent brain cells and subsequent inflammatory reactions [49, 50]. Thus, it has been shown that activated cells can both reduce the amount of A β and increase its toxic effect [48, 51, 52].

The main residents of the immune system in the brain are microglial cells and astrocytes, which participate in the immediate inflammation response. Neuroprotective microglial functions are present in transgenic mice expressing human *APP* under the control of the Thy-1 promoter (*APP23*) [53]. Moreover, CX3CR1-CX3CL1 receptors play an important role in the interaction between glial cells and neurons. The chemokine receptor CX3CR1 allows microglia to participate in synapse formation and decreases the A β level [54, 55]. The expression of the Toll-like receptors TLR-2 and TLR-4 by microglial cells also promotes the uptake of aggregated A β [56]. While investigating the role of the chemokine receptor CX3CR1 recruiting glial cells in the pathogenesis

of neuroinflammation in animal models, S. Hickman *et al.* noted that the concentration of aggregated A β and a number of senile plaques in brain tissues were lower in heterozygous APP/PS1 mice (PS1-APP-CX3CR1^{+/-}). Moreover, unlike APP/PS1 mice, the levels of A β lysing enzymes were significantly higher in the animals [57].

Considering the neuroprotective role of astrocytes, it should be mentioned that the proinflammatory cytokines TNF- α , TGF- β , and IL-1 β are released by cells at an early response, they subsequently activate adjacent microglial cells, and also degrade soluble A β with the help of apolipoproteins and, to a larger extent, ApoE2. Therefore, it is believed that astrocytes can act as a therapeutic target in Alzheimer's [51]. Yet, neuroinflammation primarily disrupts the cytokine balance and changes the microenvironment; hence, some glial cells may have a pro-inflammatory function. This is due to the synthesis of proinflammatory cytokines (IL-1 β , IL-6, TNF- α), the toxic effect of A β itself, and the suppression of the phagocytic microglia function in the brain of patients with Alzheimer's [58–60]. It was also shown that the glia surrounded by the aggregated amyloid migrates to the amyloid-free regions, skipping its activation and, as a result, their ability to degrade amyloid decreases. [60, 61].

The pathological effects of astrocytes in the brain of patients with Alzheimer's are caused by the impaired calcium exchange [62], the enhanced glutamate secretion [63] which leads to excitotoxicity, as well as the toxicity of apolipoprotein isoforms (ApoE3, ApoE4) [64]. In general, with the development of amyloidosis, activated astrocytes can both stimulate the neuroprotective functions of microglia at the early stages of Alzheimer's and suppress the activity of glial cells during the disease.

Current findings on the participation of glia cells in neuroinflammation fit into a polar model reflecting the differentiation of the activated macrophages M1 and M2 in the development of tissue inflammation. However, numerous studies show that this analogy does not describe the complex interaction in the microglia and the neuronal environment [65]. Yet, microglial cell phenotypes appear to be more diverse than expected, which is confirmed by ultrastructural analyses [66]. It is also known that glial activity depends on gender, age, and genotype [67]. Currently, five clusters of cells can be distinguished as participating in the pathogenesis of neurodegenerative diseases [68]. A hypothesis has also been formulated on the transcriptional shift mechanism of microglial cells, which highlights the transcription factors mediating neuroinflammation (NF- κ B, Activator protein-1, Interferon regulatory factors, p53 tumor suppressor, and STAT), support-

ing healthy microglia (PU-1, SALL1, MAFB), and the main factors necessary for cell survival and differentiation [69].

The last identified cluster seems more significant, and it is specified as DAM, the disease-associated microglia. The cells in this cluster are located near amyloid deposits and have a characteristic gene expression, and they contribute to pathological processes, especially at early stages of the disease [70]. The TREM2 receptor (Triggering Receptors Expressed on Myeloid cells) plays a critical role in DAM cluster activation [71] and can be used as a biomarker of an early stage of Alzheimer's [72]. Thus, TREM2 inhibition, a decrease of variability or the receptor's knockdown in animal models reduce the likelihood of the disease, phagocytic activity of microglia, as well as total activation and secretion of excitotoxic ApoE isoforms [70, 73–75].

Neuroinflammation is a complex and multifactor process where the activation of glial cells represents only an aspect of the pathological state in proteinopathies. Inflammatory processes in the brain are not only affected by the microenvironment. T-helper cells are also engaged in the process, which is evidenced in App-Tg mice and in patients with Alzheimer's [76–78]. The intestinal microbiota is also involved [79–81]. The function of the blood-brain barrier is impaired during acute and chronic inflammation. Matrix metalloproteinases (MMP-3, MMP-9), which are involved in the development of pro-inflammatory reactions, play a critical role in the molecular mechanisms of neuroinflammation pathogenesis [82–84].

Neuroinflammation is associated with neuronal loss in Parkinson's disease, which is typically under the control of microglia. Microglial activation in the substantia nigra was found in patients both with sporadic [85] and familial Parkinson's forms [86], as well as in the substantia nigra and striatum of transgenic animals modelling this pathology, as induced by an inhibitor of complex I of the respiratory chain I complex 1-methyl-4-phenyl-1,2,3,6-tetrahydropyridine (MPTP) [87]. The chronically activated or overactivated microglial condition causes redundant and uncontrolled neuroinflammatory reactions due to an abundant release of free radicals, which, in turn, leads to a self-maintained neurodegeneration cycle [88]. The molecules released from the damaged dopaminergic neurons due to impaired metabolic activity dopamine and reactive microgliosis include neuromelanin, α -synuclein, and the active form of metalloproteinase-3 (MMP-3) [17]. Insoluble extraneuronal neuromelanin granules are found in patients with juvenile idiopathic Parkinson's [89] and in patients with MPTP-induced parkinsonism [90]. In-

tracerebral neuromelanin injection causes strong microglial activation and loss of dopaminergic neurons in substantia nigra [91]. Since neuromelanin remains in the extracellular space for a very long time [90], it is considered a target molecule responsible for the triggering of a chronic neuroinflammation in Parkinson's disease [17]. The addition of aggregated human α -synuclein to a primary culture of mesencephalic neurons induced microglial activation and neurodegeneration, and the cytotoxicity was not observed in the absence of microglia [92]. Moreover, α -synuclein obtained from these neurons stimulated astrocytes to produce inflammation modulators which enhanced the activation of microglia, chemotaxis, and the proliferation of neuronal cells [93]. Gao *et al.* have shown that transgenic mice expressing mutant α -synuclein develop a persistent neuroinflammation and chronic progressive degeneration of the nigrostriatal dopamine pathway initiated by low liposaccharide levels [94]. Moreover, in response to the oxidative stress in dopaminergic neurons, the active form of MMP-3 causes the activation of microglial cells, which, in turn, leads to the formation of reactive oxygen and nitrogen species [95–99]. MMP-3 also affects protease-activated receptors, their cleavage, the removal of the N-terminal domain, and conversion of the remaining C-terminal domain into the binding ligand, which, in turn, generates intracellular signals and activates microglia [100–102]. MMP-3 also participates in the formation of interleukin-1 beta (IL-1 β) and facilitates the expression of inflammatory cytokines in activated microglia [84, 103, 104]. Thus, it has been shown that modulation of the various pathways linked to neuroinflammation can considerably contribute to the neuroprotective action of multifunctional drugs.

Role of mitochondrial stress in neurological disorders

Despite the fact that the aetiology of many neurodegenerative diseases remains largely unclear, over the last three decades the contribution of mitochondria to the development of neuropathologies has been vigorously discussed, and the accumulated evidence suggests that the dysfunction of these organelles plays an important role in the pathogenesis of a number of NDDs. Mitochondria are the most important components of eukaryotic cells, as they provide high-energy phosphates and products of intermediary metabolism, support homeostasis by participating in the regulation of the electrolyte balance, and maintain the concentration of calcium ions. Mitochondria regulate the production of the reactive oxygen species playing a key role in the initiation of apoptotic cell death; hence, their dysfunction can contribute to the development

of a number of neurodegenerative diseases, including Alzheimer's [105–107].

Evidence to support this hypothesis has been obtained in studies describing mitochondrial dysfunction (change in morphology and suppression of metabolic activity) correlated with a decrease in ATP production and an increase in the level of reactive oxygen species in the brain [107–111], fibroblasts, and the blood cells [112, 113] of patients with a neurological disorder, as well as in transgenic mice modelling Alzheimer's [106, 111, 114, 115], and in cell lines expressing the mutant precursor protein amyloid [116]. It is known that in neurodegenerative diseases, numerous mitochondrial dysfunctions are present [117]. Mitochondria undergo several cycles of division and fusion (shortening and elongation), or “mitochondrial dynamics” [118, 119]. The emerging defects in the dynamics of these organelles are associated with the changes in the expression of the fission and fusion proteins determining their morphology [120, 121], as well as the integrity and functional state [120, 122]. Therefore, fine regulation of five basic proteins Drp1, Fis1, Opa1, Mfn1 and Mfn2 controlling the dynamics of mitochondria [123] is necessary to maintain normal functioning of these organelles in brain cells. A postmortem analysis of the brain samples of patients with Alzheimer's revealed an impaired expression of these genes and, consequently, a change in the morphology of mitochondria compared to healthy patients [124]. These results were also confirmed in studies of a M17 neuroblastoma cell line overexpressing the mutant APP, where changes in the mitochondrial structure were also observed [113], while changes in the morphology of cortical mitochondria in elderly monkeys correlated with increases in active oxygen forms and memory impairment [125].

Defects in mitochondria bioenergetics manifest themselves in a disruption of the functioning of the electron transport chain, mitochondrial depolarization, increased production of reactive oxygen species, and reduced production of ATP. The respiratory chain localized in the inner mitochondrial membrane is one of the main functional and structural parts of the organelles [126], which catalyses the formation of ATP from ADP and inorganic phosphate via electron transfer between its subunits [127] and, therefore, is considered the most important and indispensable source of energy in mammalian cells. This process also leads to the formation of free radicals [128], resulting in the production of 1–5% of total cell ROS under normal physiological conditions [129]. These by-products of mitochondrial respiration [130] serve as important redox messengers in the regulation of

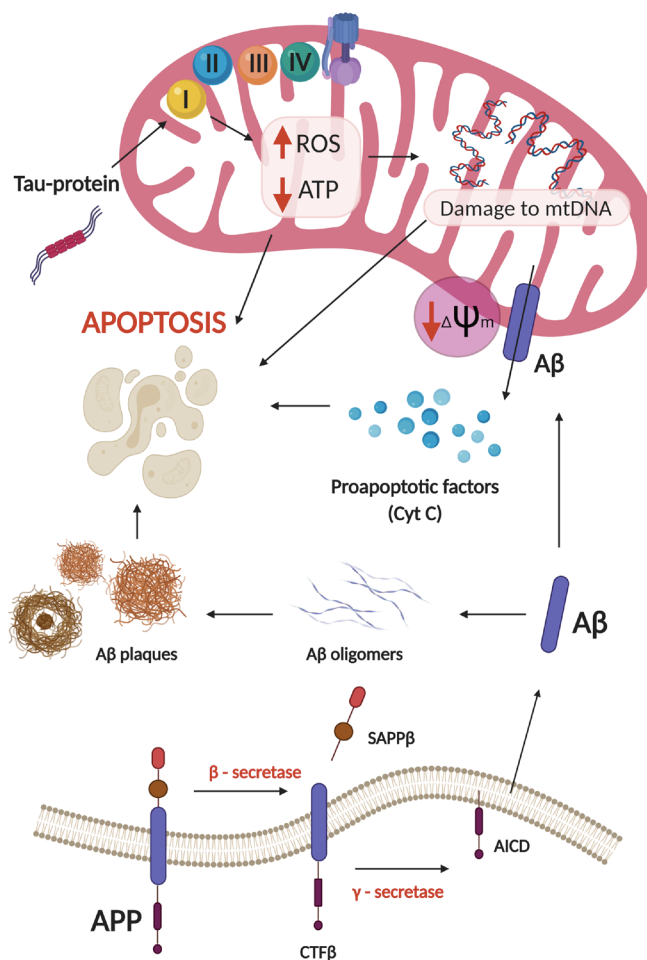


Fig. 3. The role of mitochondria and oxidative stress in the development of Alzheimer's. Mitochondrial dysfunction caused by the action of the pathological tau-protein and β-amyloid isoforms leading to respiratory chain disruption, damage to mtDNA, ROS overproduction, reduction in ATP levels, and a cascade of apoptotic death of nerve cells

various signalling pathways [17]. However, disruptions in the activity of even one of the electron transport chain complexes of mitochondria (mainly the I and IV complexes) can lead to an overproduction of superoxide radicals and other reactive oxygen species because of intensive reduction in oxygen molecules [131–133], which, in turn, contributes to the development of oxidative stress, irreversible damage to cell components and, as a consequence death of the cell through mitochondrial apoptosis [134, 135]. As a result, disruption enhances neuronal dysfunction and leads to neurodegenerative disorders [136]. Mitochondrial dysfunctions may be due to the action of a pathological Aβ peptide which destabilizes mem-

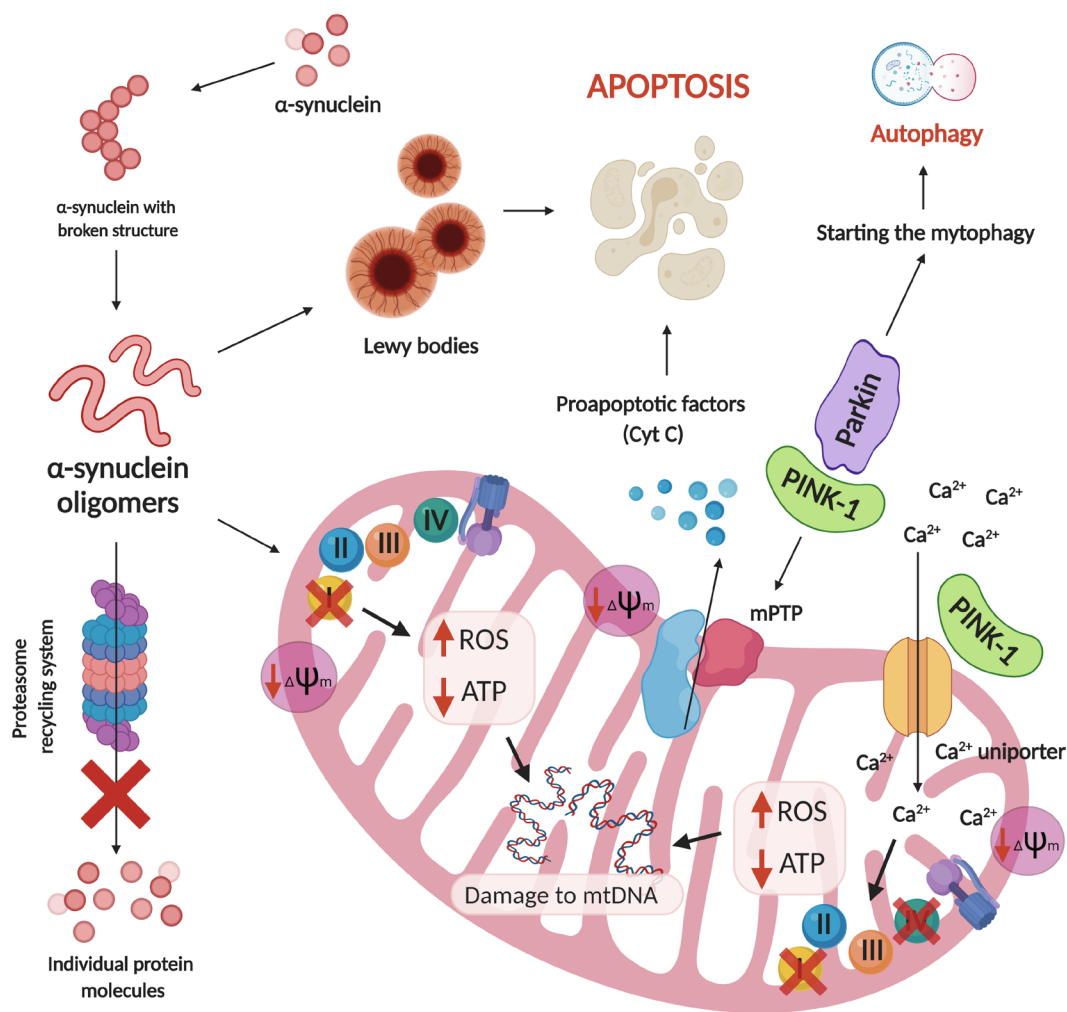


Fig. 4. The role of mitochondrial dysfunction in the development of Parkinson's. Mitochondrial dysfunction caused by overexpression of pathological α -synuclein, mutations in mitochondrial genes and calcium dysregulation lead to changes in the functioning of the electron transport chain complexes, ROS overproduction, a decrease in ATP levels and, as a result, damage to mtDNA and apoptotic neuronal death

branes and penetrates mitochondria through translocases of the outer (TOM) and inner membranes (TIM), resulting in the release of apoptogenic factors, in particular cytochrome c, and subsequent caspase activation and apoptotic cell activation [137]. The dysfunction can also be due to tau [138, 139]. The effects of tau on the mitochondrial functions and dynamics was investigated in neuroblastoma cells expressing a pathological isoform of tau (P301L), which leads to a deficiency in complex I of the respiratory electron transport chain – NADH-ubiquinone oxidoreductase, resulting in a decrease in ATP levels and increased susceptibility to oxidative stress. In addition, in-

creased expression of P301L in neuroblastoma cells also leads to a decreased mobility of mitochondria and their perinuclear clustering, resulting in an activation of the Bax proteins that increase the permeability of the outer membrane of mitochondria and cause apoptosis [140]. However, it is hard to ignore the fact that mitochondrial dysfunction can also precede the formation of pathological $A\beta$, after which the latter, in an aggregated state, penetrates the membranes of organelles and contributes to a further disruption of their functioning [141]. *Figure 3* outlines the role of mitochondria and oxidative stress in the development of Alzheimer's.

Mitochondrial dysfunction also plays a role in the pathogenesis of Parkinson's (Fig. 4). The dopaminergic neurons in the substantia nigra, which are mostly prone to progressive degradation and death in patients with the disease, are very active metabolically and largely depend on energy production as ATP by mitochondria. Any pathological situation leading to mitochondrial dysfunction can induce a significant ROS increase. Overproduction of free radicals initiates the peroxidation of mitochondrial lipids, cardiolipin in particular, and per se leads to cytochrome C release into the cytosol. In turn, this causes apoptosis. As mentioned above, electron leakage after damage to mitochondrial respiratory chain complex I induces ROS generation. Predominant death of dopaminergic neurons was observed following intraperitoneal administration of inhibitors of complex I such as rotenone and 1-methyl-4-phenyl-1,2,3,6-tetrahydropyridine to animals modelling Parkinson's disease [142]. The level of dopaminergic neurons with impairment of the electron-transport respiratory chain in mitochondria was higher in patients with Parkinson's than in age-matched controls without any signs of the disease [143]. Enough evidence of the role played by mitochondrial dysfunction and impairment of dopaminergic neurons has been gathered in studies of gene mutations in mitochondrial proteins DJ-1, Parkin, and PINK associated with inherited and sporadic Parkinson's. The cells obtained from patients with a mutation in the *Parkin* gene show a reduced complex I activation [144]. Parkin-deficient mice present a decreased activity of the respiratory chain in striatum and various types of oxidative damage [145]. *PINK1* gene mutations induce mitochondrial dysfunction, including formation of abundant free radicals [146]. The sporadic form of Parkinson's is associated with protein DJ-1, which is a redox-sensitive atypical peroxiredoxin-like peroxidase that eliminates peroxide compounds by self-oxidation. DJ-1 knockout mice accumulate more ROS in brain cells and display a fragmented mitochondrial phenotype [147]. Choi *et al.* have shown that the protein DJ-1 in the brain of patients with Parkinson's is exposed to oxidative damage [148]. They identified ten different DJ-1 subtypes using 2D gel electrophoresis and mass spectrometry and found that DJ-1 monomers containing acid fragments are selectively aggregated in the frontal cortex of patients. The authors have assumed that oxidative damage to protein DJ-1 can be related to the pathogenesis of the sporadic disease and may be used as a biomarker of an early stage of the disease. An important role in the development of pathology in Parkinson's disease is assigned to α -synuclein, which is a cytosolic protein that is capable of interacting with

mitochondrial membranes and inhibiting complex I of the mitochondrial respiratory chain (Fig. 4) [149]. Thus, impairment of the mitochondrial structure and function is found in mice with abundant expression of mutant α -synuclein [150]. It is also likely that calcium dysregulation contributes to oxidative stress and mitochondrial dysfunction in Parkinson's disease [151, 152]. This is due to the fact that the compact layer of the dopaminergic neurons in the substantia nigra includes L-type ion channels the disruption of which allows extracellular calcium to enter the cytoplasm uncontrollably [153] and thereby enhance dopamine metabolism, shifting the cytosolic concentration of the neurotransmitter to the toxic range of L-DOPA [154]. In particular, Surmeier *et al.* showed that the constant opening of L-type calcium channels in the dopaminergic neurons of the substantia nigra causes oxidative stress, and likewise leads to fluctuations in the mitochondrial potential, which is associated with a disruption of ATP production, which ultimately triggers processes associated with cell death [155]. Isradipine, an L-type calcium channel blocker, can attenuate rotenone-induced dendrite loss (shown in adult midbrain slices), as well as attenuate MPTP-induced neurodegeneration of dopaminergic neurons in mice [156].

Mitochondrial dysfunction leads to a decreased ability by the organelles to regulate intracellular calcium homeostasis and initiate mitochondrial permeability transition [157]. In other words, the increase of the intracellular calcium level can provoke degenerative changes and lead to a significantly higher probability of mitochondrial permeability with subsequent initiation of a cell death cascade via apoptosis and necrosis [158]. Importantly, higher levels of calcium can lead to excess production of active oxygen forms and oxidative stress [159]. The increased calcium levels in the neurons of 3xTg-AD transgenic mice were investigated by Lopez *et al.* [160]. In addition, the mitochondrial dysfunction associated with impaired calcium homeostasis has been described in neurodegenerative pathologies; in particular, in Huntington's disease [161]. Pronounced defects in calcium regulation were detected in the brain mitochondria of transgenic mice modelling Huntington's disease, as well as in the lymphblasts of patients with Huntington's disease [162]. Moreover, the mitochondrial function was also impaired in cell models of the disease [161, 163–165], whereas the use of mitochondria membrane permeability inhibitors such as Bongkreik acid, Nortriptyline, Desipramine, Trifluoroperazine, and Maprotiline prevented neuronal death and had a neuroprotective effect on animal models of this disorder [163]. Mitochondrial damage is also observed

in the neurons of patients with Alzheimer's, which is accompanied with membrane depolarization, reduced ability to bind Ca^{2+} ions, overproduction of reactive oxygen species and oxidative damage to mitochondrial DNA [166].

The possibility of using mitoprotectors for the treatment of neurodegenerative diseases was also confirmed by the results of studies of bioisosteric analogues of cinnamic acid and polymethoxybenzenes as potential neuroprotectors. A high ability to inhibit calcium-induced opening of the mitochondrial permeability transition pore (over 50%) was established for several compounds. Such mitoprotective activity is considered as a mechanism of the neuroprotective effect of these compounds and correlates with the presence of a cytoprotective potential on a cellular model of neurodegeneration associated with calcium stress in ionomycin-induced neurotoxicity [46]. Such ability was also shown for tetrahydro-gamma-carbolines, structural analogues of Dimebon. These compounds were more likely to inhibit calcium-induced mitochondrial permeability than the drug Dimebon, which reduced the rate of mitochondrial swelling by an average of 20%, whereas the effect of DF-407 was double [167]. Early studies of the effect of tetrahydro-gamma-carbolines on the survival of neurons in the cerebral cortex of newborn rats under glutamate-induced toxicity showed a significant decrease in the death rate of cells treated with these compounds, which may have something to do with their mitoprotective properties [47]. Preincubation of rat mitochondria with allomargaritarine, the conjugate of securinine and tryptamine, inhibits Ca^{2+} -induced mitochondrial permeability transition in a dose-dependent manner. It also effectively suppresses it when $A\beta_{35-25}$ is used as an inducer and, as a result, displays cyto(neuro)protector activity in models of excitotoxicity and toxicity mediated by trivalent iron ions and amyloid [41, 42, 168]. Moreover, allomargaritarine has the ability to reduce $A\beta$ [169]. Therefore, mitochondria represent a promising target in the search for potential neuroprotective agents aimed at preventing or slowing down the development of neurodegenerative diseases: in particular, Alzheimer's.

Histone deacetylases (HDACs) as a potential molecular target in the search for neuroprotective agents

In addition to the main pathological aspects of Alzheimer's, the formation of toxic β -amyloid aggregates and neurofibrillary tangles, epigenetic regulation mechanisms have now become increasingly important [170, 171]. Epigenetic changes are reversible, do not affect the modifications of primary DNA structure,

and can be corrected with pharmacological therapy. Chromosome DNA is enveloped in a compact structure with the specialized proteins called histones. Histones are relatively small proteins with a very large fraction

Classification of histone deacetylases

HDAC family		
Type	Co-factor	Localization
<i>Class I</i>		
HDAC1	Zn ²⁺	Nucleus
HDAC2		Nucleus
HDAC3		Nucleus/cytoplasm
HDAC8		Nucleus
<i>Class II</i>		
<i>Subclass IIa</i>		
HDAC4	Zn ²⁺	Nucleus/cytoplasm
HDAC5		Nucleus/cytoplasm
HDAC7		Nucleus/cytoplasm
HDAC9		Nucleus/cytoplasm
<i>Subclass IIb</i>		
HDAC6	Zn ²⁺	Cytoplasm
HDAC10		Cytoplasm
<i>Class III Sirtuins</i>		
Sir1	NAD ⁺	Nucleus
Sir2		Nucleus
Sir3		Nucleus/cytoplasm
Sir4		Mitochondria
Sir5		Mitochondria
Sir6		Mitochondria
Sir7		Nucleus
Sir8		Nucleolus
<i>Class IV</i>		
HDAC11	Zn ²⁺	Nucleus

of positively charged amino acids (lysine and arginine); a positive charge helps histones bind to DNA (which is negatively charged) regardless of its nucleotide sequence. Histones perform the two main functions in the cell: they are involved in the packaging of DNA in the nucleus and the epigenetic regulation of transcription, replication, and repair [172]. Histones undergo post-translation modification by acetylation, deacetylation, phosphorylation, and methylation. Histone acetylation and deacetylation are regulated by histone deacetylases (HDACs) and histone acetyltransferases (HATs) [173, 174]. These processes play a decisive role in the changing of the structure of chromatin and, as a result, regulate gene expression, cell survival, and cell differentiation [175].

There are two main subfamilies of HDAC proteins: “zinc-dependent” conventional histone deacetylases and “nicotinamide-adenine-dinucleotide (NAD⁺)-dependent” proteins sirtuins (SIRT), sometimes referred to as class III HDACs. Depending on their similarity, zinc-dependent HDACs are divided into four different classes (I, II (IIa and IIb), III and IV) which differ in their structure, enzymatic functions, subcellular localization, and expression regions (*Table*) [176]. To date, 18 deacetylases have been identified in mammals. The biological functions of individual HDACs are difficult to establish due to the lack of isoform-specific inhibitors.

The ratio between the levels of histone acetylase and histone acetyltransferases is strictly regulated in healthy neurons, whereas in neurodegenerative pathologies this ratio is disturbed [177]. HDAC6 is overexpressed in patients with Alzheimer’s, along with the formation of atypical APP, A β accumulation, A β -mediated hyperphosphorylation of the tau protein, degeneration of cholinergic neurons, and, consequently, severe cognitive decline (*Fig. 5*) [178]. Neurodegenerative diseases are accompanied by dysregulation of transcription, leading to the death of nerve cells; therefore, HDACs are considered very promising targets for the pharmacological correction of neuropathologies [179], in part because of the potential reversibility of such epigenetic modifications [180].

Hahnen *et al.* have considered the involvement of histone deacetylase inhibitors (HDACi) in the regulation of epigenetic events as relates to the development of a number of neurodegenerative processes. Histone deacetylase inhibitors, which were originally used as anti-neoplastic agents, may be effective in neurodegenerative disorders, particularly in Alzheimer’s [181]. The results of numerous studies on the effect of different compounds on HDAC show that the neuroprotective effect of histoneacetylase inhibitors might be attributed to the suppression of

A β production [182, 183] and, consequently, inhibition of A β -induced hyperphosphorylation of the tau-protein [184, 185]. The use of the histone deacetylase inhibitor Entinostat for the treatment of APP/PS1 transgenic mice modelling Alzheimer’s led to an enhanced microglial activation and a decrease in A β deposits [186]. The use of suberoylanilide hydroxamic acid (SAHA) in experiments on 20-month-old mice with age-related memory disorders showed spatial memory improvements. At the same time, in elderly mice, a decrease in the level of histone H4K12ac in the hippocampal region of CA1 was established, while SAHA led to the expression of acetylated histones, and also stimulated the activity of NMDA receptors in the hippocampus [187].

Mice overexpressing HDAC2, but not HDAC1, show a decreased synaptic plasticity, in the number of synapses formed, and impaired memory formation, while Vorinostat (an HDAC inhibitor) can restore synaptic plasticity and improve learning and memory [188]. Akhtar *et al.* showed that an increased level of HDAC2 in mature neurons affects the main excitatory neurotransmission, implying the involvement of HDAC2 in synaptic plasticity [189]. McQuown *et al.* found that, in HDAC3-Flox-modified mice (deletion of HDAC3 in the hippocampal region of CA1) or in mice treated with the selective HDAC3 inhibitor RGFP136, the histone acetylation process is enhanced and long-term memory is significantly improved [190]. Moreover, Bardai *et al.* have suggested that HDAC3 is a protein that exhibits its own strong neurotoxic activity, while its toxic effect is cell-selective. HDAC3 is phosphorylated directly by GSK-3 β , and inhibition of GSK-3 β protects mice from HDAC3-induced neurotoxicity [191]. HDAC6 is localized mainly in the cytoplasm and catalyses a number of non-histone proteins, such as tubulin and deacetylase HSP90 [192, 193].

The level of HDAC6 in the brain of patients with Alzheimer’s is significantly higher in the cortex and hippocampus compared to the brain of healthy people. Tubacin (a selective HDAC6 inhibitor) attenuates the site-specific phosphorylation of the tau-protein [194] and enhances mitochondrial migration in hippocampal neurons. GSK-3 β participates in the regulation of HDAC6 activity through its phosphorylation [195]. Selective HDAC6 inhibition ensures protection from the neurodegeneration induced by oxidative stress and contributes to the proliferation of neurites in cortical neurons [196]. HDAC4 can also play a significant role in the functioning of neuronal cells. The enzyme is predominantly found in the cytoplasm of brain cells, and abnormal expression of HDAC4 occurs in the nucleus that contributes to neuronal apoptosis. Its inactivation suppresses cell death [197].

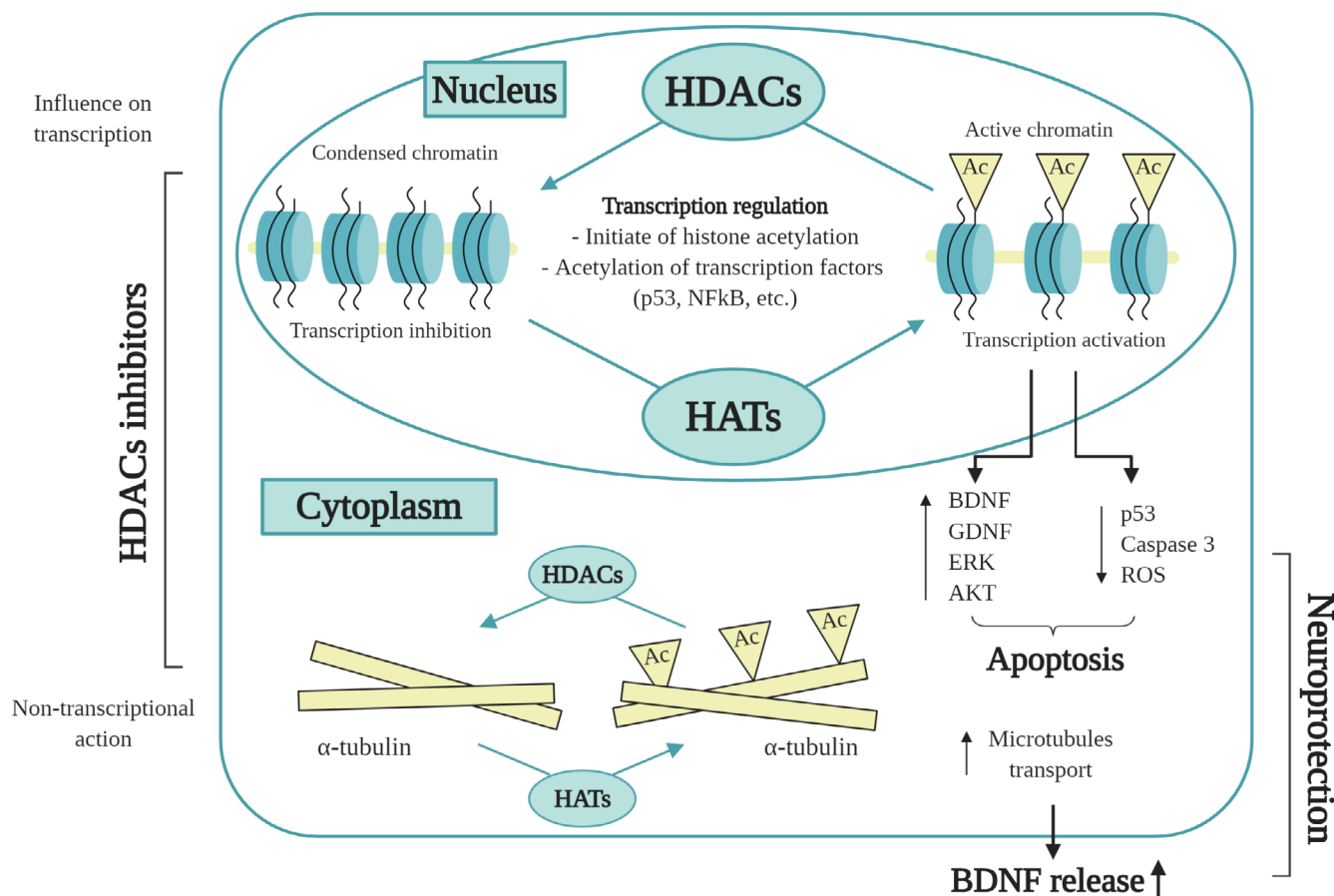


Fig. 5. Action of HDAC inhibitors in the cell in neurodegenerative diseases. Impairment of acetylation homeostasis leads to hypoacetylation of histones and, as a result, aberrant transcriptional activity. Inhibition of HDAC activity has transcriptional and non-transcriptional effects. Acetylation of histone proteins in gene promoters, as well as transcription factors, can increase the expression of multiple genes which contribute to neuroprotection, plasticity, and learning/memory. The non-transcriptional action of HDAC inhibitors leads to hyperacetylation and stabilization of microtubule proteins, increase of vesicular transport, and BDNF release

Recent findings have implicated sirtuins in the development of neurodegenerative diseases. A significant decrease in Sir1 was found in the parietal cortex of patients with Alzheimer's compared to the controls. Therefore, the accumulation of A β and tau proteins may be associated with a loss of Sir1 function [198]. In addition, memory and synaptic plasticity impairments are also found in mutant Sir1-deficient mice [199]. Moreover, abundant expression of NAD⁺-dependent deacetylase Sir1 in a mouse model of Alzheimer's decreases A β production and the formation of plaques via the activation of the gene encoding α -secretase ADAM10 [200]. Sir3 knockdown increases the generation of mitochondrial reactive oxygen species in

fertilized mouse oocytes, and the formation of mitochondrial ROS is accompanied by an increase in the amount of the p53 protein [201]. Moreover, treatment of the primary cultures of neurons in the cerebral cortex of mice with glutamate induces excessive production of ROS, as well as an increase in the level of mitochondrial Sir3, while overexpression of Sir3 significantly reduces the formation of mitochondrial ROS. Apparently, Sir3 is involved in the protection of nerve cells from oxidative stress and excitotoxicity [202].

The accumulated data support the opinion that HDAC proteins are involved in the development of neurodegenerative diseases. HDACs regulate the level

of histone acetylation and, as a consequence, affect the expression of some of the genes involved in memory formation, synaptic plasticity, and other processes necessary for the normal functioning of brain cells. HDAC inhibitors can reduce cognitive deficits in animal models with neurodegenerative disorders. HDAC inhibitors can potentially act on suppressing A β -induced hyperphosphorylation of the tau protein, as well as in regulating the expression of the genes that are involved in learning and memory (Fig. 5). The possibility of pharmacological correction of neurodegenerative diseases using HDAC inhibitors is being considered, but a number of unsolved problems remain. Most current inhibitors of histone deacetylases are pan-selective; i.e., they act against all HDACs types, which causes massive changes in gene expression leading to multiple adverse effects [203], because HDACs participate both in cell survival and death processes. Therefore, in order to develop selective HDAC inhibitors with low toxicity to normal cells, it is necessary to elucidate the exact role of individual members of the HDAC family in various neuropathologies.

Aggregation of pathogenic protein forms as a key target in the search of potential drugs for the treatment of neurological disorders

The introduction of the latest cell technologies, bioinformatics, and targeted manipulation of the genome of laboratory animals have led to rapid progress in this field and allowed us to design a new classification of the fundamental processes underlying neurodegeneration. As a result, some concepts have been revised and changes in the classification of neurodegenerative diseases have been introduced. It has been established that a wide range of neurodegenerative diseases with different clinical manifestations have a similar molecular mechanism of pathogenesis. This mechanism is based on a pathological aggregation of proteins that leads to the development of proteinopathy [204, 205]. Many neurodegenerative diseases are characterized by the presence of pathological inclusions of various types in tissues of the nervous system [206]. The cascade nature of the complex mechanism of formation of detectable inclusions is revealed, and the molecular-cellular events occurring at the main stages of this pathological process are identified. [207, 208]. For example, in Parkinson's disease, the *SNCA* gene encoding α -synuclein, a short cytoplasmic protein (140 amino acids in humans), is predominantly synthesized in the nervous system and localized in presynaptic terminals [209–211]. The most typical histopathological signs of Parkinson's are the Lewy bodies found in the dopaminergic neurons of substantia nigra and dystrophic neuritis in the tract leading

from substantia nigra to the striatum containing aggregates of various proteins [212, 213]. The key role in the formation of these deposits is played by the fibrillar form of α -synuclein, which has unique physical and chemical properties [214, 215]. It should be noted that the formation of Lewy bodies in the neurons of the cerebral cortex also results in diseases that are classified as a separate group of dementia. For example, cytoplasmic and nuclear deposits in neurons and oligodendrocytes form in multiple systemic atrophy [216–218].

In Alzheimer's, it has been established that mutations in three various genes, *APP*, presenilin-1, and presenilin-2 (*PSEN1*, *PSEN2*), lead to the development of hereditary forms of Alzheimer's with early manifestation (clinical symptoms appear before the age of 65 years) [219, 220]. At the same time, familial and sporadic forms of Alzheimer's are similar: the nervous tissues of patients contain protein aggregates of two types: amyloid plaques and neurofibrillary tangles, the main components of which are A β and hyperphosphorylated forms of the tau protein, respectively. A hypothesis about the transformation of non-toxic A β monomers into its toxic oligomers [221], which can interact with several post-synaptic components, including glutamatergic receptors (N-methyl-D-aspartate (NMDA) and metabotropic glutamate receptor 5 (mGluR5)), the prion protein, neurotrophin receptor, and the A7-nicotin acetylcholine receptor [222], and contribute to synaptic damage, is one of the predominant ones seeking to explain the order of pathogenic events leading to neurodegeneration. It is known that oligomers A β can form channels, leading to the impairment of membrane permeability and, as a result, calcium homeostasis, which in turn induces neuronal death [223, 224]. Similarly, toxic oligomers A β can modulate the activity of NMDA-subtype glutamate receptors [225], attenuate the mGluR-dependent mechanisms [226] inducing the impairment of recirculation of the synaptic glutamate contributing to synapse depression, and damaging synaptic plasticity [227].

It has also been shown that the oligomeric form of A β activates extrasynaptic NMDA-receptors in neurons which, in turn, leads to hyperphosphorylation of the tau-protein, activation of caspase-3, production of nitric oxide, and synaptic depression [228], and inhibition of this subtype of glutamate receptors protects synapses from A β -induced damage and, apparently, eliminates memory difficulties [229, 230], which clearly confirms the potential existent in using modulators of this process.

Although the exact molecular mechanisms of neurodegeneration development are still unclear, hyper-

phosphorylation of the tau-protein is one of the key roles in the pathogenesis of this pathology. To a large extent, the tau-protein is involved in the abovementioned processes, acting in parallel or in combination with A β [231]. In a model of tau-induced neurodegeneration, it was shown that an abnormally phosphorylated protein initiates the binding and stabilization of filamentous actin, which leads to mitochondrial dysfunction and oxidative stress, DNA damage and, ultimately, apoptosis [232]. Decreased tau protein levels protected both transgenic and nontransgenic mice from excitotoxicity and restored the memory function in a tauopathy model [233].

The tau-protein does not have a rigid three-dimensional structure [234]. However, its shortening and hyperphosphorylation can cause multiple pathological changes in the structure and lead to the formation of insoluble paired helical filaments and larger aggregates [234–238]. First of all, such transformations lead to a loss of the physiological function of the native protein (participation in the assembly of tubulin monomers into microtubules), and secondly, to a toxic effect on brain cells [235, 234].

Because tau plays an important role in the physiological dynamics of microtubules and thus ensures the normal functioning of cells [239], researchers are interested in the development of drugs that can act on this protein. An in-depth study of the molecular mechanisms underlying the pathological transformations of the tau protein opens up the possibility of specifically targeting the pathological modifications of tau for therapeutic purposes. At the moment, there are several approaches for the development of such agents targeting directly or indirectly the tau-protein: compounds which prevent or reverse tau aggregation [240–242], low-molecular drugs which inhibit kinases or activate tau phosphatases [243, 244], compounds that are stabilizing microtubules [245], drugs which contribute to a proteolytic degradation of incorrectly folded tau-proteins [239, 246, 247] and immunosuppressive agents [234], as well as strategies aimed at active and passive immunization [234, 248, 249].

It has been shown that monoclonal antibodies can differentiate between tau-protein isoforms and have a different effect on native than transformed proteins. Taniguchi *et al.* demonstrated that the monoclonal antibodies RTA-1 and RTA-2 binding specifically to the R1 and R2 parts of tau prevent the formation of spiral filaments *in vitro* and simultaneously stimulate tubulin assembly induced by tau [250]. At least three vaccines acting on different pathogenic forms of A β are in clinical studies. At the same time, there are currently no data on the results of these trials. In the transgenic APP animals

modeling Alzheimer's, the effectiveness of active immunization was clearly shown, which leads to a decrease in A β deposits and, as a result, alleviates the associated brain damage [251–253]. Asuni *et al.* demonstrated that active immunization with the epitope of a phosphorylated tau protein of transgenic mice expressing the P301L mutant tau in neurons reduces the amount of aggregated protein in the brain and slows down the progression of the behavioural phenotype associated with this pathology [254, 255]. Furthermore, a significant correlation was observed between motor activity values obtained in the behavioural analysis and the tau pathology in the excitable area of the cortex and brain stem, which play an evident role in motor coordination. It shows a direct correlation between the main pathological feature of the model and the related functional disorders [255] and states that immunotherapy approaches targeting the pathological tau-protein form represent a promising approach to the treatment and/or diagnosing of various tauopathies, and the Alzheimer's disease in particular.

Some other diseases can be compared in a similar way. In amyotrophic lateral sclerosis, the autopsy material of patients showed deposits containing the proteins FUS, TDP-43, OPTN, UBQLN2, as well as products of intron repetition translation in the *C9ORF72* gene [256, 257], while polyglutamine deposits had accumulated in neurons in patients with Huntington's disease as a result of the expansion of trinucleotide CAG-repetition in the huntingtin gene [258, 259]. Despite the difference in the functions of pathogenic proteins, susceptibility to aggregation is the fundamental feature of a wide range of neurodegenerative diseases; therefore, the aggregation of pathogenic protein forms can be considered as the key therapeutic target.

CONCLUSION

Our investigations of the multiple hypotheses put forth in the attempts to accurately identify the specific source of any neurodegenerative disorder failed to pinpoint any primary cause. Therefore, it appears necessary to take into account multiplicity (combination) in the context of aetiology of neurodegenerative diseases. This should be the case when a set of mutations or factors, ranging from neuroinflammatory processes to the aggregation of proteins in neuronal cells, leads to the sequential accumulation of a whole tangle of molecular pathologies. The foundational aspect in the development of new drugs should rest in a multifactorial nature of their therapeutic effect. Such drugs should have a multitarget purpose, even if they have no or little significant impact on any of the listed molecular targets. They should affect as

many targets as possible. Given the hardly conclusive, and sometimes controversial, studies that aim to identify the root causes of neurodegenerative diseases, it appears that we are only now starting to understand the key factors whose combination triggers a neurodegenerative process. ●

This work was carried out with financial support from the Russian Science Foundation (grant No. 19-73-10195) and as part of the State Assignment of the Institute of Physiologically Active Compounds, Russian Academy of Sciences, dated 2019 (No. 0090-2019-0006).

REFERENCES

1. Dementia. Information bulletin. World Health Organization. 2019. <https://www.who.int/ru/news-room/factsheets/detail/dementia>. Access date 20.01.2020.
2. McDade E., Bateman R.J. // *Nature*. 2017. V. 547. № 7662. P. 153–155. doi: 10.1038/547153a.
3. Bachurin S.O., Bovina E.V., Ustyugov A.A. // *Med Res Rev*. 2017. V. 37. № 5. P. 1186–1225. doi: 10.1002/med.21434.
4. Bachurin S.O., Gavrilova S.I., Samsonova A., Barreto G.E., Aliev G. // *Pharmacol Res*. 2018. V. 129. P. 216–226. doi: 10.1016/j.phrs.2017.11.021.
5. Reddy P.H., Reddy T.P. // *Curr Alzheimer Res*. 2011. V. 8. № 4. P. 393–409. doi: 10.2174/156720511795745401.
6. Swerdlow R.H., Khan S.M. // *Med Hypotheses*. 2004. V. 63. № 1. P. 8–20. doi: 10.1016/j.mehy.2003.12.045.
7. Moran M., Moreno-Lastres D., Marin-Buera L., Arenas J., Martin M.A., Ugalde C. // *Free Radic Biol Med*. 2012. V. 53. № 3. P. 595–609. doi: 10.1016/j.freeradbiomed.2012.05.009.
8. Zhu L., L Z., Song Y.Y. // *Zhongguo Yi Xue Ke Xue Yuan Xue Bao*. 2015. V. 37. № 4. P. 482–488. doi: 10.3881/j.issn.1000-503X.2015.04.020.
9. Chiurciu V., Orlacchio A., Maccarrone M. // *Oxid Med Cell Longev*. 2016. V. 2016. P. 7909380. doi: 10.1155/2016/7909380.
10. El-Bacha R.S., De-Lima-Filho J.L., Guedes R.C. // *Nutr Neurosci*. 1998. V. 1. № 3. P. 205–212. doi: 10.1080/1028415X.1998.11747230.
11. Mandel S., Grunblatt E., Riederer P., Gerlach M., Levites Y., Youdim M.B. // *CNS Drugs*. 2003. V. 17. № 10. P. 729–762. doi: 10.2165/00023210-200317100-00004.
12. von Arnim C.A., Gola U., Biesalski H.K. // *Nutrition*. 2010. V. 26. № 7–8. P. 694–700. doi: 10.1016/j.nut.2009.11.009.
13. Yu Y.C., Kuo C.L., Cheng W.L., Liu C.S., Hsieh M. // *J Neurosci Res*. 2009. V. 87. № 8. P. 1884–1891. doi: 10.1002/jnr.22011.
14. Zuo L., Zhou T., Pannell B.K., Ziegler A.C., Best T.M. // *Acta Physiol (Oxf)*. 2015. V. 214. № 3. P. 329–348. doi: 10.1111/apha.12515.
15. Mosley R.L., Benner E.J., Kadiu I., Thomas M., Boska M.D., Hasan K., Laurie C., Gendelman H.E. // *Clin Neurosci Res*. 2006. V. 6. № 5. P. 261–281. doi: 10.1016/j.cnr.2006.09.006.
16. Rego A.C., Oliveira C.R. // *Neurochem Res*. 2003. V. 28. № 10. P. 1563–1574. doi: 10.1023/a:1025682611389.
17. Bhat A.H., Dar K.B., Anees S., Zargar M.A., Masood A., Sofi M.A., Ganie S.A. // *Biomed Pharmacother*. 2015. V. 74. P. 101–110. doi: 10.1016/j.biopha.2015.07.025.
18. Gan L., Johnson J.A. // *Biochim Biophys Acta*. 2014. V. 1842. № 8. P. 1208–1218. doi: 10.1016/j.bbadis.2013.12.011.
19. Dias V., Junn E., Mouradian M.M. // *J Parkinsons Dis*. 2013. V. 3. № 4. P. 461–491. doi: 10.3233/JPD-130230.
20. St-Pierre J., Drori S., Uldry M., Silvaggi J.M., Rhee J., Jager S., Handschin C., Zheng K., Lin J., Yang W., et al. // *Cell*. 2006. V. 127. № 2. P. 397–408. doi: 10.1016/j.cell.2006.09.024.
21. Gill S.S., Rochon P.A., Herrmann N., Lee P.E., Sykora K., Gunraj N., Normand S.-L.T., Gurwitz J.H., Marras C., Wodchis W.P., et al. // *BMJ*. 2005. V. 330. № 7489. P. 445. doi: 10.1136/bmj.38330.470486.8F.
22. Lermontova N., Lukoyanov N., Serkova T., Lukoyanova E., Bachurin S. // *Mol. Chem. Neuropathol*. 1998. V. 33. № 1. P. 51–61. doi: 10.1007/bf02815859.
23. Berg D., Youdim M.B., Riederer P. // *Cell Tissue Res*. 2004. V. 318. № 1. P. 201–213. doi: 10.1007/s00441-004-0976-5.
24. Halliwell B. // *Acta Neurol. Scand. Suppl*. 1989. V. 126. P. 23–33. doi: 10.1111/j.1600-0404.1989.tb01779.x.
25. Cohen G. // *Oxygen Radicals Tissue Injury*. 1988. P. 130–135.
26. Greilberger J., Koidl C., Greilberger M., Lamprecht M., Schroecksnadel K., Leblhuber F., Fuchs D., Oetl K. // *Free Radic. Res*. 2008. V. 42. № 7. P. 633–638. doi: 10.1080/10715760802255764.
27. Dalfo E., Portero-Otin M., Ayala V., Martinez A., Pampolina R., Ferrer I. // *J. Neuropathol. Exp. Neurol*. 2005. V. 64. № 9. P. 816–830. doi: 10.1097/01.jnen.0000179050.54522.5a.
28. Selley M.L., Close D.R., Stern S.E. // *Neurobiol. Aging*. 2002. V. 23. № 3. P. 383–388. doi: 10.1016/s0197-4580(01)00327-x.
29. Bosco D.A., Fowler D.M., Zhang Q., Nieva J., Powers E.T., Wentworth P., Jr, Lerner R.A., Kelly J.W. // *Nat. Chem. Biol*. 2006. V. 2. № 5. P. 249–253. doi: 10.1038/nchembio782.
30. Nakabeppu Y., Tsuchimoto D., Yamaguchi H., Sakumi K. // *J. Neurosci. Res*. 2007. V. 85. № 5. P. 919–934. doi: 10.1002/jnr.21191.
31. Zeevalk G.D., Razmpour R., Bernard L.P. // *Biomed. Pharmacother*. 2008. V. 62. № 4. P. 236–249. doi: 10.1016/j.biopha.2008.01.017.
32. Thannickal T.C., Lai Y.Y., Siegel J.M. // *Brain*. 2008. V. 131. № 1. P. e87. doi: 10.1093/brain/awm221.
33. Sano M., Ernesto C., Thomas R.G., Klauber M.R., Schaffer K., Grundman M., Woodbury P., Growdon J., Cotman C.W., Pfeiffer E., et al. // *N. Engl. J. Med*. 1997. V. 336. № 17. P. 1216–1222. doi: 10.1056/NEJM199704243361704.
34. Golbe L.I., Farrell T.M., Davis P.H. // *Arch. Neurol*. 1988. V. 45. № 12. P. 1350–1353. doi: 10.1001/archneur.1988.00520360068014.
35. May J.M. // *Subcell Biochem*. 2012. V. 56. P. 85–103. doi: 10.1007/978-94-007-2199-9_6.
36. Kojo S. // *Curr. Med. Chem*. 2004. V. 11. № 8. P. 1041–1064. doi: 10.2174/0929867043455567.

37. Olabisi A.O. The chemistry of *L*-ascorbic acid derivatives in the asymmetric synthesis of C2 and C3-substituted aldo-*o*-g-lactones. Ph.D. Dissertation, 2005. College of Liberal Arts and Sciences, Wichita State University, Wichita.
38. Harikumar K.B., Aggarwal B.B. // *Cell Cycle*. 2008. V. 7. № 8. P. 1020–1035. doi: 10.4161/cc.7.8.5740.
39. Venturini C.D., Merlo S., Souto A.A., Fernandes Mda C., Gomez R., Rhoden C.R. // *Oxid. Med. Cell. Longev*. 2010. V. 3. № 6. P. 434–441. doi: 10.4161/oxim.3.6.14741.
40. Yao Z., Drieu K., Papadopoulos V. // *Brain Res*. 2001. V. 889. № 1–2. P. 181–190. doi: 10.1016/s0006-8993(00)03131-0.
41. Neganova M.E., Klochkov S.G., Afanasieva S.V., Serkova T.P., Chudinova E.S., Bachurin S.O., Reddy V.P., Aliev G., Shevtsova E.F. // *CNS Neurol. Disord. Drug Targets*. 2016. V. 15. № 1. P. 102–107. doi: 10.2174/1871527314666150821111812.
42. Neganova M.E., Serkova T.P., Klochkov S.G., Afanasieva S.V., Shevtsova E.F., Bachurin S.O. // *Nat. Techn. Sci*. 2011. V. 5. № 55. P. 86–90.
43. Neganova M.E., Blik V.A., Klochkov S.G., Chepurnova N.E., Shevtsova E.F. // *Neurochem. J*. 2011. V. 5. P. 208.
44. Kann O., Kovacs R. // *Am. J. Physiol. Cell. Physiol*. 2007. V. 292. № 2. P. C641–657. doi: 10.1152/ajpcell.00222.2006.
45. Kovacs R., Schuchmann S., Gabriel S., Kann O., Kardos J., Heinemann U. // *J. Neurophysiol*. 2002. V. 88. № 6. P. 2909–2918. doi: 10.1152/jn.00149.2002.
46. Neganova M.E., Semenov V., Semenova M., Redkozubova O.M., Aleksandrova Y.R., Lysova E.A., Klochkov S.G., Shevtsova E.F. // *Biomed. Chem. Res. Methods*. 2018. V. 1. № 3. P. e00052.
47. Vinogradova D.V., Neganova M.E., Serkova T.P., Shevtsova E.F. // *Journal of Natural and Technical Sciences (in Russian)*. 2013. V. 6. № 68. P. 73–78.
48. Kozin S.A., Makarov A.A. // *Mol. Biol. (Mosk.)*. 2019. V. 53. № 6. P. 1020–1028. doi: 10.1134/S0026898419060107.
49. Bennett C., Mohammed F., Alvarez-Ciara A., Nguyen M.A., Dietrich W.D., Rajguru S.M., Streit W.J., Prasad A. // *Biomaterials*. 2019. V. 188. P. 144–159. doi: 10.1016/j.biomaterials.2018.09.040.
50. Niranjana R. // *Neurochem. Int*. 2018. V. 120. P. 13–20. doi: 10.1016/j.neuint.2018.07.003.
51. Kim Y.S., Jung H.M., Yoon B.E. // *Anim. Cells Syst. (Seoul)*. 2018. V. 22. № 4. P. 213–218. doi: 10.1080/19768354.2018.1508498.
52. Merlo S., Spampinato S.F., Caruso G.I., Sortino M.A. // *Curr. Neuropharmacol*. 2020. V. 18. № 5. P. 446–455. doi: 10.2174/1570159X18666200131105418.
53. Wendeln A.C., Degenhardt K., Kaurani L., Gertig M., Ulas T., Jain G., Wagner J., Häslner L.M., Wild K., Skodras A., et al. // *Nature*. 2018. V. 556. № 7701. P. 332–338. doi: 10.1038/s41586-018-0023-4.
54. Mizuno T., Doi Y., Mizoguchi H., Jin S., Noda M., Sonobe Y., Takeuchi H., Suzumura A. // *Am. J. Pathol*. 2011. V. 179. № 4. P. 2016–2027. doi: 10.1016/j.ajpath.2011.06.011.
55. Parkhurst C.N., Yang G., Ninan I., Savas J.N., Yates J.R., 3rd, Lafaille J.J., Hempstead B.L., Littman D.R., Gan W.B. // *Cell*. 2013. V. 155. № 7. P. 1596–1609. doi: 10.1016/j.cell.2013.11.030.
56. Song M., Jin J., Lim J.E., Kou J., Pattanayak A., Rehman J.A., Kim H.D., Tahara K., Lalonde R., Fukuchi K. // *J. Neuroinflammation*. 2011. V. 8. P. 92. doi: 10.1186/1742-2094-8-92.
57. Hickman S.E., Allison E.K., Coleman U., Kingery-Gallagher N.D., El Khoury J. // *Front. Immunol*. 2019. V. 10. P. 2780. doi: 10.3389/fimmu.2019.02780.
58. Block M.L., Zecca L., Hong J.S. // *Nat. Rev. Neurosci*. 2007. V. 8. № 1. P. 57–69. doi: 10.1038/nrn2038.
59. Hickman S.E., Allison E.K., El Khoury J. // *J. Neurosci*. 2008. V. 28. № 33. P. 8354–8360. doi: 10.1523/JNEUROSCI.0616-08.2008.
60. Wang Y., Cao Y., Yamada S., Thirunavukkarasu M., Nin V., Joshi M., Rishi M.T., Bhattacharya S., Camacho-Pereira J., Sharma A.K., et al. // *Arterioscler. Thromb. Vasc. Biol*. 2015. V. 35. № 6. P. 1401–1412. doi: 10.1161/ATVBAHA.115.305566.
61. Eyo U.B., Mo M., Yi M.H., Murugan M., Liu J., Yarlagadda R., Margolis D.J., Xu P., Wu L.J. // *Cell Rep*. 2018. V. 23. № 4. P. 959–966. doi: 10.1016/j.celrep.2018.04.001.
62. Hashioka S., Klegeris A., McGeer P.L. // *Neuropharmacology*. 2012. V. 63. № 4. P. 685–691. doi: 10.1016/j.neuropharm.2012.05.033.
63. Bezzi P., Domercq M., Brambilla L., Galli R., Schols D., De Clercq E., Vescovi A., Bagetta G., Kollias G., Meldolesi J., et al. // *Nat. Neurosci*. 2001. V. 4. № 7. P. 702–710. doi: 10.1038/89490.
64. Liu C.C., Zhao N., Fu Y., Wang N., Linares C., Tsai C.W., Bu G. // *Neuron*. 2017. V. 96. № 5. P. 1024–1032 e1023. doi: 10.1016/j.neuron.2017.11.013.
65. Ransohoff R.M. // *Nat. Neurosci*. 2016. V. 19. № 8. P. 987–991. doi: 10.1038/nn.4338.
66. El Hajj H., Savage J.C., Bisht K., Parent M., Vallieres L., Rivest S., Tremblay M.-E. // *J. Neuroinflammation*. 2019. V. 16. № 1. P. 87. doi: 10.1186/s12974-019-1473-9.
67. Sala Frigerio C., Wolfs L., Fattorelli N., Thrupp N., Voytyuk I., Schmidt I., et al. // *Cell Rep*. 2019. V. 27. № 4. P. 1293–1306 e1296. doi: 10.1016/j.celrep.2019.03.099.
68. Hashemiaghdam A., Mroczek M. // *J. Neuroimmunol*. 2020. V. 341. P. 577185. doi: 10.1016/j.jneuroim.2020.577185.
69. Holtman I.R., Skola D., Glass C.K. // *J. Clin. Invest*. 2017. V. 127. № 9. P. 3220–3229. doi: 10.1172/JCI90604.
70. Keren-Shaul H., Spinrad A., Weiner A., Matcovitch-Natan O., Dvir-Szternfeld R., Ulland T.K., David E., Baruch K., Lara-Astaiso D., Toth B., et al. // *Cell*. 2017. V. 169. № 7. P. 1276–1290 e1217. doi: 10.1016/j.cell.2017.05.018.
71. Jay T.R., Hirsch A.M., Broihier M.L., Miller C.M., Neilson L.E., Ransohoff R.M., Lamb B.T., Landreth G.E. // *J. Neurosci*. 2017. V. 37. № 3. P. 637–647. doi: 10.1523/JNEUROSCI.21110-16.2016.
72. Suarez-Calvet M., Araque Caballero M.A., Kleinberger G., Bateman R.J., Fagan A.M., Morris J.C., Levin J., Danek A., Ewers M., Haass C. // *Sci. Transl. Med*. 2016. V. 8. № 369. P. 369ra178. doi: 10.1126/scitranslmed.aag1767.
73. Claes C., van Den Daele J., Boon R., Schouteden S., Colombo A., Monasor L.S., Fiers M., Ordovás L., Nami F., Bohrmann B., et al. // *Alzheimers Dement*. 2019. V. 15. № 3. P. 453–464. doi: 10.1016/j.jalz.2018.09.006.
74. Colonna M., Wang Y. // *Nat. Rev. Neurosci*. 2016. V. 17. № 4. P. 201–207. doi: 10.1038/nrn.2016.7.
75. Mazaheri F., Snaidero N., Kleinberger G., Madore C., Daria A., Werner G., Krasemann S., Capell A., Trümbach D., Wurst W., et al. // *EMBO Rep*. 2017. V. 18. № 7. P. 1186–1198. doi: 10.15252/embr.201743922.
76. Browne T.C., McQuillan K., McManus R.M., O'Reilly J.A., Mills K.H., Lynch M.A. // *J. Immunol*. 2013. V. 190. № 5. P. 2241–2251. doi: 10.4049/jimmunol.1200947.
77. Fisher Y., Nemirovsky A., Baron R., Monsonego A. // *PLoS One*. 2010. V. 5. № 5. P. e10830. doi: 10.1371/journal.pone.0010830.
78. Goldeck D., Larbi A., Pellicano M., Alam I., Zerr I,

- Schmidt C., Fulop T., Pawelec G. // *PLoS One*. 2013. V. 8. № 6. P. e66664. doi: 10.1371/journal.pone.0066664.
79. Atarashi K., Tanoue T., Oshima K., Suda W., Nagano Y., Nishikawa H., Fukuda S., Saito T., Narushima S., Hase K., et al. // *Nature*. 2013. V. 500. № 7461. P. 232–236. doi: 10.1038/nature12331.
80. Hsiao E.Y., McBride S.W., Hsien S., Sharon G., Hyde E.R., McCue T., Codelli J.A., Chow J., Reisman S.E., Petrosino J.F., et al. // *Cell*. 2013. V. 155. № 7. P. 1451–1463. doi: 10.1016/j.cell.2013.11.024.
81. Mayer E.A., Tillisch K., Gupta A. // *J. Clin. Invest.* 2015. V. 125. № 3. P. 926–938. doi: 10.1172/JCI76304.
82. Brkic M., Balusu S., Libert C., Vandenbroucke R.E. // *Mediators Inflamm.* 2015. V. 2015. P. 620581. doi: 10.1155/2015/620581.
83. Vafadari B., Salamian A., Kaczmarek L. // *J. Neurochem.* 2016. V. 139 Suppl 2. P. 91–114. doi: 10.1111/jnc.13415.
84. Woo M.S., Park J.S., Choi I.Y., Kim W.K., Kim H.S. // *J. Neurochem.* 2008. V. 106. № 2. P. 770–780. doi: 10.1111/j.1471-4159.2008.05430.x.
85. McGeer P.L., Itagaki S., Boyes B.E., McGeer E.G. // *Neurology*. 1988. V. 38. № 8. P. 1285–1291. doi: 10.1212/wnl.38.8.1285.
86. Yamada T., McGeer E.G., Schelper R.L., Wszolek Z.K., McGeer P.L., Pfeiffer R.F. // *Neurol. Psychiatry Brain Res.* 1993. V. 2. P. 26–35.
87. O'Callaghan J.P., Miller D.B., Reinhard J.F., Jr. // *Brain Res.* 1990. V. 521. № 1–2. P. 73–80. doi: 10.1016/0006-8993(90)91526-m.
88. Qian L., Flood P.M., Hong J.S. // *J. Neural. Transm. (Vienna)*. 2010. V. 117. № 8. P. 971–979. doi: 10.1007/s00702-010-0428-1.
89. Ishikawa A., Takahashi H. // *J. Neurol.* 1998. V. 245. № 11 Suppl 3. P. P4–9. doi: 10.1007/pl00007745.
90. Langston J.W., Forno L.S., Tetrad J., Reeves A.G., Kaplan J.A., Karluk D. // *Ann. Neurol.* 1999. V. 46. № 4. P. 598–605. doi: 10.1002/1531-8249(199910)46:4<598::aid-ana7>3.0.co;2-f.
91. Zecca L., Wilms H., Geick S., Claassen J.H., Brandenburg L.O., Holzknacht C., Panizza M.L., Zucca F.A., Deuschl G., Sievers J., et al. // *Acta Neuropathol.* 2008. V. 116. № 1. P. 47–55. doi: 10.1007/s00401-008-0361-7.
92. Lee H.J., Patel S., Lee S.J. // *J. Neurosci.* 2005. V. 25. № 25. P. 6016–6024. doi: 10.1523/JNEUROSCI.0692-05.2005.
93. Farina C., Aloisi F., Meinl E. // *Trends Immunol.* 2007. V. 28. № 3. P. 138–145. doi: 10.1016/j.it.2007.01.005.
94. Gao H.M., Zhang F., Zhou H., Kam W., Wilson B., Hong J.S. // *Environ. Hlth Perspect.* 2011. V. 119. № 6. P. 807–814. doi: 10.1289/ehp.1003013.
95. Kim Y.S., Kim S.S., Cho J.J., Choi D.H., Hwang O., Shin D.H., Chun H., Beal F., Joh T. // *J. Neurosci.* 2005. V. 25. № 14. P. 3701–3711. doi: 10.1523/JNEUROSCI.4346-04.2005.
96. Choi D.H., Kim E.M., Son H.J., Joh T.H., Kim Y.S., Kim D., Beal M.F., Hwang O. // *J. Neurochem.* 2008. V. 106. № 1. P. 405–415. doi: 10.1111/j.1471-4159.2008.05399.x.
97. Kim S.T., Kim E.M., Choi J.H., Son H.J., Ji I.J., Joh T.H., Chung S.J., Hwang O. // *Neurochem. Int.* 2010. V. 56. № 1. P. 161–167. doi: 10.1016/j.neuint.2009.09.014.
98. Kim E.M., Hwang O. // *J. Neurochem.* 2011. V. 116. № 1. P. 22–32. doi: 10.1111/j.1471-4159.2010.07082.x.
99. Kim Y.S., Choi D.H., Block M.L., Lorenz S., Yang L., Kim Y.J., Sugama S., Cho B., Hwang O., Browne S., et al. // *FASEB J.* 2007. V. 21. № 1. P. 179–187. doi: 10.1096/fj.06-5865com.
100. Lee E.J., Woo M.S., Moon P.G., Baek M.C., Choi I.Y., Kim W.K., Junn E., Kim H.-S. // *J. Immunol.* 2010. V. 185. № 1. P. 615–623. doi: 10.4049/jimmunol.0903480.
101. Vu T.K., Hung D.T., Wheaton V.I., Coughlin S.R. // *Cell*. 1991. V. 64. № 6. P. 1057–1068. doi: 10.1016/0092-8674(91)90261-v.
102. Suo Z., Wu M., Ameenuddin S., Anderson H.E., Zoloty J.E., Citron B.A., Andrade-Gordon P., Festoff B.W. // *J. Neurochem.* 2002. V. 80. № 4. P. 655–666. doi: 10.1046/j.0022-3042.2001.00745.x.
103. Schonbeck U., Mach F., Libby P. // *J. Immunol.* 1998. V. 161. № 7. P. 3340–3346.
104. Jian Liu K., Rosenberg G.A. // *Free Radic. Biol. Med.* 2005. V. 39. № 1. P. 71–80. doi: 10.1016/j.freeradbiomed.2005.03.033.
105. Aliev G., Palacios H.H., Walrafen B., Lipsitt A.E., Obrenovich M.E., Morales L. // *Int. J. Biochem. Cell. Biol.* 2009. V. 41. № 10. P. 1989–2004. doi: 10.1016/j.biocel.2009.03.015.
106. Hauptmann S., Scherping I., Drose S., Brandt U., Schulz K.L., Jendrach M., Leuner K., Eckert A., Müller W.E. // *Neurobiol. Aging.* 2009. V. 30. № 10. P. 1574–1586. doi: 10.1016/j.neurobiolaging.2007.12.005.
107. Rhein V., Song X., Wiesner A., Ittner L.M., Baysang G., Meier F., Ozmen L., Bluethmann H., Dröse S., Brandt U., et al. // *Proc. Natl. Acad. Sci. USA.* 2009. V. 106. № 47. P. 20057–20062. doi: 10.1073/pnas.0905529106.
108. Devi L., Prabhu B.M., Galati D.F., Avadhani N.G., Anandatheerthavarada H.K. // *J. Neurosci.* 2006. V. 26. № 35. P. 9057–9068. doi: 10.1523/JNEUROSCI.1469-06.2006.
109. Eckert A., Schmitt K., Gotz J. // *Alzheimers Res. Ther.* 2011. V. 3. № 2. P. 15. doi: 10.1186/alzrt74.
110. Wang Y., Xu E., Musich P.R., Lin F. // *CNS Neurosci. Ther.* 2019. V. 25. № 7. P. 816–824. doi: 10.1111/cns.13116.
111. Yao J., Irwin R.W., Zhao L., Nilsen J., Hamilton R.T., Brinton R.D. // *Proc. Natl. Acad. Sci. USA.* 2009. V. 106. № 34. P. 14670–14675. doi: 10.1073/pnas.0903563106.
112. Valla J., Schneider L., Niedzielko T., Coon K.D., Caselli R., Sabbagh M.N., Ahern G.L., Baxter L., Alexander G., Walker D.G., et al. // *Mitochondrion.* 2006. V. 6. № 6. P. 323–330. doi: 10.1016/j.mito.2006.10.004.
113. Wang X., Su B., Siedlak S.L., Moreira P.I., Fujioka H., Wang Y., Casadesus G., Zhu X. // *Proc. Natl. Acad. Sci. USA.* 2008. V. 105. № 49. P. 19318–19323. doi: 10.1073/pnas.0804871105.
114. Eckert A., Hauptmann S., Scherping I., Rhein V., Muller-Spahn F., Gotz J., Müller W.E. // *Neurodegener. Dis.* 2008. V. 5. № 3–4. P. 157–159. doi: 10.1159/000113689.
115. Li Z., Okamoto K., Hayashi Y., Sheng M. // *Cell*. 2004. V. 119. № 6. P. 873–887. doi: 10.1016/j.cell.2004.11.003.
116. Keil U., Bonert A., Marques C.A., Scherping I., Weyermann J., Strosznajder J.B., Müller-Spahn F., Haass C., Czech C., Pradier L., et al. // *J. Biol. Chem.* 2004. V. 279. № 48. P. 50310–50320. doi: 10.1074/jbc.M405600200.
117. Cabezas-Opazo F.A., Vergara-Pulgar K., Perez M.J., Jara C., Osorio-Fuentealba C., Quintanilla R.A. // *Oxid. Med. Cell. Longev.* 2015. V. 2015. P. 509654. doi: 10.1155/2015/509654.
118. Cagalinec M., Safiulina D., Liiv M., Liiv J., Choubey V., Wareski P., Veksler V., Kaasik A. // *J. Cell. Sci.* 2013. V. 126. Pt 10. P. 2187–2197. doi: 10.1242/jcs.118844.
119. Chan D.C. // *Annu. Rev. Cell. Dev. Biol.* 2006. V. 22. P. 79–99. doi: 10.1146/annurev.cellbio.22.010305.104638.
120. Twig G., Elorza A., Molina A.J., Mohamed H., Wikstrom J.D., Walzer G., Stiles L., Haigh S.E., Katz S., Las G., et al. // *EMBO J.* 2008. V. 27. № 2. P. 433–446. doi: 10.1038/sj.emboj.7601963.

121. Weststrate L.M., Drocco J.A., Martin K.R., Hlavacek W.S., MacKeigan J.P. // *PLoS One*. 2014. V. 9. № 4. P. e95265. doi: 10.1371/journal.pone.0095265.
122. Figge M.T., Reichert A.S., Meyer-Hermann M., Osiewacz H.D. // *PLoS Comput. Biol.* 2012. V. 8. № 6. P. e1002576. doi: 10.1371/journal.pcbi.1002576.
123. Chen H., Chan D.C. // *Hum. Mol. Genet.* 2009. V. 18. № R2. P. R169–176. doi: 10.1093/hmg/ddp326.
124. Trimmer P.A., Borland M.K. // *Antioxid. Redox Signal.* 2005. V. 7. № 9–10. P. 1101–1109. doi: 10.1089/ars.2005.7.1101.
125. Hara Y., Yuk F., Puri R., Janssen W.G., Rapp P.R., Morrison J.H. // *Proc. Natl. Acad. Sci. USA*. 2014. V. 111. № 1. P. 486–491. doi: 10.1073/pnas.1311310110.
126. Chen J.Q., Yager J.D., Russo J. // *Biochim. Biophys. Acta*. 2005. V. 1746. № 1. P. 1–17. doi: 10.1016/j.bbamcr.2005.08.001.
127. Ghezzi D., Zeviani M. // *Adv. Exp. Med. Biol.* 2012. V. 748. P. 65–106. doi: 10.1007/978-1-4614-3573-0_4.
128. Finkel T., Holbrook N.J. // *Nature*. 2000. V. 408. № 6809. P. 239–247. doi: 10.1038/35041687.
129. Wei Y.H., Lu C.Y., Wei C.Y., Ma Y.S., Lee H.C. // *Chin. J. Physiol.* 2001. V. 44. № 1. P. 1–11.
130. Chance B., Sies H., Boveris A. // *Physiol. Rev.* 1979. V. 59. № 3. P. 527–605. doi: 10.1152/physrev.1979.59.3.527.
131. Alexeyev M.F. // *FEBS J.* 2009. V. 276. № 20. P. 5768–5787. doi: 10.1111/j.1742-4658.2009.07269.x.
132. Castro Mdel R., Suarez E., Kraiselburd E., Isidro A., Paz J., Ferder L., Ayala-Torres S. // *Exp. Gerontol.* 2012. V. 47. № 1. P. 29–37. doi: 10.1016/j.exger.2011.10.002.
133. Voets A.M., Huigsloot M., Lindsey P.J., Leenders A.M., Koopman W.J., Willems P.H., Rodenburg R.J., Smeitink J.A., Smeets H.J. // *Biochim. Biophys. Acta*. 2012. V. 1822. № 7. P. 1161–1168. doi: 10.1016/j.bbadis.2011.10.009.
134. Hollensworth S.B., Shen C., Sim J.E., Spitz D.R., Wilson G.L., LeDoux S.P. // *Free Radic. Biol. Med.* 2000. V. 28. № 8. P. 1161–1174. doi: 10.1016/s0891-5849(00)00214-8.
135. van Houten B., Woshner V., Santos J.H. // *DNA Repair (Amst.)*. 2006. V. 5. № 2. P. 145–152. doi: 10.1016/j.dnarep.2005.03.002.
136. Guo C., Sun L., Chen X., Zhang D. // *Neural. Regen. Res.* 2013. V. 8. № 21. P. 2003–2014. doi: 10.3969/j.issn.1673-5374.2013.21.009.
137. Aleardi A.M., Benard G., Augereau O., Malgat M., Talbot J.C., Mazat J.P., Letellier T., Dachary-Prigent J., Solaini G.C., Rossignol R. // *J. Bioenerg. Biomembr.* 2005. V. 37. № 4. P. 207–225. doi: 10.1007/s10863-005-6631-3.
138. Eckert E., von Clarmann T., Kiefer M., Stiller G.P., Lossow S., Glatthor N., Degenstein D.A., Froidevaux L., Godin-Beekmann S., Leblanc T., et al. // *Atmos Chem. Phys.* 2014. V. 14. № 5. P. 2571–2589. doi: 10.5194/acp-14-2571-2014.
139. Manczak M., Reddy P.H. // *Hum. Mol. Genet.* 2012. V. 21. № 11. P. 2538–2547. doi: 10.1093/hmg/dds072.
140. Schulz S.B., Klafit Z.J., Rosler A.R., Heinemann U., Gerovich Z. // *Neuropharmacol.* 2012. V. 62. № 2. P. 914–924. doi: 10.1016/j.neuropharm.2011.09.024.
141. Swerdlow R.H. // *J. Alzheimers Dis.* 2018. V. 62. № 3. P. 1403–1416. doi: 10.3233/JAD-170585.
142. Betarbet R., Sherer T.B., Greenamyre J.T. // *Bioessays*. 2002. V. 24. № 4. P. 308–318. doi: 10.1002/bies.10067.
143. Bender A., Krishnan K.J., Morris C.M., Taylor G.A., Reeve A.K., Perry R.H., Jaros E., Hersheson J.S., Betts J., Klopstock T., et al. // *Nat. Genet.* 2006. V. 38. № 5. P. 515–517. doi: 10.1038/ng1769.
144. Muftuoglu M., Elibol B., Dalmizrak O., Ercan A., Kulaksiz G., Ogus H., Dalkara T. // *Mov. Disord.* 2004. V. 19. № 5. P. 544–548. doi: 10.1002/mds.10695.
145. Palacino J.J., Sagi D., Goldberg M.S., Krauss S., Motz C., Wacker M., Klose J., Shen J. // *J. Biol. Chem.* 2004. V. 279. № 18. P. 18614–18622. doi: 10.1074/jbc.M401135200.
146. Gandhi S., Wood-Kaczmar A., Yao Z., Plun-Favreau H., Deas E., Klupsch K., Downward J., Latchman D.S., Tabrizi S.J., Wood N.W., et al. // *Mol. Cell*. 2009. V. 33. № 5. P. 627–638. doi: 10.1016/j.molcel.2009.02.013.
147. Irrcher I., Aleyasin H., Seifert E.L., Hewitt S.J., Chhabra S., Phillips M., Lutz A.K., Rousseaux M.W.C., Bevilacqua L., Jahani-Asl A., et al. // *Hum. Mol. Genet.* 2010. V. 19. № 19. P. 3734–3746. doi: 10.1093/hmg/ddq288.
148. Choi J., Sullards M.C., Olzmann J.A., Rees H.D., Weintraub S.T., Bostwick D.E., Gearing M., Levey A.I., Chin L.S., Li L. // *J. Biol. Chem.* 2006. V. 281. № 16. P. 10816–10824. doi: 10.1074/jbc.M509079200.
149. Devi L., Raghavendran V., Prabhu B.M., Avadhani N.G., Anandatheerthavarada H.K. // *J. Biol. Chem.* 2008. V. 283. № 14. P. 9089–9100. doi: 10.1074/jbc.M710012200.
150. Martin L.J., Pan Y., Price A.C., Sterling W., Copeland N.G., Jenkins N.A., Price D.L., Lee M.K. // *J. Neurosci.* 2006. V. 26. № 1. P. 41–50. doi: 10.1523/JNEUROSCI.4308-05.2006.
151. Subramaniam S.R., Chesselet M.F. // *Prog. Neurobiol.* 2013. V. 106–107. P. 17–32. doi: 10.1016/j.pneurobio.2013.04.004.
152. Ammal Kaidery N., Thomas B. // *Neurochem. Int.* 2018. V. 117. P. 91–113. doi: 10.1016/j.neuint.2018.03.001.
153. Puopolo M., Raviola E., Bean B.P. // *J. Neurosci.* 2007. V. 27. № 3. P. 645–656. doi: 10.1523/JNEUROSCI.4341-06.2007.
154. Mosharov E.V., Larsen K.E., Kanter E., Phillips K.A., Wilson K., Schmitz Y., Krantz D.E., Kobayashi K., Edwards R.H., Sulzer D. // *Neuron*. 2009. V. 62. P. 218–229.
155. Surmeier D.J., Guzman J.N., Sanchez-Padilla J., Schumacker P.T. // *Neuroscience*. 2011. V. 198. P. 221–231. doi: 10.1016/j.neuroscience.2011.08.045.
156. Chan C.S., Guzman J.N., Ilijic E., Mercer J.N., Rick C., Tkatch T., Meredith G.E., Surmeier D.J. // *Nature*. 2007. V. 447. № 7148. P. 1081–1086. doi: 10.1038/nature05865.
157. Bezprozvanny I. // *Trends Mol. Med.* 2009. V. 15. № 3. P. 89–100. doi: 10.1016/j.molmed.2009.01.001.
158. Shevtsova E.F., Vinogradova D.V., Neganova M.E., Shevtsov P.N., Lednev B.V., Bachurin S.O. // *Biomed. Chem. Res. Meth.* 2018. V. 1. № 3. P. e00058. doi: 10.18097/BMCR00058.
159. Peng T.I., Jou M.J. // *Ann. N. Y. Acad. Sci.* 2010. V. 1201. P. 183–188. doi: 10.1111/j.1749-6632.2010.05634.x.
160. Lopez J.R., Lyckman A., Oddo S., Laferla F.M., Querfurth H.W., Shtifman A. // *J. Neurochem.* 2008. V. 105. № 1. P. 262–271. doi: 10.1111/j.1471-4159.2007.05135.x.
161. Bossy-Wetzel E., Petrilli A., Knott A.B. // *Trends Neurosci.* 2008. V. 31. № 12. P. 609–616. doi: 10.1016/j.tins.2008.09.004.
162. Panov A.V., Gutekunst C.A., Leavitt B.R., Hayden M.R., Burke J.R., Strittmatter W.J., Greenamyre J.T. // *Nat. Neurosci.* 2002. V. 5. № 8. P. 731–736. doi: 10.1038/nn884.
163. Tang T.S., Slow E., Lupu V., Stavrovskaya I.G., Sugimori M., Llinas R., Kristal B.S., Hayden M.R., Bezprozvanny I. // *Proc. Natl. Acad. Sci. USA*. 2005. V. 102. № 7. P. 2602–2607. doi: 10.1073/pnas.0409402102.
164. Zhang H., Li Q., Graham R.K., Slow E., Hayden M.R., Bezprozvanny I. // *Neurobiol. Dis.* 2008. V. 31. № 1. P. 80–88. doi: 10.1016/j.nbd.2008.03.010.
165. Wang X., Zhu S., Pei Z., Drozda M., Stavrovskaya I.G., Del Signore S.J., Cormier K., Shimony E.M., Wang H., Ferrante R.J., et al. // *J. Neurosci.* 2008. V. 28. № 38. P. 9473–

9485. doi: 10.1523/JNEUROSCI.1867-08.2008.
166. Bezprosvanny I.B. // *Acta Naturae*. 2010.T. 1. № 4. P. 80–88.
167. Bachurin S.O., Shevtsova E.P., Kireeva E.G., Oxenkrug G.F., Sablin S.O. // *Ann. N. Y. Acad. Sci.* 2003. V. 993. P. 334–344; discussion 345–339. doi: 10.1111/j.1749-6632.2003.tb07541.x.
168. Neganova M.E., Klochkov S.G., Afanasieva S.V., Chudinova E.S., Serkova T.P., Shevtsova E.F. // *Eur. Neuropsychopharmacol.* 2014. V. 24. P. 262.
169. Neganova M.E., Klochkov S.G., Petrova L.N., Shevtsova E.F., Afanasieva S.V., Chudinova E.S., Fisenko V.P., Bachurin S.O., Barreto G.E., Aliev G. // *CNS Neurol. Disord. Drug Targets*. 2017. V. 16. № 3. P. 351–355.
170. Hardy J. // *Neuron*. 2006. V. 52. № 1. P. 3–13. doi: 10.1016/j.neuron.2006.09.016.
171. Li X., Bao X., Wang R. // *Mol. Med. Rep.* 2016. V. 14. № 2. P. 1043–1053. doi: 10.3892/mmr.2016.5390.
172. Cheung P., Allis C.D., Sassone-Corsi P. // *Cell*. 2000. V. 103. № 2. P. 263–271. doi: 10.1016/s0092-8674(00)00118-5.
173. Dejligbjerg M., Grauslund M., Litman T., Collins L., Qian X., Jeffers M., Lichenstein H., Jensen P.B., Sehested M. // *Mol. Cancer*. 2008. V. 7. P. 70. doi: 10.1186/1476-4598-7-70.
174. Hrabeta J., Stiborova M., Adam V., Kizek R., Eckschlager T. // *Biomed. Pap. Med. Fac. Univ. Palacky Olomouc Czech Repub.* 2014. V. 158. № 2. P. 161–169. doi: 10.5507/bp.2013.085.
175. Chen F., Du Y., Esposito E., Liu Y., Guo S., Wang X., Lo E.H., Changhong Xing C., Ji X. // *Transl. Stroke Res.* 2015. V. 6. № 6. P. 478–484. doi: 10.1007/s12975-015-0429-3.
176. Ziemka-Nalecz M., Zaleska T. // *Acta Neurobiol. Exp. (Wars.)*. 2014. V. 74. № 4. P. 383–395.
177. Gomazkov O.A. // *Experimental and clinical pharmacology*. 2015. T. 78. № 11. P. 35–44.
178. Zhang K., Schrag M., Crofton A., Trivedi R., Vinters H., Kirsch W. // *Proteomics*. 2012. V. 12. № 8. P. 1261–1268. doi: 10.1002/pmic.201200010.
179. Ziemka-Nalecz M., Jaworska J., Sypecka J., Zaleska T. // *J. Neuropathol. Exp. Neurol.* 2018. V. 77. № 10. P. 855–870. doi: 10.1093/jnen/nly073.
180. Vaiserman A.M., Pasyukova E.G. // *Front. Genet.* 2012. V. 3. P. 224. doi: 10.3389/fgene.2012.00224.
181. Hahnen E., Hauke J., Trankle C., Eyupoglu I.Y., Wirth B., Blumcke I. // *Expert. Opin. Investig. Drugs*. 2008. V. 17. № 2. P. 169–184. doi: 10.1517/13543784.17.2.169.
182. Qing H., He G., Ly P.T., Fox C.J., Staufenbiel M., Cai F., Zhang Z., Wei S., Sun X., Chen C.-H., et al. // *J. Exp. Med.* 2008. V. 205. № 12. P. 2781–2789. doi: 10.1084/jem.20081588.
183. Ricobaraza A., Cuadrado-Tejedor M., Marco S., Perez-Otano I., Garcia-Osta A. // *Hippocampus*. 2012. V. 22. № 5. P. 1040–1050. doi: 10.1002/hipo.20883.
184. Huang J., Chen Y.J., Bian W.H., Yu J., Zhao Y.W., Liu X.Y. // *Chin. Med. J. (Engl.)*. 2010. V. 123. № 10. P. 1311–1314.
185. Zhang Z., Qin X., Tong N., Zhao X., Gong Y., Shi Y., Wu X. // *Exp. Eye Res.* 2012. V. 94. № 1. P. 98–108. doi: 10.1016/j.exer.2011.11.013.
186. Zhang Z.Y., Schluesener H.J. // *J. Neuropathol. Exp. Neurol.* 2013. V. 72. № 3. P. 178–185. doi: 10.1097/NEN.0b013e318283114a.
187. Benito E., Urbanke H., Ramachandran B., Barth J., Halder R., Awasthi A., Jain G., Capece V., Burkhardt S., Navarro-Sala M., et al. // *J. Clin. Invest.* 2015. V. 125. № 9. P. 3572–3584. doi: 10.1172/JCI79942.
188. Guan J.S., Haggarty S.J., Giacometti E., Dannenberg J.H., Joseph N., Gao J., Nieland T.J.F., Zhou Y., Wang X., Mazitschek R., et al. // *Nature*. 2009. V. 459. № 7243. P. 55–60. doi: 10.1038/nature07925.
189. Akhtar M.W., Raingo J., Nelson E.D., Montgomery R.L., Olson E.N., Kavalali E.T., Monteggia L.M. // *J. Neurosci.* 2009. V. 29. № 25. P. 8288–8297. doi: 10.1523/JNEUROSCI.0097-09.2009.
190. McQuown S.C., Barrett R.M., Matheos D.P., Post R.J., Rogge G.A., Alenghat T., Mullican S.E., Jones S., Rusche J.R., Lazar M.A., et al. // *J. Neurosci.* 2011. V. 31. № 2. P. 764–774. doi: 10.1523/JNEUROSCI.5052-10.2011.
191. Bardai F.H., D’Mello S.R. // *J. Neurosci.* 2011. V. 31. № 5. P. 1746–1751. doi: 10.1523/JNEUROSCI.5704-10.2011.
192. Bali P., Pranpat M., Bradner J., Balasis M., Fiskus W., Guo F., Rocha K., Kumaraswamy S., Boyapalle S., Atadja P., et al. // *J. Biol. Chem.* 2005. V. 280. № 29. P. 26729–26734. doi: 10.1074/jbc.C500186200.
193. Zhao Z., Xu H., Gong W. // *Protein Pept. Lett.* 2010. V. 17. № 5. P. 555–558. doi: 10.2174/092986610791112620.
194. Ding H., Dolan P.J., Johnson G.V. // *J. Neurochem.* 2008. V. 106. № 5. P. 2119–2130. doi: 10.1111/j.1471-4159.2008.05564.x.
195. Chen S., Owens G.C., Makarenkova H., Edelman D.B. // *PLoS One*. 2010. V. 5. № 5. P. e10848. doi: 10.1371/journal.pone.0010848.
196. Rivieccio M.A., Brochier C., Willis D.E., Walker B.A., D’Annibale M.A., McLaughlin K., Siddiq A., Kozikowski A.P., Jaffrey S.R., Twiss J.L., et al. // *Proc. Natl. Acad. Sci. USA*. 2009. V. 106. № 46. P. 19599–19604. doi: 10.1073/pnas.0907935106.
197. Bolger T.A., Yao T.P. // *J. Neurosci.* 2005. V. 25. № 41. P. 9544–9553. doi: 10.1523/JNEUROSCI.1826-05.2005.
198. Gao J., Wang W.Y., Mao Y.W., Graff J., Guan J.S., Pan L., Pan L., Mak G., Kim D., Su S.C., et al. // *Nature*. 2010. V. 466. № 7310. P. 1105–1109. doi: 10.1038/nature09271.
199. Julien C., Tremblay C., Emond V., Lebbadi M., Salem N., Jr., Bennett D.A., Calon F. // *J. Neuropathol. Exp. Neurol.* 2009. V. 68. № 1. P. 48–58. doi: 10.1097/NEN.0b013e3181922348.
200. Endres K., Fahrenholz F. // *FEBS J*. 2010. V. 277. № 7. P. 1585–1596. doi: 10.1111/j.1742-4658.2010.07566.x.
201. Kawamura Y., Uchijima Y., Horike N., Tonami K., Nishiyama K., Amano T., Asano T., Kurihara Y., Kurihara H. // *J. Clin. Invest.* 2010. V. 120. № 8. P. 2817–2828. doi: 10.1172/JCI42020.
202. Kim S.H., Lu H.F., Alano C.C. // *PLoS One*. 2011. V. 6. № 3. P. e14731. doi: 10.1371/journal.pone.0014731.
203. Yang S.S., Zhang R., Wang G., Zhang Y.F. // *Transl. Neurodegener.* 2017. V. 6. P. 19. doi: 10.1186/s40035-017-0089-1.
204. Sweeney P., Park H., Baumann M., Dunlop J., Frydman J., Kopito R., McCampbell A., Leblanc G., Venkateswaran A., Nurmi A., et al. // *Transl. Neurodegener.* 2017. V. 6. P. 6. doi: 10.1186/s40035-017-0077-5.
205. Weydt P., La Spada A.R. // *Expert. Opin. Ther. Targets*. 2006. V. 10. № 4. P. 505–513. doi: 10.1517/14728222.10.4.505.
206. Gandhi J., Antonelli A.C., Afridi A., Vatsia S., Joshi G., Romanov V., Murray I.V.J., Khan S.A. // *Rev. Neurosci.* 2019. V. 30. № 4. P. 339–358. doi: 10.1515/revneuro-2016-0035.
207. Chung C.G., Lee H., Lee S.B. // *Cell. Mol. Life Sci.* 2018. V. 75. № 17. P. 3159–3180. doi: 10.1007/s00018-018-2854-4.
208. Ross C.A., Poirier M.A. // *Nat. Med.* 2004. V. 10 Suppl. P. S10–17. doi: 10.1038/nm1066.
209. Kaplan B., Ratner V., Haas E. // *J. Mol. Neurosci.* 2003. V. 20. № 2. P. 83–92. doi: 10.1385/JMN:20:2:83.

210. Lavedan C. // *Genome Res.* 1998. V. 8. № 9. P. 871–880. doi: 10.1101/gr.8.9.871.
211. Tarasova TV, Lytkina O.A., Roman A.Yu., Bachurin S.O., Ustyugov A.A. // *Reports of the Academy of Sciences.* 2006. T. 466. № 5. P. 620–623. doi: 10.7868/S0869565216050285.
212. Kim W.S., Kagedal K., Halliday G.M. // *Alzheimers Res. Ther.* 2014. V. 6. № 5. P. 73. doi: 10.1186/s13195-014-0073-2.
213. Spillantini M.G., Schmidt M.L., Lee V.M., Trojanowski J.Q., Jakes R., Goedert M. // *Nature.* 1997. V. 388. № 6645. P. 839–840. doi: 10.1038/42166.
214. Mahul-Mellier A.L., Bartscher J., Maharjan N., Weerens L., Croisier M., Kuttler F., Leleu M., Knott G.W., Lashuel H.A. // *Proc. Natl. Acad. Sci. USA.* 2020. V. 117. № 9. P. 4971–4982. doi: 10.1073/pnas.1913904117.
215. Kohan V., Vankin G., Ninkina N., Bachurin S., Shamakina I. // *Problems of drug addiction.* 2012. № 1. P. 70–83.
216. Galasko D. // *Neurol. Clin.* 2017. V. 35. № 2. P. 325–338. doi: 10.1016/j.ncl.2017.01.004.
217. Kosaka K. // *Proc. Jpn. Acad. Ser. B Phys. Biol. Sci.* 2014. V. 90. № 8. P. 301–306. doi: 10.2183/pjab.90.301.
218. Sanford A.M. // *Clin. Geriatr. Med.* 2018. V. 34. № 4. P. 603–615. doi: 10.1016/j.cger.2018.06.007.
219. Chartier-Harlin M.C., Crawford F., Houlden H., Warren A., Hughes D., Fidani L., Goate A., Rossor M., Roques P., Hardy J., et al. // *Nature.* 1991. V. 353. № 6347. P. 844–846. doi: 10.1038/353844a0.
220. Goate A., Chartier-Harlin M.C., Mullan M., Brown J., Crawford F., Fidani L., Giuffra L., Haynes A., Irving N., James L., et al. // *Nature.* 1991. V. 349. № 6311. P. 704–706. doi: 10.1038/349704a0.
221. Haass C., Selkoe D.J. // *Nat. Rev. Mol. Cell. Biol.* 2007. V. 8. № 2. P. 101–112. doi: 10.1038/nrm2101.
222. Dinamarca M.C., Rios J.A., Inestrosa N.C. // *Front. Physiol.* 2012. V. 3. P. 464. doi: 10.3389/fphys.2012.00464.
223. Lashuel H.A., Hartley D., Petre B.M., Walz T., Lansbury P.T., Jr. // *Nature.* 2002. V. 418. № 6895. P. 291. doi: 10.1038/418291a.
224. Lin H., Bhatia R., Lal R. // *FASEB J.* 2001. V. 15. № 13. P. 2433–2444. doi: 10.1096/fj.01-0377com.
225. Shankar G.M., Bloodgood B.L., Townsend M., Walsh D.M., Selkoe D.J., Sabatini B.L. // *J. Neurosci.* 2007. V. 27. № 11. P. 2866–2875. doi: 10.1523/JNEUROSCI.4970-06.2007.
226. Shankar G.M., Li S., Mehta T.H., Garcia-Munoz A., Shepardson N.E., Smith I., Brett F.M., Farrell M.A., Rowan M.J., Lemere C.A., et al. // *Nat. Med.* 2008. V. 14. № 8. P. 837–842. doi: 10.1038/nm1782.
227. Li S., Hong S., Shepardson N.E., Walsh D.M., Shankar G.M., Selkoe D. // *Neuron.* 2009. V. 62. № 6. P. 788–801. doi: 10.1016/j.neuron.2009.05.012.
228. Bourdenx M., Koulakiotis N.S., Sanoudou D., Bezaud E., Dehay B., Tsaropoulos A. // *Prog. Neurobiol.* 2017. V. 155. P. 171–193. doi: 10.1016/j.pneurobio.2015.07.003.
229. Gomes G.M., Dalmolin G.D., Bar J., Karpova A., Mello C.F., Kreutz M.R., Rubin M.A. // *PLoS One.* 2014. V. 9. № 6. P. e99184. doi: 10.1371/journal.pone.0099184.
230. Talantova M., Sanz-Blasco S., Zhang X., Xia P., Akhtar M.W., Okamoto S., Dziewczapolski G., Nakamura T., Cao G., Pratt A.E., et al. // *Proc. Natl. Acad. Sci. USA.* 2013. V. 110. № 27. P. E2518–2527. doi: 10.1073/pnas.1306832110.
231. Roberson E.D., Scearce-Levie K., Palop J.J., Yan F., Cheng I.H., Wu T., Gerstein H., Yu G.Q., Mucke L. // *Science.* 2007. V. 316. № 5825. P. 750–754. doi: 10.1126/science.1141736.
232. Frost B., Gotz J., Feany M.B. // *Trends Cell Biol.* 2015. V. 25. № 1. P. 46–53. doi: 10.1016/j.tcb.2014.07.005.
233. Santacruz K., Lewis J., Spirets T., Paulson J., Kotilinek L., Ingelsson M., Guimaraes A., DeTure M., Ramsden M., McGowan E., et al. // *Science.* 2005. V. 309. № 5733. P. 476–481. doi: 10.1126/science.1113694.
234. Zilka N., Kontseikova E., Novak M. // *J. Alzheimers Dis.* 2008. V. 15. № 2. P. 169–179. doi: 10.3233/jad-2008-15203.
235. Kovacech B., Skrabana R., Novak M. // *Neurodegener. Dis.* 2010. V. 7. № 1–3. P. 24–27. doi: 10.1159/000283478.
236. Novak M., Kabat J., Wischik C.M. // *EMBO J.* 1993. V. 12. № 1. P. 365–370.
237. Wischik C.M., Novak M., Thogersen H.C., Edwards P.C., Runswick M.J., Jakes R., Walker J.E., Milstein C., Roth M., Klug A. // *Proc. Natl. Acad. Sci. USA.* 1988. V. 85. № 12. P. 4506–4510. doi: 10.1073/pnas.85.12.4506.
238. Wischik C.M., Novak M., Edwards P.C., Klug A., Tiche-laar W., Crowther R.A. // *Proc. Natl. Acad. Sci. USA.* 1988. V. 85. № 13. P. 4884–4888. doi: 10.1073/pnas.85.13.4884.
239. Dickey C.A., Petrucelli L. // *Expert. Opin. Ther. Targets.* 2006. V. 10. № 5. P. 665–676. doi: 10.1517/14728222.10.5.665.
240. Pickhardt M., von Bergen M., Gazova Z., Hascher A., Biernat J., Mandelkow E.-M., Mandelkow E. // *Curr. Alzheimer Res.* 2005. V. 2. № 2. P. 219–226. doi: 10.2174/1567205053585891.
241. Necula M., Chirita C.N., Kuret J. // *Biochemistry.* 2005. V. 44. № 30. P. 10227–10237. doi: 10.1021/bi050387o.
242. Wischik C.M., Edwards P.C., Lai R.Y., Roth M., Harrington C.R. // *Proc. Natl. Acad. Sci. USA.* 1996. V. 93. № 20. P. 11213–11218. doi: 10.1073/pnas.93.20.11213.
243. Iqbal K., Grundke-Iqbal I. // *Cell. Mol. Life Sci.* 2007. V. 64. № 17. P. 2234–2244. doi: 10.1007/s00018-007-7221-9.
244. Iqbal K., Grundke-Iqbal I. // *Curr. Drug. Targets.* 2004. V. 5. № 6. P. 495–502. doi: 10.2174/1389450043345254.
245. Zhang B., Maiti A., Shively S., Lakhani F., McDonald-Jones G., Bruce J., Lee E.B., Xie S.X., Joyce S., Li C., et al. // *Proc. Natl. Acad. Sci. USA.* 2005. V. 102. № 1. P. 227–231. doi: 10.1073/pnas.0406361102.
246. Dickey C.A., Ash P., Klosak N., Lee W.C., Petrucelli L., Hutton M., Eckman C.B. // *Mol. Neurodegener.* 2006. V. 1. P. 6. doi: 10.1186/1750-1326-1-6.
247. Dickey C.A., Eriksen J., Kamal A., Burrows F., Kasibhatla S., Eckman C.B., Hutton M., Petrucelli L. // *Curr. Alzheimer Res.* 2005. V. 2. № 2. P. 231–238. doi: 10.2174/1567205053585927.
248. Tabira T. // *Tohoku J. Exp. Med.* 2010. V. 220. № 2. P. 95–106. doi: 10.1620/tjem.220.95.
249. Schneider A., Mandelkow E. // *Neurotherapeutics.* 2008. V. 5. № 3. P. 443–457. doi: 10.1016/j.nurt.2008.05.006.
250. Taniguchi T., Sumida M., Hiraoka S., Tomoo K., Kakehi T., Minoura K., Sugiyama S., Inaka K., Ishida T., Saito N., et al. // *FEBS Lett.* 2005. V. 579. № 6. P. 1399–1404. doi: 10.1016/j.febslet.2005.01.039.
251. Sigurdsson E.M., Scholtzova H., Mehta P.D., Frangione B., Wisniewski T. // *Am. J. Pathol.* 2001. V. 159. № 2. P. 439–447. doi: 10.1016/s0002-9440(10)61715-4.
252. Janus C., Pearson J., McLaurin J., Mathews P.M., Jiang Y., Schmidt S.D., Chishti M.A., Horne P., Heslin D., French J., et al. // *Nature.* 2000. V. 408. № 6815. P. 979–982. doi: 10.1038/35050110.
253. Schenk D., Barbour R., Dunn W., Gordon G., Grajeda H., Guido T., Hu K., Huang J., Johnson-Wood K., Khan K., et al. // *Nature.* 1999. V. 400. № 6740. P. 173–177. doi: 10.1038/22124.
254. Boutajangout A., Quartermain D., Sigurdsson E.M. // *J. Neurosci.* 2010. V. 30. № 49. P. 16559–16566. doi: 10.1523/

REVIEWS

JNEUROSCI4363-10.2010.

255. Asuni A.A., Boutajangout A., Quartermain D., Sigurdson E.M. // J. Neurosci. 2007. V. 27. № 34. P. 9115–9129. doi: 10.1523/JNEUROSCI.2361-07.2007.

256. Blokhuis A.M., Groen E.J., Koppers M., van den Berg L.H., Pasterkamp R.J. // Acta Neuropathol. 2013. V. 125. № 6. P. 777–794. doi: 10.1007/s00401-013-1125-6.

257. Prasad A., Bharathi V., Sivalingam V., Girdhar A., Patel B.K. // Front. Mol. Neurosci. 2019. V. 12. P. 25. doi: 10.3389/fnmol.2019.00025.

258. Arrasate M., Finkbeiner S. // Exp. Neurol. 2012. V. 238. № 1. P. 1–11. doi: 10.1016/j.expneurol.2011.12.013.

259. Finkbeiner S. // Cold Spring Harb. Perspect. Biol. 2011. V. 3. № 6. P. a007476. doi: 10.1101/cshperspect.a007476.

Molecular Principles of Insect Chemoreception

E. L. Sokolinskaya, D. V. Kolesov, K. A. Lukyanov, A. M. Bogdanov*

Shemyakin-Ovchinnikov Institute of Bioorganic Chemistry, Moscow, 117997 Russia

*E-mail: noobissat@ya.ru

Received September 28, 2019; in final form, June 03, 2020

DOI: 10.32607/actanaturae.11038

Copyright © 2020 National Research University Higher School of Economics. This is an open access article distributed under the Creative Commons Attribution License, which permits unrestricted use, distribution, and reproduction in any medium, provided the original work is properly cited.

ABSTRACT Chemoreception, an ability to perceive specific chemical stimuli, is one of the most evolutionarily ancient forms of interaction between living organisms and their environment. Chemoreception systems are found in organisms belonging to all biological kingdoms. In higher multicellular animals, chemoreception (along with photo- and mechanoreception) underlies the functioning of five traditional senses. Insects have developed a peculiar and one of the most sophisticated chemoreception systems, which exploits at least three receptor superfamilies providing perception of smell and taste, as well as chemical communication in these animals. The enormous diversity of physiologically relevant compounds in the environment has given rise to a wide-ranging repertoire of chemoreceptors of various specificities. Thus, in insects, they are represented by several structurally and functionally distinct protein classes and are encoded by hundreds of genes. In the current review, we briefly characterize the insect chemoreception system by describing the main groups of receptors that constitute it and putting emphasis on the peculiar architecture and mechanisms of functioning possessed by these molecules.

KEYWORDS chemoreceptor, cation channel, action potential, ionotropic receptor, metabotropic receptor, odorant, olfaction, gustatory receptor, insects.

ABBREVIATIONS OSN – olfactory sensory neuron; OR – odorant (olfactory) receptor; GPCR – G protein-coupled receptor; DAG – diacylglycerol; IP3 – inositol trisphosphate; IR – ionotropic receptor; ATD – amino terminal domain; GRN – gustatory receptor neuron; GR – gustatory receptor.

INTRODUCTION

Living creatures get information about their environment via the senses: vision, hearing, smell, and taste. Perception of environmental factors in each sensory system is mediated by a small region of tissue that is sensitive to a specific physical stimulus (electromagnetic radiation in the case of vision, mechanical vibrations of air in the case of hearing, and chemicals in the case of smell and taste). In multicellular organisms, such specialized tissue structures are called *receptors*. Receptor cells convert captured light, sound, or chemicals into a nerve impulse that is transmitted to the brain for processing of the received information. The conversion of a physical stimulus to a nerve impulse is known as signal transduction. During this process, receptor cells (neurons or other specialized cells) perceive a signal using the special receptor molecules. This changes the activity of ion channels in the neuron plasma membrane and, therefore, causes a shift in the cell membrane voltage (depolarization or hyperpolarization). Depolarization triggers the action potential and then promotes the transmission of a nerve impulse in the nervous system.

Receptor molecules can either directly activate ion channels (in this case, the receptor is called ionotropic)

or run a membrane signaling cascade leading to the activation of ion channels through specialized G proteins (in this case, the receptor is called metabotropic). The ionotropic signal transduction pathway reveals its advantages for high-intensity stimuli, since it provides the fastest “start” of a neuronal excitation. On the other hand, metabotropic transduction is indispensable in the case of weak stimuli, whose perception requires signal amplification. The sensory organs of multicellular animals use both mechanisms, sometimes combining them sophisticatedly.

COMMON PRINCIPLES OF ANIMAL CHEMORECEPTION

Chemoreception is an important element in the perception and analysis of environmental information. Chemical stimulation provides recognition of taste and food quality, alerts animals to the presence of potential predators or other dangers, and directs social interactions. Smells, tastes, and other chemical stimuli are recognized and decoded by a diverse set of chemosensory systems in various animals. Chemosensory transduction is a process in which chemical stimuli – smells, tastes, nutrients, irritants, and even gases – are recognized and cause changes in the cell membrane properties or re-

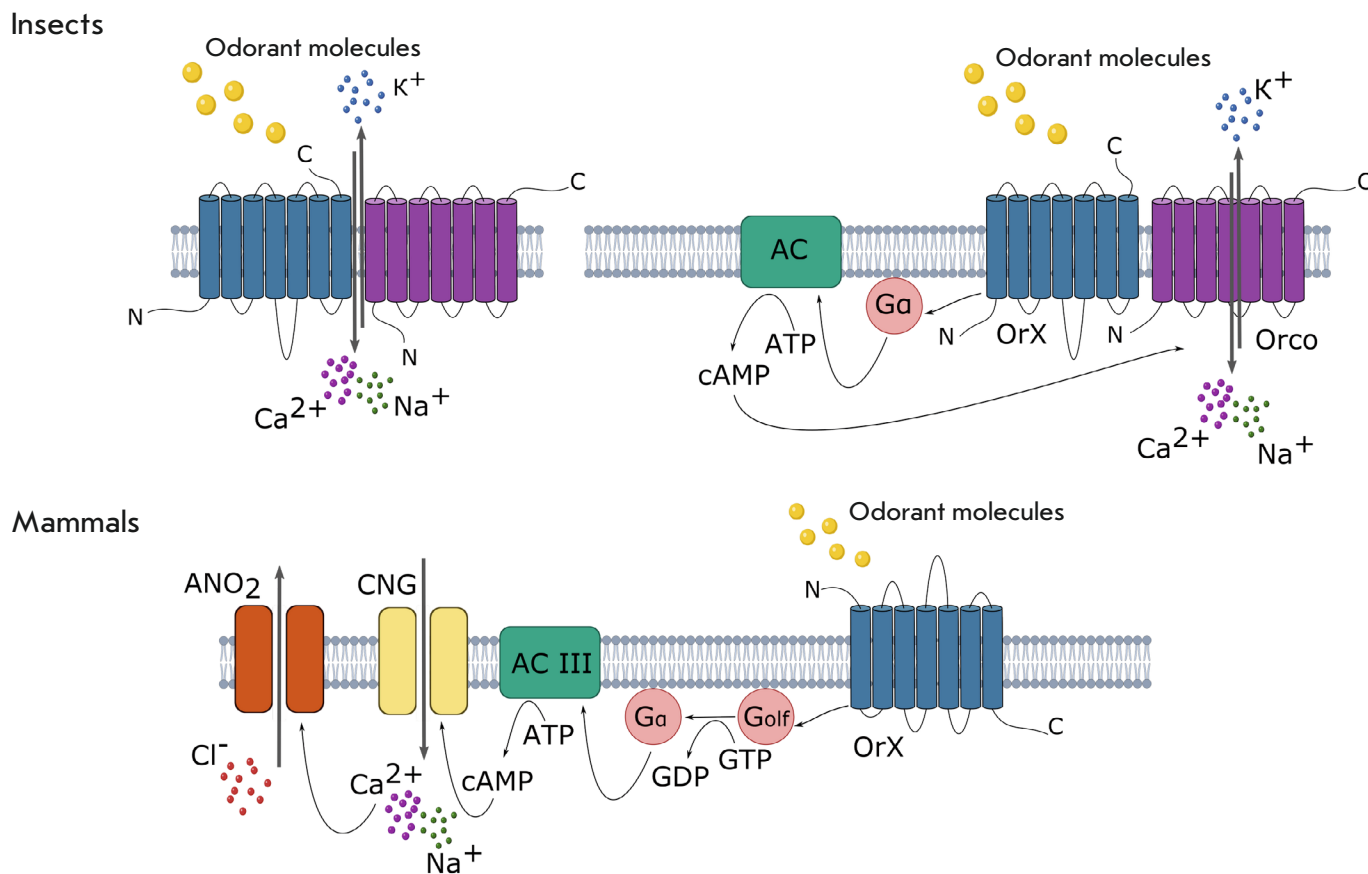


Fig. 1. Molecular mechanisms of signal transduction by the olfactory receptors of insects and mammals. The main (ionotropic) and additional (metabotropic) ways of functioning of the insect olfactory receptors are shown in the upper part of the scheme. The mammalian olfactory receptor and the membrane cascade ensuring the transduction of its signal are shown in the lower part of the scheme [2–4]. ACIII – type III adenylyate cyclase; ATP – adenosine triphosphate; cAMP – cyclic adenosine monophosphate; ANO2 – anoctamin-2 channel; CNG – a cyclic nucleotide-binding channel; G α – α -subunit of the olfactory G protein; OrX – odor-specific receptor olfactory protein Or; Orco – constant co-receptor olfactory protein; Na⁺, K⁺, Ca²⁺, Cl⁻ – sodium, potassium, calcium cations and chloride anion, respectively

lease of neurotransmitters and hormones [1]. Typically, transduction processes occur in sensitive neurons, which often form specialized subcellular compartments (cilia or microvilli) optimized for transduction. In most cases, chemosensory transduction is a multi-stage pathway in which the biochemical signal on the membrane is converted into an electrical signal, the action potential. Chemical signals (or chemical stimuli) are represented by molecules originating from various sources, such as soil, plants, or animals. These compounds can be volatile or in dissolved state. In the first case, the chemical signal is perceived by olfactory receptors; in the second one, by taste (gustatory) receptors. Among the complex chemosensory systems of higher multicellular animals, the olfactory and gustatory analyzers of insects and mammals have been the best studied at the molecular level. Interestingly, when responding to chemical stimulation, mammals rely mainly on metabotropic receptors, while insects rely on ionotropic ones [2] (Fig. 1).

INSECT CHEMORECEPTORS

Olfactory receptors

In insects, olfactory sensory neurons (OSNs), which express olfactory receptors in their dendrites, are responsible for odor perception. OSNs are localized in the forehead appendages, antennae, and maxillary palps (Fig. 2).

The sense of smell in insects is provided by three types of receptors; members of different families of transmembrane proteins. The first type is represented by the odorant (or olfactory) receptors (ORs) that recognize food odors and pheromones. ORs function as heterodimers consisting of a variable odor-specific Or receptor protein and a constant co-receptor Orco protein [5, 6] (Fig. 3).

Similarly to a typical G protein-conjugated receptor (GPCR), ORs consist of seven associated α -helices; however, they differ from GPCR in terms of helice ori-

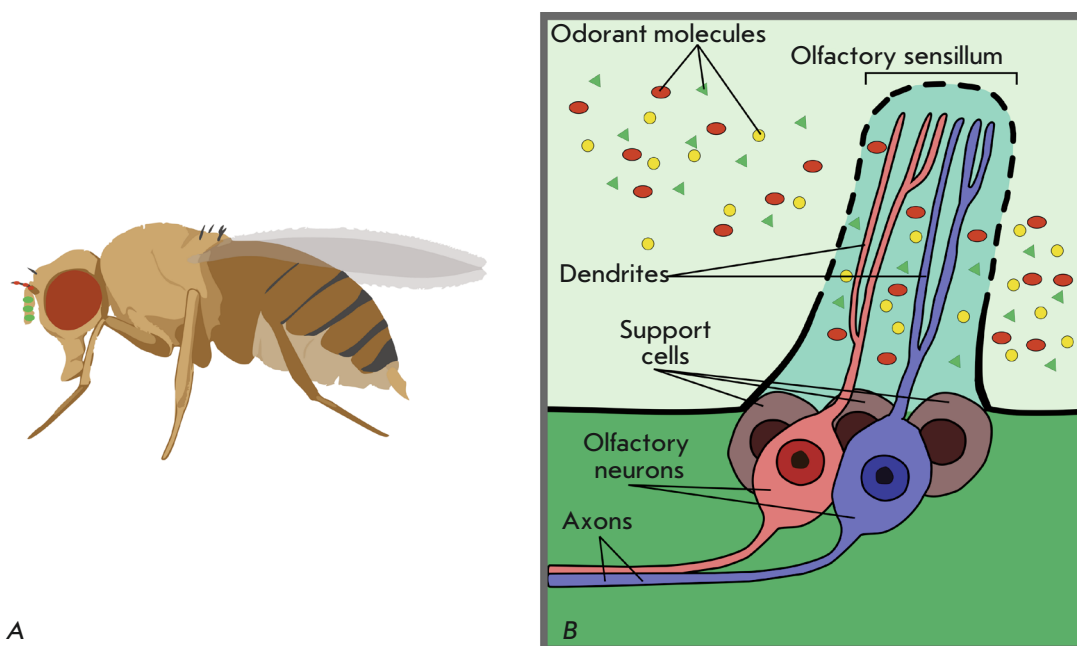


Fig. 2. The pathway of the odorant molecules entering the olfactory receptor from the environment. Molecules reach the antennae of the fly equipped with numerous sensitive hairs: sensilla (A). The surface of each sensillum has pores that allow odorant molecules to penetrate inside the sensillum, where the dendrites of the olfactory sensitive neurons (OSNs) are located (B). The olfactory receptors specifically binding odor molecules are exhibited on dendritic membranes. Adapted from [1]

entation with respect to the plasma membrane. Thus, insect ORs have a cytoplasmic N-terminus and an extracellular C-terminus [7, 8]. Although the OrX/Y-Orco heterodimer serves as an elementary functional unit of the insect olfactory system, the receptors in the membrane of olfactory neurons most likely function within large supramolecular ensembles, whose composition and topology remain poorly understood. Recent studies have shed light on the molecular organization of such complexes. Thus, the cryo-electron microscopy structure of the Orco subunit from *Apocrypta bakeri* was resolved [9]. Orco forms tetramers having a “pin-wheel” shape when viewed from above, perpendicular to the membrane plane (Fig. 4A). The tetramer is approximately 100 Å in diameter and 80 Å in the axial direction. The central pore is formed by four subunits. Each subunit has seven helical segments that penetrate the membrane at an angle of ~30°; at the same time, the C-terminus of each subunit is oriented outward of the cell, while the N-terminus has an inward orientation (Fig. 4B). In addition to the seven main helices (helices 1–7), there is an extra N-terminal helix (helix 0), which is placed under loop 4 along the outer perimeter of the channel during complex assembly. Helix 7 is closest to the central axis and consists of two parts: the cytoplasmic segment (7a) and the transmembrane segment (7b), which are separated by a β-hairpin consisting of

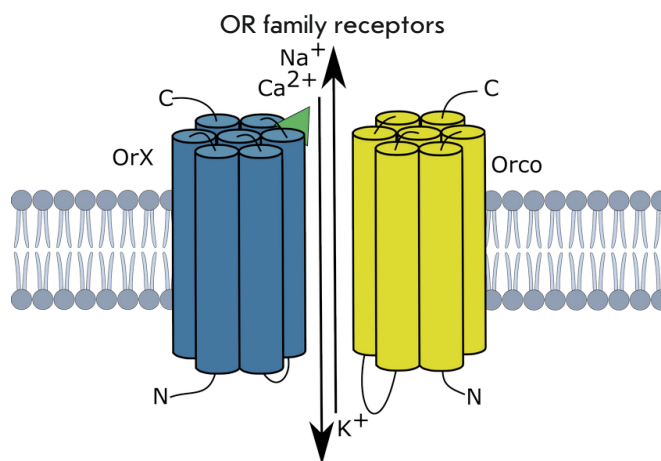


Fig. 3. Insect odorant receptors (ORs). ORs – the heterodimers consisting of Orco co-receptor and the odor-specific Or protein: OrX in the case of food odor recognition (also sensitive to odors of oviposition places, predators, toxic substances, etc.) and OrY in the case of pheromone recognition [3]. The green triangle depicts the ligand (an odorant molecule)

15 amino acid residues. Helix 7b forms the central pore, and helix 7a forms the core of the anchor domain. Helices 4, 5, and 6 extend far beyond the cell membrane (40 Å into the cytosol), where they surround helix 7a, completing the formation of the anchor domain. The

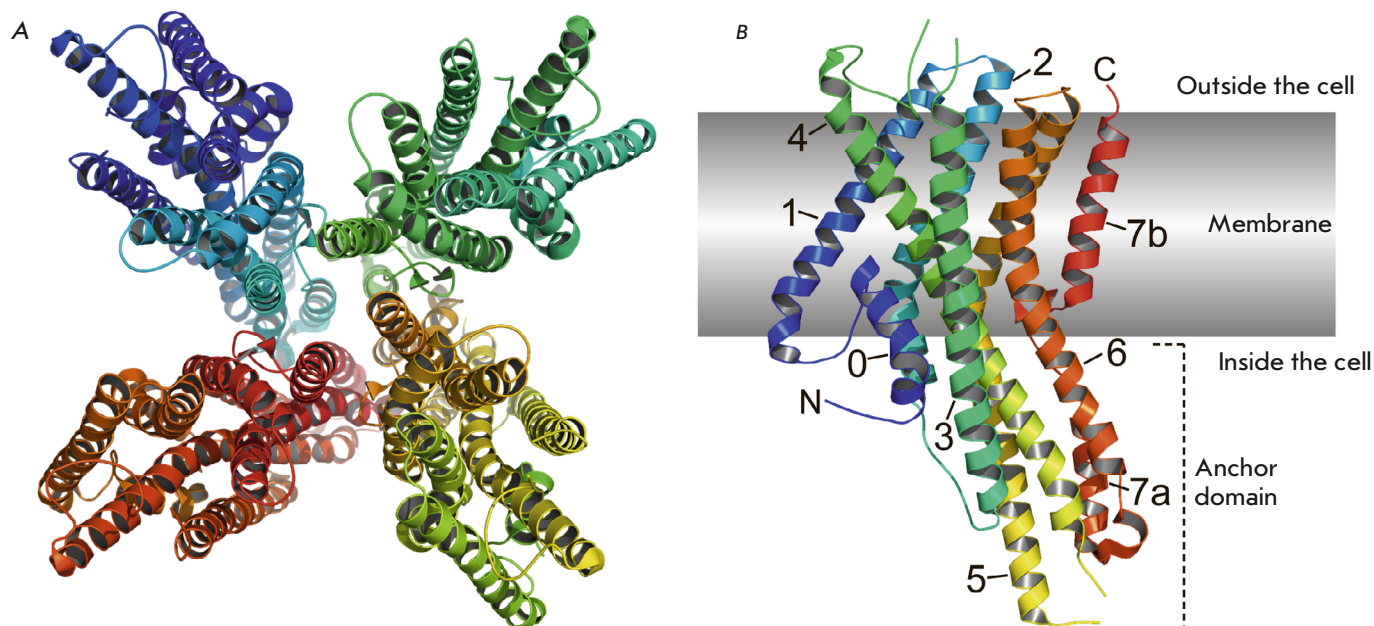


Fig. 4. The structure Orco from *Apocrypta bakeri*. (A) Structure of the homotetramer, view from the cytoplasmic side. (B) Monomer structure. The numbers indicate alpha helices. Structures are represented using the PyMol program based on PBD ID 6C70

transmembrane domain of each subunit is stabilized by the charged and polar amino acids of helices 2, 4, 5, and 6, thus forming a dense network of hydrophilic interactions within the intracellular leaflet of the membrane. Within the extracellular leaflet, helices 1–6 split to form a cleft 10 Å deep and ~ 20 Å. It is assumed that such a pocket could serve as a binding site for low-molecular-weight ligands. Mutations altering the specificity of ORs for odorants are also mapped within this pocket, indicating that there potentially exists a common structural locus for ligand binding in Orco and OR. In the Orco structure, the ordered region of the extracellular loops 3–4 restricts access to the pocket, which may interfere with odorant binding, thereby preserving odor specificity in the Orco–OR complexes.

The architecture of Or–Orco receptor complexes has not yet been established. The subject of discussion remains the topology of the receptor heterodimer itself. It is assumed that Or proteins can form heterodimers with the Orco co-receptor in a way similar to the seven-helix channelrhodopsin, where the ion channel pore is formed by opposing TM3 and TM4 helices [10, 11]. Another possible assembly option is a tetramer consisting of two dimers [12]. The relative cation permeability varies for different OrX [13, 14]. A mutation analysis of the olfactory silkworm (*Bombyx mori*) receptors showed that the OR channel pore is formed by both types of proteins, OrX and Orco [15]. Expression of Orco proteins alone (in the absence of OrX) also leads

to the formation of functional channels that do not bind odorant molecules but can be activated by cyclic nucleotides [16] or synthetic agonists [17–19].

The molecular mechanism of OR activation has not been investigated in details. In some studies, the exclusively ionotropic mechanism was found [13]; in other studies, the metabotropic signaling mechanism based on the DAG/IP₃ pathway was clearly shown [20, 21]. Finally, both signaling pathways were detected in heterologously expressed *Drosophila* OR proteins [16].

The second type of olfactory insect receptors is represented by the so-called ionotropic receptors (IRs) homologous to ionotropic glutamate receptors (involved in the formation of synaptic contacts in the nervous system of vertebrates and invertebrates) [22]. IRs are sensitive to acids, amines, and aldehydes. Receptors function as heterotetramers consisting of an odor-specific receptor protein IRX and a constant co-receptor protein IRcoY [23] (Fig. 5). However, IR receptors acting as heterodimers have also been described. Thus, the IR8a + IR75a heterodimer responds to acetic acid [23–25]. The IR8a + IR84a pair, whose specificity was characterized in *Xenopus laevis* oocytes, is activated by phenylacetaldehyde [24]. Olfactory sensilla expressing IR8a + IR64a recognize acids and free protons [24, 26]. Artificial stimulation of IR64a-positive neurons causes avoidance behavior, which corresponds to the role of these neurons in acidic stimuli detection. IR8a was shown to be associated with IR64a, thereby contribut-

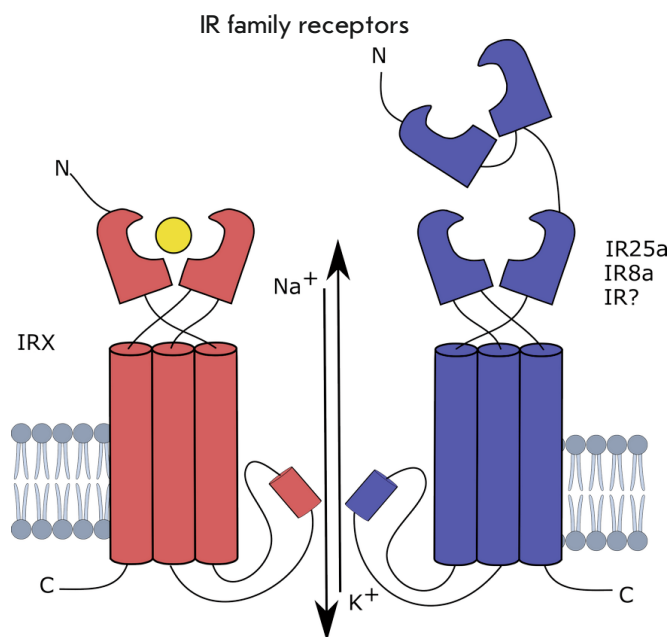


Fig. 5. Ionotropic receptors (IRs) are heterotetramers consisting of the IRcoY co-receptor protein and IRX receptor protein [3]

ing to the stability of IR64a [23]. Together, these results indicate that IR8a functions as a co-receptor in IR64a-positive neurons [27].

IRcoY also carries a ligand-binding domain; however, it is suggested that its main role is to traffic the complex onto the cell membrane but not to bind the ligand [23].

IRs can form tetramers consisting of two IRcoY:IRX dimers, or of the IRcoY monomer plus three different IRX subunits. In fruit fly, IR co-receptors are represented by IR8a and IR25a [11]. Both IRcoY and IRX consist of three transmembrane helices separated by an extracellular region containing a ligand-binding domain (LBD). IRcoY also has a massive N-terminal domain (ATD). IRs are non-selective cation channels and, upon activation, conduct Na⁺ and K⁺ ions, and some of them also Ca²⁺ cations [23].

IRs and ORs recognize odors with a complementary specificity: their ligands do not overlap. *Drosophila* OR-expressing olfactory neurons have been shown to better adapt to background odors compared to IR-expressing neurons. This feature allows insects to track odor changes over a wide range of concentrations and detect other odors even if a certain background exists. Meanwhile, despite their inability to adapt, IRs more accurately determine the absolute concentration of odorant that allows fruit fly to efficiently track food location, sexual partners, or predators [28, 29]. Most of the IR-family receptors are specifically activated by

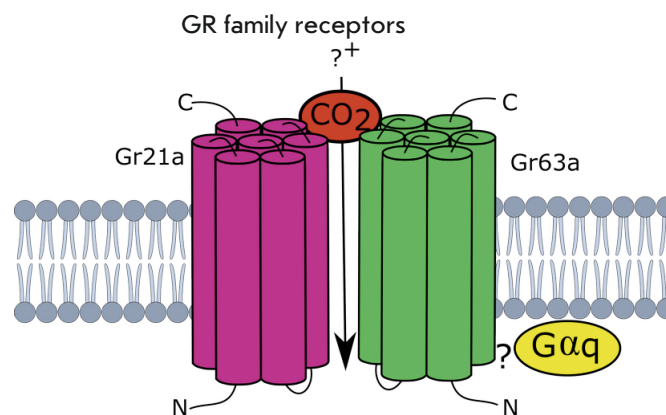


Fig. 6. Gustatory receptors (GRs) sensitive to carbon dioxide: heterodimers consisting of the Gr1/Gr2 and Gr3 subunits. GRs have structural and topological motifs that are similar to those in ORs [3]

amines and acids. The IR76b receptor is specific to low NaCl concentrations [30].

The third type of olfactory receptors is represented by specialized gustatory receptors (GRs) sensitive to carbon dioxide [31]. Like ORs, GRs belong to the family of seven-transmembrane domain receptors (7TM receptors), with the orientation of transmembrane domains opposite to that of GPCR proteins. Three *Gr* genes encoding receptors sensitive to carbon dioxide were found [32]. Receptors also form heterodimers consisting of Gr1/2 and Gr3 subunits (Fig. 6), which are represented in *Drosophila* by the Gr21a and Gr63a proteins, respectively [31, 33].

In *Drosophila*, Gr21a and Gr63a form a complex with Gαq proteins activating phospholipase C, which, in turn, activates the TRP-family ion channel through phosphoinositide hydrolysis [34–36]. Acidic odors and high carbon dioxide concentrations (> 5%) are recognized by the IR family receptor, namely IR64a [26].

Gustatory receptors

Insects are generally characterized by a complex taste sensory system. The main taste organs, taste sensilla, are located mostly on the legs and wings [37] (Fig. 7A). Receptor cells are sensitive neurons, most of which are associated with taste sensilla (Fig. 7B). Each sensillum contains several gustatory receptor neurons (GRNs), with gustatory receptors (GRs) expressed in their dendrites.

The discovery of the GR gene family in 2000 [38–40] was a breakthrough in the study of insect taste behavior and the physiology of their taste perception. The *Drosophila* genome contains 68 *Gr* genes [41], some of which are highly conserved among arthropods [42]. The *Gr* genes can be divided into two large groups. The first

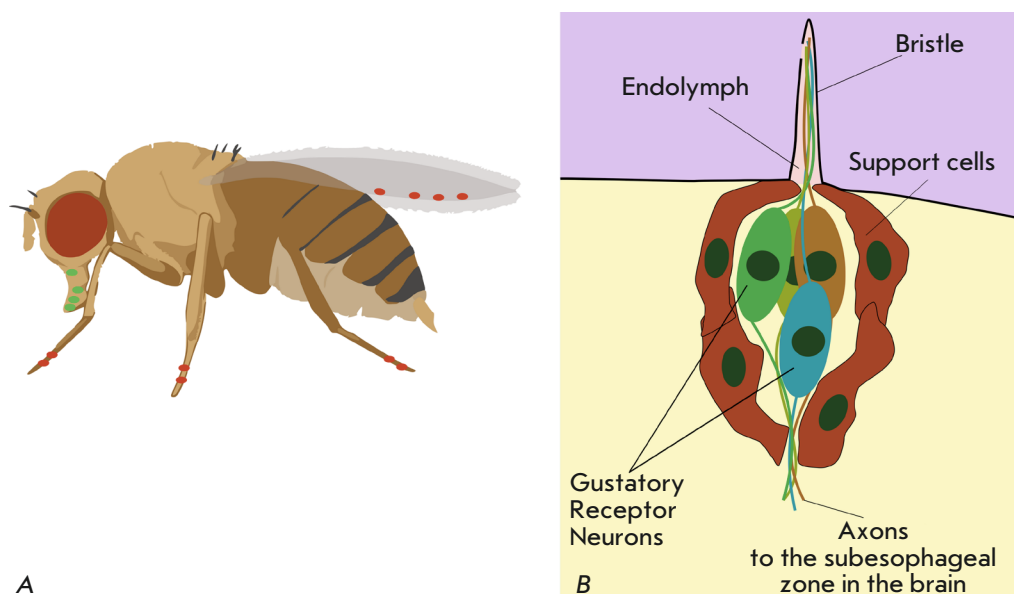


Fig. 7. Taste organs of *D. melanogaster*. (A) The main localization points of taste sensilla on the *Drosophila* body (shown with colored dots). (B) Scheme of the cellular organization of taste sensillum. Adapted from [1]

A

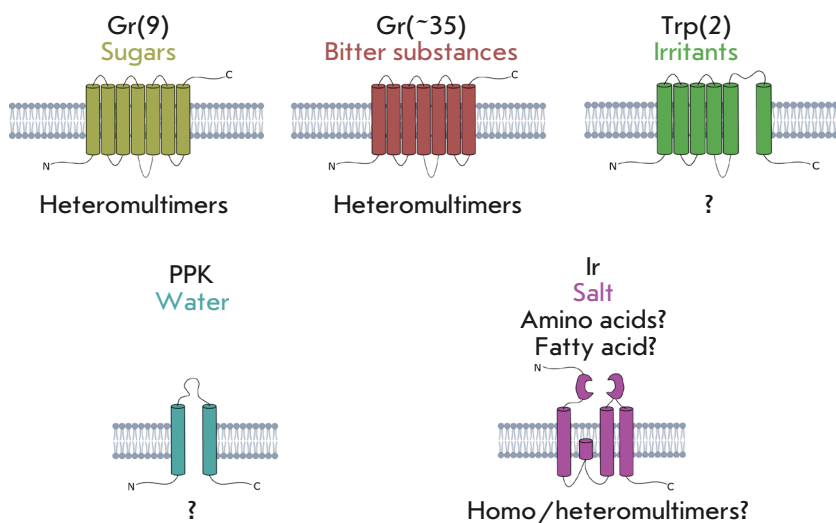


Fig. 8. Structures of different gustatory receptors in adult *D. melanogaster*. At least four types of receptors have been detected in taste neurons. Over 40 of the 68 *Gr* genes encode receptors for bitter and sweet taste. Two TRP genes were shown to encode taste-sensitive receptors (aristocholic acid and allyl isothiocyanate). At least one molecule (PPK28 channel) is used to determine the taste of water. The role of IR family receptors in taste perception is poorly understood, but expression in gustatory neurons has been shown for 15 genes. At least one example sensitive to sodium chloride taste (IR76b) has been reported. Adapted from [1]

group includes most *Gr* genes (about 35), which are expressed in neurons that recognize bitter and salty tastes [43]. The second group consists of eight genes expressed exclusively in neurons sensitive to the sweet taste [44] (Fig. 8).

Gr receptors of sweet taste

Recognition of the sweet taste of sugars is the best studied form of taste perception in *Drosophila*. Unlike mammals, where the only heterodimeric G protein-coupled receptor complex recognizes all sugars and even sweet-tasting proteins [45, 46], *Drosophila* was found to have eight *Gr* receptors involved in determining the sweet taste and encoded by the *Gr5a*, *Gr61a* and a cluster of six *Gr64a-f* genes [44]. All the genes en-

coding *Gr* receptors sensitive to the sweet taste are expressed in the paws, with a single exception for *Gr64a*, which is expressed in the palps [44]. Functional sweet taste receptors are heterodimers [47]. However, receptors that can function as homomultimers or monomers (*Gr43a*-like) are also known [48]. Below one can find a brief description of *Gr* genes encoding sweet taste receptors (Table 1) [1]. The data on specificity were obtained based on knockouts of the corresponding genes.

Bitter taste receptors

Similarly to mammals, *Drosophila* and other insects have systems that are well-tuned to detect potentially dangerous substances, usually bitter and lacking nutritional value. Insects meet a wide range of bitter sub-

stances from various sources. For example, many plants produce bitter substances as secondary metabolites that they use to protect against herbivorous insects [1]. For *Drosophila* and other insects consuming fruits, microorganisms inhabiting rotting fruits are a source of dangerous bitter substances. Bitter substances are represented by a wide range of components with diverse structures, such as alkaloids, terpenoids, and phenols. Therefore, most of the gustatory receptors (about 35) are sensitive to bitter substances [49]. However, only four bitter taste Gr receptors were functionally characterized. These receptors are presented in the table below (Table 2).

It is assumed that bitter taste Gr receptors also consist of several subunits, and that Gr33a and Gr66a are the core subunits of such multimeric complexes [49, 50].

Gustatory signal transduction

The signaling pathways of gustatory receptors are poorly understood. There are two reasons for the lack of knowledge in this research field. First, the gustatory neurons in *Drosophila* are not susceptible to electrophysiological studies using the patch-clamp method, which makes it impossible to study the neurophysiological processes underlying receptor activation. Second, most of the attempts to express gustatory receptors in a heterologous system have failed. The only exception is representatives of the so-called Gr43a-like clade, a family of receptors classified as taste receptors for fructose by phylogenetic analysis [51].

Available data suggest that insect receptors belonging to the Gr43a-like clade (conserved in many holometabolous insects) are ionotropic homosubunit chemoreceptors. Orthologs of the *DmGr43a* fruit fly gene are represented by *BmGr9* in *B. mori*, *HarmGr4* in *H. armigera*, and *AmGr3* in *A. mellifera*. Recently, *DmGr43a* paralogs have been discovered in *T. castaneum* (*TcGr20*) and *B. mori* (*BmGr10*). In 2011, Japanese scientists succeeded in an heterologous expression of the *BmGr9* gene from silkworm (*B. mori*) and its ortholog *DmGr43a* from *Drosophila* [52]. The *BmGr9* gene was expressed in human embryonic kidney cells (HEK293T line) and in *Xenopus* oocytes; *DmGr43a*, in COS-7 cell line (fibroblast-like cells from monkey kidneys). Using the patch-clamp method, the authors showed that D-fructose is the ligand for the *BmGr9* and *DmGr43a* receptors. Recording of the fluorescence dynamics of calcium indicator after D-fructose application confirmed the electrophysiological results. It was shown that the *BmGr9* receptor functions as a ligand-gated cation channel: inhibition of G protein-coupled signaling with the U73122 agent (phospholipase C inhibitor) did not prevent the entry of Ca²⁺ ions upon application of fructose onto cells expressing *BmGr9*.

Table 1. Brief description of the *Gr* genes encoding sweet taste receptors

Gene	Ligand	Partner
<i>Gr5a</i>	Trehalose	Gr64f
<i>Gr61a</i>	Glucose	?
<i>Gr64a</i>	Maltose Fructose	Gr64e
<i>Gr64b</i>	Glycerol	Gr64e
<i>Gr64c</i>	Sucrose Maltose Arabinose	?
<i>Gr64e</i>	Glycerol	Gr64a/Gr64b
<i>Gr64f</i>	Glucose Sucrose Fructose Maltose Trehalose Melezitose	Gr5a
<i>Gr43a</i>	Fructose Sucrose	None

Table 2. *Gr* receptors of bitter taste

Gene	Ligand	Partner
<i>Gr8a</i>	L-canavanine	?
<i>Gr66a</i>	Caffeine Diethyltoluamide Papaverine Strychnine Lobeline	?
<i>Gr93a</i>	Caffeine	?
<i>DmRX</i>	L-canavanine	None

Note: L-Canavanin is a non-proteinogenic amino acid found in some leguminous plants; an insecticide. Diethyltoluamide is an artificially synthesized organic compound with a repellent and insecticidal effect.

Moreover, stimulation with a cyclic nucleotide analog and adenylate cyclase activator (compounds essential for G protein-coupled signaling) failed to produce a calcium response in *BmGr9*-expressing HEK293T cells.

It was later shown that the *BmGr10* receptor sensitive to *myo*- and *epi*-inositol (whose gene is a paralogue of *BmGr9*) is also a ligand-dependent cation channel [53]. The presence of an inward calcium current upon inhibition of G protein cascades with U73122 proved the ionotropic nature of the receptor.

Insect Gr receptors continue to be actively studied. Thus, it has recently been shown that the *TcGr20* receptor in *Tribolium castaneum* is sensitive to sorbitol and mannitol [54]. *Tribolium castaneum* (red flour beetle), a common pest of dry goods, has 207 Gr genes. Apparently, such a wide repertoire of gustatory receptors is necessary for universal consumer species (which

Table 3. Sweet taste Gr receptors with a reported signal transduction mechanism

Receptor	Ligand	Natural source of receptors	Description of receptors in the literature
<i>BmGr9</i>	D-fructose	<i>Bombyx mori</i> (domestic silkworm)	[52]
<i>BmGr10</i>	<i>myo</i> -inositol <i>epi</i> -inositol	<i>Bombyx mori</i> (domestic silkworm)	[53]
<i>TcGr20</i>	mannitol sorbitol	<i>Tribolium castaneum</i> (red flour beetle)	[54]

consume various types of products and are not tied to a specific type of food) (Table 3) [54].

Thus, the members of the Gr43a-clade are insect gustatory receptors with the best-studied functioning mechanism. Moreover, the possibility of heterologous expression of their genes and such chemoreceptor properties as ionotropy and homomery provide ample opportunities to study them in detail in various model systems *in cellulo* and *in vitro* and even for the development of electrophysiological instruments based on them.

The expression features of insect chemoreceptors

Insects and vertebrates differ not only in the structure of chemoreceptors, but also in their gene expression strategies. Thus, in each of the approximately 10 million vertebral olfactory neurons, strictly one receptor gene is expressed. The implementation of the “one receptor – one neuron” rule is ensured by regulation at the transcriptional level. It is assumed that after the functional type of the receptor expressed in a particular cell is selected, transcription of the remaining receptor genes is suppressed by the feedback principle [55]. The mechanism used by a neuron to “choose” its olfactory receptor and arrest the expression of the receptors of all the other specificities is still poorly understood [56]. Most likely, following the “one receptor – one neuron” rule is important for accurate “decoding” of olfactory signals, which implies that the given population of olfactory neurons responds to a limited number of odorants, and that the olfactory center uniquely identifies the origin of incoming signals [56].

In *Drosophila*, most of the ~2,600 available olfactory neurons express two olfactory receptor genes: one is cell type-specific (odor-specific Or subunit), and the second one is the *Or83b* (Orco co-receptor). Dimerization of *Or83b* with a specific receptor provides trafficking of the functional complex toward the olfactory sensilla [6]. At the first glance, this principle seems synonymous with the vertebrate “one receptor – one neuron” rule described above; however, *Drosophila* has

more flexible expression conditions. For example, in 6 out of 8 classes of olfactory antenna neurons, two genes of the odor-specific Or subunit are expressed in addition to *Or83b* [57]. Moreover, all the neurons of a particular sensillum always express the same Or receptor, although *Drosophila* has not been found to suppress the expression of other genes through the feedback principle characteristic of vertebrates [58].

In the *Drosophila* genome, the OR protein family is encoded by 60 genes and several pseudogenes. It consists of 62 receptor proteins (*Or46a* and *Or69a* encode two proteins each via alternative splicing [41]). Some OR genes are grouped into clusters of two or three genes (probably because they appeared as a result of duplication), but most genes are widely distributed across the genome [41]. The expression analysis of OR genes showed that 45 members of the family are expressed in the antennae and maxillary palps of adult animals, while 25 genes function only in the larva olfactory system [57].

Interestingly, OR family receptors were found only in flying insects. Some authors suggest that the dual transduction system characteristic of OR is an adaptation to smell source recognition during flight [59, 60].

The IR receptor family is extremely divergent and demonstrates a shared amino acid sequence identity of 10–70%. Like the OR genes, IR genes are scattered throughout the *Drosophila* genome, mainly as individual genes, but some also form clusters [22]. Genomic analysis of *Drosophila* revealed 66 genes belonging to the IR family, including 9 presumable pseudogenes [22]. Notably, 16 representatives of the family are expressed in olfactory antenna neurons (IR receptors sensitive to organic acids and amines), and 44 in the taste organs (32 at the larval stage, 27 in the adult insect) – labellum, legs, pharynx, and the anterior wing margin [61].

The genome of *Drosophila* also contains 60 genes of the GR family, which encode 68 proteins including those produced via alternative splicing [61]. GR proteins are extremely divergent in amino acid sequences (only 8% identity). The GR family members are expressed in the taste organs of adult animals (the labellum, legs, and pharynx), in the gustatory organs of larvae, as well as in various other tissues of adult animals, including antenna, maxillary palps, enteroendocrine cells of the gut, multidendritic cells of the abdominal body wall, in neurons innervating reproductive organs, and even in the brain [61].

Expression of chemoreceptors is affected by the physiological state of the insect’s organism, which, in turn, depends on environmental factors. Thus, a study of the mRNA levels of the 21 IR, 12 GR, and 43 OR receptors in the antennae of *Bactrocera dorsalis* oriental

fruit fly revealed that expression significantly depends on the nutritional and sexual behavior of insects and even on the time of day [62]. Interestingly, the direction of regulation and its quantitative characteristics appears to be completely different for receptors of different types and individuals of different sexes. These data presumably illustrate the dynamic adaptation of insect physiology to changes in external conditions, providing a certain degree of flexibility in the implementation of behavioral programs.

An analysis of the transcriptomes of eusocial insects, and *Reticulitermes speratus* termites in particular, revealed a differential expression of the *Or*, *Ir*, and *Gr* genes associated with sex, age, and specialization (caste affiliation) of the studied individuals [63]. It is likely that similar expression features may be characteristic of other social insects (ants, bees, etc.), and that the architecture of the chemoreceptor system plays an important role in the formation of polyethism and community building.

CONCLUSION

Insects possess a complexly organized chemoreception system based on proteins that belong to three superfamilies (Table 4). A characteristic feature of this system is lack of a strict correspondence between the receptor type and its functional role. Thus, ionotropic receptors (IRs) are involved both in the sense of smell (acid odors, amine odors) and taste perception (low con-

centrations of sodium chloride). The situation is similar with GR receptors, which, as their name suggests, are mainly involved in taste perception (bitter and sweet taste), while at the same time they can also be involved in olfaction (carbon dioxide). Only odorant receptors (ORs) are strictly olfactory.

The architecture of the chemosensory system reflects the development of the evolutionary adaptations that allow insects to accurately and adequately respond to external chemical stimulation. Thus, GR and IR receptors demonstrate complementary sensitivity to carbon dioxide and acidic odors: low carbon dioxide concentrations are recognized by GR heterodimers (e.g., Gr21a and Gr63a in *Drosophila*), whereas high CO₂ concentrations are recognized by IR heterodimers (IR8a-IR64a in *Drosophila*). The olfactory receptors of the IR and OR families, in turn, demonstrate complementary specificity and unequal sensitization ability, which apparently enables insects to accurately determine changes in the concentration of specific odorants even in the presence of a wide range of “background” molecules.

Evolutionary adaptations would probably also include unusual signal transduction mechanisms characteristic of insect chemoreceptors. For instance, odorant receptors (ORs) use both the ionotropic and metabotropic pathways of “chemical” signal transduction. The first way is important probably for a quick response to high concentrations of odorant,

Table 4. Comparative characteristic of the three main groups of insect chemoreceptors

Chemoreceptor superfamily	ORs (odorant receptors)	IRs (ionotropic receptors)	GRs (gustatory receptors)
Function in insect chemoreceptor system	Food odor and pheromone perception	Odor perception (acids and amines) and low-salt taste perception	Taste perception and carbon dioxide sensing
Protein quaternary structure/oligomeric status	heterodimers	· heterotetramers · heterodimers (acidic odors)	· monomers (Gr43a-like receptors) · heterodimers (sweet taste, carbon dioxide)
Response mechanism	ionotropic + metabotropic	ionotropic	· ionotropic (Gr43a-like receptors) · metabotropic (carbon dioxide sensing receptors)
Type of sensory neurons responsible for signal transduction in the central nervous system	Olfactory sensory neurons – OSNs		Gustatory receptor neurons – GRNs
Localization of sensory neurons in insects	Appendages of the forehead, antennae, maxillary palps		Legs and wings
Model systems used for the conducted studies	· <i>Drosophila melanogaster</i> “empty neuron”* · <i>Xenopus laevis</i> oocyte · Mammalian cells (HEK293)	· <i>Drosophila melanogaster</i> “empty neuron”* · <i>Xenopus laevis</i> oocyte	· <i>Drosophila melanogaster</i> “empty neuron”* · <i>Xenopus laevis</i> oocyte · Mammalian cells (HEK293)

**Drosophila melanogaster* olfactory neuron lacking an endogenous receptor.

while the second one provides signal amplification when recognizing weak odors. The molecular mechanisms of IRs and GRs functioning have been studied much less, but the available data generally indicate a preferentially ionotropic transduction pathway of their signal. This, however, does not exclude the presence of alternative mechanisms. Thus, carbon dioxide receptors from the GR superfamily are characterized by a metabotropic response mediated by Gαq proteins and activating ion channels of the TRP family. It has been suggested that olfactory IR receptors can also interact with G proteins [55].

An ionotropic signal transduction pathway is quite common among all types of insect chemoreceptors. This fact is responsible for the significant peculiarity of their chemosensory system. However, we would like to note that a significant amount of blank spots remains on the “chemoreceptor map” of arthropods in general and insects, in particular. Both the specificity, molecular structure, and the signaling pathways of these receptors are still being studied. ●

This work was supported by the Russian Foundation for Basic Research (RFBR), project no. 18-34-20087.

REFERENCES

- Frank Z., Munger S. Chemosensory transduction: the detection of odors, tastes, and other chemostimuli. London (UK): Elsevier, 2016. 404 p.
- Silbering A.F., Benton R. // *EMBO Rep.* 2010. V. 11. № 3. P. 173–179.
- Wicher D. // *Prog. Mol. Biol. Transl. Sci.* 2015. V. 130. P. 37–54.
- Kaupp U.B. // *Nat Rev Neurosci.* 2010. V. 11. № 3. P. 188–200.
- Larsson M.C., Domingos A.I., Jones W.D., Chiappe M.E., Amrein H., Vosshall L.B. // *Neuron.* 2004. V. 43 № 5. P. 703–714.
- Neuhaus E.M., Gisselmann G., Zhang W., Dooley R., Störtkuhl K., Hatt H. // *Nat. Neurosci.* 2005. V. 8. № 1. P. 15–17.
- Benton R., Sachse S., Michnick S.W., Vosshall L.B. // *PLoS Biol.* 2006. V. 4. № 2. P. 240–257.
- Lundin C., Ka L., Kreher S.A., Kapp K., Sonnhammer E.L., Carlson J.R., Heijne G. Von, Nilsson I. // *FEBS Lett.* 2007. V. 581 № 29. P. 5601–5604.
- Butterwick J.A., Mármol J., Kim K.H., Kahlson M.A., Rogow J.A., Walz T., Ruta V. // *Nature.* 2018. V. 560. № 7719. P. 447–452.
- Kato H.E., Zhang F., Yizhar O., Ramakrishnan C., Nishizawa T., Hirata K., Ito J., Deisseroth K., Nureki O. // *Nature.* 2012. V. 482 № 7385. P. 369–374.
- Müller M., Bamann C., Bamberg E., Kühlbrandt W. // *J. Mol. Biol.* 2011. V. 414. № 1. P. 86–95.
- Penna A., Demuro A., Yeromin A.V., Zhang S.L., Safrina O., Parker I., Cahalan M.D. // *Nature.* 2008. V. 456. № 7218. P. 116–120.
- Sato K., Pellegrino M., Nakagawa T., Nakagawa T., Vosshall L.B., Touhara K. // *Nature.* 2008. V. 452 № 7190. P. 1002–1006.
- Rinker D.C., Zwiebel L.J., Pask G.M., Jones P.L., Rützler M. // *PLoS One.* 2011. V. 6. № 12. P. 4–10.
- Nakagawa T., Pellegrino M., Sato K., Vosshall L.B., Touhara K. // *PLoS One.* 2012. V. 7. № 3. P. 1–9.
- Wicher D., Stensmyr M.C., Heller R., Heinemann S.H., Scha R., Hansson B.S. // *Nature.* 2008. V. 452. № 7190. P. 1007–1012.
- Jones P.L., Pask G.M., Rinker D.C., Zwiebel L.J. // *PNAS.* 2011. V. 108 № 21. P. 8821–8825.
- Chen S., Luetje C.W. // *PLoS One.* 2012. V. 7. № 5. P. 1–9.
- Taylor R.W., Romaine I.M., Liu C., Murthi P., Jones P.L., Waterson A.G., Sulikowski G.A., Zwiebel L.J. // *ACS Chem Biol.* 2012. V. 7. № 10. P. 1647–1652.
- Stengl M. // *J Comp Physiol A.* 1994. V. 174. № 2. P. 187–194.
- Krieger J., Breer H. // *Science.* 1999. V. 286. № 5440. P. 720–723.
- Benton R., Vannice K.S., Gomez-diaz C., Vosshall L.B. // *Cell.* 2009. V. 136. № 1. P. 149–162.
- Abuin L., Ulbrich M.H., Isacoff E.Y., Kellenberger S., Benton R. // *Neuron.* 2011. V. 69. № 1. P. 44–60.
- Silbering A.F., Rytz R., Grosjean Y., Abuin L., Ramdya P., Jefferis G.S., Benton R. // *J Neurosci.* 2011. V. 31. № 38. P. 13357–13375.
- Prieto-godino L.L., Rytz R., Bargeton B., Abuin L., Arguello J.R., Peraro M.D., Benton R. // *Nature.* 2016. V. 539. № 7627. P. 93–97.
- Ai M., Min S., Grosjean Y., Leblanc C., Bell R., Benton R., Suh G.S.B. // *Nature.* 2010. V. 468. № 7324. P. 691–695.
- Rimal S., Lee Y. // *Insect Mol Biol.* 2018. V. 27. № 1. P. 1–7.
- Cao L., Jing B., Yang D., Zeng X., Shen Y., Tu Y. // *PNAS.* 2015. V. 113 № 7. P. 902–911.
- Getahun M.N., Wicher D., Hansson B.S., Olsson S.B., Fontanini A., Brook S. // *Front Cell Neurosci.* 2012. V. 6. № 54. P. 1–11.
- Zhang Y.V., Ni J., Montell C. // *Science.* 2013. V. 340. № 6138. P. 1334–1338.
- Jones W.D., Cayirlioglu P., Kadow I.G., Vosshall L.B. // *Nature.* 2007. V. 445. № 7123. P. 86–90.
- Robertson H.M., Kent L.B. // *J Insect Sci.* 2009. V. 9. № 19. P. 1–14.
- Kwon J.Y., Dahanukar A., Weiss L.A., Carlson J.R. // *PNAS.* 2007. V. 104. № 9. P. 3574–3578.
- Yao C.A., Carlson J.R. // *J Neurosci.* 2010. V. 30. № 13. P. 4562–4572.
- Sturgeon R.M., Magoski N.S. // *J Neurosci.* 2018. V. 38. № 35. P. 7622–7634.
- Badsha F., Kain P., Prabhakar S., Sundaram S., Padinjat R., Rodrigues V., Hasan G. // *PLoS One.* 2012. V. 7. № 11. P. 1–11.
- Stocker R.F. // *Cell Tissue Res.* 1994. V. 275. № 1. P. 3–26.
- Clyne P.J., Warr C.G., Carlson J.R. // *Science.* 2000. V. 287. № 5459. P. 1830–1834.
- Scott K., Brady R., Cravchik A., Morozov P., Rzhetsky A., Zuker C., Axel R., York N., York N. // *Cell.* 2001. V. 104. № 5. P. 661–673.
- Dunipace L., Meister S., Mcnealy C., Amrein H. // *Curr Biol.* 2001. V. 11. № 11. P. 822–835.
- Robertson H.M., Warr C.G., Carlson J.R. // *PNAS.* 2003. V. 100. P. 14537–14542.
- Kent L.B., Robertson H.M. // *BMC Evol Biol.* 2009. V. 9. № 41. P. 1–20.
- Weiss L.A., Dahanukar A., Kwon J.Y., Banerjee D., Carlson J.R. // *Neuron.* 2011. V. 69. № 2. P. 258–272.

REVIEWS

44. Fujii S., Yavuz A., Slone J., Jagge C., Song X., Amrein H. // *Curr. Biol.* 2015. V. 25. № 5. P. 621–627.
45. Nelson G., Hoon M.A., Chandrashekar J., Zhang Y., Ryba N.J., Zuker C.S. // *Cell.* 2001. V. 106. № 3. P. 381–390.
46. Montmayeur J., Liberles S.D., Matsunami H., Buck L.B. // *Nat Neurosci.* 2001. V. 4. № 5. P. 492–498.
47. Yavuz A., Jagge C., Slone J., Amrein H. // *Fly (Austin)*. 2015. V. 8. № 4. P. 189–196.
48. Miyamoto T., Slone J., Song X., Amrein H. // *Cell.* 2012. V. 151. № 5. P. 1113–1125.
49. Moon S.J., Lee Y., Jiao Y. // *Curr. Biol.* V. 2009. V. 19. № 19. P. 1623–1627.
50. Lee Y., Jun S., Montell C. // *PNAS.* 2009. V. 106. № 11. P. 4495–4500.
51. Smadja C., Shi P., Butlin R.K., Robertson H.M. // *Mol. Biol. Evol.* 2008. V. 26. № 9. P. 2073–2076.
52. Sato K., Tanaka K., Touhara K. // *PNAS.* 2011. V. 108. № 28. P. 11680–116805.
53. Kikuta S., Endo H., Tomita N., Takada T., Morita C., Asaoka K., Sato R. // *Insect Biochem. Mol. Biol.* 2016. V. 74. P. 12–20.
54. Takada T., Sato R., Kikuta S. // *PLoS One.* 2017. V. 12. № 10. P. 1–16.
55. Serizawa S., Miyamichi K., Nakatani H., Suzuki M., Saito M., Yoshihara Y., Sakano H. // *Science.* 2003. V. 302. № 5653. P. 2088–2094.
56. Touhara K., Vosshall L.B. // *Annu Rev Physiol.* 2009. V. 71. P. 307–332.
57. Couto A., Alenius M., Dickson B.J. // *Curr Biol.* 2005. V. 15. № 17. P. 1535–1547.
58. Dobritsa A.A., van der Goes van Naters W., Warr C.G., Steinbrecht R.A., Carlson J.R., Haven N., Vic C. // *Neuron.* 2003. V. 37. № 5. P. 827–841.
59. Missbach C., Dweck H.K.M., Vogel H., Vilcinskas A., Stensmyr M.C., Hansson B. S., Grosse-Wilde E. // *eLife.* 2014. V. 3. P. 1–22.
60. Getahun M.N., Thoma M., Lavista-Llanos S., Keesey I., Fandino R.A., Knaden M., Wicher D., Olsson S.B., Hansson B.S. // *J Exp Biol.* 2016. V. 219. № 21. P. 3428–3438.
61. Joseph R.M., Carlson J.R. // *Trends Genet.* 2015. V. 31. № 12. P. 683–695.
62. Jin S., Zhou X., Gu F., Zhong G., Yi X. // *Front Physiol.* 2017. V. 8. № 627. P. 1–12.
63. Mitaka Y., Kobayashi K., Mikheyev A., Tin M.M.Y., Watanabe Y., Matsuura K. // *PLoS One.* 2016. V. 11. № 1. P. 1–16.
64. John H. Byrne. *The Oxford Handbook of Invertebrate Neurobiology.* Oxford (UK): Oxford University Press, 2017. 792 p.

Cytokine Profile As a Marker of Cell Damage and Immune Dysfunction after Spinal Cord Injury

G. B. Telegin^{1*}, A. S. Chernov¹, N. A. Konovalov², A. A. Belogurov³, I. P. Balmasova⁴,
A. G. Gabibov³

¹Branch of Shemyakin and Ovchinnikov Institute of Bioorganic Chemistry Russian Academy of Sciences, Pushchino, 142290 Russia

²N.N. Burdenko National Scientific and Practical Center for Neurosurgery, RF Health Ministry, Moscow, 125047 Russia

³Shemyakin and Ovchinnikov Institute of Bioorganic Chemistry Russian Academy of Sciences, Moscow, 117997 Russia

⁴Evdokimov Moscow State University of Medicine and Dentistry of Russia's Ministry of Health, Moscow, 127473 Russia

*E-mail: telegin@bibch.ru

Received July 20, 2020; in final form, September 8, 2020

DOI: 10.32607/actanaturae.11096

Copyright © 2020 National Research University Higher School of Economics. This is an open access article distributed under the Creative Commons Attribution License, which permits unrestricted use, distribution, and reproduction in any medium, provided the original work is properly cited.

ABSTRACT This study reviews the findings of recent experiments designed to investigate the cytokine profile after a spinal cord injury. The role played by key cytokines in eliciting the cellular response to trauma was assessed. The results of the specific immunopathogenetic interaction between the nervous and immune systems in the immediate and chronic post-traumatic periods are summarized. It was demonstrated that it is reasonable to use the step-by-step approach to the assessment of the cytokine profile after a spinal cord injury and take into account the combination of the pathogenetic and protective components in implementing the regulatory effects of individual cytokines and their integration into the regenerative processes in the injured spinal cord. This allows one to rationally organize treatment and develop novel drugs.

KEYWORDS Spinal cord injury, cytokines, cellular response.

ABBREVIATIONS BBB – blood–brain barrier; SC – spinal cord; SCI – spinal cord injury; CNS – central nervous system.

INTRODUCTION

Spinal cord injury (SCI) is a serious global health problem which often leads to severe lifelong disability [1, 2]. According to the WHO, up to 500,000 people, including young patients aged 20–35 years, suffer from SCI annually in the world [3].

Broad opportunities for studying the morphological and pathophysiological changes in patients with SCI, which are necessary for developing rational treatment strategies, have made it possible to progress from clinical observations to developing experimental models [4]. This approach has allowed one to elucidate many pathogenetically significant mechanisms that underly the development of this pathology, including those associated with the immune responses to the injury; so, these responses were classified into immediate and chronic post-traumatic reactions [5].

1. IMMUNE AND CYTOKINE RESPONSES DURING THE ACUTE POST-TRAUMATIC PHASE AFTER A SPINAL CORD INJURY

Two different phases are distinguished in the pathogenesis of the immediate post-traumatic period of spinal cord injury. Each of them leads to a complex of pathophysiological reactions in response to the damage to the nervous system [6, 7].

The first post-traumatic phase that starts on the first day after trauma exposure involves the damage mechanisms and disorders associated with it. Neurons, astrocytes, oligodendrocytes, and other components of nerve signal transmission are physically affected, which is accompanied by disorders in vascular components, including the blood–brain barrier (BBB) [8–10]. This results in tissue infiltration by inflammatory cells [11–13].

The second post-traumatic phase involves the endogenously induced degradation of the nervous tissue and associated consequences [14]. Increased glutamate level in the damaged spinal cord (SC) tissue causes neuronal excitotoxicity, a pathological process leading to neurotransmitter-mediated damage and death of nerve cells, due to the excess of intracellular Ca^{2+} . This promotes the accumulation of reactive oxygen species [15–17], which, in turn, damage cellular components, such as nucleic acids, proteins, and phospholipids, and cause significant cell loss and subsequent neurological dysfunction [18, 19].

The inflammatory response to primary structural changes in the spinal cord is accompanied by the release of a large number of regulatory peptides, including proinflammatory ones, and cytokines [20, 21]. Cytokines are synthesized by activated macro- and microglia, damaged vascular endothelium, as well as the immune system cells mobilized from the systemic circulation to the injury site and the adjacent areas, due to changes in the BBB permeability [22].

Figure 1 shows the main pathogenetic mechanisms involved in the immediate post-traumatic phase of SCI, as well as the general role played by immune system cells and cytokines in its development.

It was found that a series of immunologically significant molecules, including tumor necrosis factor (TNF- α), inducible nitric oxide synthase (iNOS), nuclear factor (NF)- κ B, interleukin (IL)-1 β , and/or a factor of the apoptosis Fas ligand (FasL), are activated as early as within a few minutes after SCI [23–25]. Activation of these molecules further results in inflammation and other forms of important neurological disorders [14].

Activated astrocytes are the main source of all these factors: they account for about 30% of all cellular components; overexpression of the microRNA miR-136-5p in these cells during SCI is one of the inducers of proinflammatory factors and chemokines (primarily TNF- α and IL-1 β) [26–28]. This process triggers an inflammatory immune response involving type 17 T-helpers [29]. Angiogenesis is another concomitant effect of SCI mediated by microRNA (miR-210) [30, 31].

It should be emphasized that it is the endogenous cells (neurons and glial cells) of the human spinal cord but not white blood cells that contribute to the early production of IL-1 β , IL-6, and TNF- α in the post-traumatic inflammatory response [32–34].

However, one should not underestimate the role played by immune cells as a source of proinflammatory

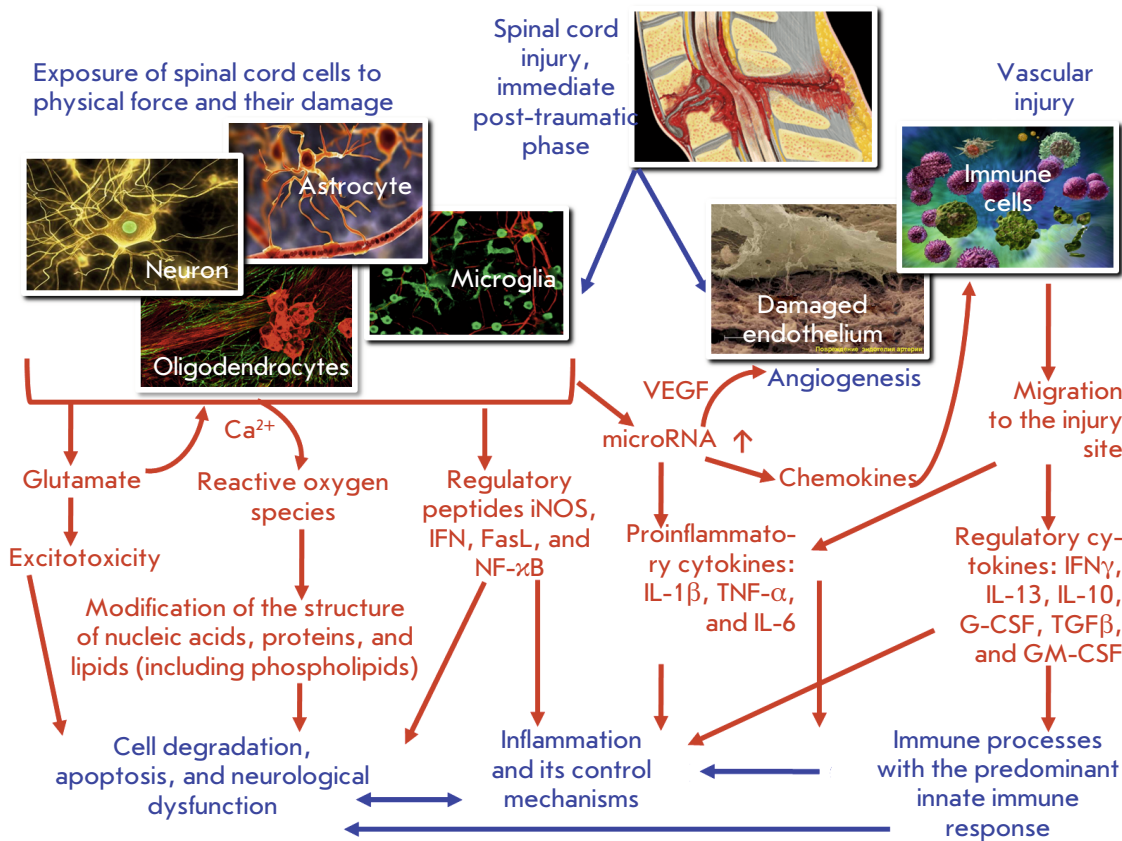


Fig. 1. The pathogenetic mechanisms of the immediate post-traumatic phase after SCI that trigger the innate immune system response.

cytokines in a spinal cord injury. This is facilitated by hemorrhage in the spinal cord tissue after damage to it [35, 36], which enables infiltration of the affected areas by neutrophils, monocytes/macrophages, and T cells [37–40] (i.e., cells releasing the same factors TNF- α , IL-1 α , IL-1 β , and IL-6) [41, 42].

In general, these cytokines reach their peak level 6–12 h after the injury; they also induce an inflammatory response in acute and subacute periods and expand the lesion in the rostral and caudal directions [43–45]. Activated microglia and macrophages infiltrating the spinal cord have been shown to be responsible for the subsequent necrosis and apoptosis of neurons, astrocytes, and oligodendrocytes at the injury site [46, 47], thus worsening the neurological outcome [48, 49].

As for the signals of cytokine release, they can enter the cells through the Toll-like receptors (TLRs) of the spinal cord [50, 51]. TLRs are best known as the structures for pathogen recognition and initiation of the innate immune response [52, 53]. However, they can also detect tissue damage and trigger sterile inflammation by binding to endogenous ligands typical of stressed or damaged cells. In addition to the cells associated with the immune system, TLRs have also been revealed in the neurons of the central nervous system (CNS) and glial components, including microglia, astrocytes, and oligodendrocytes [54, 55]. Considering the above, Toll-like receptors can play both a direct and indirect role in a spinal cord injury [56]. The indirect effects are most likely mediated by microglia or the immune cells penetrating the damaged CNS tissue [57]. It was also revealed that the restorative responses in ischemic disorders after a spinal cord injury occur with predominant involvement of Toll-like receptor 3 and subsequent regulation by TLR4 [58].

Modulation of proinflammatory and immune effects in the spinal cord tissue during injury occurs with the involvement of interferons due to the increased concentration of stimulators of the interferon genes (STING) in the tissue [59, 60].

Another immunological effect is observed during the first 24 h after the spinal cord injury: the number of natural killer (NK) cells with an activated phenotype increases significantly, manifesting itself as overexpression of CD69, HLA-DR, NKG2D, and NKp30 on their membrane, as well as enhanced cytotoxic activity [61]. Furthermore, an increased level of the brain-derived neurotrophic factor (BDNF), which can be secreted by vascular endothelial cells, was found in patients' plasma samples, which strongly correlated with the percentage of NK cells and the level of activation molecules CD69 and NKp30 on their surface during this phase after SCI. [62].

Early intervention to reduce inflammation and prevent apoptosis has long been a strategy in treating spinal cord injury. However, the growing body of knowledge in this field suggests that the inflammatory process has apparent protection aspects that should not be ignored during therapy [63].

One of the mechanisms of innate immune defense during inflammatory response after a spinal cord injury is associated with the unique role played by mast cells [64]. Mast cells are abundant in the CNS and play a rather complex role in the development of neuroinflammatory disorders. In particular, astrogliosis and infiltration of T cells increase in mast-cell-deficient mice, while functional recovery after a spinal cord injury is significantly reduced in these animals [65]. Moreover, these mice have significantly increased levels of cytokines MCP-1, NF α , IL-10, and IL-13 in the spinal cord. Data have been obtained on the relationship between these phenomena and the fact that, at an equal number and functional activity of mast cells, their chymases cleave MCP-1, IL-6, and IL-13, thus indicating the protective role played by these cellular elements in the development of inflammatory changes in the nervous tissue during a spinal cord injury [66].

The pattern of cytokine and hormone secretion after spinal cord injury largely depends not only on the mechanisms of induction and immune response, but also on injury severity. For instance, experiments in a rat model clearly demonstrated similar differences in the secretion of the vascular endothelial growth factor (VEGF), leptin, interferon- γ -induced chemokine IP-10, IL-10, IL-18, the granulocyte colony-stimulating factor (G-CSF), and chemokine fractalkine in animals' plasma. In contrast to the thoracic spine trauma, injury to the cervical spine is accompanied by a reduced expression of these mediators; this is probably due to sympathetic dysregulation, which is associated with higher injury severity [67, 68]. Experiments on mice have also demonstrated that the involvement of the cytokine profile in the systemic changes of interleukins such as IL-3, IL-6, IL-10, IL-13, and G-CSF after a spinal cord injury to the lower thoracic region (Th910) is accompanied by the activation of T lymphocytes and neutrophils during the immediate post-traumatic phase of the observed changes [69].

It should be noted that, in addition to astrocytes and microglia, IL-10 is also produced by macrophages, B cells, and Th2 cells [70, 71]. Being an immunomodulator, IL-10 stimulates the formation of regulatory T cells, while suppressing the activity of Th1 and NK cells [72].

Thus, the immunopathogenetic mechanisms primarily associated with innate immune cells and predominantly proinflammatory cytokines are induced during

the immediate post-traumatic phase after a spinal cord injury. *Figure 2* is an attempt to summarize the linking mechanisms of these pathogenetically significant immune responses to the spinal cord injury described in modern publications. The following information regarding the interaction between immunocytes can be added to the scheme.

Damaged neurons and neuroglial cells after a spinal cord injury are a source of chemokines (fractalkine, MCP-1, and IP-10) [67, 69] that target monocytes/macrophages, as well as lymphocytes and promote their entry into the lesion site. Mast cells are one of the first cells (among the innate immune cells) to exert an effect on the injury site. As already mentioned, mast cells can regulate chemokine secretion; however, their role is far from clear. On the one hand, these cells can be a source of cytokines and other mediators that promote inflammation [73]. On the other hand, chymases released from mast cells during their activation and subsequent degranulation can destroy chemokines and proinflammatory cytokines, thus limiting the intensity of the inflammatory responses [66].

Most chemokines produced by the cells of an injured spinal cord promote the recruitment of monocytes/

macrophages [74], which eliminate cell debris, while chemokine IP-10 also recruits NK cells [75]. The involvement of NK cells in the innate immune response is also facilitated by the fact that spinal cord cells express injury patterns in trauma. These, in particular, include stress-induced molecules (MICA, MICB), which are ligands for NKG2D receptors [76]. In turn, they are overexpressed by NK cells in a spinal cord injury [60]. At first glance, manifestations of the cytotoxic activity of NK cells against the nervous tissue in a spinal cord injury significantly aggravate the destructive processes during trauma [60]. However, the involvement of NK cells in the elimination of exclusively cells carrying injury patterns contributes to a more rapid suppression of destructive processes at the site of a spinal cord lesion.

This study, focused on another crucial player, macrophages, under conditions of tissue damage has demonstrated that their activation involves two stages. During the first stage, these cells acquire an inflammatory (M1) phenotype, which is mediated by endogenous molecules released during cellular damage. At later stages, when reparative processes are triggered in response to damage, the activated macrophages are

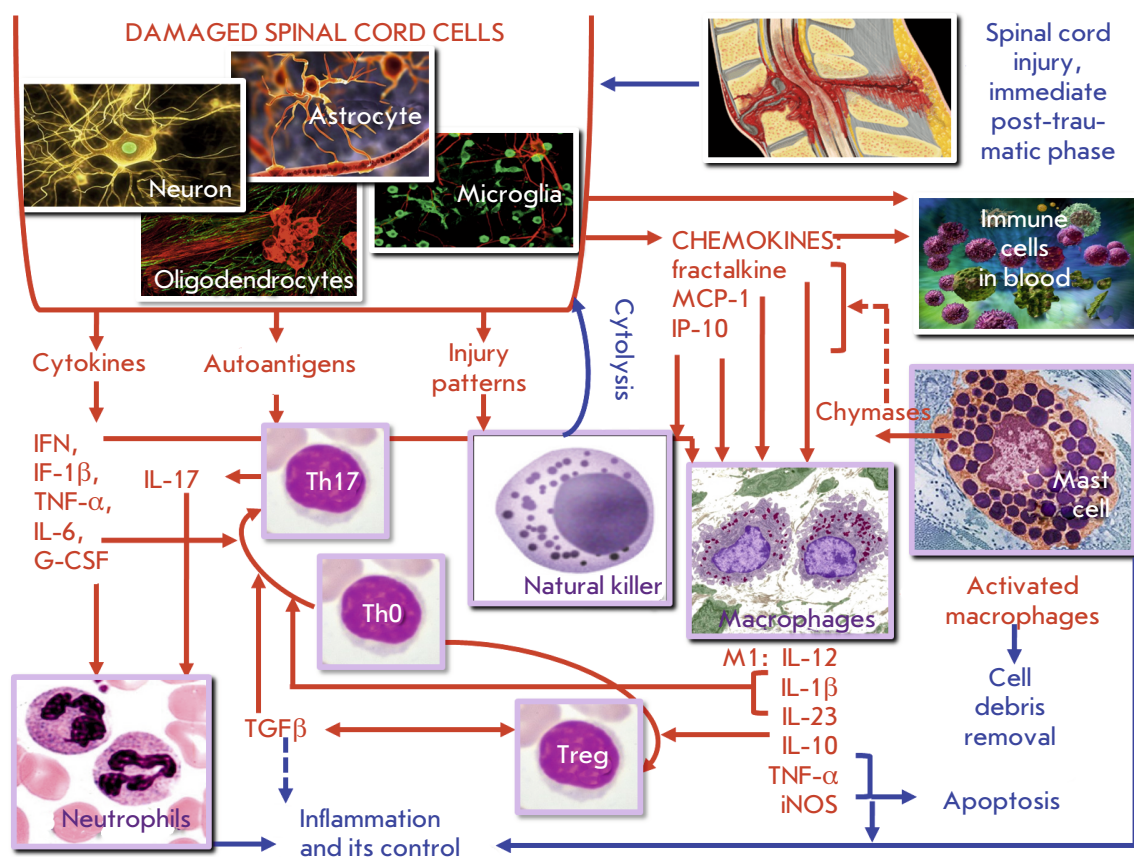


Fig. 2. Specific characteristics of the immune response in the immediate post-traumatic phase after SCI

polarized into the resident (M2) phenotype [77]. In this regard, one can assume that M1 macrophages are predominantly produced during the immediate post-traumatic phase of spinal cord injury. Their induction is also mediated by interferons [78], which accumulate, as has already been reported, in damaged tissues during a spinal cord injury [59]. These macrophages secrete IL-12, IL-10, IL-1 β , IL-6, IL-23, IL-21, TNF- α , and iNOS, characteristic of this phenotype; high levels of these factors are typical of the pathology [67, 69, 77].

These cytokines have different functions: IL-12 promotes further induction of adaptive cellular responses; IL-10 has an immunosuppressive effect and is involved in the induction of regulatory T cells; IL-1 β , IL-6, IL-21, IL-23, and TNF- α exert a proinflammatory effect; TNF- α and iNOS provoke cellular damage [78, 79].

The predominant cytokine profile, as well as the presence of M1 macrophage-producing cells in combination with the effect of autoantigens of the damaged spinal cord, suggests that the population of T lymphocytes involved in the immune response at the initial stage includes Th17 cells whose functional significance during the immediate post-traumatic period of a spinal cord injury has already been proved. The functional role of this subpopulation is closely related to the formation of the balance T helper 17/regulatory T cells (Th17/Treg). Q. Fu et al. [29] described these processes as follows: the Th17/Treg cell balance is regulated by the molecules ROR γ T and FoxP3, while FoxP3 expression can be inhibited by ROR γ T expression. As mentioned above, a spinal cord injury is accompanied by the migration of M1 macrophages to the injury site and release of proinflammatory cytokines, including IL-6 and IL-21. This allows T-helpers (CD⁴⁺ T lymphocytes) to differentiate into CD⁴⁺IL-17A⁺ Th17, which contribute to the inflammatory response by recruiting neutrophilic granulocytes. In combination with proinflammatory cytokines secreted at the injury site by macrophages, neurons, and neuroglia cells, the products of Th17 and neutrophils greatly exacerbate the inflammation, which is regarded as a quite undesirable aspect of the pathogenesis of post-traumatic changes in the spinal cord.

It should also be emphasized that Th17 induction during the initial phase requires one more cytokine, the transforming growth factor β (TGF β), which is mainly secreted by Treg cells. The formation of these cells that play an important role in the Th17/Treg balance is mainly mediated by IL-10, which is also secreted by M1 macrophages in relatively small amounts during the initial phase of tissue damage. Like TGF β , IL-10 also has an immunosuppressive effect, thus limiting the redundancy of the autoimmune inflammatory process after a spinal cord injury [77, 80].

Thus, the innate immune response and T cell-mediated responses that prevail during the immediate pre-traumatic phase of a spinal cord injury should be assessed in a different manner. On the one hand, they aim to eliminate cells in the damaged spinal cord tissue through apoptosis or cytolysis, as well as induce an inflammatory response that enhances neurological dysfunction. On the other hand, these reactions contribute to the elimination of the destroyed cell elements, along with the corresponding autoantigens, injury patterns, and inflammation mediators, and they also involve the mechanisms that regulate inflammatory responses. These conclusions require one not to use a simplified approach to assess the role played by immune processes in a spinal cord injury. They also affect the chosen therapeutic strategy during the immediate post-traumatic period, as one needs to evaluate the balance between the immune mechanisms that prevail in each particular case and exhibit either a protective or pathogenetic action, rather than individual parameters.

2. THE IMMUNE AND CYTOKINE PROCESSES ACCOMPANYING THE CHRONIC PHASE OF A SPINAL CORD INJURY

As early as during the immediate post-traumatic phase, a spinal cord injury causes a severe inflammatory response [81] and a strong immune response both within and beyond the injury site [82]; these responses do not tend to resolve. In this case, the interaction takes place between the CNS and the immune system (i.e., the two main systems maintaining homeostasis in the entire body). That is why the process involves not only the response of immune cells in the site of the spinal cord injury but also affects one's entire immune system [83].

The functions of the immune system change significantly as the immediate post-traumatic phase after the injury progresses to a chronic phase. The loss or dysfunction of vegetative innervation in the lymphatic and endocrine tissues causes immune response disorders that last quite a long time after the initial trauma [84]. The main manifestations of such disorders are immune depression and the autoimmune process [83], although inflammatory reactions also remain pathogenetically significant.

Thus, starting on day 7 after a spinal cord injury, signs of regeneration of the myelin sheath of neurons, accompanied by a biochemically detectable activity of oligodendrocytes and production of the proinflammatory cytokines TNF- α , IL-1 β , and IL-6, were observed [85]. Meanwhile, it was noted that the higher the level of proinflammatory cytokines during the chronic phase, the sooner the remission after the spinal cord injury occurs [86].

The fact is that proinflammatory cytokines trigger the activation of astrocytes in the spinal cord [87]. Astrocytes undergo proliferation and acquire one of two phenotypes; astrocytes that have one phenotype and actively secrete a glial fibrillary acidic protein (GFAP), which contributes to neuroregeneration. Contrariwise, astrocytes that have the other phenotype and secrete the glutamine synthase that is involved in the glutamate uptake and slows down neuronal regeneration in the injured spinal cord region. The balance between astrocytes with these two phenotypes determines the efficiency of neuroregeneration [88]. Neurons secrete neuregulin-1 (Nrg-1), which stimulates cell regeneration, contributes to the preservation of the spinal cord white matter, and positively regulates the functions of macrophages, T cells, and B cells. Today, it is even recommended as a medicinal product for patients with spinal cord injury [89].

Although this positive regulation is possible, one should take into account the fact that all the aforementioned processes take place in the CNS; therefore, they can have both local and systemic manifestations.

Systemic changes at the level of cell populations and lymphocyte subpopulations during the chronic phase of a spinal cord injury are mainly related to T cell-mediated adaptive immunity. Thus, it has been demonstrated that the total count of T cells (CD3+) and T helper cell subpopulation (CD3+ CD4+) in the blood is reduced, although the count of activated CD4+ T cells (HLA-DR+CD4+) remains elevated [90]. This is possible if the count of T helper cells in the blood decreases because they migrate to the affected organ.

Regulatory T cells (Tregs) that exhibit suppressive properties are particularly interesting in this case. These cells have a CD3+CD4+CD25+CD127lo phenotype; the activated CCR4+HLA-Dr+ fraction being the predominant one. The level of the transforming growth factor β (TGF β), the main cytokine in these cells, is significantly higher in patients with spinal cord injury, which largely explains the observed immune dysfunction and its sequelae, such as impaired defense against infections and/or persistent chronic inflammation [5, 38].

The deficiency of T-cell-mediated immunity at a systemic level is also accompanied by a significant reduction in NK cell count during the chronic phase of SCI, which eventually often leads to the development of a lethal infection [91].

Speaking about one of the key mechanisms of induction of the observed changes, we would like to provide the data obtained by C.J. Ferrante and S.J. Leibovich [77]. They reported that after the immediate tissue damage phase, the macrophage phenotype switched abruptly from M1 to M2, which significantly differs

from the typical M2 cells in terms of cytokine secretion. This variety was called the angiogenic M2d phenotype. The main products of M2d macrophage secretion included the vascular endothelial growth factor (VEGF) and IL-10 inducing the formation of regulatory T cells. That is why the angiogenic and immunosuppressive effects are predominant (see *Fig. 3*). Similar transformations also took place for macrophage microglial cells [92].

Special attention should be paid to the autoimmune processes associated with a spinal cord injury. D.P. Ankeny et al. [93] demonstrated that a spinal cord injury and the immunodepression accompanying it cause profound long-lasting changes in the functions of B cells in the peripheral lymphoid tissue (the bone marrow and spleen) and the injured spinal cord; in particular, after differentiation-activated B cells become able to secrete autoantibodies that bind to CNS proteins and nuclear antigens, including DNA and RNA. In patients with systemic lupus erythematosus, anti-DNA antibodies cross-reactively interact with glutamate receptors to cause excitotoxicity [94]. The same phenomenon is observed for the autoantibodies produced in patients after SCI that exhibit similar neurotoxic properties.

After a spinal cord injury, the autoimmunity can also promote CNS re-generation and/or neuroprotection, although there still can be a tendency towards neurotoxicity manifestations. Myelin-reactive T cells exhibit a similar neuroprotective effect in a rat model of SCI [95]. The data on the role played by autoantibodies are rather inconsistent, because the antibodies specific to CNS proteins can promote axonal re-generation and remyelination [96], as well as demyelination, because antimyelin antibodies can be involved in the formation of a “bridge” between myelin of nerve fibers and oligodendrocytes [97]. In any case, despite the ambiguity of the effects and their interpretations, it has been established that B cells infiltrate the injured spinal cord during the chronic phase [93].

The presented analysis demonstrates that interpreting the results is challenging, because it is rather difficult to differentiate between local and systemic effects after a spinal cord injury. In this regard, the possibility of differentiating between the local and systemic manifestations of the immune response opens some prospects. For example, significant changes in the cytokine profile after SCI, especially during the chronic phase, were observed not only in the blood. The changes in the cytokine profile in CSF were even more informative. Thus, A.R. Taylor et al. [98] determined the levels of the IL-2, IL-6, IL-7, IL-8, IL-10, IL-15, IL-18, granulocyte-macrophage colony-stimulating factor (GM-CSF), interferon- γ (IFN γ), keratinocyte chemoattractant (KC-like protein), IFN γ -inducible

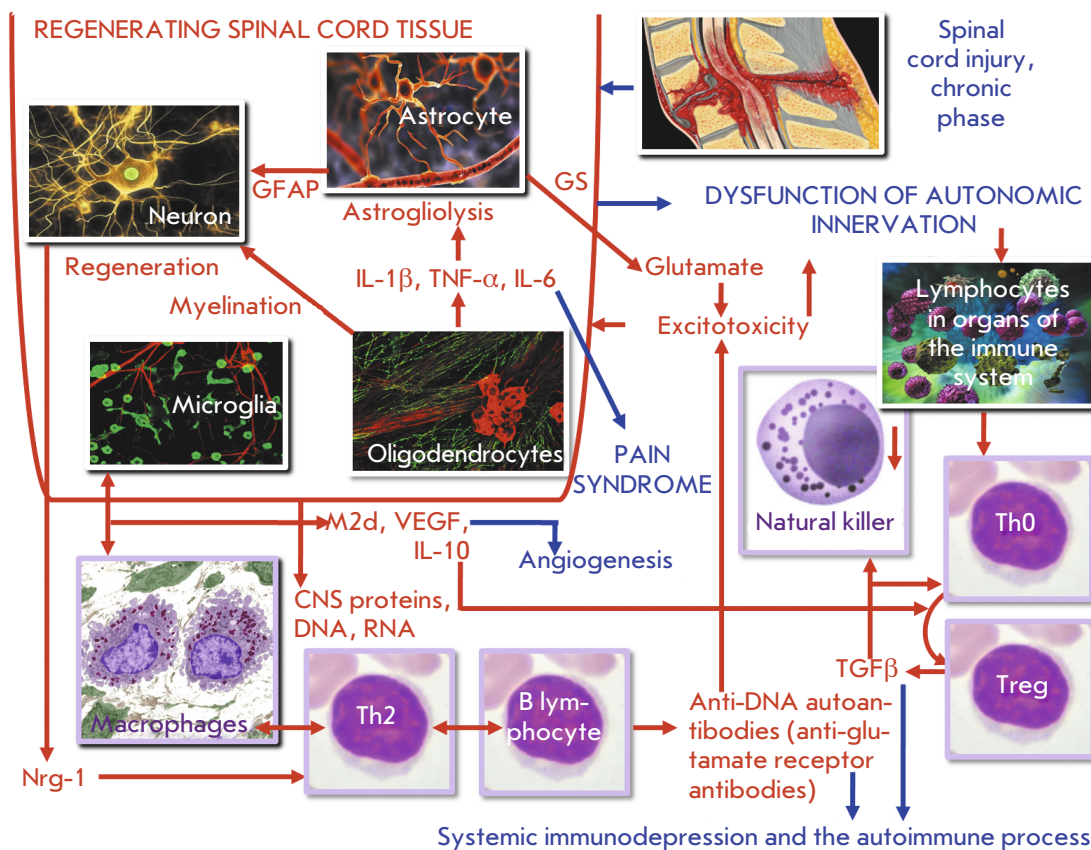


Fig. 3. Specific immunopathogenic characteristics of the chronic post-traumatic phase after SCI

protein 10 (IP-10), monocyte chemotactic protein-1 (MCP-1), and tumor necrosis factor α (TNF- α) in the cerebrospinal fluid as a criteria for evaluating the intensity of a chronic inflammation. The concentrations of most cytokines and chemokines in CSF of animals after SCI correlated with injury duration, injury severity at sampling, and the long-term neurological outcome. Thus, the IL-8 level after a spinal cord injury was significantly higher than in the healthy control but showed a negative correlation with injury duration; the levels of colony-stimulating factors and MCP-1 negatively correlated with a long-term positive outcome.

Particular focus is to be directed at the role played by tumor necrosis factor α during the chronic phase after a spinal cord injury. The fact is that the level of brain-derived neurotrophic factor (BDNF) decreases in the hippocampus while increasing in the lateral part of the spinal cord. Deletion within the gene encoding the TNF- α receptor cancels this effect, but the presence of this cytokine restores it. These findings suggest that the various structural synaptic changes in the spinal cord and hippocampal neurons are mediated by overproduction of TNF- α by activated microglial cells, which can be associated with the development of

chronic neuropathic pain and memory deficit after a spinal cord injury [99].

IL-1 β that reduces the efficiency of the calcium pump function in neurons is also involved in the development of neuropathic pain [100].

Hence, cytokines contribute rather significantly to the pathogenesis of a traumatic disease after a spinal cord injury and are responsible for many of its manifestations. The cytokines can be secreted by the immune cells; however, the neurons of the damaged spinal cord are the main source of these biologically active substances. Therefore, the cytokine profile in patients with SCI plays a special diagnostic and prognostic role. It also characterizes both the immune and neurological status of patients with this pathology.

CONCLUSIONS

This review of publications focused on the problem of the immune (including cytokine) processes accompanying a spinal cord injury demonstrates that the available data are ambiguous and difficult to interpret.

The complexity of the problem is primarily to do with the fact that both the nervous and immune systems have important regulatory functions in the body

and are tightly interrelated, while the mechanisms behind this interrelation are very diverse. Both local and systemic manifestations accompany the neurological and immune changes that occur after a spinal cord injury.

Along with these general aspects, it is important to take into account the phases of local and systemic changes in the central nervous system and the immune processes associated with SCI [101, 102]. Each phase is characterized by its own predominant pathogenetic mechanism, which is initially associated with the response to the injury and aims to eliminate the damaged cells; then, the focus moves towards the inflammatory response aiming to confine the affected area to a minimum. Finally, a transition from local responses to systemic processes takes place during the last stages;

the outcome of the pathological process depends on the efficiency of these phases. Each phase is accompanied by its own category of immune response; various cell subpopulations characteristic of innate and adaptive immunity or cytokines, the secretory products of these cells, can act as markers of these types of immune response [103, 104].

A specific feature of cytokines as markers of pathological changes after a spinal cord injury is that they are secreted not only by immune cells, but also by the cells of the damaged spinal cord. The interaction between the nervous and immune systems can be observed using the cytokine profile model, which is both of fundamental interest and diagnostic importance as it allows one to identify the key targets of therapeutic action. ●

REFERENCES

- Karsy M., Hawryluk G. // *Neurosurg. Clin. N. Am.* 2017. V. 28. № 1. P. 49–62.
- La Placa M.C., Simon C.M., Prado G.R., Cullen D.K. // *Prog. Brain Res.* 2007. V. 161. P. 13–26.
- Bracken M.B. // *Cochrane Database Syst. Rev.* 2012. V. 1. CD001046.
- Minakov A.N., Chernov A.S., Asutin D.S., Kononov N.A., Telegin G.B. // *Acta Nature.* 2018. V. 10. № 3. P. 4–10.
- Monahan R., Stein A., Gibbs K., Bank M., Bloom O. // *Immunol. Res.* 2015. V. 63. № 1–3. P. 3–10.
- Oyinbo C.A. // *Acta Neurobiol. Exp. (Wars.)*. 2011. V. 71. № 2. P. 281–299.
- Zhang N., Yin Y., Xu S.J., Wu Y.P., Chen W.S. // *Indian J. Med. Res.* 2012. V. 135. № 3. P. 287–296.
- Wilcox J.T., Satkunendrarajah K., Nasirzadeh Y., Laliberte A.M., Lip A., Cadotte D.W., Foltz W.D., Fehling M.G. // *Neurobiol. Dis.* 2017. V. 105. P. 194–212.
- Cruz C.D., Coelho A., Antunes-Lopes T., Cruz F. // *Adv. Drug Deliv. Rev.* 2015. V. 82–83. P. 153–159.
- Figley S.A., Khosravi R., Legasto J.M., Tseng Y.-F., Fehlings M.G. // *J. Neurotrauma.* 2014. V. 31. № 6. P. 541–552.
- Kunis G., Baruch K., Rosenzweig N., Kertser A., Miller O., Berkutzki T., Schwartz M. // *Brain.* 2013. V. 136. № 11. P. 3427–3440.
- Li Y., Lucas-Osma A.M., Black S., Bandet M.V., Stephens M.J., Vavrek R., Sanelli L., Fenrich K.K., Di Narzo A.F., Dracheva S., et al. // *Nat. Med.* 2017. V. 23. № 6. P. 733–741.
- Shechter R., Miller O., Yovel O.G., Rosenzweig N., London A., Ruckh J., Kim K.-W., Klein E., Kalchenko V., Bendel P., et al. // *Immunity.* 2013. V. 38. № 3. P. 555–569.
- Jorge A., Taylor T., Agarwal N., Hamilton D.K. // *World Neurosurg.* 2019. V. 132. P. 138–147.
- Breckwoldt M.O., Pfister F.M., Bradley P.M., Marinković P., Williams P.R., Brill M.S., Plomer B., Schmalz A., St Clair D.K., Naumann R., et al. // *Nat. Med.* 2014. V. 20. № 5. P. 555–560.
- Ouardouz M., Coderre E., Basak A., Chen A., Zamponi G.W., Hameed S., Rehak R., Yin X., Trapp B.D., Stys P.K. // *Ann. Neurol.* 2009. V. 65. № 2. P. 151–159.
- Yin H.Z., Hsu C.I., Yu S., Rao S.D., Sorkin L.S., Weiss J.H. // *Exp. Neurol.* 2012. V. 238. № 2. P. 93–102.
- Khayrullina G., Bermudez S., Byrnes K.R. // *J. Neuroinflammation.* 2015. V. 12. P. 172–182.
- von Leden R.E., Khayrullina G., Moritz K.E., Byrnes K.R. // *J. Neuroinflammation.* 2017. V. 14. № 1. P. 161–174.
- Goss J.R., Taffe K.M., Kochanek P.M., DeKosky S.T. // *Exp. Neurol.* 1997. V. 146. № 1. P. 291–294.
- Ren H., Chen X., Tian M., Zhou J., Ouyang H., Zhang Z. // *Adv. Sci.* 2018. V. 5. № 11. P. 1800529.
- Sutherland T.C., Mathews K.J., Mao Y., Nguyen T., Gorrie C.A. // *Front. Cell Neurosci.* 2017. V. 10. P. 310.
- Shohami E., Bass R., Wallach D., Yamin A., Gallily R. // *J. Cereb. Blood Metabol.* 1996. V. 16. № 3. P. 378–384.
- Yu W.R., Fehlings M.G. // *Acta Neuropathol.* 2011. V. 122. № 6. P. 747–761.
- Chen S., Ye J., Chen X., Shi J., Wu W., Lin W., Li Y., Fu H., Li S. // *J. Neuroinflammation.* 2018. V. 15. № 1. P. 150–163.
- Deng G., Gao Y., Cen Z., He J., Cao B., Zeng G., Zong S. // *Cell Biochem.* 2018. V. 50. № 2. P. 512–524.
- He J., Zhao J., Peng X., Shi X., Zong S., Zeng G. // *Cell Physiol. Biochem.* 2017. V. 44. № 3. P. 1224–1241.
- Beilerli O.A., Azizova S.H.T., Kononov N.A., Akhmedov A.D., Gareev I.F., Belogurov A.A. // *Voprosu neirohirurgii im. N.N. Burdenko.* 2020. V. 84. № 4. P. 104–110.
- Fu Q., Liu Y., Liu X., Zhang Q., Chen L., Peng J., Ao J., Li Y., Wang S., Song G., et al. // *Am. J. Transl. Res.* 2017. V. 9. № 9. P. 3950–3966.
- Cao Y., Wu T.D., Wu H., Lang Y., Li D.Z., Ni S.F., Lu H.B., Hu J.Z. // *Brain Res.* 2017. V. 1655. P. 55–65.
- Ujigo S., Kamei N., Hadoush H., Fujioka Y., Miyaki S., Nakasa T., Tanaka N., Nakanishi K., Eguchi A., Sunagawa T., et al. // *Spine.* 2014. V. 39. № 14. P. 1099–1107.
- Pineau I., Lacroix S. // *J. Comp. Neurol.* 2007. V. 500. № 2. P. 267–285.
- Yang L., Blumbergs P.C., Jones N.R., Manavis J., Sarvestani G.T., Ghabriel M.N. // *Spine.* 2004. V. 29. № 9. P. 966–971.
- Yang L., Jones N.R., Blumbergs P.C., van den Heuvel C., Moore E.J., Manavis J., Sarvestani G.T., Ghabriel M.N. // *J. Clin. Neurosci.* 2005. V. 12. № 3. P. 276–284.
- Saiwai H., Ohkawa Y., Yamada H., Kumamaru H., Harada A., Okano H., Yokomizo T., Iwamoto Y., Okada S. // *Am.*

- J. Pathol. 2010. V. 176. № 5. P. 2352–2366.
36. Yokota K., Saito T., Kobayakawa K., Kubota K., Hara M., Murata M., Ohkawa Y., Iwamoto Y., Okada S. // *Sci. Rep.* 2016. V. 6. P. 25673–25684.
37. Ankeny D.P., Guan Z., Popovich P.G. // *J. Clin. Invest.* 2009. V. 119. № 10. P. 2990–2999.
38. Beck K.D., Nguyen H.X., Galvan M.D., Salazar D.L., Woodruff T.M., Anderson A.J. // *Brain.* 2010. V. 133. Pt. 2. P. 433–447.
39. Raposo C., Graubardt N., Cohen M., Eitan C., London A., Berkutzki T., Schwartz M. // *J. Neurosci.* 2014. V. 34. № 31. P. 10141–10155.
40. Saiwai H., Kumamaru H., Ohkawa Y., Kubota K., Kobayakawa K., Yamada H., Yokomizo T., Iwamoto Y., Okada S. // *J. Neurochem.* 2013. V. 125. № 1. P. 74–88.
41. Kumamaru H., Saiwai H., Ohkawa Y., Yamada H., Iwamoto Y., Okada S. // *J. Cell Physiol.* 2012. V. 227. № 4. P. 1335–1346.
42. Nguyen D.H., Cho N., Satkunendrarajah K., Austin J.W., Wang J., Fehlings M.G. // *J. Neuroinflammation.* 2012. V. 9. P. 224–237.
43. Min K.J., Jeong H.K., Kim B., Hwang D.H., Shin H.Y., Nguyen A.T., Kim J.H., Jou I., Kim B.G., Joe E.H. // *J. Neuroinflammation.* 2012. V. 9. P. 100–112.
44. Smith P.D., Puskas F., Meng X., Lee J.H., Cleveland J.C. Jr., Weyant M.J., Fullerton D.A., Reece T.B. // *Circulation.* 2012. V. 126. № 11(1). P. 110–117.
45. Zhu P., Li J.X., Fujino M., Zhuang J., Li X.K. // *Mediators Inflamm.* 2013. V. 2013. P. 701970.
46. Akhmetzyanova E., Kletenkov K., Mukhamedshina Y., Rizvanov A. // *Front. Syst. Neurosci.* 2019. V. 13. P. 37–48.
47. Chu G.K., Yu W., Fehlings M.G. // *Neuroscience.* 2007. V. 148. № 3. P. 668–682.
48. Floriddia E.M., Rathore K.I., Tedeschi A., Quadrato G., Wuttke A., Lueckmann J.M., Kigerl K.A., Popovich P.G., Di Giovanni S. // *J. Neurosci.* 2012. V. 32. № 40. P. 13956–13970.
49. Horn K.P., Busch S.A., Hawthorne A.L., van Rooijen N., Silver J. // *J. Neurosci.* 2008. V. 28. № 38. P. 9330–9341.
50. Azam S., Jakaria M., Kim I.S., Kim J., Haque M.E., Choi D.K. // *Front. Immunol.* 2019. V. 10. P. 1000.
51. Kigerl K.A., Popovich P.G. // *Curr. Top Microbiol. Immunol.* 2009. V. 336. P. 121–136.
52. Hug H., Mohajeri M.H., La Fata G. // *Nutrients.* 2018. V. 10. № 2. P. 203.
53. Kawasaki T., Kawai T. // *Front. Immunol.* 2014. V. 5. P. 461.
54. Marinelli C., Di Liddo R., Facci L., Bertalot T., Conconi M.T., Zusso M., Skaper S.D., Giusti P. // *J. Neuroinflammation.* 2015. V. 12. P. 244.
55. Trudler D., Farfara D., Frenkel D. // *Mediators Inflamm.* 2010. V. 2010. P. 497987.
56. Lacagnina M.J., Watkins L.R., Grace P.M. // *Pharmacol. Ther.* 2018. V. 184. P. 145–158.
57. Heiman A., Pallottie A., Heary R.F., Elkabes S. // *Brain Behav. Immun.* 2014. V. 42. P. 232–245.
58. Lobenwein D., Tepekoylu C., Kozarin R. // *J. Am. Heart Assoc.* 2015. V. 4. № 10. e002440.
59. Roselli F., Chandrasekar A., Morganti-Kossmann M.C. // *Front. Neurol.* 2018. V. 9. P. 458.
60. Wang Y.Y., Shen D., Zhao L.J., Zeng N., Hu T.H. // *Biochem. Biophys. Res. Commun.* 2019. V. 517. № 4. P. 741–748.
61. Laginha I., Kopp M.A., Druschel C., Schaser K.D., Brommer B., Hellmann R.C., Watzlawick R., Ossami-Saidi R.R., Prüss H., Failli V., et al // *BMC Neurol.* 2016. V. 16. № 1. P. 170.
62. Xu L., Zhang Y., Zhang R., Zhang H., Song P., Ma T., Li Y., Wang X., Hou X., Li Q., et al. // *Int. Immunopharmacol.* 2019. V. 74. P. 105722.
63. Rust R., Kaiser J. // *J. Neurosci.* 2017. V. 37. № 18. P. 4658–4660.
64. Mittal A., Sagi V., Gupta M., Gupta K. // *Front. Cell Neurosci.* 2019. V. 13. P. 110–115.
65. Vanganswinkel T., Geurts N., Quanten K., Nelissen S., Lemmens S., Geboes L., Dooley D., Vidal P.M., Pejler G., Hendrix S. // *FASEB J.* 2016. V. 30. № 5. P. 2040–2057.
66. Nelissen S., Vanganswinkel T., Geurts N., Geboes L., Lemmens E., Vidal P.M., Lemmens S., Willems L., Boato F., Dooley D., et al // *Neurobiol. Dis.* 2014. V. 62. P. 260–272.
67. Hong J., Chang A., Zavvarian M.M., Wang J., Liu Y., Fehlings M.G. // *Int. J. Mol. Sci.* 2018. V. 19. № 8. P. 2167–2178.
68. Hong J., Chang A., Liu Y., Wang J., Fehlings M.G. // *Int. J. Mol. Sci.* 2019. V. 20. № 15. P. 3762.
69. Yuan X., Wu Q., Tang Y., Jing Y., Li Z., Xiu R. // *Life Sci.* 2019. V. 221. P. 47–55.
70. Rutz S., Ouyang W. // *Adv. Exp. Med. Biol.* 2016. V. 941. P. 89–116.
71. Rutz S., Ouyang W. // *Curr. Opin. Immunol.* 2011. V. 23. № 5. P. 605–612.
72. Lobo-Silva D., Carriche G.M., Castro A.G., Roque S., Saraiva M. // *J. Neuroinflammation.* 2016. V. 13. № 1. P. 297.
73. Tcibulkina V.N., Tcibulkin V.N. // *Allergology and immunology in pediatric.* 2017. № 2 (49). P. 4–11.
74. Sarbaeva N.N., Ponomareva Yu.V., Miliakova M.N. // *Genes and cells.* 2016. V. XI. № 1. P. 9–17.
75. Zhang Y., Gao Z., Wang D., Zhang T., Sun B., Mu L., Wang J., Liu Y., Kong Q., Liu X., et al. // *J. Neuroinflammation.* 2014. V. 11. P. 79.
76. Balmasova I.P., Shmeleva E.V., Eremina O.F., Dunda N.I. // *Allergology and immunology.* 2009. V. 10. № 2. P. 169.
77. Ferrante C.J., Leibovich S.J. // *Adv. Wound Care (New Rochelle).* 2012. V. 1. № 1. P. 10–16.
78. Balmasova I.P., Nestereva I.V., Malova E.S., Sepiashvili R.I. Structural and functional organization of the immune system. M.: Practical medicine, 2019. 72 p.
79. Chybenko V.A. // *Practical oncology.* 2016. V. 17. № 2. P. 99–109.
80. Fasching P., Stradner M., Graninger W., Dejaco C., Fessler J. // *Molecules.* 2017. V. 22. № 1. P. 134.
81. Rice T., Larsen J., Rivest S., Yong V.W. // *J. Neuropathol. Exp. Neurol.* 2007. V. 66. № 3. P. 184–195.
82. Irwin M.R., Cole S.W. // *Nat. Rev. Immunol.* 2011. V. 11. № 9. P. 625–632.
83. Schwab J.M., Zhang Y., Kopp M.A., Brommer B., Popovich P.G. // *Exp. Neurol.* 2014. V. 258. P. 121–129.
84. Zhou Y., Li N., Zhu L., Lin Y., Cheng H. // *Neuropsychiatr. Dis Treat.* 2018. V. 14. P. 2401–2413.
85. Zhang Y., Guan Z., Reader B., Shawler T., Mandrekar-Colucci S., Huang K., Weil Z., Bratasz A., Wells J., Powell N.D., et al. // *J. Neurosci.* 2013. V. 33. № 32. P. 12970–12981.
86. Moghaddam A., Child C., Bruckner T., Gerner H.J., Daniel V., Biglari B. // *Int. J. Mol. Sci.* 2015. V. 16. № 4. P. 7900–7916.
87. Sanz P., Garcia-Gimeno M.A. // *Int. J. Mol. Sci.* 2020. V. 21. № 11. P. 4096–4112.
88. Pekny M., Pekna M. // *Physiol. Rev.* 2014. V. 94. № 4. P. 1077–1098.
89. Alizadeh A., Santhosh K.T., Kataria H., Gounni A.S., Karimi-Abdolrezaee S. // *J. Neuroinflammation.* 2018. V. 15. № 1. P. 53–73.

REVIEWS

90. Monahan R., Stein A., Gibbs K., Bank M., Bloom O. // *Immunol. Res.* 2015. V. 63. № 1–3. P. 3–10.
91. Herman P., Stein A., Gibbs K., Korsunsky I., Gregersen P., Bloom O. // *J. Neurotrauma.* 2018. V. 35. № 15. P. 1819–1829.
92. Gensel J.C., Zhang B. // *Brain Res.* 2015. V. 1619. P. 1–11.
93. Ankeny D.P., Lucin K.M., Sanders V.M., McGaughy V.M., Popovich P.G. // *J. Neurochem.* 2006. V. 99. P. 1073–1087.
94. DeGiorgio L.A., Konstantinov K.N., Lee S.C., Hardin J.A., Volpe B.T., Diamond B. // *Nat. Med.* 2001. V. 7. № 11. P. 1189–1193.
95. Hauben E., Butovsky O., Nevo U., Yoels E., Moalem G., Agranov E., Mor F., Leibowitz-Amit R., Pevsner E., Akse-rod S., et al. // *J. Neurosci.* 2000. V. 20. № 17. P. 6421–6430.
96. Huang D.W., McKerracher L., Braun P.E., David S. // *Neuron.* 1999. V. 24. № 3. P. 639–647.
97. Kotter M.R., Li W.W., Zhao C., Franklin R.J. // *J. Neurosci.* 2006. V. 26. № 1. P. 328–332.
98. Taylor A.R., Welsh C.J., Young C., Spoor E., Kerwin S.C., Griffin J.F., Levine G.J., Cohen N.D., Levine J.M. // *J. Neurotrauma.* 2014. V. 31. № 18. P. 1561–1569.
99. Liu Y., Zhou L.J., Wang J., Li D., Ren W.J., Peng J., Wei X., Xu T., Xin W.J., Pang R.P., et al. // *J. Neurosci.* 2017. V. 37. № 4. P. 871–881.
100. Mirabelli E., Ni L., Li L., Acioglu C., Heary R.F., Elkabes S. // *J. Neuroinflammation.* 2019. V. 16. № 1. P. 207.
101. Bradbury E.J., Burnside E.R. // *Nat. Commun.* 2019. V. 10. P. 3879.
102. Telegin G.B., Minakov A.N., Chernov A.S., Manskikh V.N., Asyutin D.S., Konovalov N.A., Gabibov A.G. // *Acta Naturae.* 2019. V. 11. № 3(42). P. 75–81.
103. Sergeeva S.P., Erofeeva L.M., Gultiaev M.M., Balmasova I.P. // *Immunopathology, allergology, infectology.* 2010. № 3. P. 27–31.
104. Belogurov A.A., Ivanova O.M., Lomakin Y.A., Ziganshin R.X., Vaskina M.I., Knorre V.D., Klimova E.A., Gabibov A.G., Ivanov V.T., Govorun V.M. // *Biochemistry.* 2016. V. 81. № 11. P. 1540–1552.

Near-Infrared Activated Cyanine Dyes As Agents for Photothermal Therapy and Diagnosis of Tumors

E. I. Shramova^{1*}, A. B. Kotlyar², E. N. Lebedenko¹, S. M. Deyev^{1,3}, G. M. Proshkina¹

¹Shemyakin-Ovchinnikov Institute of Bioorganic Chemistry, Russian Academy of Sciences, Moscow, 117997 Russia

²Tel Aviv University, Ramat Aviv, Tel Aviv, 69978 Israel

³National Research Tomsk Polytechnic University, Tomsk, 634050 Russia

*E-mail: shramova.e.i@gmail.com

Received May 28, 2020; in final form, July 24, 2020

DOI: 10.32607/actanaturae.11028

Copyright © 2020 National Research University Higher School of Economics. This is an open access article distributed under the Creative Commons Attribution License, which permits unrestricted use, distribution, and reproduction in any medium, provided the original work is properly cited.

ABSTRACT Today, it has become apparent that innovative treatment methods, including those involving simultaneous diagnosis and therapy, are particularly in demand in modern cancer medicine. The development of nanomedicine offers new ways of increasing the therapeutic index and minimizing side effects. The development of photoactivatable dyes that are effectively absorbed in the first transparency window of biological tissues (700–900 nm) and are capable of fluorescence and heat generation has led to the emergence of phototheranostics, an approach that combines the bioimaging of deep tumors and metastases and their photothermal treatment. The creation of near-infrared (NIR) light-activated agents for sensitive fluorescence bioimaging and phototherapy is a priority in phototheranostics, because the excitation of drugs and/or diagnostic substances in the near-infrared region exhibits advantages such as deep penetration into tissues and a weak baseline level of autofluorescence. In this review, we focus on NIR-excited dyes and discuss prospects for their application in photothermal therapy and the diagnosis of cancer. Particular attention is focused on the consideration of new multifunctional nanoplatforams for phototheranostics which allow one to achieve a synergistic effect in combinatorial photothermal, photodynamic, and/or chemotherapy, with simultaneous fluorescence, acoustic, and/or magnetic resonance imaging.

KEYWORDS cyanines, near infrared, photothermal therapy.

ABBREVIATIONS BSA – bovine serum albumin; HSA – human serum albumin; ICG – indocyanine green; IR – infrared; PDT – photodynamic therapy; PEG – polyethylene glycol; PEI – polyethyleneimine; PLGA – polylactide glycolide; PTT – photothermal therapy; PTX – paclitaxel; RB – Rose Bengal; ROS – reactive oxygen species; UNP – upconverting nanoparticle.

INTRODUCTION

The phototherapy of tumors using organic compounds dates back to 1972, when experiments by I. Diamond and colleagues on rats showed the promise of hematoporphyrin as a powerful phototherapeutic agent for selective destruction of glioma cells [1]. Since then, a large number of organic compounds based on porphyrin, cyanine, and polymer dyes have been developed for phototherapy, some of which are used in medical practice today [2, 3].

This review is devoted to the use of organic infrared (IR) dyes as agents for the photothermal therapy and diagnosis of tumors. The theoretical aspects of phototherapy and the physicochemical properties of the agents used in phototherapy are described in detail in reviews [4–7].

Phototherapy is based on a selective destruction of tumor cells under the influence of light. Dyes absorb light and convert its energy into heat, thereby causing cell damage and death. Phototherapy with dyes

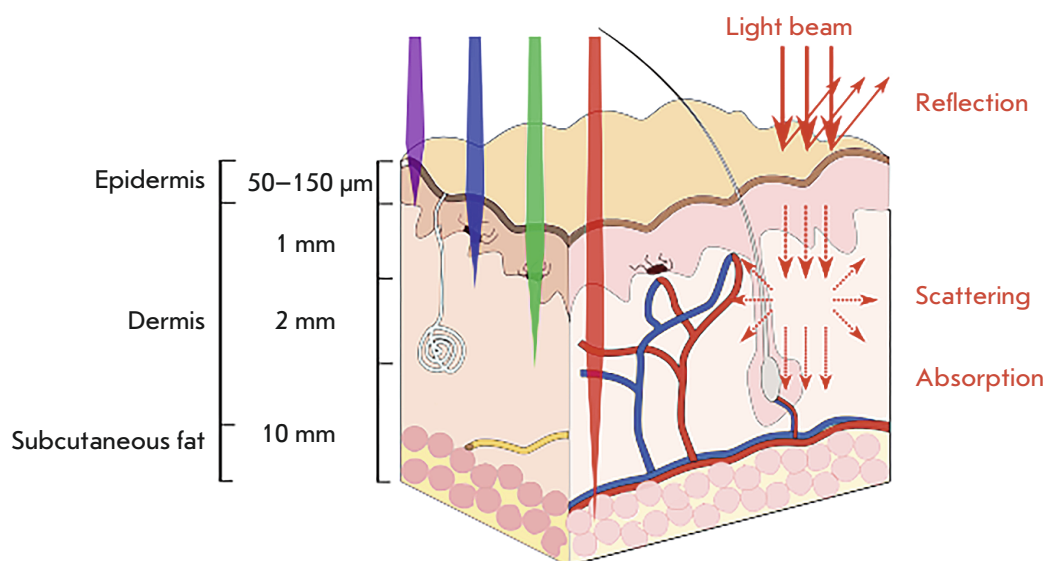


Fig. 1. Depth of light penetration of human tissues

includes photodynamic therapy (PDT) and photothermal therapy (PTT). In the case of PDT [7], light induces chemical reactions, the products of which have a negative effect on the vital activity of cells. In the case of PTT [8], the dye directly transforms light energy into heat, causing thermal damage to cells.

Due to the intense absorption of visible and ultraviolet light quanta by biological tissues (Fig. 1), phototherapy with light in an indicated range is used in clinical practice only to treat superficial tumors exposed to external light sources. It is known that proteins, nucleic acids, vitamins, and most cofactors efficiently absorb in the ultraviolet region of the spectrum; oxyhemoglobin, deoxyhemoglobin, and melanin intensively absorb in the visible region of the spectrum (400–650 nm). Therefore, the preferred excitation wavelengths in medicine (transparency window) are near-IR light in a range of 700–900 nm [4]. Light in a range of 900 to 1,100 nm cannot be used due to the strong absorption of water (Fig. 2).

Phototherapy has several obvious advantages, including non-invasiveness, ability to affect deep body tissues, small area and accuracy of irradiation, and regulation of the degree of tumor exposure via changing of the irradiation dose. In addition to these advantages, when using near-infrared light in phototherapy, the excitation light penetrates deeply into biological tissues and causes less background fluorescence; also, infrared dyes are characterized by extremely rare activation by visible light.

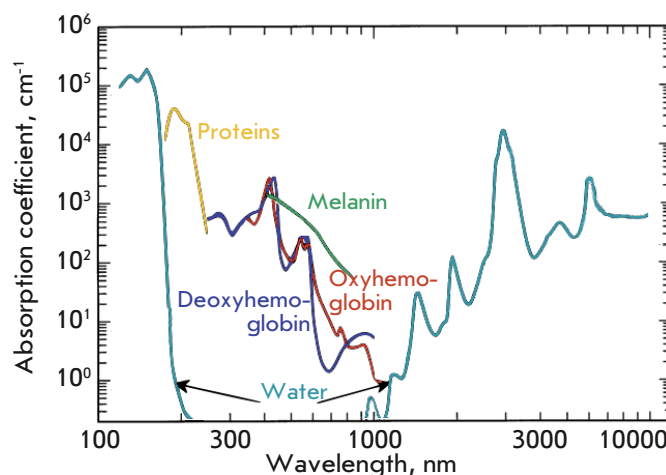


Fig. 2. Visible and infrared absorption spectra of biological tissues (adapted from [9])

In recent years, phototherapy has significantly advanced thanks to the use of lasers as light sources; nano-objects for the delivery of sensitizers [10–13]; targeted dyes [14, 15]; increased dye circulation time in the blood [16]; and sustained release of dyes [17]. Also, conjugation of dyes with immunoadjuvants is promising in photoimmunotherapy because it leads to the triggering of a systemic immune response [18].

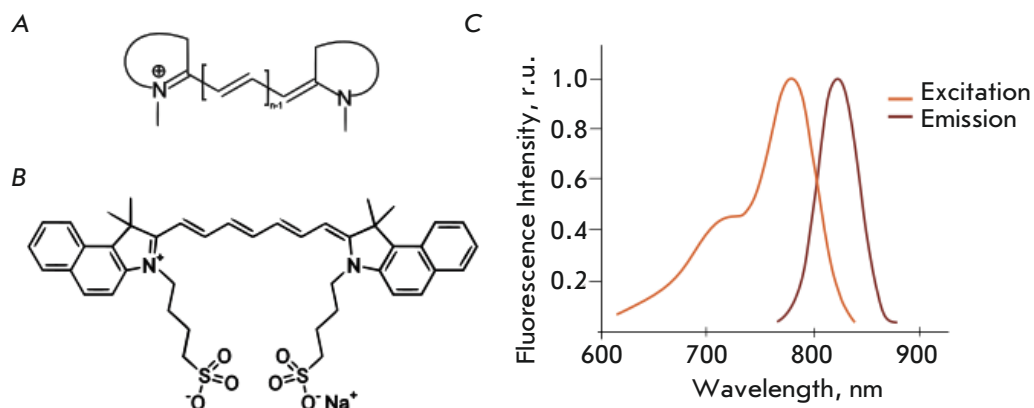


Fig. 3. General structure of cyanine dyes (A); structure of indocyanine green (ICG) (B); excitation and emission spectra of ICG (C)

Hypoxia is well known as a distinctive feature of solid tumors [19]. That is why the phototherapy of such tumors should use substances that act not photodynamically, but photothermally.

Today, PTT is a clinically approved technique that is used to treat patients with solid tumors of the liver, kidneys, lungs, adrenal glands, prostate, and bones [20]. An increase in the tumor temperature of up to 42°C renders cancer cells more susceptible to traditional treatment techniques (radiotherapy and chemotherapy), because an increase in temperature enhances the permeability of biological membranes and accelerates endocytosis and blood circulation [21]. An increase in tissue temperature to 45°C or above leads to necrosis of tumor cells [22].

In recent years, nanotechnology has been actively used to develop photothermal sensitizing agents, such as gold nanoparticles [23], gold nanorods [10], upconverting nanoparticles [14, 24–28], carbon nanotubes, graphene and its derivatives, and many others [8].

In biomedical imaging and phototherapy, organic dyes, thanks to their versatile photophysical properties and simplicity of large-scale synthesis, hold a special place among photoactivatable agents. Organic dyes can be conjugated to various specific biomolecules, which expands the range of their applications for therapy. The disadvantage of most dyes is their instability and rapid elimination from the bloodstream.

Photothermal agents should exhibit several basic properties, such as: 1) strong absorption in the near infrared region (extinction coefficients $> 1 \times 10^5 \text{ M}^{-1}\text{cm}^{-1}$); 2) biocompatibility and biodegradability; and 3) real-time imaging to control therapy [29]. Cyanine-based dyes, which are widely used in the phototherapy of tumors, fully possess these properties.

Cyanines are synthetic organic dyes (Fig. 3A) that are excited by infrared light (780–820 nm) and excellent for fluorescence imaging and phototherapy.

INDOCYANINE GREEN AND NANOSYSTEMS FOR ITS DELIVERY

Indocyanine green (ICG) (Fig. 3B, C) is a carbocyanine dye widely used in medical diagnostics [30]. Thanks to its spectral characteristics, this dye can be used as a contrast agent for optical imaging in angiography [31, 32], the biopsy of sentinel lymph nodes in breast cancer [33], assessment of blood plasma volume after cardiovascular surgery [34, 35], and evaluation of the functional reserves of the liver in hepatology [36]. Also, ICG is one of the least toxic contrast agents approved for use in medical practice [37]. The only known adverse reaction to ICG is anaphylactic shock in rare cases [38]. Under the action of an IR laser ($\lambda = 808 \text{ nm}$; radiation flux density, 155 W/cm^2), ICG converts most of the excitation energy into heat and, after 30 s of irradiation, causes local heating of the tissue to 75°C [39]. In this case, part of the energy is spent on the production of singlet oxygen, so ICG can be used for combined photothermal (PTT) and photodynamic therapy (PDT) [40].

After intratumoral injection, ICG was shown to accumulate well in tumor tissues and sentinel lymph nodes [41]. As shown in *in vitro* experiments, irradiated ICG induces the death of squamous cell carcinoma [42], colon cancer [43], and human pancreatic cancer [44] cells.

ICG has a low quantum yield of fluorescence [45, 46] and is susceptible to photobleaching, which limits its use in long-term bioimaging *in vivo* [39, 47, 48]. Many researchers have noted that ICG molecules

are oxidized and dimerized in an aqueous medium, which leads to decreased absorption of exciting light, reduced fluorescence, and a maximum absorption wavelength shift [30, 49, 50–55]. In addition, upon systemic administration, ICG cannot specifically accumulate in tumors because it quickly binds to blood plasma albumin and is rapidly excreted from the body (2–4 min) [49, 52, 56].

Various nanocarrier systems have been developed to increase the circulation time of ICG in the body. For example, to date, ICG-containing nanoparticles have been developed based on polymeric complexes [57, 58], peptides [59], proteins [60–62], micelles [63, 64], magnetic [65] and polylactide glycolide (PLGA) [66] particles. Encapsulation of the dye in PLGA particles improved the stability of ICG in water and increased its thermal stability [66]. Eight-hour incubation of PLGA particles under physiological conditions resulted in 78% dye leakage. To overcome this problem, silica polymer composite microcapsules were developed. This resulted in a 17% reduction in ICG leakage [39], but it required increasing the particle size to 1 μm . In addition, polymeric shells were found not to protect encapsulated dye molecules from dimerization or photoisomerization, as evidenced by an absorption peak wavelength shift to longer wavelengths [39, 67, 68] and a significant decrease in the fluorescence peak intensity [66]. The properties of encapsulated ICG molecules were improved by using organically modified silicates as carriers [69]; however, even in this case, the sizes of the produced particles were not small enough and amounted to about 100 nm, which corresponds to the upper size limit of the carriers used in *in vivo* experiments [70].

Several studies have proposed biodegradable calcium phosphate nanoparticles as ICG carriers for therapy and bioimaging [71–73]. The mean particle size in suspension is about 16 nm, and functionalization of the outer particle surface with carboxylate or polyethylene glycol (PEG) preserves the stability of the particles in physiological solutions for a long time and simultaneously preserves the high quantum yield and photostability of the dye. Upon intravenous administration, ICG-loaded particles coated with PEG were shown to accumulate, due to increased capillary permeability and impaired lymphatic drainage in tumor tissue, in xenografted tumors of model animals; in this case, the dye was detected *in vivo* within four days after its administration. In this case, the surface of the loaded nanoparticles can be functionalized with targeted antibodies to enhance the directed accumulation of particles in the tumor, which was demonstrated in breast tumors via targeting of the transferrin receptor CD71 [72]; pancreatic cancer

cells via targeting of the gastrin receptor [72]; and leukemia cells via targeting of the receptor tyrosine kinase CD117 and type I transmembrane glycoprotein CD96 [73].

The ICG–polyethyleneimine (PEI) complexes incorporated into silicon dioxide nanoparticles [74] had improved photophysical properties compared to those of the dye. The interaction with PEI prevented ICG aggregation and quenching of dye fluorescence, and it stopped dye leakage from the particles. The use of an ICG–PEI complex in combination with silicon nanoparticles enabled detection of IR signals at a depth of up to 2 cm from the body surface during bioimaging. The interaction between ICG and proteins changes the dye fluorescence parameters, a property used to create targeted IR probes. After binding to receptors and internalization, the dye dissociated from antibodies, which led to a restoration of the initial parameters of dye fluorescence. Targeted probes have been developed based on ICG complexes with daclizumab, trastuzumab, or panitumumab, which interact with interleukin-2 (CD25) receptors and human epidermal growth factor II and I (HER2 and HER1) receptors, respectively [75].

Targeted delivery of ICG into cells by lipid nanoparticles functionalized with folic acid molecules (*Fig. 4A*) is an alternative method for targeted delivery of a dye into cells [76]. These biocompatible particles were found to have good monodispersity, retain photostability, and to be characterized by a longer circulation time in the bloodstream compared to that of free ICG. *In vivo* experiments confirmed the targeted uptake of the described particles by the tumor, which makes lipid nanoparticles ideal agents for intravital bioimaging and early cancer diagnosis.

For bimodal phototherapy combining both PTT and PDT, a nanoplatform based on hybrid chitosan nanospheres with encapsulated gold nanorods and ICG was proposed (*Fig. 4B*) [77]. The hybrid nanospheres had a diameter of 180 nm and absorbed in a range of 650 to 900 nm. ICG inside the nanospheres was protected from rapid hydrolysis in biological fluids, which increased the dye's lifetime and its effect on the cells. Bimodal phototherapy demonstrated a high synergistic effect and improved the therapeutic efficacy of either ICG or gold nanorods alone. For example, after the irradiation of nanosphere-pretreated model animals with an IR laser, the tumor volume increased only 16-fold in mice of the experimental group and 58-fold in mice of the control group.

Tungsten oxide ($\text{W}_{18}\text{O}_{49}$) nanorods and ICG can also be used for bimodal phototherapy [78]. In such a design, tungsten oxide nanorods simultaneously act as an effective photothermal agent for PTT and as

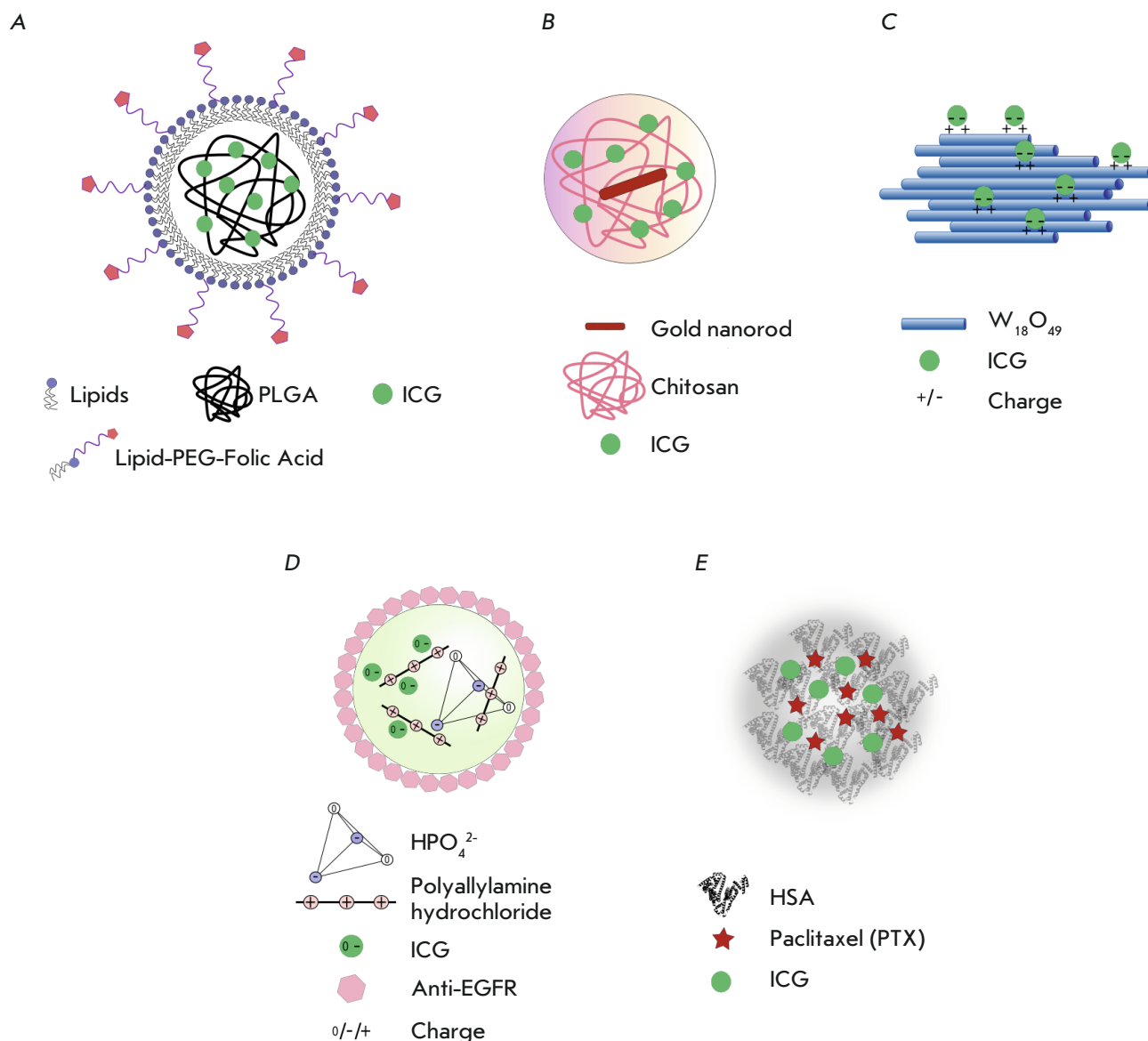


Fig. 4. Nanosystems for the delivery of ICG to tumor cells. **A** – folic acid-functionalized multilayer lipid nanoparticles loaded with ICG [76]; **B** – chitosan nanospheres with encapsulated gold nanorods and ICG [77]; **C** – wolfram oxide nanorods with surface-bound ICG [78]; **D** – polyallylamine hydrochloride–phosphoric acid salt nanospheres loaded with ICG and functionalized with anti-human epidermal growth factor receptor (EGFR) antibodies [57]; **E** – self-organized nanoparticles consisting of human serum albumin (HSA), paclitaxel (PTX), and ICG [79]

a nanocarrier that electrostatically binds ICG molecules on its surface (*Fig. 4C*). As in the case of gold nanorods, bimodal therapy triggered by irradiation of tungsten oxide nanorods was accompanied by increased lethality of HeLa cells compared to monomodal therapy (PTT or PDT alone). Experiments on animals have shown that tungsten nanorods with

bound dye molecules effectively destroy solid tumors when exposed to light (808 nm), thus demonstrating the high potential of these nanocomposites in tumor therapy.

The use of ICG spherical composite capsules consisting of polyallylamine hydrochloride molecules and orthophosphoric acid salts (*Fig. 4D*) for PTT was re-

ported in [57]. The capsule surface was functionalized with anti-human epidermal growth factor receptor (EGFR) antibodies targeting EGFR-positive cancer cells. In *in vitro* experiments, the irradiation of cells with an IR laser (808 nm) with an irradiation intensity of 6 W/cm² caused almost 100% death of cells treated with anti-EGFR nanocapsules loaded with ICG, while the death rate of cells treated with a free dye amounted to only 15%.

A nanotheranostic platform consisting of three clinically approved agents, human serum albumin (HSA), paclitaxel (PTX), and ICG, was developed for PTT and bioimaging (Fig. 4E) [79]. Mixing of HSA, PTX, and ICG molecules was shown to lead to the formation of stable 80 nm nanoparticles. In this system, HSA plays the role of a biocompatible carrier, PTX is an effective antitumor drug, and ICG acts both as a probe for fluorescence imaging and as a photothermal agent. These three-component nanoparticles (HSA-ICG-PTX) were shown to possess higher stability and a more extended lifetime in the bloodstream than the HSA-ICG complex. Moderate photothermal heating caused by irradiation of ICG with an IR laser increases the intracellular uptake of HSA-ICG-PTX, which enhances the cytotoxicity of the complex. *In vivo* experiments using intravital bioimaging have demonstrated that nanocomplexes efficiently accumulate in the primary tumor and lung metastases. In the case of subcutaneous tumors and metastases, therapy with three-component nanoparticles produces an excellent synergistic effect based on chemical and photothermal effects. The described theranostic nanoplatform, which consists of clinically approved agents, is very promising for both non-invasive detection of a disease focus and treatment of oncological diseases.

Targeted liposome particles loaded with a dye and superficially functionalized with folic acid [80] were successfully used to suppress MCF-7 human breast adenocarcinoma cells overexpressing folate receptors on their surface. These liposomal particles were shown to be effective in PTT *in vitro* and *in vivo*.

INDOCYANINE GREEN ANALOGS WITH IMPROVED PROPERTIES

Along with ICG, recent studies have used a number of dye analogs that are characterized by improved photo-optical properties and increased stability in biological media [81, 82] (Table, Fig. 5).

IR780, IR783, IR800, and IR808 dyes have been successfully used for bioimaging [86, 93–96]. IR780, IR783, and IR808 water-soluble dyes were found to preferentially accumulate in tumor cells *in vitro* and *in vivo*. However, like ICG, they are rapidly cleared from the bloodstream and are characterized by short

retention in the tumor, which limits the time window for phototherapy [97].

IRDye800CW (IR800) is a water-soluble analog of ICG. It is approved for clinical use and used for biomedical imaging and fluorescence surgery, a technique involving a fluorescent contrast agent to improve intraoperative tumor imaging [96, 98]. Conjugates of IR800 with various antibodies targeting growth factors and proteoglycans have been successfully used in preclinical and clinical trials for phototheranostics of brain tumors [96, 99–101], breast cancer [102], and head and neck cancer [103–105].

The use of highly efficient hydrophobic analogs of ICG required the development of systems for delivery of the dyes to the disease focus, based on various nanocarriers [106, 107]. For example, in 2017 [108], a phototheranostic nanoplatform based on a hydrophobic analog of ICG, IR775, was developed for bimodal therapy (PDT and PTT) in combination with real-time bioimaging. Water-insoluble IR775 was loaded into 40-nm biocompatible PEG-poly-caprolactone polymeric nanoparticles for delivery to tumors. Nanoparticle-encapsulated IR775 causes heating of a test liquid up to 55°C and triggers production of reactive oxygen species upon irradiation. *In vivo* experiments have shown that, after systemic administration, nanoparticle-encapsulated IR775 efficiently accumulates in cancerous tumors, produces a clear fluorescent signal upon IR irradiation, and leads to complete destruction of a tumor resistant to traditional chemotherapy after only a single session of combinatorial phototherapy.

For multimodal PTT with simultaneous fluorescence and photoacoustic imaging, a theranostic nanoplatform based on ferritin nanoparticles loaded with IR820, called “chameleon,” was developed [62]. The absorption spectrum of free IR820 contains a minor peak at 550 nm. Excitation of both the free and particle-encapsulated versions of the dye with a light source at 550 nm produced an emission with a maximum at 604 nm. Excitation of the dye at a main absorption peak wavelength (770 nm) resulted in an emission with a maximum at 834 nm. This property of IR820 enabled excitation of nanoparticles at 550 nm for fluorescence imaging and excitation with an IR laser at 808 nm for photoacoustic imaging and highly efficient PTT. Intravenous injection of nanoparticles to model animals, followed by low intensity (0.5 W/cm²) IR irradiation, resulted in complete disappearance of tumors without significant toxicity or relapses.

Combination therapy also uses upconverting nanoparticles (UCNPs) (Fig. 6A). To increase solubility and stability in physiological fluids, UCNPs were coated with bovine serum albumin (BSA). In this case, two

REVIEWS

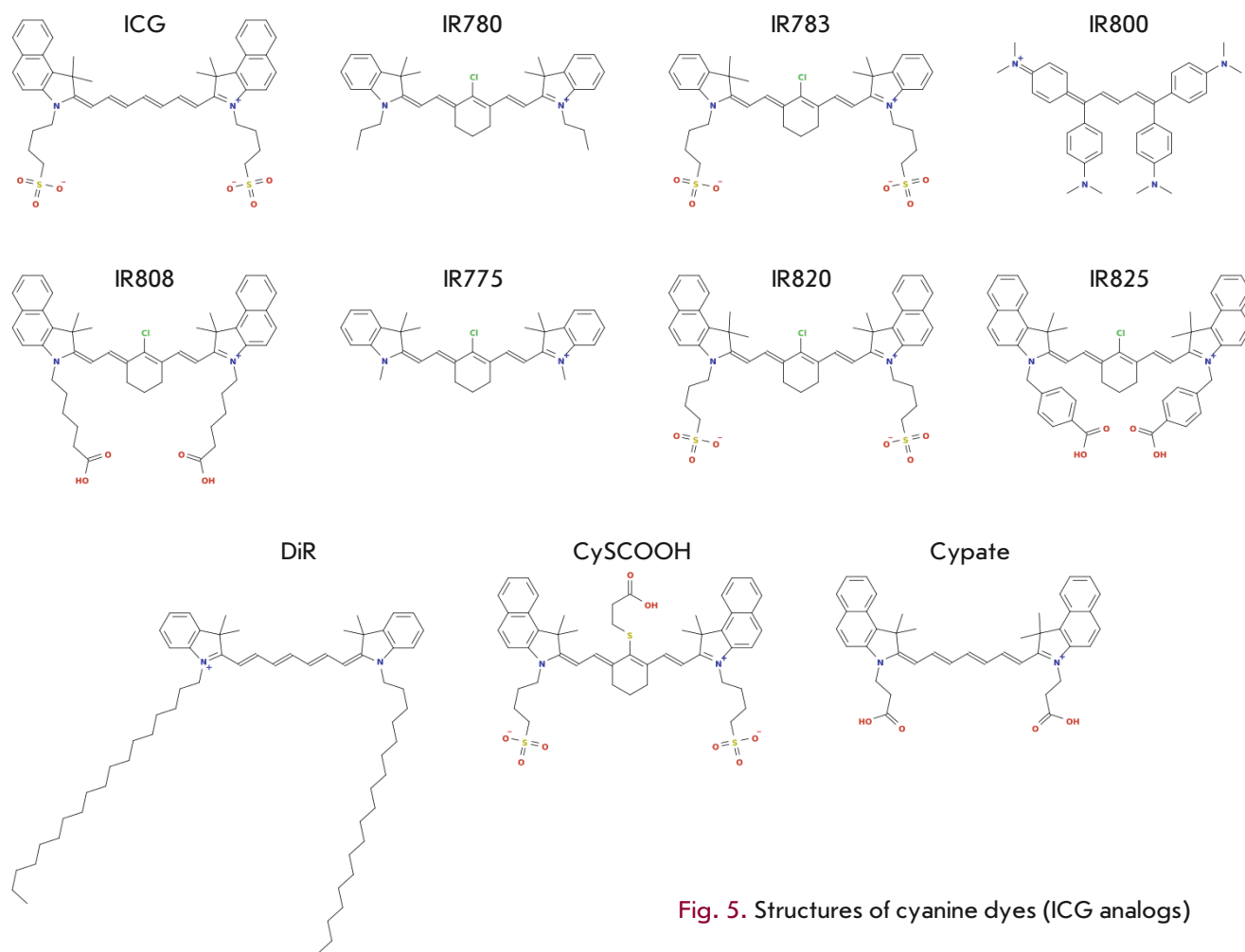


Fig. 5. Structures of cyanine dyes (ICG analogs)

Basic photophysical properties of ICG and its IR analogs

	IR dye	Absorption λ_{\max} , nm	Emission λ_{\max} , nm	Extinction coefficient, ϵ ($\times 10^5$ M ⁻¹ cm ⁻¹)	Quantum yield of singlet oxygen, %*	Quantum yield of fluorescence, %	Reference
1	ICG	785	822	2.04	0.8	7.8 ^M	[82]
2	IR780	780	798–823**	2.65	12.7	0.07–0.17%**	[83, 84]
3	IR783	783	804	1.17	3	4	[82]
4	IR800	774	794	2.40	N/D	9	[85]
5	IR808	783 ^M	816	3.00	N/D	5.9	[86, 87]
6	IR775	775 ^M	792	2.37	N/D	7	[88]
7	IR820	820	850	2.02	2	4.4	[82]
8	IR825	825 ^M	–	1.14	N/D	< 0.1 ^M	[89]
9	DiR	747 ^M	774 ^M	2.70	N/D	28	[90]
10	CySCOOH	820	840	N/D	N/D	N/D	[91]
11	Cypate	785	822	2.16	2	6.5	[92]

*Relative to Rose Bengali [82]; **depending on the solvent.
N/D – no data; M – in methanol.

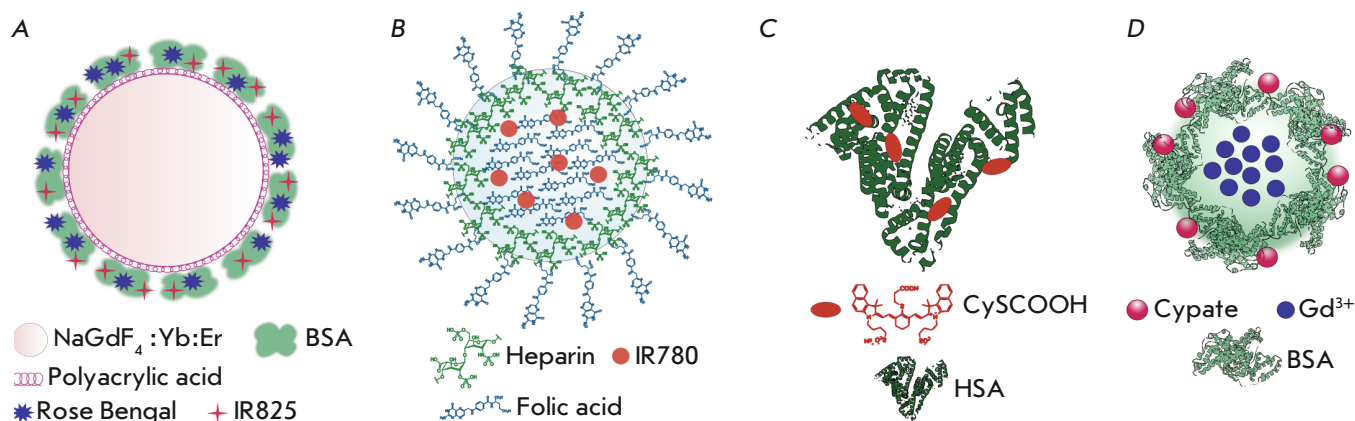


Fig. 6. Multifunctional platforms based on ICG dye analogs for phototheranostics. **A** – upconverting nanoparticles with bovine serum albumin (BSA) incorporating Rose Bengal and IR825 [109]; **B** – heparin and folic acid-based nanoparticles loaded with IR780 [58]; **C** – conjugates of human serum albumin (HSA) and CySCOOH [91]; **D** – gadolinium nanoparticles coated with a BSA-Cypate conjugate [113]

dyes, Rose Bengal (RB) absorbing at 560 nm and IR825 absorbing at 808 nm, were integrated directly into the protein coat of the BSA-UCNP complex [109]. When excited by a laser at 980 nm, UCNPs re-emit light in the green region of the spectrum, thereby exciting RB that, via the generation of ROS, exerts a photodynamic effect. The IR825 dye is excited by a laser at 808 nm and generates heat. The synergistic effect of the developed bimodal system was proven in *in vitro* and *in vivo* experiments.

On the basis of micelles loaded with the IR780 dye and radioactive isotope rhenium-188 (¹⁸⁸Re), a multifunctional platform was developed for PTT, fluorescence imaging, and single-photon emission tomography [110]. This platform enables real-time monitoring of the accumulation and distribution of micelles in the tumor, as well as the release kinetics of the drugs loaded into the micelles. In *in vivo* PTT experiments on model animals with xenograft tumors (rectal cancer), inhibition of tumor growth was achieved in 82.6% of the animals of the experimental group. A histopathological analysis revealed irreversible necrotic tissue damage, decreased proliferative activity, enhanced cell apoptosis, and increased expression of heat shock proteins in tumors treated by PTT.

Water-soluble heparin-folic acid nanoparticles (Fig. 6B) were shown to bind the water-insoluble dye IR780 [58]. Water-insoluble folic acid molecules form a hydrophobic core, with IR780 incorporated in the

particle center, while heparin molecules form a hydrophilic layer on the particle surface. A small fraction of folic acid molecules are located on the particle surface, forming an address for targeting tumor cells expressing the folate receptor. These particles exhibit good monodispersity, high stability, and specificity for folate-positive MCF-7 cells. *In vivo* experiments have demonstrated that folic acid-heparin particles not only exert a photothermal effect upon irradiation, but also serve as a tool to visualize the tumor focus.

Another iodinated analog of ICG, DiR (1,1-dioctadecyl-3,3,3,3-tetramethylindotricarbocyanine iodide) absorbing at 808 nm, was used for IR visualization and simultaneous photothermal ablation of breast cancer tumors and metastases [64]. The dye is passively delivered in polymeric nanoparticles to inflammatory foci. DiR possesses both photothermal and photodynamic properties: injection of the dye directly into a tumor, followed by irradiation, causes the destruction of cancer cells through the simultaneous generation of heat and reactive oxygen species by the dye [111].

The cyanine dye CySCOOH, which is produced by introducing a rigid cyclohexenyl ring into the heptamethine chain of ICG (Table and Fig. 5), conjugated with HSA (Fig. 6C), showed improved accumulation and longer retention in a tumor compared to the free dye CySCOOH. *In vitro* and *in vivo* experiments demon-

strated that the dye could be used for photoacoustic imaging, IR fluorescence bioimaging, and thermal therapy [91]. In *in vivo* experiments, complete photothermal tumor ablation was achieved with a single intravenous injection of the drug, followed by IR irradiation (808 nm, 1 W/cm², 5 min).

The carbocyanine dye Cypate is another cyanine dye that absorbs in the near IR region (~800 nm, *Table*) and exhibits photoacoustic and photothermal effects upon irradiation [81, 112]. Protein-coated gadolinium nanoparticles were used to deliver this dye (*Fig. 6D*) [113]. The dye molecules were covalently attached to the protein shell using a carbodiimide reaction. *In vivo* experiments demonstrated that these nanoparticles perfectly visualize the tumor focus by photoacoustic, magnetic resonance, and fluorescent imaging, passively accumulate in tumor cells, and cause complete photothermal tumor ablation after one phototherapy session.

CONCLUSION

Photothermal therapy of tumor neoplasms using near-infrared organic dyes is an actively developing and promising area of biomedicine. Thanks to the relatively low (compared to other photothermal agents) cost of the used dyes, their ability to passively accumulate in tumors, the possibility of housing them in a wide range of nanocarriers for active delivery (including targeted delivery), and thanks to the minimal invasiveness of the treatment and minor side effects in comparison with inorganic photothermal agents, organic dyes have been attracting increasing attention from researchers. To improve the biocompatibility and enhance the phototheranostic properties of indocyanine dyes, along with the development of new modifications of the dyes,

new methods for their delivery by nanoagents are being developed.

The ability of photoactivated dyes for multimodal imaging, e.g., simultaneous infrared fluorescence and photoacoustic imaging, makes them choice agents for cancer phototheranostics. An area of growth in this research field is the development of multifunctional nanoplatforms that combine the ability, when irradiated, not only to fluoresce, but also to exhibit photothermal and/or photodynamic properties. The multimodal nanoplatforms described in this review enable not only therapy that combines different therapeutic approaches leading to impressive synergistic effects, but also simultaneous visualization of disease foci, as well as non-invasive monitoring of the response to treatment.

The particular attention of researchers is focused on the development of targeted drugs that can minimize the adverse toxicity and side effects of cancer therapy. At present, this direction is rapidly developing not only thanks to the use of traditional antibodies, but also thanks to new targeted non-immunoglobulin scaffolds (affibodies, anticalins, designed ankyrin repeat proteins, etc.).

In the opinion of these authors, the development of similar multimodal theranostic nanoplatforms will represent the leading edge of experimental oncology, enabling solutions to the most vexing problems of non-invasive diagnostics, highly effective precision treatment, and real-time monitoring of treatment efficacy. ●

This study was supported by a Russian Foundation for Basic Research grant No. 19-54-06001 “Development of new technologies for specific destruction of cancer cells and tumors”.

REFERENCES

1. Diamond I., Mcdonagh Antony F., Wilson Charles B., Granelli Steven G., Nielsen S., Jaenicke R. // *Lancet*. 1972. V. 300. № 7788. P. 1175–1177.
2. Lucky S.S., Soo K.C., Zhang Y. // *Chem. Rev.* 2015. V. 115. № 4. P. 1990–2042.
3. Zhang P., Hu C., Ran W., Meng J., Yin Q., Li Y. // *Theranostics*. 2016. V. 6. № 7. P. 948–968.
4. Plaetzer K., Krammer B., Berlanda J., Berr F., Kiesslich T. // *Lasers Med. Sci.* 2009. V. 24. № 2. P. 259–268.
5. Wilson B.C., Patterson M.S. // *Phys. Med. Biol.* 2008. V. 53. № 9. P. R61–R109.
6. Fan W., Huang P., Chen X. // *Chem. Soc. Rev.* 2016. V. 45. № 23. P. 6488–6519.
7. Agostinis P., Berg K., Cengel K.A., Foster T.H., Girotti A.W., Gollnick S.O., Hahn S.M., Hamblin M.R., Juzeniene A., Kessel D., et al. // *CA. Cancer J. Clin.* 2011. V. 61. № 4. P. 250–281.
8. Zhang H., Chen G., Yu B., Cong H. // *Rev. Adv. Mater. Sci.* 2018. V. 53. № 2. P. 131–146.
9. Vogel A., Venugopalan V. // *Chem. Rev.* 2003. V. 103. № 2. P. 577–644.

10. Proshkina G., Deyev S., Ryabova A., Tavanti F., Menziani M.C., Cohen R., Katrivas L., Kotlyar A. // *ACS Appl. Mater. Interfaces*. 2019. V. 11. № 38. P. 34645–34651.
11. Shipunova V.O., Zelepukin I.V., Stremovskiy O.A., Nikitin M.P., Care A., Sunna A., Zvyagin A.V., Deyev S.M. // *ACS Appl. Mater. Interfaces*. 2018. V. 10. № 20. P. 17437–17447.
12. Shipunova V.O., Kotelnikova P.A., Aghayeva U.F., Stremovskiy O.A., Novikov I.A., Schulga A.A., Nikitin M.P., Deyev S.M. // *J. Magn. Magn. Mater.* 2019. V. 469. P. 450–455.
13. Belova M.M., Shipunova V.O., Kotelnikova P.A., Babenyshv A.V., Rogozhin E.A., Cherednichenko M.Yu., Deyev S.M. // *Acta Naturae*. 2019. V. 11. № 2. P. 47–53.
14. Guryev E.L., Volodina N.O., Shilyagina N.Y., Gudkov S.V., Balalaeva I.V., Volovetskiy A.B., Lyubeshkin A.V., Sen' A.V., Ermilov S.A., Vodeneev V.A., et al. // *Proc. Natl. Acad. Sci. USA*. 2018. V. 115. № 39. P. 9690–9695.
15. Shilova O.N., Deyev S.M. // *Acta Naturae*. 2019. V. 11. № 4. P. 42–53.
16. Zelepukin I.V., Yaremenko A.V., Shipunova V.O., Babenyshv A.V., Balalaeva I.V., Nikitin P.I., Deyev S.M., Nikitin M.P. // *Nanoscale*. 2019. V. 11. № 4. P. 1636–1646.
17. Pekkanen A.M., Dewitt M.R., Rylander M.N. // *J. Biomed. Nanotechnol.* 2014. V. 10. № 9. P. 1677–1712.
18. Chen W.R., Huang Z., Korbelik M., Nordquist R.E., Liu H. // *J. Environ. Pathol. Toxicol. Oncol.* 2006. V. 25. № 1–2. P. 281–292.
19. Harris A.L. // *Nat. Rev. Cancer*. 2002. V. 2. № 1. P. 38–47.
20. Huang H.-W., Liauh C.-T. // *J. Med. Biol. Eng.* 2012. V. 32. № 1. P. 1.
21. Hong G., Wu J.Z., Robinson J.T., Wang H., Zhang B., Dai H. // *Nat. Commun.* 2012. V. 3. № 1. P. 700.
22. Hildebrandt B. // *Crit. Rev. Oncol. Hematol.* 2002. V. 43. № 1. P. 33–56.
23. Deyev S., Proshkina G., Ryabova A., Tavanti F., Menziani M.C., Eidelshstein G., Avishai G., Kotlyar A. // *Bioconjug. Chem.* 2017. V. 28. № 10. P. 2569–2574.
24. Grebenik E.A., Generalova A.N., Nechaev A.V., Khaydukov E.V., Mironova K.E., Stremovskiy O.A., Lebedenko E.N., Zvyagin A.V., Deyev S.M. // *Acta Naturae*. 2014. V. 6. № 4. P. 48–53.
25. Grebenik E.A., Kostyuk A.B., Deyev S.M. // *Russ. Chem. Rev.* 2016. V. 85. № 12. P. 1277–1296.
26. Guryev E.L., Shilyagina N.Y., Kostyuk A.B., Sencha L.M., Balalaeva I.V., Vodeneev V.A., Kutova O.M., Lyubeshkin A.V., Yakubovskaya R.I., Pankratov A.A., et al. // *Toxicol. Sci.* 2019. V. 170. № 1. P. 123–132.
27. Mironova K.E., Khochenkov D.A., Generalova A.N., Rocheva V.V., Sholina N.V., Nechaev A.V., Semchishen V.A., Deyev S.M., Zvyagin A.V., Khaydukov E.V. // *Nanoscale*. 2017. V. 9. № 39. P. 14921–14928.
28. Khaydukov E.V., Mironova K.E., Semchishen V.A., Generalova A.N., Nechaev A.V., Khochenkov D.A., Stepanova E.V., Lebedev O.I., Zvyagin A.V., Deyev S.M., et al. // *Sci. Rep.* 2016. V. 6. № 1. P. 35103.
29. Melancon M.P., Zhou M., Li C. // *Acc. Chem. Res.* 2011. V. 44. № 10. P. 947–956.
30. Landsman M.L., Kwant G., Mook G.A., Zijlstra W.G. // *J. Appl. Physiol.* 1976. V. 40. № 4. P. 575–583.
31. Schutt F., Fischer J., Kopitz J., Holz F.G. // *Clin. Exp. Ophthalmol.* 2002. V. 30. № 2. P. 110–114.
32. Benson R.C., Kues H.A. // *Phys. Med. Biol.* 1978. V. 23. № 1. P. 159–163.
33. Motomura K., Inaji H., Komoike Y., Kasugai T., Noguchi S., Koyama H. // *Jpn. J. Clin. Oncol.* 1999. V. 29. № 12. P. 604–607.
34. Ishihara H., Okawa H., Iwakawa T., Umegaki N., Tsubo T., Matsuki A. // *Anesth. Analg.* 2002. V. 94. № 4. P. 781–786.
35. Ott P. // *Pharmacol. Toxicol.* 1998. V. 83. P. 1–48.
36. Sakka S.G. // *J. Clin. Monit. Comput.* 2018. V. 32. № 5. P. 787–796.
37. Frangioni J. // *Curr. Opin. Chem. Biol.* 2003. V. 7. № 5. P. 626–634.
38. Olsen T.W. // *Arch. Ophthalmol.* 1996. V. 114. № 1. P. 97.
39. Yu J., Yaseen M.A., Anvari B., Wong M.S. // *Chem. Mater.* 2007. V. 19. № 6. P. 1277–1284.
40. Chen W.R., Adams R.L., Higgins A.K., Bartels K.E., Nordquist R.E. // *Cancer Lett.* 1996. V. 98. № 2. P. 169–173.
41. Li X., Beauvoit B., White R., Nioka S., Chance B., Yodh A.G. // *Optical tomography, photon migration, and spectroscopy of tissue and model media: Theory, human studies, and instrumentation / Eds Chance B., Alfano R.R.* SPIE, 1995. V. 2389. P. 789–797.
42. Abels C., Fickweiler S., Weiderer P., Bäuml W., Hofstädter F., Landthaler M., Szeimies R.-M. // *Arch. Dermatol. Res.* 2000. V. 292. № 8. P. 404–411.
43. Bäuml W., Abels C., Karrer S., Weiß T., Messmann H., Landthaler M., Szeimies R.-M. // *Br. J. Cancer.* 1999. V. 80. № 3–4. P. 360–363.
44. Tseng W.W., Saxton R.E., Deganutti A., Liu C.D. // *Pancreas*. 2003. V. 27. № 3. P. e42–e45.
45. Philip R., Penzkofer A., Bäuml W., Szeimies R.M., Abels C. // *J. Photochem. Photobiol. Chem.* 1996. V. 96. № 1–3. P. 137–148.
46. Soper S.A., Mattingly Q.L. // *J. Am. Chem. Soc.* 1994. V. 116. № 9. P. 3744–3752.
47. Sevcik-Muraca E.M., Houston J.P., Gurfinkel M. // *Curr. Opin. Chem. Biol.* 2002. V. 6. № 5. P. 642–650.
48. Yan J., Estévez M.C., Smith J.E., Wang K., He X., Wang L., Tan W. // *Nano Today*. 2007. V. 2. № 3. P. 44–50.
49. Desmettre T., Devoisselle J.M., Mordon S. // *Surv. Ophthalmol.* 2000. V. 45. № 1. P. 15–27.
50. Gathje J., Steuer R.R., Nicholes K.R. // *J. Appl. Physiol.* 1970. V. 29. № 2. P. 181–185.
51. Holzer W., Mauerer M., Penzkofer A., Szeimies R.-M., Abels C., Landthaler M., Bäuml W. // *J. Photochem. Photobiol. B*. 1998. V. 47. № 2–3. P. 155–164.
52. Mordon S., Devoisselle J.M., Soulie-Begu S., Desmettre T. // *Microvasc. Res.* 1998. V. 55. № 2. P. 146–152.
53. Maarek J.-M.I., Holschneider D.P., Harimoto J. // *J. Photochem. Photobiol. B*. 2001. V. 65. № 2–3. P. 157–164.
54. Zhang Y., Wang M. // *Mater. Lett.* 2000. V. 42. № 1–2. P. 86–91.
55. Saxena V., Sadoqi M., Shao J. // *J. Pharm. Sci.* 2003. V. 92. № 10. P. 2090–2097.
56. Muckle T.J. // *Biochem. Med.* 1976. V. 15. № 1. P. 17–21.
57. Yu J., Javier D., Yaseen M.A., Nitin N., Richards-Kortum R., Anvari B., Wong M.S. // *J. Am. Chem. Soc.* 2010. V. 132. № 6. P. 1929–1938.
58. Yue C., Liu P., Zheng M., Zhao P., Wang Y., Ma Y., Cai L. // *Biomaterials*. 2013. V. 34. № 28. P. 6853–6861.
59. Huang P., Gao Y., Lin J., Hu H., Liao H.-S., Yan X., Tang Y., Jin A., Song J., Niu G., et al. // *ACS Nano*. 2015. V. 9. № 10. P. 9517–9527.
60. Sheng Z., Hu D., Zheng M., Zhao P., Liu H., Gao D., Gong P., Gao G., Zhang P., Ma Y., et al. // *ACS Nano*. 2014. V. 8. № 12. P. 12310–12322.
61. Chen Q., Liang C., Wang X., He J., Li Y., Liu Z. // *Biomaterials*. 2014. V. 35. № 34. P. 9355–9362.
62. Huang P., Rong P., Jin A., Yan X., Zhang M.G., Lin J., Hu

- H., Wang Z., Yue X., Li W., et al. // *Adv. Mater.* 2014. V. 26. № 37. P. 6401–6408.
63. Zheng M., Yue C., Ma Y., Gong P., Zhao P., Zheng C., Sheng Z., Zhang P., Wang Z., Cai L. // *ACS Nano.* 2013. V. 7. № 3. P. 2056–2067.
64. He X., Bao X., Cao H., Zhang Z., Yin Q., Gu W., Chen L., Yu H., Li Y. // *Adv. Funct. Mater.* 2015. V. 25. № 19. P. 2831–2839.
65. Ma Y., Tong S., Bao G., Gao C., Dai Z. // *Biomaterials.* 2013. V. 34. № 31. P. 7706–7714.
66. Saxena V., Sadoqi M., Shao J. // *J. Photochem. Photobiol. B.* 2004. V. 74. № 1. P. 29–38.
67. Gomes A.J., Lunardi L.O., Marchetti J.M., Lunardi C.N., Tedesco A.C. // *Photomed. Laser Surg.* 2006. V. 24. № 4. P. 514–521.
68. Rodriguez V.B., Henry S.M., Hoffman A.S., Stayton P.S., Li X., Pun S.H. // *J. Biomed. Opt.* 2008. V. 13. № 1. P. 014025.
69. Kim G., Huang S.-W., Day K.C., O'Donnell M., Agayan R.R., Day M.A., Kopelman R., Ashkenazi S. // *J. Biomed. Opt.* 2007. V. 12. № 4. P. 044020.
70. Goldberg M., Langer R., Jia X. // *J. Biomater. Sci. Polym. Ed.* 2007. V. 18. № 3. P. 241–268.
71. Altinoğlu E.I., Russin T.J., Kaiser J.M., Barth B.M., Eklund P.C., Kester M., Adair J.H. // *ACS Nano.* 2008. V. 2. № 10. P. 2075–2084.
72. Barth B.M., Sharma R., Altinoğlu E.İ., Morgan T.T., Shanmugavelandy S.S., Kaiser J.M., McGovern C., Matters G.L., Smith J.P., Kester M., et al. // *ACS Nano.* 2010. V. 4. № 3. P. 1279–1287.
73. Barth B.M., Altinoğlu E., Shanmugavelandy S.S., Kaiser J.M., Crespo-Gonzalez D., DiVittore N.A., McGovern C., Goff T.M., Keasey N.R., Adair J.H., et al. // *ACS Nano.* 2011. V. 5. № 7. P. 5325–5337.
74. Quan B., Choi K., Kim Y.-H., Kang K.W., Chung D.S. // *Talanta.* 2012. V. 99. P. 387–393.
75. Ogawa M., Kosaka N., Choyke P.L., Kobayashi H. // *Cancer Res.* 2009. V. 69. № 4. P. 1268–1272.
76. Zheng C., Zheng M., Gong P., Jia D., Zhang P., Shi B., Sheng Z., Ma Y., Cai L. // *Biomaterials.* 2012. V. 33. № 22. P. 5603–5609.
77. Chen R., Wang X., Yao X., Zheng X., Wang J., Jiang X. // *Biomaterials.* 2013. V. 34. № 33. P. 8314–8322.
78. Deng K., Hou Z., Deng X., Yang P., Li C., Lin J. // *Adv. Funct. Mater.* 2015. V. 25. № 47. P. 7280–7290.
79. Chen Q., Liang C., Wang C., Liu Z. // *Adv. Mater.* 2015. V. 27. № 5. P. 903–910.
80. Zheng M., Zhao P., Luo Z., Gong P., Zheng C., Zhang P., Yue C., Gao D., Ma Y., Cai L. // *ACS Appl. Mater. Interfaces.* 2014. V. 6. № 9. P. 6709–6716.
81. Luo S., Zhang E., Su Y., Cheng T., Shi C. // *Biomaterials.* 2011. V. 32. № 29. P. 7127–7138.
82. James N.S., Chen Y., Joshi P., Ohulchanskyy T.Y., Ethirajan M., Henary M., Strekowski L., Pandey R.K. // *Theranostics.* 2013. V. 3. № 9. P. 692–702.
83. Singh A.K., Hahn M.A., Gutwein L.G., Rule M.C., Knapik J.A., Moudgil B.M., Grobmyer S.R., Brown S.C. // *Int. J. Nanomedicine.* 2012. V. 7. P. 2739–2750.
84. Alves C.G., Lima-Sousa R., de Melo-Diogo D., Louro R.O., Correia I.J. // *Int. J. Pharm.* 2018. V. 542. № 1–2. P. 164–175.
85. Marshall M.V., Draney D., Sevick-Muraca E.M., Olive D.M. // *Mol. Imaging Biol.* 2010. V. 12. № 6. P. 583–594.
86. Tan X., Luo S., Wang D., Su Y., Cheng T., Shi C. // *Biomaterials.* 2012. V. 33. № 7. P. 2230–2239.
87. Deng G., Li S., Sun Z., Li W., Zhou L., Zhang J., Gong P., Cai L. // *Theranostics.* 2018. V. 8. № 15. P. 4116–4128.
88. Strehmel B., Schmitz C., Kütahya C., Pang Y., Drewitz A., Mustroph H. // *Beilstein J. Org. Chem.* 2020. V. 16. P. 415–444.
89. Cheng L., He W., Gong H., Wang C., Chen Q., Cheng Z., Liu Z. // *Adv. Funct. Mater.* 2013. V. 23. № 47. P. 5893–5902.
90. Texier I., Goutayer M., Da Silva A., Guyon L., Djaker N., Josserand V., Neumann E., Bibette J., Vinet F. // *J. Biomed. Opt.* 2009. V. 14. № 5. P. 054005.
91. Rong P., Huang P., Liu Z., Lin J., Jin A., Ma Y., Niu G., Yu L., Zeng W., Wang W., et al. // *Nanoscale. Royal Soc. Chem.,* 2015. V. 7. № 39. P. 16330–16336.
92. Achilefu S., Dorshow R.B., Bugaj J.E., Rajagopalan R. // *Invest. Radiol.* 2000. V. 35. № 8. P. 479–485.
93. Zhang C., Liu T., Su Y., Luo S., Zhu Y., Tan X., Fan S., Zhang L., Zhou Y., Cheng T., et al. // *Biomaterials.* 2010. V. 31. № 25. P. 6612–6617.
94. Yang X., Shi C., Tong R., Qian W., Zhou H.E., Wang R., Zhu G., Cheng J., Yang V.W., Cheng T., et al. // *Clin. Cancer Res.* 2010. V. 16. № 10. P. 2833–2844.
95. Luo S., Tan X., Qi Q., Guo Q., Ran X., Zhang L., Zhang E., Liang Y., Weng L., Zheng H., et al. // *Biomaterials.* 2013. V. 34. № 9. P. 2244–2251.
96. Miller S.E., Tummers W.S., Teraphongphom N., van den Berg N.S., Hasan A., Ertsey R.D., Nagpal S., Recht L.D., Plowey E.D., Vogel H., et al. // *J. Neurooncol.* 2018. V. 139. № 1. P. 135–143.
97. Haugland R.P. *Handbook of fluorescent probes and research products.* 9. ed. Eugene, Or.: Molecular Probes, Inc, 2002.
98. van Keulen S., Nishio N., Fakurnejad S., Birkeland A., Martin B.A., Lu G., Zhou Q., Chirita S.U., Forouzanfar T., Colevas A.D., et al. // *J. Nucl. Med.* 2019. V. 60. № 6. P. 758–763.
99. Warram J.M., de Boer E., Korb M., Hartman Y., Kovar J., Markert J.M., Gillespie G.Y., Rosenthal E.L. // *Br. J. Neurosurg.* 2015. V. 29. № 6. P. 850–858.
100. Kovar J.L., Curtis E., Othman S.F., Simpson M.A., Michael Olive D. // *Anal. Biochem.* 2013. V. 440. № 2. P. 212–219.
101. Polikarpov D.M., Campbell D.H., McRobb L.S., Wu J., Lund M.E., Lu Y., Deyev S.M., Davidson A.S., Walsh B.J., Zvyagin A.V., et al. // *Cancers.* 2020. V. 12. № 4. P. 984.
102. Sampath L., Kwon S., Ke S., Wang W., Schiff R., Mawad M.E., Sevick-Muraca E.M. // *J. Nucl. Med.* 2007. V. 48. № 9. P. 1501–1510.
103. Heath C.H., Deep N.L., Beck L.N., Day K.E., Sweeny L., Zinn K.R., Huang C.C., Rosenthal E.L. // *Otolaryngol. Neck Surg.* 2013. V. 148. № 6. P. 982–990.
104. Rosenthal E.L., Warram J.M., de Boer E., Chung T.K., Korb M.L., Brandwein-Gensler M., Strong T.V., Schmalbach C.E., Morlandt A.B., Agarwal G., et al. // *Clin. Cancer Res.* 2015. V. 21. № 16. P. 3658–3666.
105. Zinn K.R., Korb M., Samuel S., Warram J.M., Dion D., Killingsworth C., Fan J., Schoeb T., Strong T.V., Rosenthal E.L. // *Mol. Imaging Biol.* 2015. V. 17. № 1. P. 49–57.
106. Mérian J., Gravier J., Navarro F., Texier I. // *Molecules.* 2012. V. 17. № 5. P. 5564–5591.
107. Yuan A., Wu J., Tang X., Zhao L., Xu F., Hu Y. // *J. Pharm. Sci.* 2013. V. 102. № 1. P. 6–28.
108. Duong T., Li X., Yang B., Schumann C., Albarqi H.A., Taratula O. // *Nanomed. Nanotechnol. Biol. Med.* 2017. V. 13. № 3. P. 955–963.
109. Chen Q., Wang C., Cheng L., He W., Cheng Z., Liu Z. // *Biomaterials.* 2014. V. 35. № 9. P. 2915–2923.
110. Peng C.-L., Shih Y.-H., Lee P.-C., Hsieh T.M.-H., Luo T.-

REVIEWS

- Y., Shieh M.-J. // ACS Nano. 2011. V. 5. № 7. P. 5594–5607.
111. Cao J., Chi J., Xia J., Zhang Y., Han S., Sun Y. // ACS Appl. Mater. Interfaces. 2019. V. 11. № 29. P. 25720–25729.
112. Yang H., Mao H., Wan Z., Zhu A., Guo M., Li Y., Li X., Wan J., Yang X., Shuai X., et al. // Biomaterials. 2013. V. 34. № 36. P. 9124–9133.
113. Wang Y., Yang T., Ke H., Zhu A., Wang Y., Wang J., Shen J., Liu G., Chen C., Zhao Y., et al. // Adv. Mater. 2015. V. 27. № 26. P. 3874–3882.

Preclinical Studies of Immunogenicity, Protectivity, and Safety of the Combined Vector Vaccine for Prevention of the Middle East Respiratory Syndrome

I. V. Dolzhikova¹, D. M. Grousova¹, O. V. Zubkova¹, A. I. Tikhvatulin¹, A. V. Kovyrshina¹, N. L. Lubenets¹, T. A. Ozharovskaia¹, O. Popova¹, I. B. Esmagambetov¹, D. V. Shcheblyakov¹, I. M. Evgrafova¹, A. A. Nedorubov³, I. V. Gordeichuk^{1,2,3}, S. A. Gulyaev³, A. G. Botikov¹, L. V. Panina¹, D. V. Mishin¹, S. Y. Loginova⁴, S. V. Borisevich⁴, P. G. Deryabin¹, B. S. Naroditsky^{1,2}, D. Y. Logunov^{1*}, A. L. Gintsburg^{1,2}

¹N.F. Gamaleya National Research Center for Epidemiology and Microbiology of the Ministry of Health of the Russian Federation, Moscow, 123098 Russia

²I.M. Sechenov Institute of Evolutionary Physiology and Biochemistry of the Russian Academy of Sciences, Moscow, 119435 Russia

³M.P. Chumakov Federal Scientific Center for Research and Development of Immune-and-Biological Products of the Russian Academy of Sciences, Moscow, 108819 Russia

⁴The 48th Central Research Institute of the Ministry of Defense of the Russian Federation, Moscow, 141306 Russia

*E-mail: logunov@gamaleya.org

Received October 21, 2019; in final form, May 29, 2020

DOI: 10.32607/actanaturae.11042

Copyright © 2020 National Research University Higher School of Economics. This is an open access article distributed under the Creative Commons Attribution License, which permits unrestricted use, distribution, and reproduction in any medium, provided the original work is properly cited.

ABSTRACT The Middle East Respiratory Syndrome (MERS) is an acute inflammatory disease of the respiratory system caused by the MERS-CoV coronavirus. The mortality rate for MERS is about 34.5%. Due to its high mortality rate, the lack of therapeutic and prophylactic agents, and the continuing threat of the spread of MERS beyond its current confines, developing a vaccine is a pressing task, because vaccination would help limit the spread of MERS and reduce its death toll. We have developed a combined vector vaccine for the prevention of MERS based on recombinant human adenovirus serotypes 26 and 5. Studies of its immunogenicity have shown that vaccination of animals (mice and primates) induces a robust humoral immune response that lasts for at least six months. Studies of the cellular immune response in mice after vaccination showed the emergence of a specific CD4⁺ and CD8⁺ T cell response. A study of the vaccine protectivity conducted in a model of transgenic mice carrying the human DPP4 receptor gene showed that our vaccination protected 100% of the animals from the lethal infection caused by the MERS-CoV virus (MERS-CoV EMC/2012, 100LD₅₀ per mouse). Studies of the safety and tolerability of the developed vaccine in rodents, rabbits, and primates showed a good safety profile and tolerance in animals; they revealed no contraindications for clinical testing.

KEYWORDS adenoviral vector, Middle East Respiratory Syndrome (MERS), immunogenicity, safety assessment.

ABBREVIATIONS 95% CI – 95% confidence interval; Ad5 – recombinant human serotype 5 adenovirus; Ad26 – recombinant human serotype 26 adenovirus; Ad41 – recombinant human serotype 41 adenovirus; APC – allophycocyanin; ChAdOx1 – recombinant chimpanzee adenovirus vector; DPP4 – dipeptidyl peptidase 4; MVA – modified vaccinia virus Ankara; RBD – receptor-binding domain of MERS-CoV S glycoprotein; RBD-Fc – receptor-binding domain of MERS-CoV S glycoprotein fused to the Fc domain of human IgG1; RBD-G – receptor-binding domain of MERS-CoV S glycoprotein fused to the transmembrane domain of the glycoprotein G of vesicular stomatitis virus; S – MERS-CoV glycoprotein; S-G – MERS-CoV glycoprotein with the transmembrane domain of the glycoprotein G of vesicular stomatitis virus; ALT – alanine aminotransferase; AST – aspartate aminotransferase; MERS – Middle East Respiratory Syndrome; MERS-CoV – Middle East Respiratory Syndrome coronavirus; v.p. – viral particles; IFN-gamma – interferon gamma; ALP – alkaline phosphatase.

INTRODUCTION

The Middle East Respiratory Syndrome (MERS) is an acute inflammatory disease of the respiratory system that was first diagnosed in June 2012 in Saudi Arabia [1, 2]. The disease is caused by the MERS-CoV coronavirus, a member of the genus *Betacoronavirus* of the family *Coronaviridae*. One-humped camels are the natural reservoir of the virus; human infection occurs through contact with camels and consumption of unpasteurized camel milk; an aerosol transmission of infection is also possible [3, 4]. According to the WHO, a total of 2,458 laboratory-confirmed cases of MERS had been registered by September 12, 2019, 848 of which resulted in a fatal outcome (a 34.5% mortality rate) [5]. Most MERS cases were registered in Saudi Arabia [6]. However, the disease was also detected in 27 other countries (the United Arab Emirates, South Korea, Yemen, etc.); cases of imported infection were reported in Europe, North Africa, and North America [5]. Because of the lack of effective preventive and therapeutic drugs for MERS, the high mortality rate of the disease, and the widespread character of the infection reservoir, WHO experts classify MERS-CoV as a virus with the potential to cause a pandemic. There have been no cases of MERS in Russia. However, due to the high mortality of MERS and the continuing threat that it could spread outside the endemic areas [5], development of a vaccine is an urgency. Vaccination can limit the spread of MERS and reduce its mortality [7].

To date, several candidate vaccine preparations based on a protective antigen, MERS-CoV S glycoprotein and its derivatives (S1 subunit, receptor-binding domain), are known: vector vaccines (based on recombinant adenoviruses and vaccinia virus), a DNA vaccine based on plasmid DNA, as well as vaccines based on recombinant proteins and virus-like particles [8–15]. Since the formation of a humoral and cellular immune response is important to protect against MERS-CoV, the use of recombinant viral vectors for antigen delivery seems promising for the development of anti-MERS vaccines. These vectors provide long-term expression of the antigen in the cells of the immunized organism, which results in a protective immune response as early as after the first or second immunization. Repeated vaccination is effective in inducing the most pronounced and lasting immune response, while heterologous vaccination involving the use of different viral vectors for primary and secondary immunization is the most optimal regimen. This regimen was successfully implemented in the development of a vaccine against the disease caused by the Ebola virus; the vaccine has been registered in the Russian Federation for medical use and already undergone post-registration clinical trials in the African Republic of Guinea [16].

We have developed a combined vector vaccine for the prevention of MERS based on recombinant human adenovirus serotypes 26 and 5 expressing MERS-CoV glycoprotein (MERS-CoV EMC/2012 isolate). Here, we present the results of a study of the post-vaccination humoral and cellular immune responses in mice and primates, as well as the results of preclinical studies of the safety of the developed vaccine against MERS.

EXPERIMENTAL

Study drug

The combined vector vaccine against MERS consists of two components.

Component 1 presents viral particles of recombinant human adenovirus serotype 26 carrying the gene for the receptor-binding domain of MERS-CoV glycoprotein, 10^{11} viral particles (v.p.) per dose.

Component 2 presents viral particles of recombinant human adenovirus serotype 5 carrying the gene for the full-length MERS-CoV glycoprotein and the gene for the receptor-binding domain of MERS-CoV glycoprotein, 10^{11} viral particles (v.p.) per dose.

Both components are lyophilisates for the preparation of solutions for intramuscular administration. The drug was obtained in compliance with the conditions of biotechnological production at the Medgamal branch of the Gamaleya National Research Center for Epidemiology and Microbiology of the Ministry of Health of the Russian Federation.

Laboratory animals

All experiments on animals were carried out in strict accordance with the recommendations of the National Standard of the Russian Federation (GOST R 53434-2009, “Principles of Good Laboratory Practice”). Six-week-old female C57BL/6 mice (18–20 g) were purchased from the Pushchino Breeding Facility (Russia). Transgenic F1 hybrid mice were obtained by crossing transgenic homozygous $+/+$ males carrying the human DPP4 receptor gene (hDPP4) (Medical University of Texas, USA) and non-transgenic C57BL/6 females (Pushchino, Russia). Expression of the transgene in F1 hybrid mice was confirmed by immunoblotting. All mice had free access to water and food and were housed in an ISOcage animal housing system (Tecniplast, Italy).

Common marmosets (*Callithrix jacchus*) were born and kept in a specialized animal facility at the Chumakov Federal Scientific Center for Research and Development of Immune-and-Biological Products RAS (Moscow, Russia). The animals were kept at the Laboratory for Modeling Immunobiological Processes with the Experimental Clinic of Callitrichidae (Chumakov

Federal Scientific Center for Research and Development of Immune-and-Biological Products RAS) in accordance with the requirements for housing laboratory primates. All experimental procedures with marmosets were carried out by a specialist who had received certification from the Federation of European Laboratory Animal Science Associations (FELASA) and completed a course on working with primates ("Laboratory Animal Science for Researchers: Non-Human Primates," Karolinska Institute, Stockholm, Sweden). All animals were identified by a radio chip implanted subcutaneously and having a unique 15-digit code (Globalvet, Moscow).

Immunization of mice and marmosets and collection of their serum samples

The mice were immunized intramuscularly using the widest possible dose range, 5×10^{11} to 10^5 v.p. per mouse. Immunization was carried out twice successively with component 1 and then component 2 with a 21-day interval. Mouse serum samples were collected at the following time points: 14 and 28 days, three and six months after immunization.

The marmosets were immunized intramuscularly at a dose of 10^{11} v.p. per animal. Immunization was conducted twice successively with component 1 and then component 2 with a 21-day interval. Plasma samples were collected at the following time points: before immunization, seven and 24 days, as well as three and six months, after immunization.

Determination of antibody titer by enzyme-linked immunosorbent assay (ELISA)

The titer of glycoprotein-specific antibodies in serum/plasma was determined by enzyme immunoassay. The following recombinant proteins were used: S glycoprotein (40069-V08B; Sino Biological, China) and RBD (40071-V08B1; Sino Biological). A PBS solution in 0.1% Tween-20 (PBS-T) containing 5% non-fat dry milk (A0830; AppliChem, Spain) was used for blocking. Serum/plasma was titrated in two steps in a PBS-T solution containing 3% non-fat dry milk. Anti-mouse IgG horseradish peroxidase-linked secondary antibodies (NXA931; GE Healthcare, USA) were used to detect mouse IgG. Serum of a rabbit immunized with marmoset IgG and anti-rabbit IgG horseradish peroxidase-linked secondary antibodies (NA934V; GE Healthcare, USA) were used to detect marmoset IgG. A Tetramethylbenzidine solution (NIIOPiK, Russia) was used as a chromogenic agent. The reaction was stopped by adding 1 M H_2SO_4 ; optical density was measured at 450 nm (OD_{450}) using a Multiskan FC microplate reader (Thermo Fisher Scientific, USA). The IgG titer was defined as the maximum serum dilution at which the

OD_{450} value of the serum sample from the immunized animal exceeded that of the control serum/plasma (serum/plasma of the control animal or animal before immunization) more than twofold.

Determination of the titer of neutralizing antibodies

The titer of virus-neutralizing antibodies (VNAs) in the plasma of immunized animals was determined in a neutralization reaction (NR) by suppressing the cytopathic effect caused by the MERS-CoV virus (MERS-CoV EMC/2012) in the monolayer of Vero B cells. The neutralization reaction was carried out in the "constant viral dose/serum dilution" mode. Monkey plasma was incubated at $56^\circ C$ for 30 min to remove non-specific inhibitors. All serum samples were diluted in a DMEM medium supplemented with 2% inactivated fetal bovine serum, starting from the 1 : 10 ratio, then with two-fold dilution to 1 : 5,120. Dilutions of the MERS-CoV virus suspension were prepared in a DMEM medium supplemented with 2% inactivated fetal bovine serum. The concentration of the MERS-CoV virus in the prepared dilution was 1,000 TCID₅₀/ml. A mixture of equal volumes of plasma and the virus suspension was incubated at $37^\circ C$ for 60 min. Vero B cells were plated in 96-well plates at 4×10^4 cells per well at a volume of 100 μl and then supplemented with 100 μl of the mixture of plasma and the virus suspension. The cytopathic effect was assessed after four days. The VNA titer of the studied plasma was defined as its highest dilution at which the cytopathic effect was suppressed in two out of three wells (compared to the control serum samples).

Analysis of the T cell response (lymphocyte proliferation assay) and production of interferon gamma (IFN-gamma) in mice

The mice were euthanized on day eight after immunization. The spleens were collected and homogenized through a 100- μm sieve in sterile PBS. Splenocytes were isolated by Ficoll (1.09 g/ml; PanEco, Russia) density gradient centrifugation (800 g, 30 min). For T cell proliferation assay, the splenocytes were stained with carboxyfluorescein using the Carboxyfluorescein succinimidyl ester (CFSE) tracer kit (Invitrogen, USA) as previously described [17]. Cells were seeded in 96-well plates at 2×10^5 cells per well in a RPMI 1640 medium and re-stimulated with the recombinant MERS-CoV S protein (40069-V08B; Sino Biological) at 1 μg per well. After 72 h, the media were collected for a IFN-gamma analysis and the cells were harvested, washed with PBS, stained with antibodies specific to CD3, CD4, and CD8: allophycocyanin (APC)-labelled anti-CD3, APC-Cy7-labelled anti-CD8, and phycoerythrin-labelled anti-CD4 (BD Biosciences, USA), and then fixed in 1%

paraformaldehyde. Proliferating CD4⁺ and CD8⁺ T lymphocytes were evaluated in the cell mixture using a BD FACS Aria III flow cytometer (BD Biosciences). The resulting percentage of proliferating cells (X) was determined using the following formula: $X = \%st - \%$, where %st is the percentage of proliferating cells after splenocyte re-stimulation with recombinant MERS-CoV S glycoprotein, and % is the percentage of proliferating cells in the absence of splenocyte re-stimulation (intact cells).

The concentration of IFN-gamma in the medium was measured by ELISA using a commercial kit (mouse IFN- γ ELISA kit; Invitrogen) according to the manufacturer's protocol. The increase in the concentration of IFN-gamma was determined using the following formula: $X = Cst/Cint$, where X is the fold increase in the concentration of IFN-gamma, Cst is the concentration of IFN-gamma in the medium of stimulated cells (pg/ml), and Cint is the concentration of IFN-gamma in the medium of unstimulated (intact) cells (pg/ml).

Assessment of the protective efficacy

The protective efficacy of the vaccine was studied in a model of lethal infection in transgenic mice carrying the human DPP4 receptor gene and obtained by crossing homozygous transgenic hDPP4^{+/+} males and non-transgenic C57BL/6 females. The animals were immunized intramuscularly twice successively with component 1 and then component 2 with a 21-day interval. Seven days after the injection of component 2, the mice were infected intranasally with the MERS-CoV virus (MERS-CoV EMC/2012) at a dose of 100 LD₅₀ per animal, and then the survival rate was analyzed for a period of 30 days.

Preclinical safety study

Preclinical studies of the safety of the combined vector vaccine against MERS were conducted in collaboration with the Autonomous Non-commercial Organization "Institute of Biomedical Research and Technology" and FSAEI HE I.M. Sechenov First Moscow State Medical University, in compliance with the Guidelines for Pre-clinical Trials of Medicinal Products [18] and Guidelines for experimental (preclinical) study of new pharmacological substances [19]. The safety study included the analysis of the toxicity of a single and repeated administration, as well as an assessment of the reproductive and ontogenetic toxicity, immunogenicity, and allergenicity. A total of 670 mice, 725 rats, 24 rabbits, 120 guinea pigs, and six common marmosets were used in the preclinical safety study.

Tolerability of the vaccine in primates was analyzed daily by assessing the physical condition of the animals and based on the presence of general symptoms of in-

toxication, which included an assessment of behavior, appearance, and physiological functions. Vaccine tolerance in marmosets was studied in the laboratory by monitoring the body weight, rectal temperature, and blood biochemical parameters: total bilirubin, direct bilirubin, aspartate aminotransferase (AST), alanine aminotransferase (ALT), creatinine, total protein, and alkaline phosphatase (ALP). The studies were carried out on fully automatic analyzers CA-180 and B-200 (Furuno, Japan) using DiaSys reagent kits (Germany).

Statistical analysis

Statistical analysis of the data was performed using the GraphPad 7.0 software. Either the Student's t-test for independent samples or the Mann-Whitney U-test was used for the analysis of the data of unpaired samples depending on the data distribution normality [20]. Either the Student's t-test for paired samples or Wilcoxon's test was used for the analysis of the data of related samples depending on the data distribution normality [20]. Distribution normality was determined using the generalized D'Agostino-Pearson test [21].

RESULTS

Immunization of the animals with the combined vector vaccine induces a robust long-term humoral immune response to MERS-CoV glycoprotein in mice and primates

In order to select an effective dose, mice were immunized intramuscularly with the vaccine at doses of 10⁵–10¹⁰, 5 × 10¹⁰ v.p. per mouse; serum samples were collected, and the titers of glycoprotein-specific antibodies were analyzed two and four weeks after immunization. Next, the intensity of the post-vaccination humoral immune response was assessed based on the titer of glycoprotein-specific IgG (*Fig. 1*).

Analysis of the obtained results demonstrates a dose-dependent increase in the serum titer of glycoprotein-specific IgG. The minimum dose of the combined vector vaccine required to induce a robust humoral immune response was 10⁶ v.p. per mouse for all vaccinated animals. Analysis of the duration of post-vaccination humoral immunity showed that glycoprotein-specific antibodies were detected at a high titer in the mouse serum six months after immunization (the geometric mean titer was 1 : 182,456, *Fig. 2*).

Next, we studied the level of humoral immunity in primates vaccinated with the developed vaccine. In order to determine the level of humoral immunity in common marmosets (*C. jacchus*), they were immunized with the combined vaccine according to the regimen intended for clinical use, i.e. successively with component 1 (at a dose of 10¹¹ v.p. per animal) and then com-

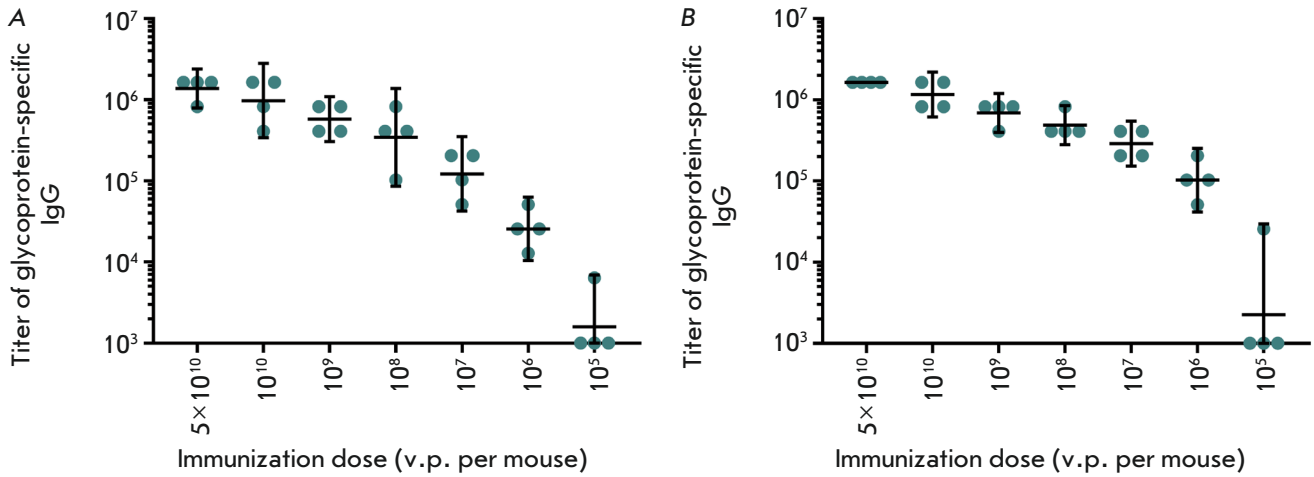
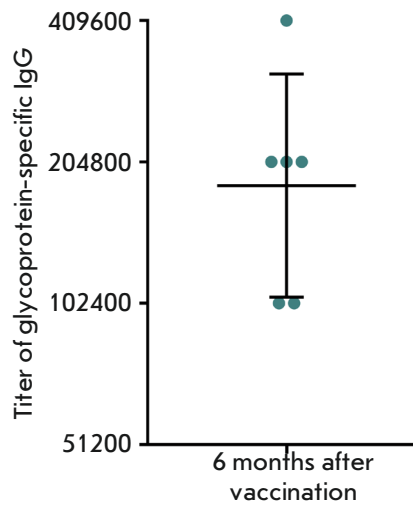


Fig. 1. Titers of glycoprotein-specific IgGs in the serum of immunized animals two weeks (A) and four weeks (B) after boosting of the vaccination. The abscissa axis represents immunization doses (v.p. per mouse); the ordinate axis shows reciprocal IgG titers. The geometric mean titers and 95% confidence intervals are indicated

Fig. 2. Titers of glycoprotein-specific IgGs in the serum of immunized animals six months after vaccination. The ordinate axis shows reciprocal IgG titers. The geometric mean titer and the 95% confidence interval (n = 6) are indicated



ponent 2 (at a dose of 10^{11} v.p. per animal) with a 21-day interval. Further, plasma samples were collected from animals for the analysis of the titer of glycoprotein-specific IgG seven and 24 days, as well as three and six months, after the boosting of immunization (Fig. 3A). Immunization of primates was shown to induce robust humoral immunity, which persists for at least six months. For instance, the titers of glycoprotein-specific IgG in primates six months after immunization did not differ from the titers after three months, which is an indication of the induction of long-term immunity. Analysis of the titer of neutralizing antibodies to the MERS-CoV virus in the plasma of immunized monkeys showed that VNAs were detected in the animals as early as seven days after booster immunization, while

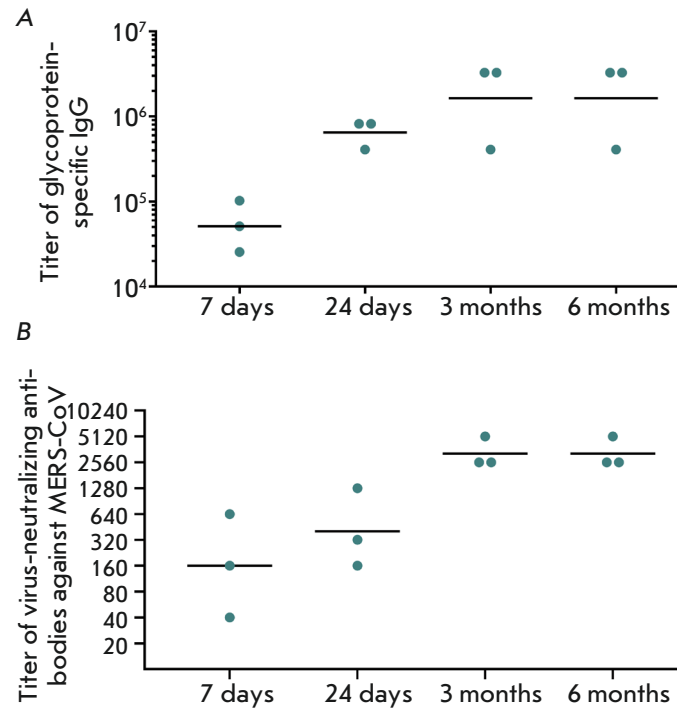


Fig. 3. A – Titers of glycoprotein-specific IgG in the plasma of immunized marmosets after vaccination. IgG titers are shown on the ordinate axis; time after immunization is represented on the abscissa axis. Individual titers for each studied animal and the geometric mean titer (n = 3) are indicated. B – Titers of virus-neutralizing antibodies in the plasma of immunized marmosets after vaccination. Virus-neutralizing antibody titers are shown on the ordinate axis; time after immunization is represented on the abscissa axis. Individual titers for each studied animal and the geometric mean titer (n = 3) are indicated

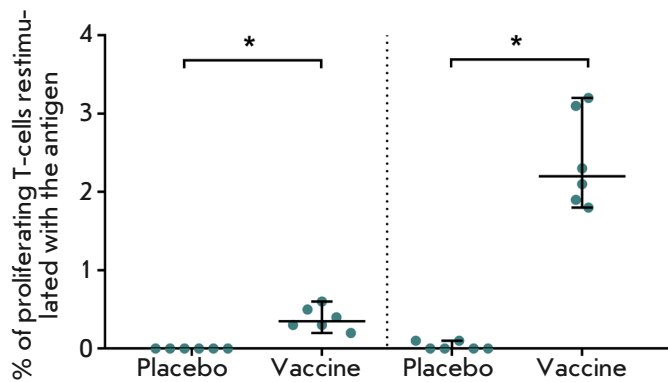


Fig. 4. Study of the lymphoproliferative activity of splenocytes in mice immunized with the vaccine or placebo. The levels (in %) of proliferating CD4⁺ and CD8⁺ T cells re-stimulated with recombinant MERS-CoV S glycoprotein on the 18th day after vaccination are presented. Medians of the percentage of proliferating cells after re-stimulation and 95% CI for the median for each group (n = 6) are indicated. * – p < 0.05

the maximum VNA titer was reached three and six months after immunization (Fig. 3B). No VNAs were detected in the plasma of the control animals and the animals before immunization.

Thus, our analysis of the level of post-vaccination immunity showed that immunization of mice and primates induces a robust humoral immune response, which persists for at least six months after immunization.

Immunization of mice with the candidate vaccine induces a robust cellular immune response

In order to assess the level of post-vaccination cellular immunity, the mice were immunized with the candidate vaccine against MERS once at a dose of 10⁷ v.p. per mouse. Spleens were collected from the animals 18 days after immunization; splenocytes were isolated, and the number of proliferating CD4⁺ and CD8⁺ T lymphocytes was determined in the splenocyte culture *in vitro* after cell re-stimulation with the recombinant MERS-CoV S protein (Fig. 4). The obtained data demonstrate that introduction of the combined vector vaccine induces the formation of S-specific CD4⁺ and CD8⁺ T cells.

Activation of cellular immunity was also analyzed by measuring the expression of IFN-gamma. The results of the study of an increase in the IFN-gamma concentration in an *in vitro* culture of mouse splenocytes after repeated stimulation of the cells with the recombinant MERS-CoV S protein are presented in Fig. 5. Administration of the vaccine increased the concentration of IFN-gamma in the medium upon stimulation of the splenocytes of immunized mice with the MERS-CoV S

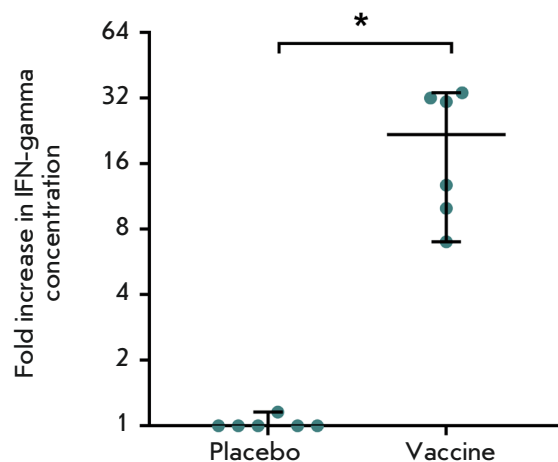


Fig. 5. Increase in the concentration of IFN-gamma in the splenocyte media of immunized and non-immunized mice after re-stimulation with recombinant MERS-CoV S glycoprotein. Median increase in the concentration of IFN-gamma after re-stimulation and 95% CI for the median for each group (n = 6) are indicated. * – p < 0.05

glycoprotein. The concentration of IFN-gamma in the medium increased by an average of 22 times.

Summarizing the data of our analysis of the antigen-specific lymphoproliferative activity of CD4⁺ and CD8⁺ T cells and the level of IFN-gamma expression by re-stimulated splenocytes, we can conclude that immunization of animals with the combined vaccine against MERS results in the formation of glycoprotein-specific cellular immunity.

Combined vector vaccine protects animals against lethal infection with the MERS-CoV virus

The study was carried out in a model of lethal infection caused by MERS-CoV in transgenic mice carrying the human DPP4 receptor gene. Mice were immunized successively with component 1 and then component 2 with a 21-day interval. One week after administration of component 2 of the vaccine, animals were infected intranasally with the MERS-CoV virus (MERS-CoV EMC/2012) at a dose of 100 LD₅₀ per animal, and the survival rate was assessed during 30 days. Immunization of the animals with the combined vector vaccine was shown to protect 100% of animals from lethal infection caused by the MERS-CoV virus. All control (unvaccinated) animals died (Fig. 6).

The combined vector vaccine for the prevention of MERS has favorable safety and tolerability profiles in animals

General and specific toxicity (the toxicity of single and repeated administration, assessment of the local

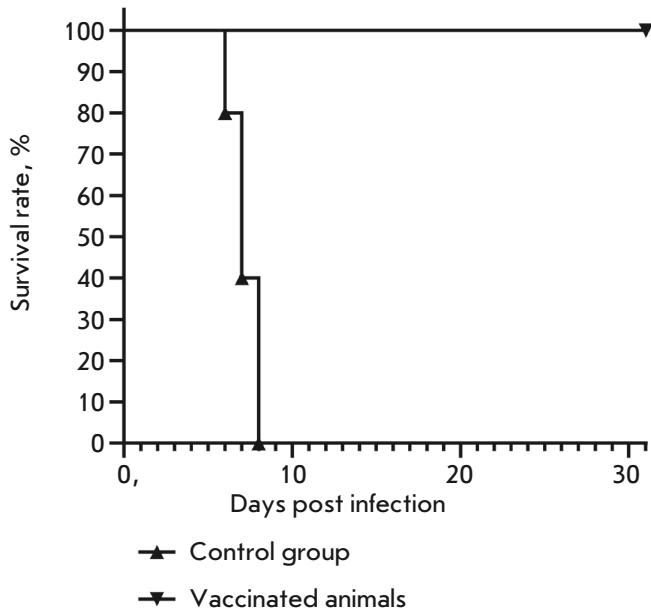


Fig. 6. Survival of vaccinated ($n = 10$) and non-vaccinated (control group, $n = 10$) animals after a lethal infection of MERS-CoV. The ordinate axis shows the survival rate of animals (%). The abscissa axis represents time after immunization (days)

irritation effect, immunotoxicity, allergenic properties, and reproductive toxicity) were evaluated in rodents (mice, rats, and guinea pigs) and large animals (rabbits). The combined vector vaccine against MERS did not cause any toxic effects, did not have an allergenic or immunotoxic effect, did not affect the generative function, did not have a local irritation effect, and can be recommended for clinical studies.

Vaccine tolerability was also studied in primates. No abnormalities in the analyzed parameters of physical condition (behavioral reactions, appearance, and physiological functions) were found in the animals immunized with the combined vector vaccine against MERS and the control animals during the observation period. Rectal temperature, changes in body weight, and biochemical parameters were within the normal range for the species in all animals during the experiment (*Fig. 7*). Summarizing the obtained data, we can conclude that the combined vector vaccine against MERS has shown good tolerability in the common marmoset model.

DISCUSSION

Currently, there are no specific prophylactic and therapeutic agents against the Middle East Respiratory Syndrome in the World. Intensive studies on the development of vaccines for this disease are currently underway in the United States, Germany, Korea, China, Great Britain, and other countries. Among the prophylactic

drugs with the highest efficiency demonstrated in preclinical studies, the following candidate vaccines can be mentioned: vaccines based on adenoviral vectors (Ad5, Ad41, ChAdOx1) [22, 23], Modified Vaccinia virus Ankara (MVA) [24] encoding MERS-CoV protective antigen S, as well as preparations of recombinant MERS-CoV protective antigen S [25, 26]. Two drugs are currently undergoing clinical trials: two vaccines based on recombinant viral vectors MERS001 (based on chimpanzee adenovirus, phase 1) [27] and MVA-MERS-S (based on vaccinia virus, phase 2) [28]. Clinical studies of the first phase of a vaccine based on plasmid DNA (GLS-5300), as well as a vaccine based on a vaccinia virus (MVA-MERS-S), have been completed [29, 30].

All vaccines that have reached clinical trials are based on MERS-CoV S glycoprotein. This glycoprotein performs one of the most important roles in the viral life cycle: it enables virus internalization via interaction with the DPP4 receptor on the cell surface. Neutralization of this interaction limits penetration of the virus into the cell, thus decreasing its replication.

Since the formation of not only a humoral, but also cellular immune response is important for protection against MERS, the development of vaccines based on recombinant viral vectors seems promising. Such vectors effectively deliver antigen-encoding genetic material to the cells, which results in the cellular expression of the antigen and induction of a robust cellular and humoral immunity. An important property of recombinant viral vectors is that they induce protective immunity as early as after the first or second immunization, which is extremely important when developing a vaccine for the prevention of dangerous and extremely dangerous infections and is intended for use during an epidemic or in the case of an infection that spreads beyond non-endemic areas.

We have conducted a study of the immunogenicity of various forms of MERS-CoV S glycoprotein: full-length glycoprotein (S), full-length glycoprotein with the transmembrane domain of the G protein (S-G) of the vesicular stomatitis virus, a secreted glycoprotein receptor-binding domain (RBD), a secreted glycoprotein RBD fused to the Fc fragment of human IgG1 (RBD-Fc), and the membrane form of the glycoprotein RBD (RBD-G) [31]. The obtained data demonstrated that the membrane form of the RBD is the most effective in inducing a robust cellular immune response, while full-length glycoprotein is most efficient in inducing a robust cellular immunity. When choosing an immunization regimen, one should take into account the fact that repeated heterologous vaccination, which involves the use of two different recombinant viral vectors for primary and secondary immunization, is advisable for inducing long-term immunity. For this

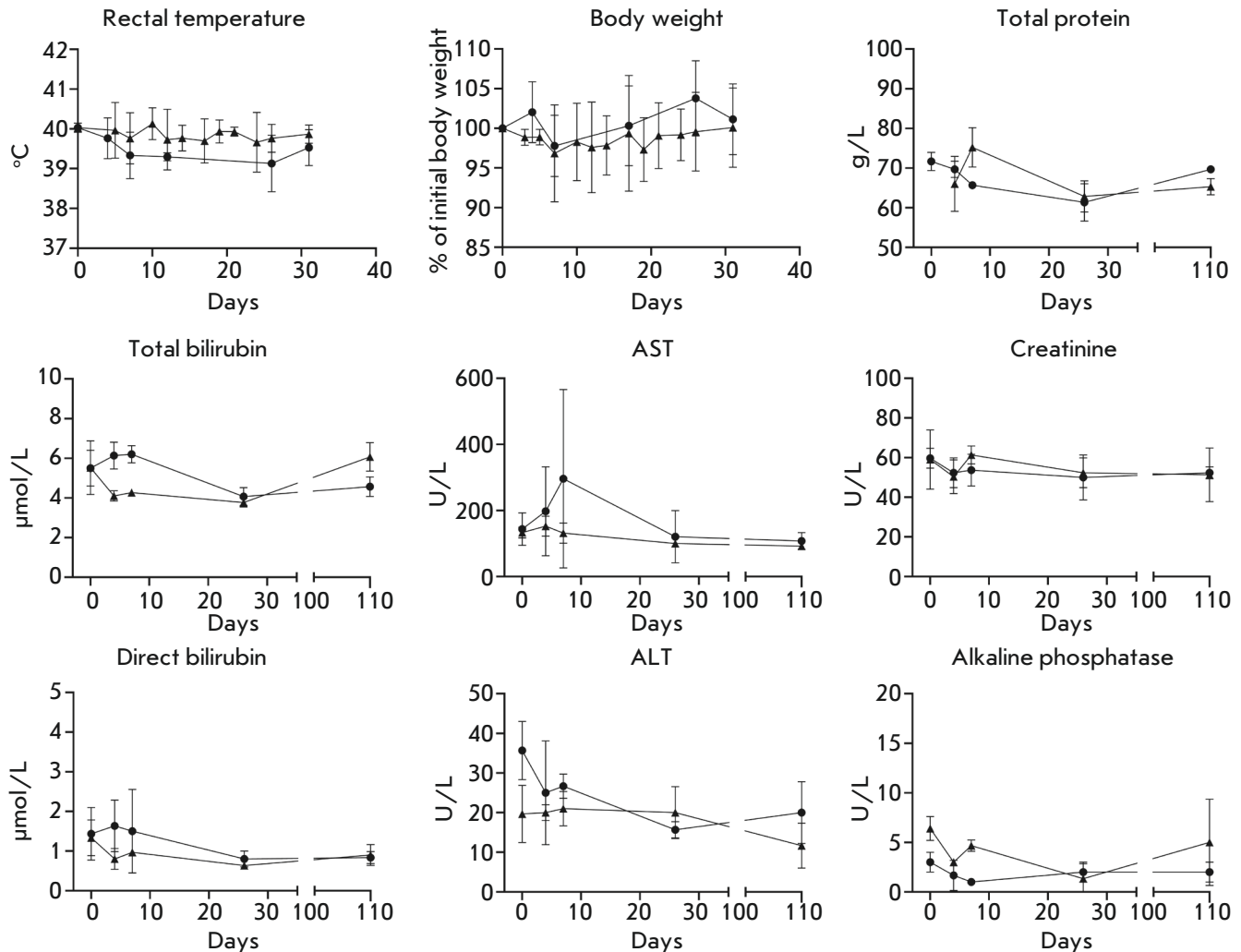


Fig. 7. Rectal temperature, body weight, and biochemical blood parameters in primates (common marmosets) immunized with the combined vector vaccine against MERS (indicated by triangles) and control animals (marked by circles)

reason, the combined vaccine against MERS included two recombinant vectors based on human adenovirus serotypes 26 and 5. Component 1 included the rAd26-RBD-G recombinant vector, while component 2 was comprised of two recombinant vectors: rAd5-S and rAd5-RBD-G.

Studies of the immunogenicity of the combined vector vaccine revealed the induction of long-term humoral immunity in mice, while the mean titer of glycoprotein-specific antibodies equaled 1 : 121,775 two weeks after vaccination at a dose of 10^7 v.p. per mouse. A similar antibody titer was observed by Alharbi et al. in mice 28 days after immunization with a vaccine against MERS based on chimpanzee adenovirus ChAdOx1 MERS [12]; however, the authors used a dose of 10^8 v.p. per mouse for immunization. In

another study by Munster et al. [13], immunization of transgenic mice carrying the human DPP4 receptor gene with a ChAdOx1 MERS vaccine at a dose 10^8 v.p. per mouse was shown to protect 100% of the animals from a lethal infection with MERS-CoV. Hashem et al. developed a rAd5-based drug carrying the MERS-CoV S1 sequence and demonstrated that repeated immunization of mice with the drug at a dose of 10^9 v.p. per mouse induced a humoral immune response [32]. The titer of glycoprotein-specific IgG was 1 : 70,000 three weeks after the second immunization (one and a half months from the beginning of immunization); the drug also provided 100% protection to animals from MERS-CoV infection [32].

Glycoprotein-specific antibodies were found at a titer range of 1 : 25,600 to 1 : 102,400 in the plasma of the

animals as early as a week after the boosting of immunization. It is important to note that Muthumani et al. [33] detected glycoprotein-specific antibodies at a titer of 1 : 20,000 for a period of six weeks in primates after long-term thrice immunization with a DNA vaccine; the authors also showed that immunization of primates with the DNA vaccine protects them from a MERS-CoV infection.

The study of post-vaccination humoral immunity in mice and primates demonstrated that an intense humoral immune response persists in the animals for at least six months after vaccination. Analysis of the cellular component of the immunity in the mice showed that administration of the developed vaccine induces a robust cellular response. It is important to note that not only a CD4⁺ but also CD8⁺ T cell response is observed, which can play an important role in protection against MERS-CoV [34, 35]

Having completed studies of the immunogenicity of the combined vector vaccine in a model of lethal infection in transgenic mice carrying the human DPP4 receptor gene, we studied the protective effect of the vaccine. The vaccine was shown to provide 100% protection to animals from lethal infections of MERS-CoV. Our series of preclinical studies of vaccine safety

revealed no contraindications for the clinical testing of the developed vaccine.

CONCLUSION

In this work, we have studied the immunogenicity and safety of a combined vector vaccine for the prevention of the Middle East Respiratory Syndrome. The following conclusions were obtained:

Vaccination of animals with the vaccine induces a robust humoral immune response to the MERS-CoV S glycoprotein persisting for at least six months.

Vaccination of animals induces a robust cellular immune response to the MERS-CoV S glycoprotein.

Vaccination of animals induces a protective immune response, which protects 100% of animals from a lethal infection of MERS-CoV.

Preclinical studies of the vaccine safety did not reveal any contraindications to clinical testing. ●

Conflict of interests. The authors declare no obvious or potential conflicts of interests related to the publication of this article.

This study was funded by the Ministry of Health of the Russian Federation (State Assignments No. 056-00108-18-00 and 056-00078-19-00).

REFERENCES

- de Groot R.J., Baker S.C., Baric R.S., Brown C.S., Drosten C., Enjuanes L., Fouchier R.A.M., Galiano M., Gorbalenya A.E., Memish Z.A., et al. // *J. Virol.* 2013. V. 87. № 14. P. 7790–7792.
- Zaki A.M., van Boheemen S., Bestebroer T.M., Osterhaus A.D., Fouchier R.A. // *N. Engl. J. Med.* 2012. V. 367. № 19. P. 1814–1820.
- Memish Z.A., Cotten M., Meyer B., Watson S.J., Alshafi A.J., Al Rabeeah A.A., Corman V.M., Sieberg A., Makhdoom H.Q., Assiri A., et al. // *Emerg. Infect. Dis.* 2014. V. 20. № 6. P. 1012–1015.
- Reusken C.B., Farag E.A., Jonges M., Godeke G.J., El-Sayed A.M., Pas S.D., Raj V.S., Mohran K.A., Moussa H.A., Ghobashy H., et al. // *Euro Surveill.* 2014. V. 19. № 23. P. 1–5.
- World Health Organisation. Middle East respiratory syndrome coronavirus (MERS-CoV). 2019. URL: <http://www.who.int/emergencies/mers-cov/en/> (access date: 15.10.19).
- Aly M., Elrobh M., Alzayer M., Aljuhani, S., Balkhy H. // *PLoS One.* 2017. V. 12. № 10. P. 1–11.
- World Health Organisation. WHO Research and Development Blueprint: 2017 Annual review of diseases prioritized under the Research and Development Blueprint). 2017. URL: <http://www.who.int/blueprint/what/research-development/2017-Prioritization-Long-Report.pdf> (access date: 15.10.19).
- Okba N.M., Raj V.S., Haagmans B.L. // *Curr. Opin. Virol.* 2017. V. 23. P. 49–58.
- Ma C., Wang L., Tao X., Zhang N., Yang Y., Tseng C.T.K., Li F., Zhou Y., Jiang S., Du L. // *Vaccine.* 2014. V. 32. № 46. P. 6170–6176.
- Nyon M.P., Du L., Tseng C.K., Seid C.A., Pollet J., Naceanceno K.S., Agrawal A., Algaissi A., Peng B.H., Tai W., et al. // *Vaccine.* 2018. V. 36. № 14. P. 1853–1862.
- Tai W., Zhao G., Sun S., Guo Y., Wang Y., Tao X., Tseng C.K., Li F., Jiang S., Du L., et al. // *Virology.* 2016. V. 499. P. 375–382.
- Alharbi N.K., Padron-Regalado E., Thompson C.P., Kupke A., Wells D., Sloan M.A., Grehan K., Temperton N., Lambe T., Warimwe G., et al. // *Vaccine.* 2017. V. 35. № 30. P. 3780–3788.
- Munster V.J., Wells D., Lambe T., Wright D., Fischer R.J., Bushmaker T., Saturday G., Van Doremalen N., Gilbert S.C., De Wit E., et al. // *NPJ Vaccines.* 2017. V. 2. P. 28.
- Malczyk A.H., Kupke A., Prüfer S., Scheuplein V.A., Hutzler S., Kreuz D., Beissert T., Bauer S., Hubich-Rau S., Tondera C., et al. // *J. Virol.* 2015. V. 89. № 22. P. 11654–11667.
- Modjarrad K. // *Vaccine.* 2016. V. 34. № 26. P. 2982–2987.
- International Multicenter Study of the Immunogenicity of Medicinal Product GamEvac-Combi. ClinicalTrials.gov Identifier: NCT03072030. URL: <https://clinicaltrials.gov/ct2/show/NCT03072030> (access date: 15.10.19).
- Quah B.J., Warren H.S., Parish C.R. // *Nat. Protoc.* 2007. V. 2. № 9. P. 2049–2056.
- Mironov A.N., editor. Guidelines for Preclinical Trials of Medicinal Products. // Moscow: Grif i K; 2012. (in Russian)
- Khabriev R.U., editor. Guidelines for experimental (preclinical) study of new pharmacological substances // Moscow: Medicine, 2005. (in Russian)
- Unguryanu T.N., Grzhibovskiy A.M. // *Ekologiya che-*

- loveka. 2011. V. 5. P. 55–60.
21. Petri A, Sabin K. *Per. With the English*. Ed. VP Leonov. Visual medical statistics. 3rd ed. Pererab. and additional. Moscow: GEOTAR-Media; 2015.
 22. Guo X., Deng Y., Chen H., Lan J., Wang W., Zou X., Hung T., Lu Z., Tan W. // *Immunology*. 2015. V. 145. № 4. P. 476–484.
 23. Kim E., Okada K., Kenniston T., Raj V.S., AlHajri M.M., Farag E.A., AlHajri F., Osterhaus A.D., Haagmans B.L., Gambotto A. // *Vaccine*. 2014. V. 32. № 45. P. 5975–5982.
 24. Volz A., Kupke A., Song F., Jany S., Fux R., Shams-Eldin H., Schmidt J., Becker C., Eickmann M., Becker S., et al. // *J. Virol*. 2015. V. 89. № 16. P. 8651–8656.
 25. Coleman C.M., Venkataraman T., Liu Y.V., Glenn G.M., Smith G.E., Flyer D.C., Frieman M.B. // *Vaccine*. 2017. V. 35. № 12. P. 1586–1589.
 26. Tang J., Zhang N., Tao X., Zhao G., Guo Y., Tseng C.T., Jiang S., Du L., Zhou Y. // *Hum. Vaccin. Immunother*. 2015. V. 11. № 5. P. 1244–1250.
 27. Safety and Immunogenicity of a Candidate MERS-CoV Vaccine (MERS001). *ClinicalTrials.gov Identifier: NCT03399578* URL: <https://clinicaltrials.gov/ct2/show/NCT03399578> (access date: 15.10.19).
 28. Randomized, Double-blind, Placebo-controlled, Phase Ib Study to Assess the Safety and Immunogenicity of MVA-MERS-S_DF-1. *ClinicalTrials.gov Identifier: NCT04119440* URL: <https://clinicaltrials.gov/ct2/show/NCT04119440> (access date: 15.10.19).
 29. Phase I, Open Label Dose Ranging Safety Study of GLS-5300 in Healthy Volunteers *ClinicalTrials.gov Identifier: NCT02670187* URL: <https://clinicaltrials.gov/ct2/show/NCT02670187> (access date: 15.10.19).
 30. Safety, Tolerability and Immunogenicity of Vaccine Candidate MVA-MERS-S. *ClinicalTrials.gov Identifier: NCT03615911* URL: <https://clinicaltrials.gov/ct2/show/NCT03615911> (access date: 15.10.19).
 31. Ozharovskaia T.A., Zubkova O.V., Dolzhikova I.V., Gromova A.S., Grousova D.M., Tukhvatulin A.I., Popova O., Shcheblyakov D.V., Scherbinin D.N., Dzharullaeva A.S., et al. // *Acta Naturae*. 2019. V. 11. № 1. P. 38–47.
 32. Hashem A.M., Algaissi A., Agrawal A.S., Al-Amri S.S., Alhabbab R.Y., Sohrab S.S., Almasoud A., Alharbi N.K., Peng B.H., Russell M. et al. // *J. Infect. Dis*. 2019. V. 220. № 10. P. 1558–1567.
 33. Muthumani K., Falzarano D., Reuschel E.L., Tingey C., Flingai S., Villarreal D.O., Wise M., Patel A., Izmirly A., Aljuaid A., et al. // *Sci. Transl. Med*. 2015. V. 7. № 301. P. 301ra132.
 34. Zhao J., Li K., Wohlford-Lenane C., Agnihothram S.S., Fett C., Zhao J., Gale M.J. Jr., Baric R.S., Enjuanes L., Gallagher T., et al. // *Proc. Natl. Acad. Sci. USA*. 2014. V. 111. № 13. P. 4970–4975.
 35. Zhao J., Alshukairi A.N., Baharoon S.A., Ahmed W.A., Bokhari A.A., Nehdi A.M., Layqah L.A., Alghamdi M.G., Al Gethamy M.M., Dada A.M., et al. // *Sci. Immunol*. 2017. V. 2. № 14. P. eaan5393.

GLAD-PCR Assay of R(5mC)GY Sites in the Regulatory Region of Tumor-Suppressor Genes Associated with Gastric Cancer

B. S. Malyshev¹, N. A. Netesova¹, N. A. Smetannikova¹, M. A. Abdurashitov², A. G. Akishev², E. V. Dubinin^{2*}, A. Z. Azanov³, I. V. Vihlyanov⁴, M. K. Nikitin⁴, A. B. Karpov⁵, S. Kh. Degtyarev^{1,2}

¹State Research Center of Virology and Biotechnology «Vector», Novosibirsk region, Koltsovo, 630559 Russia

²EpiGene LLC, Novosibirsk, 630090 Russia

³Regional Clinical Oncology Center, Kemerovo, 650036 Russia

⁴Altai Regional Oncology, Center Altai region, Barnaul, 656049 Russia

⁵Seversk Biophysical Research Centre, Tomsk region, Seversk, 636039 Russia

*E-mail: evgeny.dubinin@epigene.ru

Received January 20, 2020; in final form, July 22, 2020

DOI: 10.32607/actanaturae.11070

Copyright © 2020 National Research University Higher School of Economics. This is an open access article distributed under the Creative Commons Attribution License, which permits unrestricted use, distribution, and reproduction in any medium, provided the original work is properly cited.

ABSTRACT At early stages of carcinogenesis, the regulatory regions of some tumor suppressor genes become aberrantly methylated at RCGY sites, which are substrates of DNA methyltransferase Dnmt3. Identification of aberrantly methylated sites in tumor DNA is considered to be the first step in the development of epigenetic PCR test systems for early diagnosis of cancer. Recently, we have developed a GLAD-PCR assay, a method for detecting the R(5mC)GY site in the genome position of interest even at significant excess of DNA molecules with a non-methylated RCGY site in this location. The aim of the present work is to use the GLAD-PCR assay to detect the aberrantly methylated R(5mC)GY sites in the regulatory regions of tumor suppressor genes (*brinp1*, *bves*, *cacna2d3*, *cdh11*, *cpeb1*, *epha7*, *fgf2*, *galr1*, *gata4*, *hopx*, *hs3st2*, *irx1*, *lrrc3b*, *pcdh10*, *rprm*, *runx3*, *sfrp2*, *sox17*, *tcf21*, *tfpi2*, *wnt5a*, *zfp82*, and *znf331*) in DNA samples obtained from gastric cancer (GC) tissues. The study of the DNA samples derived from 29 tumor and 25 normal gastric tissue samples demonstrated a high diagnostic potential of the selected RCGY sites in the regulatory regions of the *irx1*, *cacna2d3*, and *epha7* genes; the total indices of sensitivity and specificity for GC detection being 96.6% and 100%, respectively.

KEYWORDS gastric cancer, tumor suppressor genes, DNA methylation, GLAD-PCR assay, methyl-directed DNA endonuclease GlI.

INTRODUCTION

Gastric cancer (GC) is one of the most lethal and widespread malignancies in the world. GC's ranks third among cancer mortality rates in the world; this disease is responsible for over 700,000 deaths every year [1]. According to WHO data, more than 1,000,000 new diagnoses were made and about 783,000 patients died from gastric cancer in 2018 [2].

The prognosis of the disease largely depends on its clinical stage but in general remains quite unfavorable: only 40% of patients have the potential to be cured of the disease at the time of their diagnosis. The chances of a 5-year survival period do not exceed 25–30% in most countries [3, 4], while detection of GC at early

stages (IA–IB) increases that chance of survival by up to 80% or more [5, 6].

Epigenetic DNA diagnostics involving the identification of the aberrantly methylated regulatory regions of the tumor suppressor genes that are inactivated by such a modification is considered a promising tool for early cancer detection and monitoring. Such an aberrant methylation has been shown for most sporadic cancers at early stages of malignant neoplasms (more than 90% of all cases) [7, 8].

The DNA methyltransferases Dnmt3a and Dnmt3b perform *de novo* DNA methylation, including aberrant methylation. These enzymes predominantly recognize the RCGY sites (where R stands for A or G; Y stands

for T or C) and modify cytosine, yielding the R(5mC)GY sequence in both DNA strands. DNA methyltransferase Dnmt1 maintains the methylation of the RCGY sites after DNA replication [9].

The methyl-directed site-specific DNA endonuclease *GlaI* recognizes and cleaves precisely the R(5mC)GY sites, making it a convenient tool for studying DNA methylation [10]. Based on *GlaI* unique specificity, we have developed a GLAD-PCR assay, a method for detecting the R(5mC)GY sites of interest even at a significant excess of DNA molecules with the corresponding non-methylated RCGY site [11].

The GLAD-PCR assay of R(5mC)GY sites displays a higher accuracy and reproducibility compared to the conventionally used method of bisulfite conversion of DNA. DNA bisulfite treatment often causes serious DNA degradation and a significant loss of material [11].

Recently, we have studied the methylation of the tumor suppressor genes in DNA samples derived from colorectal cancer tissues using the GLAD-PCR assay. Abnormal methylation of the RCGY sites in the *fbn1*, *cnrip1*, *adhfe1*, *ryr2*, *sept9l*, and *eid3* genes was proved for more than 75% of the tumor DNA samples [12,13].

This work aimed to use the GLAD-PCR assay to detect the R(5mC)GY sites in the regulatory regions of tumor suppressor genes in DNA samples derived from gastric cancer tissues.

EXPERIMENTAL

DNA samples intraoperatively isolated from the tumors of gastric mucosal tissue from 29 patients were used as study material. In all cases, the patients were diagnosed with gastric adenocarcinomas with varying degrees of differentiation.

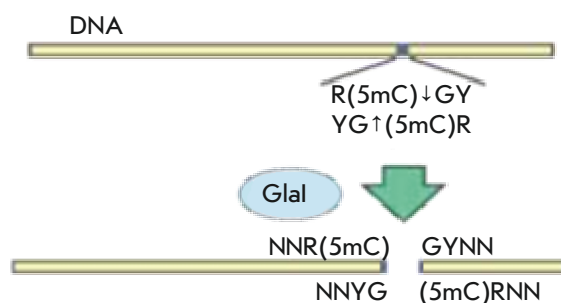
Five patients had clinical stage I of the disease (T1N0-1M0, T2N0M0); 11 patients, stage II (T1N2-3M0, T2N1-2M0, T3N0-1M0, T4aN0M0); 10 patients, stage III (T2N3M0, T3N2-3M0, T4aN1-3M0, T4bN0-3M0); and three patients had stage IV gastric cancer (presence of distant metastases (M1) in any variants of the primary tumor size (T) and the presence or absence of metastatic lesions on regional lymph nodes (N)).

DNA samples from morphologically unchanged gastric mucosal tissue obtained from 25 GC patients during surgery on the resection line (at a distance of at least 5 cm from the macroscopically determined tumor edge) were used as the controls.

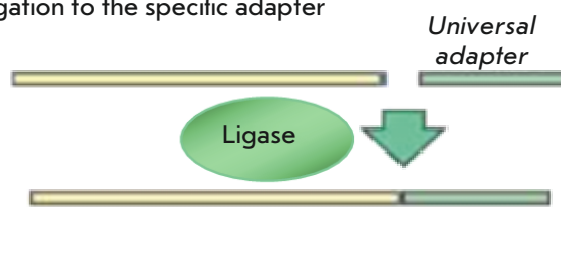
All the patients enrolled in this study have provided written informed consent.

Tissue samples obtained during surgery were placed in a test tube containing a RNA-later solution and refrigerated for 24 h at +4°C, then transferred to a freezer and stored at -20°C [12].

1) *GlaI* hydrolysis



2) Ligation to the specific adapter



3) Real-time PCR

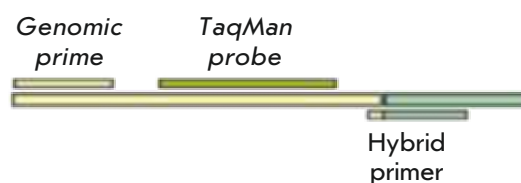


Fig. 1. GLAD-PCR assay

DNA isolation was performed using the standard phenol-chloroform method [14].

GLAD-PCR assay

The GLAD-PCR assay of DNA samples involved three stages: (1) DNA hydrolysis with the *GlaI* enzyme; (2) ligation of the resulting DNA hydrolysates with a universal adapter; and (3) subsequent real-time PCR using a fluorescent probe and the first primer complementary to the target DNA region, as well as the second primer corresponding to the adapter sequence and the DNA region near the determined *GlaI* site (Fig. 1).

Reagents produced by SibEnzyme Ltd were used for setting all the GLAD-PCR stages.

Enzymatic DNA hydrolysis was performed for 30 min at 30°C. The reaction mixture (volume, 21.5 µL) included 9.0 ng of the test DNA sample, 1 × SE TMN buffer (10 mM Tris-HCl (pH 7.9), 5 mM MgCl₂, 25 mM NaCl), 2.0 % dimethyl sulfoxide (DMSO), 2.0 µg of bovine serum albumin (BSA), and 1.5 AU of *GlaI*.

For ligation of the hydrolysis products with the adapter (in a volume of 30.0 µL), ATP and a universal

double-stranded adapter (5'-CCTGCTCTTTCATCG-3'/3'-p-GGACGAGAAAGTAGC-p-5') were added to each sample units to the final concentration of 0.5 μM , as well as 240 AU of highly active T4-DNA ligase. The reaction was performed for 15 min at 25°C.

At the final stage, PCR components were added to the reaction mixture to the following concentrations in the final volume 60.0 μL : 1 \times SE-GLAD buffer (50 mM Tris-SO₄ (pH 9.0), 30 mM KCl, 10 mM [NH₄]₂SO₄), 3 mM MgCl₂, dNTP mixture (0.2 mM each), 0.1 $\mu\text{g}/\mu\text{L}$ BSA, the respective mixture of two primers and a probe (0.4 μM each), and 0.05 AU of SP Taq DNA polymerase. To improve the amplification efficiency of the GC-rich regions in the *tfpi2* gene, extra DMSO was added to the PCR mixture to a total concentration of 4%.

Then, 20.0 μL of the resulting mixture was transferred into three separate microtubes and real-time PCR was performed in a CFX-96 detecting amplifier (Bio-Rad Lab., USA) according to the following program: 3 min at 95°C; 45 cycles lasting 10 s at 95°C, 15 s at 61°C (*bves*, *gata4*, *sox17*, *tcf21*) or 62°C (*cacna2d3*, *galr1*, *hs3st2*, *pcdh10*, *rprm*, *sfrp2*, *wnt5a*) or 63°C (*cdh11*, *cpeb1*, *fgf2*, *hopx*, *tfpi2*, *zfp82*), and 20 s at 72°C. To eliminate the influence of possible initial fluctuations on the shape of the amplification curve, the fluorescence of the first five PCR cycles was not recorded.

Designing specific primers and probes

To design the specific primers and probes, we used nucleotide sequences from the GenBank database according to the GRCh38/hg38 version of the human genome (<http://ncbi.nlm.nih.gov/genbank>), the Vector NTI 11.5 software family (Invitrogen, USA), and the NCBI BLAST online resource (<http://blast.ncbi.nlm.nih.gov>). The primer and probe structures are shown in *Table 1*.

The hybrid primers corresponding to the R(5mC)GY sites, methylated with the highest frequency, were selected experimentally. The nucleotide sequence of each hybrid primer was 5'-CCTGCTCTTTCATCG-GYNN-3', where 15 of 5'-terminal nucleotides corresponded to the adapter, and four of 3'-terminal nucleotides (underlined) were complementary to the genomic sequence at the DNA hydrolysis site. By using hybrid primers corresponding to the terminal tetranucleotides obtained after the hydrolysis of the NNR(5mC) \downarrow GYNN sequence, all RCGY sites – located within ~ 200 bp of the hybridization site of the fluorescent probe – in the regulatory region of each gene were analyzed. The lowest cycle threshold (Cq) value meant maximum methylation of the R(5mC)GY site [12, 13].

Statistical analysis

The experimental data were statistically processed using the MedCalc 15.11 software (MedCalc Software,

Belgium). Based on the Cq values of the DNA samples for the analyzed RCGY sites, characteristic curves (ROC curves; Receiver Operating Characteristic Curves) were obtained with a 95% confidence interval. The area under the ROC curve (AUC) shows a correlation between the sensitivity and specificity of a diagnostic test. AUC is an integral indicator of the diagnostic efficiency of a tumor marker site. AUC is an integral indicator of the diagnostic efficiency of a tumor marker site (for the “perfect” test AUC = 1) [15].

RESULTS

A number of candidate epigenetic GC markers have been identified thus far. Based on the results of a literature search for the epigenetically downregulated genes involved in gastric carcinogenesis, we have formed a panel of 23 tumor suppressor genes to study the methylation of the RCGY sites in their regulatory regions by GLAD-PCR assay. This list includes the *brinp1* [16], *bves* [17], *cacna2d3* [18], *cdh11* [16], *cpeb1* [19], *epha7*, *fgf2*, *galr1* [16], *gata4* [20], *hopx* [21], *hs3st2* [16], *irx1* [17], *lrrc3b* [22], *pcdh10* [23], *rprm* [24], *runx3*, *sfrp2* [17], *sox17* [25], *tcf21* [26], *tfpi2* [27], *wnt5a* [17], *zfp82* [18], and *znf331* [28] genes.

Identification of RCGY sites in DNA from GC tissues for a GLAD-PCR analysis. At this step, we used ten random DNA samples from gastric cancer tissues to select the most frequently methylated RCGY sites within the regulatory regions of tumor suppressor genes as described earlier [12, 13]

The real-time PCR threshold cycle Cq value was used as a criterion for selecting RCGY sites promising for the GLAD-PCR assay, which should be less than 30 in at least one of the ten DNA samples from the gastric cancer tissue.

According to the results of the preliminary analysis, a single RCGY site in each of the *brinp1*, *bves*, *cacna2d3*, *cdh11*, *cpeb1*, *epha7*, *fgf2*, *galr1*, *gata4*, *hopx*, *hs3st2*, *irx1*, *lrrc3b*, *pcdh10*, *rprm*, *runx3*, *sfrp2*, *sox17*, *tcf21*, *tfpi2*, *wnt5a*, *zfp82*, and *znf331* genes was selected to further study the full collection of DNA samples derived from tumor (n = 29) and morphologically unchanged (n = 25) stomach mucosa tissues of GC patients (*Table 2*).

GLAD-PCR assay of RCGY sites in DNAs from the clinical samples

GLAD-PCR assay of selected RCGY sites was performed in triplets of 3 ng of DNA (~ 10³ copies of the studied gene region) in the reaction mixture. *Figure 2* presents the diagrams of the average Cq values for the studied RCGY sites.

Table 1. The structures of primers and fluorescent probes for a GLAD-PCR assay of gastric cancer tumor marker genes

Gene ^a	Protein encoded name ^a	Chromosomal location ^a	Primer/probe sequence ^b
<i>brinp1</i>	BMP / retinoic acid inducible neural specific 1	9q33.1	FAM-CCGTAAAGTCCCCTTCGCTGGTCCC-BHQ1 GAGCCGGGATTTCATGCCTGTC
<i>bves</i>	Blood vessel epicardial substance	6q21	CCGGCGGCATTTCGTCTGTT FAM-CCCTACCCGGACCGCACTTCTCGAA-BHQ1
<i>cacna2d3</i>	Calcium voltage-gated channel auxiliary subunit alpha2delta 3	3p21.1-p14.3	FAM-CGCACTCGGGAAAAGCTAAGAGCCTC-BHQ1 CGAGGGAGAAGGACTGCTACCGA
<i>cdh11</i>	Cadherin 11	16q21	CGCTCCAGCTGGCCAGGC FAM-CTTCCCCCAACCACCATCCCAGGC-BHQ1
<i>cpeb1</i>	Cytoplasmic polyadenylation element binding protein 1	15q25.2	CTGCCCTGGGCTCAGTTTCC FAM-CCCCTGGAGCGCGCGCG-BHQ1
<i>epha7</i>	EPH receptor A7	6q16.1	FAM-CCAAGCACGGAGCCCGACAGTGA-BHQ1 CCCAGCCCCGGAGGTTTC
<i>fgf2</i>	Fibroblast growth factor 2	4q28.1	CGGGGTCCGGGAGAAGAGC FAM-CCGACCCGCTCTCTCCGCCTCATT-BHQ1
<i>galr1</i>	Galanin receptor 1	18q23	FAM-TGCAGCAGAGAAGCCCCTGGCACC-BHQ1 GGCGAGAGCTCTTTTGGGAGGC
<i>gata4</i>	GATA binding protein 4	8p23.1	CCTTTCTGGCCGGCCTCCT FAM-AGTCCCTGGACCCAGCCCCGA-BHQ1
<i>hopx</i>	HOP homeobox	4q12	CGGGCAGAAGCGATGGGAGA FAM-CCCGCCGGCTGCCCTCC-BHQ1
<i>hs3st2</i>	Heparan sulfate-glucosamine 3-sulfotransferase 2	16p12.2	GCCTCCCCGAGGAGTACTATGCC FAM-CACCTTCGTTTCACCGCCCCAAAGC-BHQ1
<i>irx1</i>	Iroquois homeobox 1	5p15.33	GCCAGGGAGCGGGTAGCGA FAM-CTCCACGGGCTGCTTCTGCGG-BHQ1
<i>lrrc3b</i>	Leucine rich repeat containing 3B	3p24.1	FAM-TGCTCACCCCGTGTGTGCACTTG-BHQ1 GGGCTGGGGGAAGGGCAA
<i>pcdh10</i>	Protocadherin 10	4q28.3	CCGGCCCTGTATCTCTGGTGC FAM-CCGCCATCTCTGCTCCACAACG-BHQ1
<i>rprm</i>	Reprimo, TP53 dependent G2 arrest mediator homolog	2q23.3	CCCCGTTCAAATTTCGACGC FAM-CCCCCAACCCCTTCTCCACAATGA-BHQ1
<i>runx3</i>	Runt related transcription factor 3	1p36.11	FAM-CCCTCCCAACTGTAGCCGGCCCC-BHQ1 CTGGGGCGATAATTCCGAATGA
<i>sfrp2</i>	Secreted frizzled related protein 2	4q31.3	FAM-CTCCCTTGCTCCCCCACCCTCC-BHQ1 CCAGCCCTCCTCGGATTACCC
<i>sox17</i>	SRY (sex determining region Y)-Box 17	8q11.23	CGCCCTCCGACCCTCCAA FAM-TCCCGGATTCCCCAGGTGGCC-BHQ1
<i>tcf21</i>	Transcription factor 21	6q23.2	FAM-TGCCCCCGACACCAAGCTCTCC-BHQ1 CCAGCCTGAGCGTGTCCAGC
<i>tfpi2</i>	Tissue factor pathway inhibitor 2	7q21.3	CCGAGCGGAGGGGCCTCT FAM-AGCGAGTCCCCCTGCCAGCG-BHQ1
<i>wnt5a</i>	Wnt family member 5A	3p14.3	FAM-CCCTTCCCTGCCCTCCCCACAGC-BHQ1 CAGGTGTGGGGTGGGAGGGA
<i>zfp82</i>	Zinc finger protein 82	19q13.12	FAM-CAGCTGCAGAGAAATGGCCCTCGGTC-BHQ1 CCCCAGCATCCTCTGCCCCAC
<i>znf331</i>	Zinc finger protein 331	19q13.42	FAM-CCGCACACTCGCTGGCCCTTTCAC-BHQ1 GCCCGATCCCGACCAGTCAC

^aGene symbol, protein encoded name, and chromosomal location are given in accordance with the approved guidelines from the HUGO Gene Nomenclature Committee (<http://www.genenames.org>).

^bDirect genomic primer structure is indicated before the probe structure, the one for the reverse genomic primer is provided after the probe structure; FAM – 6-carboxyfluorescein, BHQ1 – Black Hole Quencher 1.

Table 2. RCGY sites selected for a GLAD-PCR assay, their locations, and the structure of the respective hybrid primers

Gene	Target site	Site location ^a	Hybrid primer ^b
<i>brinp1</i>	GCGC	chr9: 119369161–119369164	CCTGCTCTTTCATCGGCGG
<i>bves</i>	GCGC	chr6:105137614–105137617	CCTGCTCTTTCATCGGCGC
<i>cacna2d3</i>	GCGC	chr3:54120898–54120901	CCTGCTCTTTCATCGGCGA
<i>cpeb1</i>	GCGC	chr15: 82648343–82648347	CCTGCTCTTTCATCGGCGG
<i>epha7</i>	GCGC	chr6:93419955–93419958	CCTGCTCTTTCATCGGCGA
<i>galr1</i>	GCGC	chr18:77249828–77249831	CCTGCTCTTTCATCGGCGG
<i>irx1</i>	GCGC	chr5:3596424–35966427	CCTGCTCTTTCATCGGCGG
<i>lrrc3b</i>	GCGC	chr3:26623493–26623500	CCTGCTCTTTCATCGGCGG
<i>pcdh10</i>	GCGT	chr4:133152953–133152956	CCTGCTCTTTCATCGGCGA
<i>runx3</i>	GCGT	chr1:24931357–24931360	CCTGCTCTTTCATCGGTGG
<i>sfrp2</i>	GCGC	chr4:153789030–15379033	CCTGCTCTTTCATCGGCGC
<i>pcf21</i>	GCGC	chr6:133889653–133889658	CCTGCTCTTTCATCGGCGA
<i>tspi2</i>	GCGC	chr7:93890478–93890481	CCTGCTCTTTCATCGGCGC
<i>znf331</i>	GCGT	chr19:53521737–53521740	CCTGCTCTTTCATCGGTCT

^aSite locations are given in accordance with the recent human genome assembly GRCh38/hg38.

^bUnderlined is the 3'-terminal tetranucleotide sequence (pentanucleotide one for *SOX17* gene) of the hybrid primer, which is complementary to the genomic sequence at the point of GlI hydrolysis.

The results of the analysis of the R(5mC)GY sites in the *bves*, *cacna2d3*, *cpeb1*, *epha7*, *galr*, and *tspi2* genes show that the Cq values (23–27) for most tumor DNA samples are on average three or more cycles lower than those for the corresponding DNA samples derived from healthy tissues. Meanwhile, for the *brinp1*, *lrrc3b*, *runx3*, *pcf21*, and *znf331* markers, this difference in the Cq value for most DNA samples is small (less than 1.5 cycles), which makes it difficult to use them to detect tumor tissue because of a possible overlap of the range of standard deviations.

The ROC curves obtained by a statistical analysis of the experimental data from the GLAD-PCR assay for 14 RCGY sites are shown in *Fig. 3*. Meanwhile, *Table 3* summarizes the numerical results of calculated parameter values. Columns 2 and 3 indicate the number of positive results for tumor tissues for each gene and the sensitivity of determination for the site, respectively. Columns 4 and 5 show the number of negative results of the GLAD-PCR assay of the DNA samples derived from morphologically unchanged tissues and specificity in detecting tumor DNA. Column 6 lists the values

of the areas under the ROC curve (AUC) expressed as a fraction of the total area of the square, indicating the standard error of measurement. Finally, column 7 lists the 95% confidence intervals for determining this parameter.

The statistical analysis of the results of the GLAD-PCR assay (*Fig. 2* and *Table 3*) shows that most of the tested markers are characterized by high sensitivity and specificity and makes it possible to differentiate between the DNA samples derived from tumor and normal tissues of gastric cancer.

The RCGY sites in the tumor suppressor genes *irx1* and *cpeb1* have the highest diagnostic potential; the AUC values for them are above 0.91.

The overall diagnostic characteristics of all the investigated RCGY sites were assessed using the logistic regression method (sequential inclusion/exclusion algorithm), which made it possible to select the optimal combination of markers providing the maximum area under the ROC curve and distinguish between DNA samples derived from tumor and normal tissues with the greatest efficiency. As one can see in *Table 3*, analy-

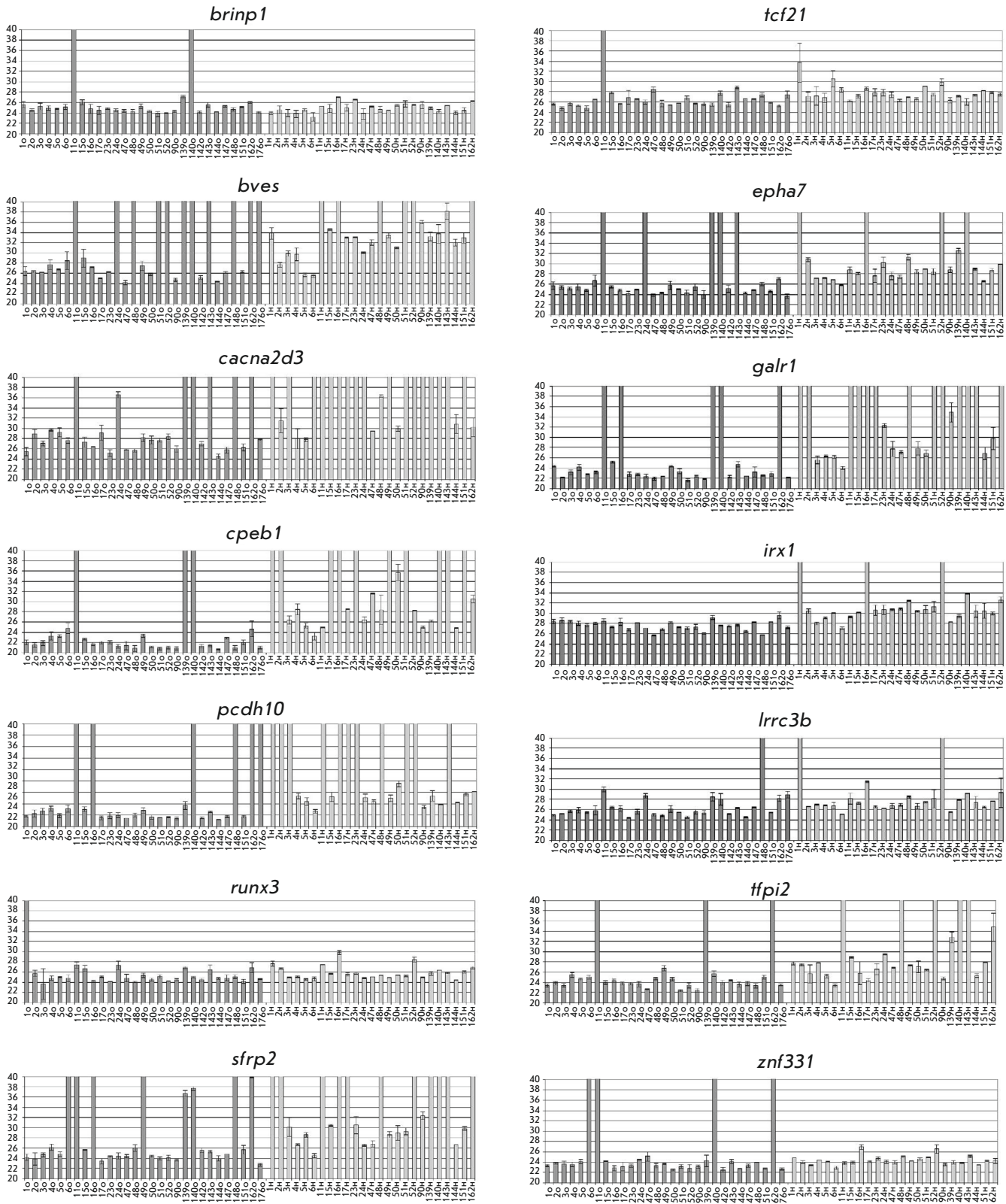


Fig. 2. The Cq values (with the standard deviation ranges) for selected R(5mC)GY sites obtained using the GLAD-PCR assay of tissue DNAs. Sample designations are given below each diagram (T – tumor tissue, N – normal tissue)

Table 3. Receiver operating characteristics for the diagnosis of GC versus normal mucosa determined by means of a GLAD-PCR assay of selected RCGY sites (sorted by AUC values)

Gene (region)	Number of detected GC samples/total number of GC samples	Sensitivity, %	Number of negative controls/total number of normal lung tissue controls	Specificity, %	AUC (standard error)	95% CI
<i>irx1</i>	27/29	93.1	22/25	88.0	0.934 (0.038)	0.83–0.984
<i>cpeb1</i>	25/29	86.2	24/25	96.0	0.911 (0.047)	0.802–0.971
<i>galr1</i>	24/29	82.7	24/25	96.0	0.866 (0.054)	0.745–0.943
<i>tfpi2</i>	23/29	79.3	22/25	88.0	0.846 (0.059)	0.721–0.929
<i>cacna2d3</i>	21/29	72.4	23/25	92.0	0.834 (0.054)	0.708–0.921
<i>epha7</i>	22/29	75.7	24/25	96.0	0.832 (0.066)	0.706–0.920
<i>pcdh10</i>	22/29	75.9	24/25	96.0	0.830 (0.061)	0.703–0.918
<i>sfrp2</i>	21/29	72.4	24/25	96.0	0.795 (0.064)	0.663–0.893
<i>tcf21</i>	15/29	51.7	25/25	100.0	0.790 (0.063)	0.657–0.889
<i>lrrc3b</i>	21/29	72.4	22/25	88.0	0.762 (0.070)	0.627–0.867
<i>znf331</i>	14/29	48.3	24/25	96.00	0.698 (0.075)	0.558–0.815
<i>runx3</i>	14/29	48.3	21/25	84.0	0.673 (0.074)	0.532–0.795
<i>bves</i>	18/29	62.1	22/25	88.0	0.627 (0.082)	0.485–0.755
<i>brinp1</i>	3/29	10.3	25/25	100.0	0.514 (0.081)	0.374–0.652
Panel of <i>irx1</i> , <i>cacna2d3</i> and <i>epha7</i> genes	28/29	96.6	25/25	100.0	0.985 (0.016)	0.907–1.000

sis of a combination of the markers *irx1*, *cacna2d3*, and *epha7* allows for such differentiation with 100% specificity and 96.6% sensitivity.

Thus, a diagnostic panel of RCGY sites was formed using the GLAD-PCR analysis of DNA preparations from clinical samples of tumor and normal tissues from patients with gastric cancer, which makes it possible to identify tumor tissues.

DISCUSSION

Four molecular subtypes of GC differing in their DNA methylation profiles are known [17]. They include (a) the EBV-positive subtype, associated with the Epstein-Barr virus; (b) MSI (MLH1 silencing), characterized by functional inactivation of the *mhl1* locus; (c) the option with stable microsatellite repeats; and (d) the subtype carrying a large number of mutations in microsatellite repeats. However, the histological type of gastric cancer is mostly adenocarcinoma (> 90%).

A significant number of genes with different biological functions have currently been identified in which the promoter regions or the first exon are methylated in gastric cancer [30]. Meanwhile, methylation of the

regulatory regions of the *bves*, *irx1*, *runx3*, *cacna2d3*, *lrrc3b*, and *sfrp2* genes presented in Table 3 is associated with at least three subtypes of gastric cancer [17]. In the study of DNA methylation at the genome level, the bisulfite conversion method is used, followed by sequencing on the NGS platform. Sepulveda J.L. et al. applied this approach to the study of DNA preparations derived from normal mucous and tumor tissue and showed that methylation of CpG-dinucleotides is significantly increased in the *brinp1*, *epha7*, and *galr1* genes in gastric cancer [16].

The conclusions drawn in the listed studies were based on a comparison of the median methylation degrees in tissue samples without determining the frequency indicators of methylation or gene expression for the “normal” and “tumor” groups. Such indicators are described for the remaining five genes presented in Table 3.

Silencing of the *cpeb1* gene during promoter methylation was observed in all nine studied gastric cancer cell lines and in 91% of primary tumors [19]. The same results were obtained for the *pcdh10* gene, whose methylation was established in 82% of gastric tumors

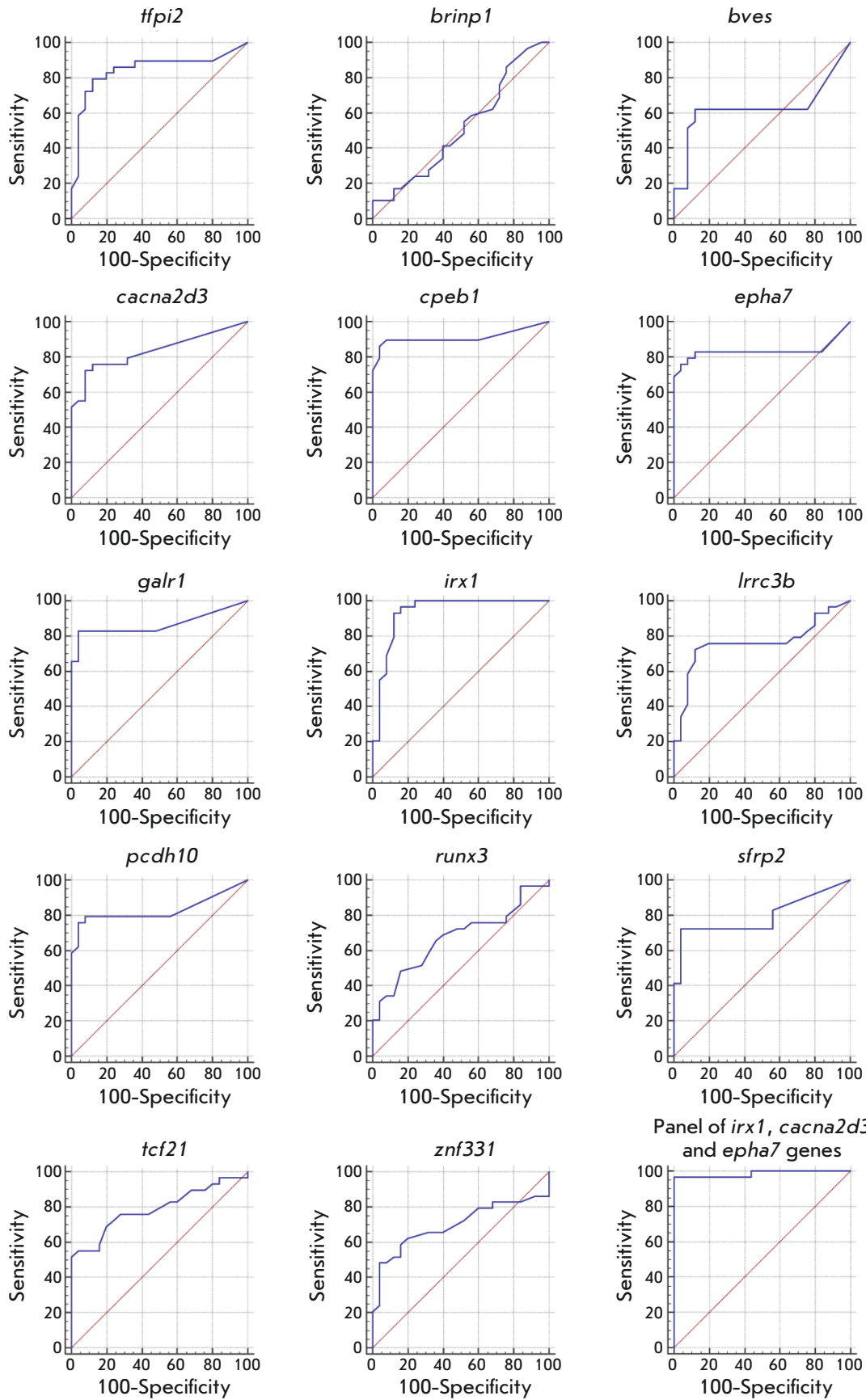


Fig. 3. The ROC curves for a GLAD-PCR analysis of R(5mC)GY sites in GC versus normal gastric mucosa tissues

and 94% of gastric tumor cell lines [23]. Methylation of the *tfpi2* gene promoter was also detected in more than 80% of gastric tumor samples [27]. In 71% of the pancreatic cell lines, the *znf331* gene was turned off. This effect was also observed in a significant number of DNA samples from tumor tissues, while this gene was non-methylated in morphologically unchanged tissues, including gastric tissue [28]. Methylation of the promoter region of the *tcf21* gene was observed only in 65% of the cases [26]. The results are presented in *Table 3* and correlate well with the previously obtained quantitative data on gene methylation in tumors of gastric cancer [19, 23, 26–28].

The list of genes with aberrant methylated sites in tumors of gastric cancer (*Table 3*) significantly differs from the earlier obtained list of genes in colorectal cancer [13]. The *sfrp2* gene is an exception; its regulatory region's methylation in tumor DNA is observed in both cases with almost the same frequency (72% for colorectal cancer).

Potential of GLAD-PCR assay for gastric cancer diagnosis

The results obtained in this study agree with the previously published data and demonstrate that a GLAD-PCR analysis allows one to determine aberrant methylated R(5mC)GY sites in the regulatory regions of tumor suppressor genes in DNA samples isolated from GC tissue. Site methylation negatively correlates with the threshold cycle value (C_q) in real-time PCR.

A combination of RCGY sites in the regulatory regions of the *irx1*, *cacna2d3*, and *epha7* genes was the optimal complex marker of gastric cancer. This panel of genes allows one to achieve 100% specificity in differentiation between tumor and morphologically un-

changed tissues, while the analysis sensitivity increases to 96.6% (*Table 3*).

At the moment, the so-called “liquid biopsy” technique is the most promising and actively evolving method of oncodiagnosis, which is based on an analysis of freely circulating DNA in blood. One of the main sources of such DNA in cancer patients is tumor cells, which are destroyed as a result of apoptosis and necrosis [31].

We plan to continue working with the obtained panel of markers to perform tests using DNA samples isolated from the peripheral blood of gastric cancer patients in order to develop a sensitive method for a laboratory diagnosis of gastric cancer.

CONCLUSIONS

The R(5mC)GY sites emerging during aberrant methylation of the regulatory regions of tumor suppressor genes in DNA samples from gastric cancer tissues have been identified by GLAD-PCR assay. A panel of sites in the *irx1*, *cacna2d3*, and *epha7* genes, which are epigenetic markers of gastric cancer, has been proposed. The high diagnostic efficiency of this panel was proved in the differentiation of DNA from morphologically unchanged and tumor tissues. The overall sensitivity and specificity of the panel are 96.6% and 100%, respectively.

We believe that the selected RCGY sites can be used to develop systems for the diagnosis of gastric cancer by the GLAD-PCR of DNA samples isolated from the blood of patients.

This work was supported by the Skolkovo Foundation grant No. G102/16 dated December 6, 2016.

REFERENCES

1. IARC, Stewart BW, Wild CP, ed. World Cancer Report 2014. Geneva: WHO Press; 2014.
2. IARC. Press release N 263. WHO, Geneva, Switzerland; 2018. <https://www.who.int/cancer/PRGlobocanFinal.pdf>. Accessed 25 Sep 2019.
3. Siegel R., Ma J., Zou Z., Jemal A. // *CA Cancer J Clin.* 2014. V. 64. № 1. P. 9–29.
4. Cancer.net. Doctor-Approved Patient Information from ASCO. <https://www.cancer.net/cancer-types/stomach-cancer/statistics>. Accessed 25 Sep 2019.
5. International medical center ONCLINIC. https://www.onclinic.ru/articles/zabolevaniya/onkologiya/vyzhivae-most_pri_rake_zheludka. Accessed 25 Sep 2019.
6. American Cancer Society. <https://www.cancer.org/cancer/stomach-cancer/detection-diagnosis-staging/survival-rates.html>. Accessed 25 Sep 2019.
7. de Cáceres I., Cairns P. // *Clin Transl Oncol.* 2007. V. 9. № 7. P. 429–437.
8. Langevin S.M., Kratzke R.A., Kelsey K.T. // *Transl Res.* 2015. V. 165. № 1. P. 74–90.
9. Handa V., Jeltsch A. // *J Mol Biol.* 2005. V. 348. № 5. P. 1103–1112.
10. Tarasova G.V., Nayakshina T.N., Degtyarev S.K. // *BMC Mol Biol.* 2008. V. 9. P. 7.
11. Kuznetsov V.V., Akishev A.G., Abdurashitov M.A., Degtyarev S.K. // Patent RU 2525710 (in Russian). IPC C12Q 1/68 (2006.01). 2014.
12. Evdokimov A.A., Netesova N.A., Smetannikova N.A., Abdurashitov M.A., Akishev A.G., Davidovich E.S., Ermolaev Yu.D., Karpov A.B., Sazonov A.E., Tahauov R.M. et al. // *Prob Oncol (Voprosy Onkologii, in Russian).* 2016. V. 62. P. 117–121.
13. Evdokimov A.A., Netesova N.A., Smetannikova N.A., Abdurashitov M.A., Akishev A.G., Malyshev B.S., Davidovich E.S., Fedotov V.V., Kuznetsov V.V., Ermolaev Yu.D. et al. // *Biol Med (Aligarh).* 2016. V. 8. P. 342.
14. Smith K., Klko S., Cantor Ch. Genome analysis. *Methods.*

RESEARCH ARTICLES

- Davis K, ed. (in Russian) Moscow: Mir, 1990. 244 p.
15. Pepe M.S. The statistical evaluation of medical tests for classification and prediction. New York: Oxford, 2003. 320 p.
 16. Sepulveda J.L., Gutierrez-Pajares J.L., Luna A., Yao Y., Tobias J.W., Thomas S. Woo Y., Giorgi F., Komissarova E.V., et al // *Mod Pathol.* 2016. V. 29. № 2. P. 182–193.
 17. Lim B., Kim J.H., Kim M., Kim S.Y. // *World J Gastroenterol.* 2016. V. 22. № 3. P. 1190–1201.
 18. Yuasa Y., Nagasaki H., Akiyama Y., Hashimoto Y., Takizawa T., Kojima K., Kawano T., Sugihara K., Imai K., Nakachi K. // *Int. J. Cancer.* 2009. V. 124. № 11. P. 2677–2682.
 19. Caldeira J., Simoes-Correia J., Paredes J., Pinto M.T., Sousa S., Corso G., Marrelli D., Roviello F., Pereira P.S., Weil D., et al. // *Gut.* 2012. V. 61. № 8. P. 1115–1123.
 20. Akiyama Y., Watkins N., Suzuki H., Jair K.W., van Engeland M., Esteller M., Sakai H., Ren C.Y., Yuasa Y., Herman J.G., et al. // *Mol. Cell. Biol.* 2003. V. 23. № 23. P. 8429–8439.
 21. Ooki A., Yamashita K., Kikuchi S., Sakuramoto S., Katada N., Kokubo K., Kobayashi H., Kim M.S., Sidransky D., Watanabe M. // *Oncogene.* 2010. V. 29. P. 3263–3275.
 22. Kim M., Kim J.H., Jang H.R., Kim H.M., Lee C.W., Noh S.M., Song K.S., Cho J.S., Jeong H.Y., Hahn Y., et al. // *Cancer Res.* 2008. V. 68. P. 7147–7155.
 23. Yu J., Cheng Y.Y., Tao Q., Cheung K.F., Lam C.N., Geng H., Tian L.W., Wong Y.P., Tong J.H., Ying J.M., et.al. // *Gastroenterology.* 2009. V. 136. № 2. P. 640–651.
 24. Wang H., Zheng Y., Lai J., Luo Q., Ke H., Chen Q. // *PLoS One.* 2016. V. 11. № 12. P. e0168635.
 25. Oishi Y., Watanabe Y., Yoshida Y., Sato Y., Hiraishi T., Oikawa R., Maehata T., Suzuki H., Toyota M., Niwa H., et.al. // *Tumour Biol.* 2012. V. 33. № 2. P. 383–393.
 26. Yang Z., Li D.M., Xie Q., Dai D.Q. // *J. Cancer Res. Clin. Oncol.* 2015. V. 141. № 2. P. 211–220.
 27. Jee C.D., Kim M.A., Jung E.J., Kim J., Kim W.H. // *Eur. J. Cancer.* 2009. V. 45. № 7. P. 1282–1293.
 28. Yu J., Liang Q.Y., Wang J., Cheng Y., Wang S., Poon T.C., Go M.Y., Tao Q., Chang Z., Sung J.J. // *Oncogene.* 2013. V. 32. № 3. P. 307–317.
 29. Wang S., Cheng Y., Du W., Lu L., Zhou L., Wang H., Kang W., Li X., Tao Q., Sung J.J., et.al. // *Gut.* 2013. V. 62. № 6. P. 833–841.
 30. Qu Y., Dang S., Hou P. // *Clin. Chim. Acta.* 2013. V. 424. P. 53–65.
 31. Tamkovich S.N., Vlasov V.V., Laktionov P.P. // *Mol. Biol.* 2008. V. 42. № 1. P. 12–23.

Synthesis and Antiviral Properties of 1-Substituted 3-[ω -(4-Oxoquinazolin-4(3H)-yl)alkyl]uracil Derivatives

M. P. Paramonova¹, A. L. Khandzhinskaya^{2*}, A. A. Ozerov¹, S. N. Kochetkov², R. Snoeck³, G. Andrei³, M. S. Novikov¹

¹Department of Pharmaceutical & Toxicological Chemistry, Volgograd State Medical University, Volgograd, 400131 Russia

²Engelhardt Institute of Molecular Biology, Russian Academy of Science, Moscow, 119991 Russia

³Rega Institute for Medical Research, KU Leuven, B-3000 Leuven, Belgium.

*E-mail: khandzhinskaya@bk.ru

Received May 05, 2020; in final form, May 28, 2020

DOI: 10.32607/actanaturae.10983

Copyright © 2020 National Research University Higher School of Economics. This is an open access article distributed under the Creative Commons Attribution License, which permits unrestricted use, distribution, and reproduction in any medium, provided the original work is properly cited.

ABSTRACT A series of uracil derivatives containing a 4-oxoquinazoline fragment bound to the nitrogen atom N³ of the pyrimidine ring by a short methylene bridge was synthesized to search for new antiviral agents. Some compounds in this series are shown to exhibit high inhibitory activity against human cytomegalovirus and the varicella zoster virus in a HEL cell culture.

KEYWORDS Uracil derivatives, 4-oxoquinazoline, synthesis, antiviral activity, human cytomegalovirus, varicella zoster virus.

ABBREVIATIONS HCMV – human cytomegalovirus; HIV – human immunodeficiency virus; AIDS – acquired immunodeficiency syndrome; VZV – varicella zoster virus; DMF – dimethylformamide.

INTRODUCTION

Human cytomegalovirus (HCMV) is a member of the *Herpesviridae* family and belongs to the *Betaherpesvirinae* subfamily [1]. One of the key characteristics of herpes viruses, including HCMV, is their ability to induce a latent infection that can reactivate when one's immunity is weakened [2]. Up to 90% of the adult urban population is infected with HCMV. The spectrum of diseases associated with HCMV infection ranges from a nearly asymptomatic infection to a severe multiple-organ dysfunction syndrome characterized by significant morbidity and mortality [3]. The risk group for severe HCMV infection includes transplant recipients undergoing immunosuppressive therapy [4], people with HIV infection [5], and children during the prenatal period [6]. Loss of adaptive immunity in transplant recipients and HIV-infected patients is a major risk factor for a disseminated HCMV infection, while it is assumed that immaturity of the fetal immune system predisposes infants infected *in utero* to a severe infection, congenital malformations, and stillbirths [7]. Even with the widespread use of highly active antiretroviral therapy in HIV-infected patients, HCMV is associated with a higher mortality rate not because of AIDS, but due

to cerebrovascular and cardiovascular diseases [8]. In addition, studies have shown that HCMV can cause not only vascular diseases in transplant recipients [9], but also chronic inflammatory diseases such as the inflammatory bowel disease [11], accelerated immune senescence in elderly patients [11], and the development of malignant tumors [12, 13].

Ganciclovir, cidofovir, and foscarnet are the anti-HCMV drugs currently used in clinical practice to treat a HCMV infection [14]. These drugs inhibit the synthesis catalyzed by HCMV polymerase and reduce viral replication in patients presenting the clinical symptoms of an HCMV infection. However, these medicinal products cause a number of adverse effects. In particular, all of them exhibit marked toxicity [15]. In addition, these drugs are characterized by low bioavailability and need to be administered intravenously for a target blood drug concentration to be achieved. Furthermore, long-term therapy is needed for a positive outcome in the treatment of a HCMV infection; in turn, this leads to the emergence of resistant HCMV variants [16–18]. The recently approved letermovir and maribavir drugs have a significantly lower toxicity, but their prolonged use in the treatment and prevention

of HCMV infections also leads to the emergence of resistant HCMV strains [19, 20]. Therefore, searching for new, highly effective anti-HCMV agents is a pressing task.

Earlier, we synthesized a series of 1-[ω -(aryloxy)alkyl]uracil derivatives containing an *N*-(4-phenoxyphenyl)acetamide fragment at the N³ nitrogen atom of the pyrimidine ring. These compounds inhibited the replication of HCMV, VZV [21], and HCV [22]. Replacing the acetamide fragment with a coumarin residue has given rise to a number of compounds that also effectively inhibit the replication of HCMV and VZV [23]. In continuation of our research focused on effective viral replication blockers, we synthesized a number of 1-[ω -(aryloxy)alkyl]uracil derivatives carrying a quinazolin-4(3H)-one moiety bound to the N³ atom in the pyrimidine ring by a linker consisting of two or three methylene groups.

EXPERIMENTAL

All reagents were procured from Sigma and Acros Organics at the highest grade available, and they were used without further purification, unless otherwise indicated. Anhydrous DMF and isopropyl alcohol were purchased from Sigma-Aldrich Co. Anhydrous 1,2-dichloroethane and ethyl acetate were obtained by distillation over P₂O₅. Thin-layer chromatography (TLC) was performed on Merck TLC Silica gel 60 F₂₅₄ plates by eluting with 1 : 1 ethyl acetate–hexane or a 1 : 1 ethyl acetate–1,2-dichloroethane mixture that was developed using a VL-6.LC UV lamp (Vilber). The Acros Organics (Belgium) silica gel (Kieselgur 60–200 μ m, 60 A) was used for column chromatography. Yields refer to spectroscopically (¹H and ¹³C NMR) homogeneous materials. The melting points were determined in glass capillaries on a Mel-Temp 3.0 apparatus (Laboratory Devices Inc., USA). The NMR spectra were recorded using Bruker Avance 400 (400 MHz for ¹H and 100 MHz for ¹³C) and Bruker Avance 600 (600 MHz for ¹H and 150 MHz for ¹³C) spectrometers in DMSO-*d*₆ or CDCl₃ with tetramethylsilane used as an internal standard.

The starting 3-(ω -bromoalkyl)quinazolin-4(3H)-one derivatives **4–7** were obtained in accordance with the previously described methods [24].

General procedure for synthesizing 3-(ω -bromoalkyl)quinazolin-4(3H)-one derivatives **4–7**

A mixture of quinazolin-4(3H)-one **1–3** (27.37 mmol), 1,2-dibromoethane or 1,3-dibromopropane (0.116 mmol), and K₂CO₃ (5.0 g, 36.18 mmol) was stirred in a DMF solution (80 mL) at 70°C for 36 h. The reaction mass was evaporated to dryness in vacuo; the residue was treated with water (100 mL); the solid residue was

filtered off, dried at room temperature, purified by flash chromatography eluting with ethyl acetate; and the fractions containing the product were combined and evaporated under reduced pressure. The residue was recrystallized from a 1 : 2 ethyl acetate–hexane mixture.

3-(2-Bromoethyl)quinazolin-4(3H)-one (4). Yield, 58%; mp, 109.5–111°C; R_f, 0.26 (ethyl acetate–hexane, 1:1). ¹H NMR spectrum (DMSO-*D*₆) δ , ppm, *J* (Hz): 3.86 (2H, t, *J* = 6.3, BrCH₂), 4.40 (2H, t, *J* = 6.3, NCH₂), 7.55 (1H, dt, *J* = 7.2 and 1.1, H-5), 7.69 (1H, d, *J* = 8.1, H-8), 7.84 (1H, dt, *J* = 8.6 and 1.6, H-7), 8.17 (1H, dd, *J* = 9.0 and 1.1, H-6), 8.43 (1H, s, H-2). ¹³C NMR spectrum (DMSO-*D*₆) δ , ppm: 31.1, 47.9, 121.8, 126.5, 127.5, 127.7, 135.0, 148.1, 148.4, 160.6.

3-(3-Bromopropyl)quinazolin-4(3H)-one (5). Yield, 59%; mp, 111–112.5°C; R_f, 0.22 (ethyl acetate–hexane, 1:1). ¹H NMR spectrum (DMSO-*D*₆) δ , ppm, *J* (Hz): 2.27 (2H, q, *J* = 6.8, CH₂), 3.57 (2H, t, *J* = 6.5, BrCH₂), 4.09 (2H, t, *J* = 7.0, NCH₂), 7.53 (1H, dt, *J* = 7.0 and 1.0, H-5), 7.66 (1H, d, *J* = 8.1, H-8), 7.81 (1H, dt, *J* = 7.0 and 1.4, H-7), 8.15 (1H, dd, *J* = 7.9 and 1.2, H-6), 8.35 (1H, s, H-2). ¹³C NMR spectrum (DMSO-*D*₆) δ , ppm: 31.4, 45.0, 121.6, 126.0, 126.9, 127.1, 134.2, 147.9, 160.2.

3-(2-Bromoethyl)-6-methylquinazolin-4(3H)-one (6). Yield, 52%; mp, 157.5–159°C; R_f, 0.27 (ethyl acetate–hexane, 1:1). ¹H NMR spectrum (DMSO-*D*₆) δ , ppm, *J* (Hz): 2.44 (3H, s, CH₃), 3.85 (2H, t, *J* = 6.3, BrCH₂), 4.39 (2H, t, *J* = 6.2, NCH₂), 7.58 (1H, d, *J* = 8.3, H-7), 7.65 (1H, dd, *J* = 8.4 and 2.0, H-8), 7.95 (1H, t, *J* = 0.8, H-5), 8.37 (1H, s, H-2). ¹³C NMR spectrum (DMSO-*D*₆) δ , ppm: 21.3, 31.1, 40.6, 47.9, 125.9, 127.3, 136.2, 136.3, 137.5, 146.0, 147.7.

3-(2-Bromoethyl)-7-chloroquinazolin-4(3H)-one (7). Yield, 63%; mp, 138.5–140°C; R_f, 0.41 (ethyl acetate–hexane, 1:1). ¹H NMR spectrum (DMSO-*D*₆) δ , ppm, *J* (Hz): 3.81 (2H, t, *J* = 6.3, BrCH₂), 4.36 (2H, t, *J* = 6.2, NCH₂), 7.56 (1H, dd, *J* = 8.5 and 1.9, H-5), 7.72 (1H, d, *J* = 1.7, H-8), 8.13 (1H, d, *J* = 8.6, H-6), 8.41 (1H, s, H-2). ¹³C NMR spectrum (DMSO-*D*₆) δ , ppm: 30.5, 47.4, 120.2, 126.4, 127.4, 128.1, 139.2, 148.9, 149.3, 159.6.

General procedure for synthesizing 1-[ω -(4-bromophenoxy)alkyl]-3-[ω' -(4-oxoquinazolin-4(3H)-yl)alkyl]uracil derivatives **9–18**

A suspension of 1-[ω -(4-bromophenoxy)alkyl]uracil derivative **8** (1.538 mmol) and K₂CO₃ (0.3 g, 2.171 mmol) was stirred in a DMF solution (10 mL) at 80°C for 1 h; bromide **4–7** (1.541 mmol) was added, and the resulting mixture was stirred at the same temperature for

24 h. The reaction mass was evaporated in vacuo; the residue was treated with water (100 mL); the solid residue was filtered off, dried at room temperature, and purified by flash chromatography on silica gel eluting with ethyl acetate; the fractions containing the product were combined and evaporated under reduced pressure; the residue was recrystallized from a 1 : 1 ethyl acetate–1,2-dichloroethane mixture.

1-[3-(4-Bromophenoxy)propyl]-3-[2-(4-oxoquinazolin-4(3H)-yl)ethyl]uracil (9). Yield, 78%; mp, 178.5–179.5°C; R_f , 0.45 (1,2-dichloroethane–MeOH, 10:1). ^1H NMR spectrum (DMSO- D_6) δ , ppm, J (Hz): 1.82 (2H, q, $J = 6.3$, CH_2), 3.72 (2H, t, $J = 6.6$, N^1CH_2), 3.86 (2H, t, $J = 6.2$, OCH_2), 4.15–4.20 (4H, m, $\text{CH}_2 \times 2$), 5.52 (1H, d, $J = 7.8$, H^5), 6.83 (2H, d, $J = 9.1$, H-3', H-5'), 7.40 (2H, d, $J = 9.0$, H-2', H-6'), 7.45 (1H, dt, $J = 7.6$ and 1.0, H-5''), 7.54 (1H, d, $J = 7.9$, H^6), 7.58 (1H, d, $J = 8.1$, H-8''), 7.74 (1H, dt, $J = 7.7$ and 1.5, H-7''), 8.03 (1H, dd, $J = 8.0$ and 1.2, H-6''), 8.18 (1H, s, H-2''). ^{13}C NMR spectrum (DMSO- D_6) δ , ppm: 27.8, 44.4, 46.9, 65.5, 100.4, 112.5, 117.3, 121.9, 126.5, 127.3, 127.6, 132.6, 134.6, 145.0, 148.2, 151.6, 158.1, 161.1, 163.0.

1-[4-(4-Bromophenoxy)butyl]-3-[2-(4-oxoquinazolin-4(3H)-yl)ethyl]uracil (10). Yield, 76%; mp, 191–192°C; R_f , 0.45 (1,2-dichloroethane–MeOH, 10:1). ^1H NMR spectrum (DMSO- D_6) δ , ppm, J (Hz): 1.47–1.56 (4H, m, $\text{CH}_2 \times 2$), 3.59 (2H, t, $J = 6.3$, N^1CH_2), 3.81 (2H, t, $J = 6.0$, OCH_2), 4.17–4.22 (4H, m, $\text{CH}_2 \times 2$), 5.57 (1H, d, $J = 7.9$, H^5), 6.84 (2H, d, $J = 9.0$, H-3', H-5'), 7.40 (2H, d, $J = 9.0$, H-2', H-6'), 7.42 (1H, dt, $J = 7.2$ and 1.2, H-5''), 7.56 (1H, d, $J = 8.1$, H-8''), 7.61 (1H, d, $J = 7.9$, H^6), 7.71 (1H, dt, $J = 7.7$ and 1.5, H-7''), 8.04 (1H, dd, $J = 8.0$ and 1.1, H-6''), 8.17 (1H, s, H-2''). ^{13}C NMR spectrum (DMSO- D_6) δ , ppm: 25.2, 25.8, 44.4, 48.9, 67.8, 100.4, 112.3, 117.2, 121.9, 126.5, 127.2, 127.5, 132.6, 134.5, 144.9, 148.2, 148.3, 151.7, 158.3, 161.1, 162.9.

1-[5-(4-Bromophenoxy)pentyl]-3-[2-(4-oxoquinazolin-4(3H)-yl)ethyl]uracil (11). Yield, 73%; mp, 174.5–176°C; R_f , 0.47 (1,2-dichloroethane–MeOH, 10:1). ^1H NMR spectrum (DMSO- D_6) δ , ppm, J (Hz): 1.23 (2H, q, $J = 5.6$, CH_2), 1.38 (2H, q, $J = 7.0$, CH_2), 1.58 (2H, q, $J = 7.3$, CH_2), 3.54 (2H, t, $J = 7.1$, N^1CH_2), 3.86 (2H, t, $J = 6.2$, OCH_2), 4.16–4.20 (4H, m, $\text{CH}_2 \times 2$), 5.55 (1H, d, $J = 7.9$, H^5), 6.85 (2H, d, $J = 9.0$, H-3', H-5'), 7.39 (2H, d, $J = 9.0$, H-2', H-6'), 7.44 (1H, dt, $J = 7.5$ and 1.2, H-5''), 7.55–7.60 (2H, m, H^6 , H-8''), 7.71 (1H, dt, $J = 7.9$ and 1.6, H-7''), 8.05 (1H, ddd, $J = 7.9$, 1.5 and 0.4, H-6''), 8.16 (1H, s, H-2''). ^{13}C NMR spectrum (DMSO- D_6) δ , ppm: 22.6, 28.2, 28.5, 44.4, 49.1, 68.0, 100.4, 112.2, 117.3, 122.0, 126.5, 127.2, 127.5, 132.6, 134.5, 144.9, 148.2, 148.4, 151.6, 158.4, 161.0, 162.3.

1-[6-(4-Bromophenoxy)hexyl]-3-[2-(4-oxoquinazolin-4(3H)-yl)ethyl]uracil (12). Yield, 78%; mp, 178.5–179.5°C; R_f , 0.48 (1,2-dichloroethane–MeOH, 10:1). ^1H NMR spectrum (DMSO- D_6) δ , ppm, J (Hz): 1.32 (2H, q, $J = 6.5$, CH_2), 1.58–1.70 (4H, m, $\text{CH}_2 \times 2$), 1.94 (2H, q, $J = 7.1$, CH_2), 3.68 (2H, t, $J = 7.1$, N^1CH_2), 3.84 (2H, t, $J = 7.0$, OCH_2), 3.87–3.98 (4H, m, $\text{CH}_2 \times 2$), 5.64 (1H, d, $J = 7.9$, H^5), 6.81 (2H, d, $J = 9.0$, H-3', H-5'), 7.35 (2H, d, $J = 9.0$, H-2', H-6'), 7.49 (1H, dt, $J = 7.5$ and 1.2, H-5''), 7.58 (1H, dd, $J = 7.6$ and 0.5, H-8''), 7.65 (1H, d, $J = 7.9$, H^6), 7.78 (1H, dt, $J = 7.8$ and 1.7, H-7''), 8.05 (1H, dd, $J = 8.0$ and 1.1, H-6''), 8.37 (1H, s, H-2''). ^{13}C NMR spectrum (DMSO- D_6) δ , ppm: 22.8, 27.5, 28.5, 28.6, 38.2, 44.5, 48.9, 68.0, 100.6, 112.2, 117.2, 122.0, 126.5, 127.4, 127.6, 132.5, 134.6, 144.6, 148.4, 151.5, 158.4, 160.6, 162.9.

1-[8-(4-Bromophenoxy)octyl]-3-[2-(4-oxoquinazolin-4(3H)-yl)ethyl]uracil (13). Yield, 77%; mp, 171.5–173°C; R_f , 0.33 (ethyl acetate). ^1H NMR spectrum (DMSO- D_6) δ , ppm, J (Hz): 1.15–1.36 (10H, m, $\text{CH}_2 \times 5$), 1.68 (2H, q, $J = 7.1$, CH_2), 3.54 (2H, t, $J = 6.9$, N^1CH_2), 3.94 (2H, t, $J = 6.3$, OCH_2), 4.23 (4H, s, $\text{CH}_2 \times 2$), 5.60 (1H, d, $J = 7.8$, H^5), 6.89 (2H, d, $J = 8.6$, H-3', H-5'), 7.42 (2H, d, $J = 8.6$, H-2', H-6'), 7.49 (1H, t, $J = 7.5$, H-5''), 7.61–7.64 (2H, m, H-8'', H^6), 7.78 (1H, t, $J = 7.5$, H-7''), 8.09 (1H, d, $J = 7.8$, H-6''), 8.20 (1H, s, H-2''). ^{13}C NMR spectrum (DMSO- D_6) δ , ppm: 25.8, 26.0, 28.4, 29.0, 40.6, 44.4, 49.2, 68.2, 100.3, 112.2, 117.2, 121.9, 126.5, 127.2, 127.5, 132.5, 134.5, 144.9, 148.2, 151.6, 158.4, 161.0, 162.9.

1-[10-(4-Bromophenoxy)decyl]-3-[2-(4-oxoquinazolin-4(3H)-yl)ethyl]uracil (14). Yield, 80%; mp, 161–162°C; R_f , 0.38 (ethyl acetate). ^1H NMR spectrum (DMSO- D_6) δ , ppm, J (Hz): 1.15–1.40 (14H, m, $\text{CH}_2 \times 7$), 1.70 (2H, q, $J = 7.3$, CH_2), 3.54 (2H, t, $J = 7.1$, N^1CH_2), 3.94 (2H, t, $J = 6.5$, OCH_2), 4.20–4.24 (4H, m, $\text{CH}_2 \times 2$), 5.60 (1H, d, $J = 7.8$, H^5), 6.90 (2H, d, $J = 9.1$, H-3', H-5'), 7.43 (2H, d, $J = 9.0$, H-2', H-6'), 7.50 (1H, t, $J = 7.0$, H-5''), 7.62 (1H, d, $J = 7.5$, H-8''), 7.64 (1H, d, $J = 7.9$, H^6), 7.77 (1H, dt, $J = 8.6$ and 1.6, H-7''), 8.09 (1H, dd, $J = 7.9$ and 1.1, H-6''), 8.21 (1H, s, H-2''). ^{13}C NMR spectrum (DMSO- D_6) δ , ppm: 25.9, 26.1, 28.4, 28.96, 29.02, 29.16, 29.22, 29.3, 44.4, 49.2, 68.2, 100.3, 112.2, 117.2, 121.9, 126.5, 127.2, 127.5, 132.5, 134.5, 144.9, 148.2, 148.3, 151.6, 158.4, 161.0, 163.0.

1-[12-(4-Bromophenoxy)dodecyl]-3-[2-(4-oxoquinazolin-4(3H)-yl)ethyl]uracil (15). Yield, 73%; mp, 150–152°C; R_f , 0.39 (ethyl acetate). ^1H NMR spectrum (DMSO- D_6) δ , ppm, J (Hz): 1.17–1.41 (18H, m, $\text{CH}_2 \times 9$), 1.70 (2H, q, $J = 7.6$, CH_2), 3.56 (2H, t, $J = 7.3$, N^1CH_2), 3.95 (2H, t, $J = 6.5$, OCH_2), 4.21–4.26 (4H, m, $\text{CH}_2 \times 2$), 5.58 (1H, d, $J = 7.9$, H^5), 6.89 (2H, d, $J = 9.0$, H-3', H-5'), 7.41

(2H, d, $J = 9.0$, H-2', H-6'), 7.49 (1H, dt, $J = 7.1$ and 1.1 , H-5"), 7.60 (1H, d, $J = 7.8$, H-8"), 7.62 (1H, d, $J = 7.9$, H⁶), 7.78 (1H, dt, $J = 8.5$ and 1.6 , H-7"), 8.11 (1H, dd, $J = 7.9$ and 1.2 , H-6"), 8.17 (1H, s, H-2"). ¹³C NMR spectrum (DMSO-D₆) δ , ppm: 25.9, 26.2, 28.5, 29.0, 29.15, 29.24, 29.3, 44.4, 49.2, 68.4, 100.4, 112.2, 117.3, 122.0, 126.5, 127.2, 127.5, 132.5, 134.4, 144.8, 148.1, 148.4, 151.6, 158.6, 161.0, 162.9.

1-[5-(4-Bromophenoxy)pentyl]-3-[2-(7-chloro-4-oxoquinazolin-4(3H)-yl)ethyl]uracil (16). Yield, 82%; mp, 154–155°C; R_f , 0.59 (1,2-dichloroethane-MeOH, 10:1). ¹H NMR spectrum (DMSO-D₆) δ , ppm, J (Hz): 1.24 (2H, q, $J = 8.0$, CH₂), 1.37 (2H, q, $J = 7.5$, CH₂), 1.59 (2H, q, $J = 7.6$, CH₂), 3.55 (2H, t, $J = 7.3$, N¹CH₂), 3.88 (2H, t, $J = 6.5$, OCH₂), 4.17–4.20 (4H, m, CH₂ × 2), 5.57 (1H, d, $J = 7.8$, H⁵), 6.87 (2H, d, $J = 8.9$, H-3', H-5'), 7.40 (2H, d, $J = 8.9$, H-2', H-6'), 7.49 (1H, dd, $J = 8.5$ and 1.9 , H-5"), 7.61 (1H, d, $J = 7.9$, H⁶), 7.65 (1H, d, $J = 1.8$, H-8"), 8.05 (1H, d, $J = 8.6$, H-6), 8.25 (1H, s, H-2"). ¹³C NMR spectrum (DMSO-D₆) δ , ppm: 22.1, 27.7, 28.1, 44.1, 48.6, 67.5, 99.8, 111.7, 116.7, 120.2, 126.2, 127.1, 128.1, 132.1, 138.8, 144.5, 148.9, 149.2, 151.1, 157.9, 160.0, 162.4.

1-[5-(4-Bromophenoxy)pentyl]-3-[3-(4-oxoquinazolin-4(3H)-yl)propyl]uracil (17). Yield, 87%; mp, 103.5–104.5°C; R_f , 0.48 (1,2-dichloroethane-MeOH, 10:1). ¹H NMR spectrum (DMSO-D₆) δ , ppm: 1.31 (2H, q, $J = 5.6$, CH₂), 1.36–1.70 (4H, m, CH₂ × 2), 1.94 (2H, q, $J = 7.0$, CH₂), 3.68 (2H, t, $J = 7.1$, N¹CH₂), 3.81–3.91 (4H, m, CH₂ × 2), 3.95 (2H, t, $J = 7.3$, OCH₂), 5.64 (1H, d, $J = 7.9$, H⁵), 6.81 (2H, d, $J = 9.0$, H-3', H-5'), 7.34 (2H, d, $J = 9.0$, H-2', H-6'), 7.48 (1H, dt, $J = 7.5$ and 1.1 , H-5"), 7.61 (1H, dd, $J = 7.6$ and 0.5 , H-8"), 7.64 (1H, d, $J = 7.9$, H⁶), 7.77 (1H, dt, $J = 7.7$ and 1.6 , H-7"), 8.05 (1H, dd, $J = 8.0$ and 1.1 , H-6"), 8.37 (1H, s, H-2"). ¹³C NMR spectrum (DMSO-D₆) δ , ppm: 22.8, 27.5, 28.5, 28.6, 38.3, 44.5, 49.0, 68.0, 100.6, 112.2, 117.2, 122.0, 126.5, 127.4, 127.6, 132.5, 134.6, 144.6, 148.4, 151.5, 158.4, 160.6, 162.9.

1-[5-(4-Bromophenoxy)pentyl]-3-[2-(6-methyl-4-oxoquinazolin-4(3H)-yl)ethyl]uracil (18). Yield, 79%; mp 180–181.5°C; R_f , 0.29 (ethyl acetate). ¹H NMR spectrum (DMSO-D₆) δ , ppm: 1.28 (2H, q, $J = 6.5$, CH₂), 1.39 (2H, q, $J = 6.8$, CH₂), 1.60 (2H, q, $J = 7.2$, CH₂), 2.40 (3H, s, CH₃), 3.58 (2H, t, $J = 7.1$, N¹CH₂), 3.89 (2H, t, $J = 6.4$, OCH₂), 4.21 (4H, m, CH₂ × 2), 5.61 (1H, d, $J = 7.8$, H⁵), 6.89 (2H, d, $J = 9.1$, H-3', H-5'), 7.44 (2H, d, $J = 9.0$, H-2', H-6'), 7.51 (1H, d, $J = 8.3$, H-7"), 7.58 (1H, dd, $J = 8.3$ and 1.9 , H-8"), 7.64 (1H, d, $J = 7.9$, H⁶), 7.88 (1H, s, H-5"), 8.15 (1H, s, H-2"). ¹³C NMR spectrum (DMSO-D₆) δ , ppm: 21.2, 22.6, 28.2, 28.5, 44.3, 49.1, 67.9, 100.3, 112.2, 117.2, 121.7, 125.8, 127.4, 132.6, 135.8, 137.0, 144.9, 146.3, 147.4, 151.6, 158.4, 161.0, 162.9.

Antiviral assays

The compounds were evaluated against human cytomegalovirus (HCMV, strains AD-169 and Davis) and the varicella zoster virus (VZV, strains OKA and YS). The antiviral assays were based on the inhibition of virus-induced cytopathicity or plaque formation in human embryonic lung (HEL) fibroblasts. Confluent cell cultures in 96-well microplates were inoculated with 100 CCID₅₀ of the virus (1 CCID₅₀ being the virus dose to infect 50% of the cell culture) or 10 or 100 plaque-forming units (PFU) (for VZV and HCMV) in the presence of varied concentrations of the test compounds. Viral cytopathicity or plaque formation was recorded as soon as it reached completion in the control virus-infected cell cultures not treated with the test compounds. Antiviral activity was expressed as the EC₅₀ or compound concentration required to reduce virus-induced cytopathogenicity or viral plaque formation by 50%.

Cytostatic activity assays

All assays were performed in 96-well microplates. A given amount of the test compound and $(5-7.5) \times 10^4$ tumor cells were added to each well. The cells were allowed to proliferate for 48 h (murine leukemia L1210 cells) or 72 h (human lymphocytic CEM and human cervix carcinoma HeLa cells) at 37°C in a humidified CO₂-controlled atmosphere. At the end of the incubation period, the cells were counted using a Coulter counter. The IC₅₀ (50% inhibitory concentration) was defined as the concentration of the compound that inhibited cell proliferation by 50%.

RESULTS AND DISCUSSION

Synthesis of the compounds

The compounds in this series were synthesized according to *Scheme*. The starting 3-(ω -bromoalkyl)-quinazolin-4(3H)-one **4-7** derivatives were obtained in accordance with the previously described method [24]. Treating quinazolin-4(3H)-ones **1-3** with a 4-fold molar excess of 1,2-dibromoethane or 1,3-dibromopropane in a DMF solution in the presence of K₂CO₃ gave rise to the corresponding bromides **4-7** with 52–63% yields. The 1-[ω -(4-bromophenoxy)alkyl]uracil derivatives described earlier [25] were treated with bromides **4-7** in the DMF solution in the presence of K₂CO₃ to give the target 3-[ω -(4-oxoquinazolin-4(3H)-yl)alkyl]uracils **9-18** with yields of 73–87%.

Antiviral properties

The antiviral properties of the 3-[ω -(4-oxoquinazolin-3-(4H)-yl)alkyl] derivatives of uracil **9-18** against cytomegalovirus (HCMV, AD-169 and Davis strains)

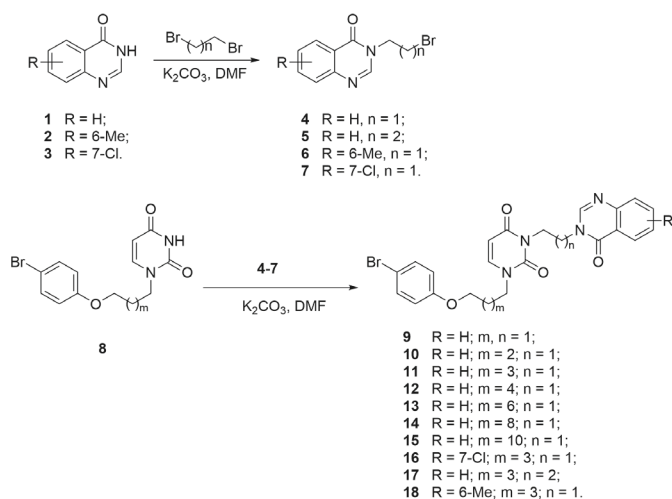
Anti-HCMV activity of 3-[ω-(4-oxoquinazolin-4(3H)-yl)alkyl]uracil derivatives **9–18** in the HEL cell culture

Compound	Antiviral activity, EC ₅₀ /μM ^a				Cytotoxicity	
	HCMV AD-169	HCMV Davis	VZV Oka (TK ⁺)	VZV 07-1 (TK ⁻)	Cell morphology MCC/μM ^b	Cell growth CC ₅₀ /μM ^c
9 (Z779)	> 100	> 100	> 100	> 100	100	-
10 (Z780)	> 20	> 100	> 20	> 100	20	-
11 (Z785)	> 20	> 20	> 20	> 100	100	-
12 (Z786)	> 100	> 20	> 100	> 100	100	-
13 (Z796)	100	> 100	> 100	> 100	> 100	12.8
14 (Z797)	> 100	> 100	> 100	> 100	> 100	> 100
15 (Z798)	> 100	> 100	> 100	> 100	≥ 100	> 100
16 (Z770)	> 20	> 20	> 20	> 100	20	-
17 (Z696)	7.31	5.23	28.96	28.96	20	1.81
18 (Z799)	> 100	> 100	>100	> 100	> 100	> 100
Ganciclovir	2.4	2.01	-	-	350	196.41
Cidofovir	0.38	0.38	-	-	300	129.43
Acyclovir	-	-	1.6	30.37	> 440	> 100
Brivudine	-	-	0.039	6.04	> 300	> 100

^a Effective concentration required to reduce virus plaque formation by 50%.

^b Minimum cytotoxic concentration that causes a microscopically detectable alteration of cell morphology.

^c Cytotoxic concentration required to reduce cell growth by 50%.



and the varicella zoster virus (VZV, OKA and 07-1 strains) were tested in the HEL cell culture. The results are presented in *Table*. Compound **17** exhibited significant anti-HCMV activity: it blocked viral replication at concentrations (EC₅₀) of 7.31 μM (AD-169 strain) and 5.23 μM (Davis strain). However, any structure

modification, such as changing the length of the bridge *m*, either increasing (compounds **12–15**) or decreasing (compounds **9** and **10**), reducing the length of the bridge *n* (compound **11**) or inserting substituents in the quinazoline moiety (compounds **16** and **18**), led to a complete loss of inhibitory properties against HCMV. Compound **17** also showed some inhibitory activity against the varicella zoster virus (VZV) and inhibited the replication of both strains of VZV at a concentration (EC₅₀) of 28.96 μM. The remaining compounds were inactive (see *Table*).

CONCLUSIONS

Thus, we have discovered an efficient inhibitor of HCMV and VZV replication in a cell culture which contains a 4-oxoquinazoline moiety linked to the uracil residue by a chain consisting of three methylene groups. Compound **17** can be a platform to perform targeted searches of anti-HCMV drugs. ●

This work was supported by the Russian Foundation for Basic Research (project № 19-015-00094 A). The biological part of the work was supported by KU Leuven.

REFERENCES

1. Cytomegaloviruses. From molecular pathogenesis to intervention. Edited by M.J. Reddehase, N.A.W. Lemmermann, Caister Academic Press, Norfolk, 2013.
2. Griffiths P.D. // *J. Virol. Methods*. 1988. V. 21. P. 79–86.
3. Zanghellini F, Boppana S.B., Emery V.C., Griffiths P.D., Pass R.F. // *J. Infect. Dis.* 1999. V. 180. P. 702–707.
4. Fehr T, Cippà P.E., Mueller N.J. // *Transpl. Int.* 2015. V. 28. P. 1351–1356.
5. Gianella S., Letendre S. // *J. Infect. Dis.* 2016. V. 214. Suppl. 2. P. S67–S74.
6. Griffiths P., Baraniak I., Reeves M. // *J. Pathol.* 2015. V. 235. P. 288–297.
7. Pereira L. // *J. Infect. Dis.* 2011. V. 203. P. 1510–1512.
8. Lichtner M., Cicconi P., Vita S., et al. // *J. Infect. Dis.* 2015. V. 211. P. 178–186.
9. Weis M., Kledal T.N., Lin K.Y., et al // *Circulation*. 2004. V. 109. P. 500–505.
10. Pillet S., Pozzetto B., Roblin X. // *World J. Gastroenterol.* 2016. V. 22. P. 2030–2045.
11. Effros R.B. // *Mech. Ageing. Dev.* 2016. V. 158. P. 46–52.
12. Herbein G. // *Viruses*. 2018. V. 10. P. 408.
13. Elgert P.A., Yee-Chang M., Simsir A. // *Diagn. Cytopathol.* 2018. V. 46. P. 593–599.
14. Ahmed A. // *Infect. Disord. Drug Targets*. 2011. V. 11. P. 475–503.
15. Bedard J., May S., Lis M., et al // *Antimicrob. Agents Chemother.* 1999. V. 43. P. 557–567.
16. Smith I.L., Taskintuna I., Rahhal F.M., et al // *Arch. Ophthalmol.* 1998. V. 116. P. 178–185.
17. Limaye A.P., Corey L., Koelle D.M., Davis C.L., Boeckh M. // *Lancet*. 2000. V. 356. P. 645–649.
18. Weinberg A., Jabs D.A., Chou S., et al // *J. Infect. Dis.* 2003. V. 187. P. 777–784.
19. Gerna G., Lilleri D., Baldanti F. // *Expert Opin. Pharmacother.* 2019. V. 20. P. 1429–1438.
20. Piret J., Boivin G. // *Antiviral Res.* 2019. V. 163. P. 91–105.
21. Babkov D.A., Khandazhinskaya A.L., Chizhov A.O., et al // *Bioorg. Med. Chem.* 2015. V. 23. P. 7035–7044.
22. Magri A., Ozerov A.A., Tunitskaya V., et al // *Sci. Report.* 2016. V. 6. P. 29487.
23. Paramonova M.P., Ozerov A.A., Chizhov A.O., et al // *Mendeleev Commun.* 2019. V. 29. P. 638–639.
24. Liu G., Liu C.P., Ji C.N., et al // *Asian J. Chem.* 2013. V. 25. P. 9853–9856.
25. Novikov M.S., Babkov D.A., Paramonova M.P., et al // *Bioorg. Med. Chem.* 2013. V. 21. P. 4151–4157.

UDK 577.152.1

Identification of a Novel Substrate-Derived Spermine Oxidase Inhibitor

T. T. Dunston¹, M. A. Khomutov², S. B. Gabelli^{1,3,4}, T. M. Stewart¹, J. R. Foley¹, S. N. Kochetkov², A. R. Khomutov^{2*}, R. A. Casero Jr.^{1*}

¹Sidney Kimmel Comprehensive Cancer Center, The Johns Hopkins University School of Medicine, Baltimore, MD 21287 USA

²Engelhardt Institute of Molecular Biology, Russian Academy of Sciences, Moscow, 119991 Russia

³Department of Medicine, The Johns Hopkins University School of Medicine, Baltimore, MD 21205, USA

⁴Department of Oncology, The Johns Hopkins University School of Medicine, Baltimore, MD 21287, USA

*E-mail: alexkhom@list.ru, rcasero@jhmi.edu

Received May 08, 2020; in final form, July 07, 2020

DOI: 10.32607/actanaturae.10992

Copyright © 2020 National Research University Higher School of Economics. This is an open access article distributed under the Creative Commons Attribution License, which permits unrestricted use, distribution, and reproduction in any medium, provided the original work is properly cited.

ABSTRACT Homeostasis of the biogenic polyamines spermine (Spm) and spermidine (Spd), present in μM - mM concentrations in all eukaryotic cells, is precisely regulated by coordinated activities of the enzymes of polyamine synthesis, degradation, and transport, in order to sustain normal cell growth and viability. Spermine oxidase (SMOX) is the key and most recently discovered enzyme of polyamine metabolism that plays an essential role in regulating polyamine homeostasis by catalyzing the back-conversion of Spm to Spd. The development of many types of epithelial cancer is associated with inflammation, and disease-related inflammatory stimuli induce SMOX. MDL72527 is widely used *in vitro* and *in vivo* as an irreversible inhibitor of SMOX, but it is also potent towards N^1 -acetylpolyamine oxidase. Although SMOX has high substrate specificity, Spm analogues have not been systematically studied as enzyme inhibitors. Here we demonstrate that 1,12-diamino-2,11-bis(methylidene)-4,9-diazadodecane (2,11-Met₂-Spm) has, under standard assay conditions, an IC₅₀ value of 169 μM towards SMOX and is an interesting instrument and lead compound for studying polyamine catabolism.

KEYWORDS Spermine oxidase, inhibitors, MDL72527, spermine analogues, 2,11-Met₂-Spm.

ABBREVIATIONS Spm – spermine; Spd – spermidine; SMOX – spermine oxidase; PAOX – N^1 -acetylpolyamine oxidase; MDL72527 – $\{N^1, N^4$ -*bis*(2,3-butadienyl)-1,4-butanediamine $\}$; 2,11-Met₂-Spm – 1,12-diamino-2,11-bis(methylidene)-4,9-diazadodecane; 2,11-Me₂-Spm – 1,12-diamino-2,11-dimethyl-4,9-diazadodecane.

INTRODUCTION

The biogenic polyamines spermine (Spm) and spermidine (Spd), and their diamine precursor putrescine (Put), are organic polycations present in all eukaryotic cells in μM - mM concentrations that *a priori* determine the diversity of their functions, many of which are vitally important [1, 2]. Polyamine intracellular levels are strictly controlled by precise regulation of the activity, biosynthesis and degradation of key enzymes of their metabolism. Polyamines are tightly involved in these regulatory processes, and the cell spends considerable energy to maintain polyamine homeostasis [3]. Disturbances of polyamine metabolism and homeostasis are associated with many diseases [1–6], but they may be most essential to cancer cells, which can have

elevated requirements for polyamines. Compounds capable of specifically decreasing the polyamine pool have potential as anticancer drugs [5] and for chemoprevention [6].

FAD-dependent spermine oxidase (SMOX, *Fig. 1*) converts Spm to Spd with the formation of hydrogen peroxide, a source of ROS, and 3-aminopropanal, which can spontaneously form highly toxic acrolein (*Fig. 1*). SMOX has been demonstrated to contribute to cancer, including prostate, colon and gastric cancer induced by infection and inflammation [7–9]. In gastric cancer, *Helicobacter pylori* infection induces SMOX in gastric epithelial cells that results in the generation of hydrogen peroxide and acrolein-producing 3-aminopropanal; these lead to DNA damage and apoptosis [10].

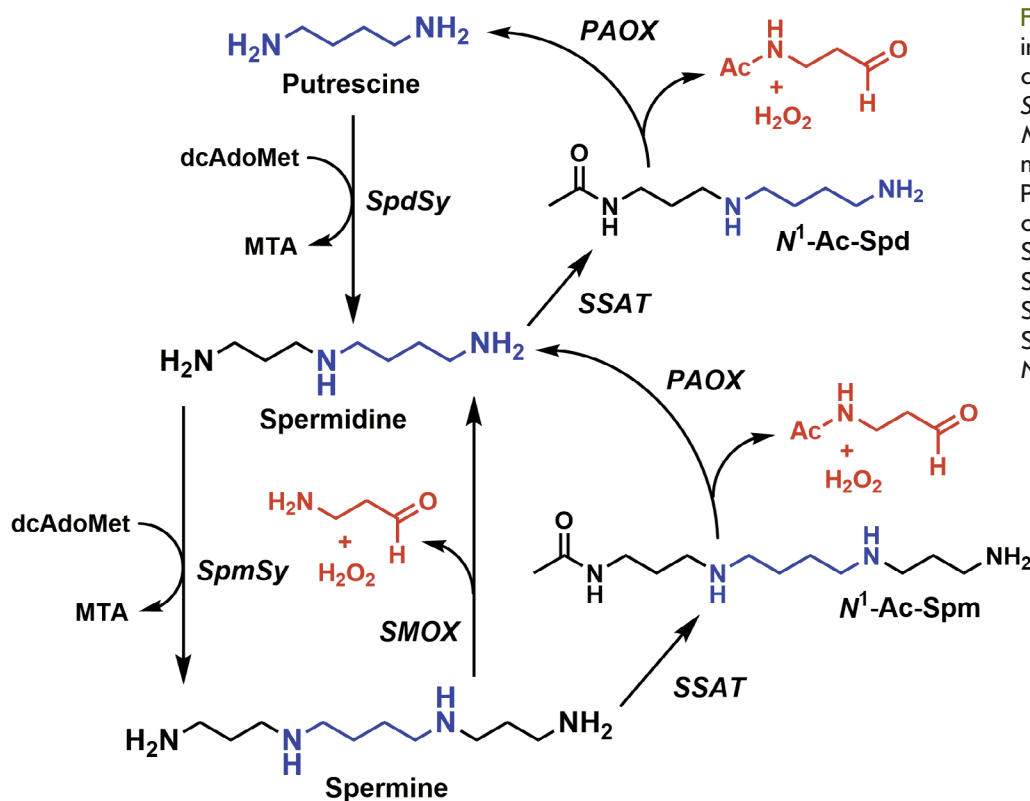


Fig. 1. Polyamine interconversions. dcAdoMet – decarboxylated S-adenosylmethionine; MTA – 5'-deoxy-5'-methylthioadenosine; PAOX – N¹-acetylpolyamine oxidase; SMOX – spermine oxidase; SpdSy – spermidine synthase; SpmSy – spermine synthase; SSAT – spermidine/spermine-N¹-acetyltransferase

Inhibition of SMOX with the N¹-acetylpolyamine oxidase (PAOX, Fig. 1) irreversible inhibitor MDL72527 {N¹,N⁴-(bis(2,3-butadienyl)-1,4-butanediamine)} [11], which has an IC₅₀ value of 90 μM towards SMOX, reduces these effects [8, 9]. However, in some cases it is necessary to discriminate the individual impact of SMOX and PAOX in an integral biological effect or development of the disease and MDL72527, which has been successfully and widely used for decades and inhibits both enzymes. Specific, effective and irreversible inhibitors of SMOX are lacking, partly because the X-ray structure of the enzyme is not available. The analysis of structure/activity relationships of polyamine analogues for PAOX and SMOX has indicated that both enzymes recognize two positively charged amino groups and have hydrophobic pocket(s) located close to the substrate binding site [12]. Therefore, a number of N-substituted diamines were investigated as potential inhibitors of SMOX. However, the problem of specific inhibition of each enzyme has still not been completely solved.

C9-4 (N¹-nonyl-1,4-diaminobutane) is a Put derivative having an IC₅₀ value of 2.6 μM towards PAOX and an IC₅₀ value of 88 μM towards SMOX. This compound reduced the volume of brain infarction in a mouse model more effectively than MDL72527 [13]. The *nor*-Spd derivative SI-4650 (N-(3-{[3-(dimethylamino)

propyl]amino}propyl)-8-quinolinecarboxamide) has an IC₅₀ value of 380 μM towards SMOX and an IC₅₀ value of 35 μM towards PAOX. SI-4650 inhibited cell growth, induced apoptosis, and promoted autophagy, making it a compound of interest for cancer treatment [12]. Recently, among a family of N-substituted 3,5-diamino-1,2,4-triazoles, an efficient and specific inhibitor of SMOX, N⁵-(2-([1,1'-biphenyl]-4-yloxy)benzyl)-1H-1,2,4-triazole-3,5-diamine, was identified as having an IC₅₀ value of 25 μM (the compound had an IC₅₀ value of >200 μM towards PAOX); this compound efficiently inhibited SMOX in cell culture [14]. Currently, this is the one compound that is significantly more effective towards SMOX than PAOX. Moreover, this N-substituted 3,5-diamino-1,2,4-triazole is 3.5-fold more potent against SMOX *in vitro* if compared with MDL72527 and is a promising tool to study the effects of specific SMOX inhibition on polyamine metabolism [14].

Properly designed Spm derivatives/analogues have never been widely studied as specific inhibitors of SMOX. However, taking into consideration that Spm is a substrate of SMOX and not a substrate of PAOX, one may expect that Spm derivatives may be a useful source of specific SMOX inhibitors. In the present paper, we started such investigations using 2,11-Met₂-Spm (Fig. 2A) for the inhibition of SMOX.

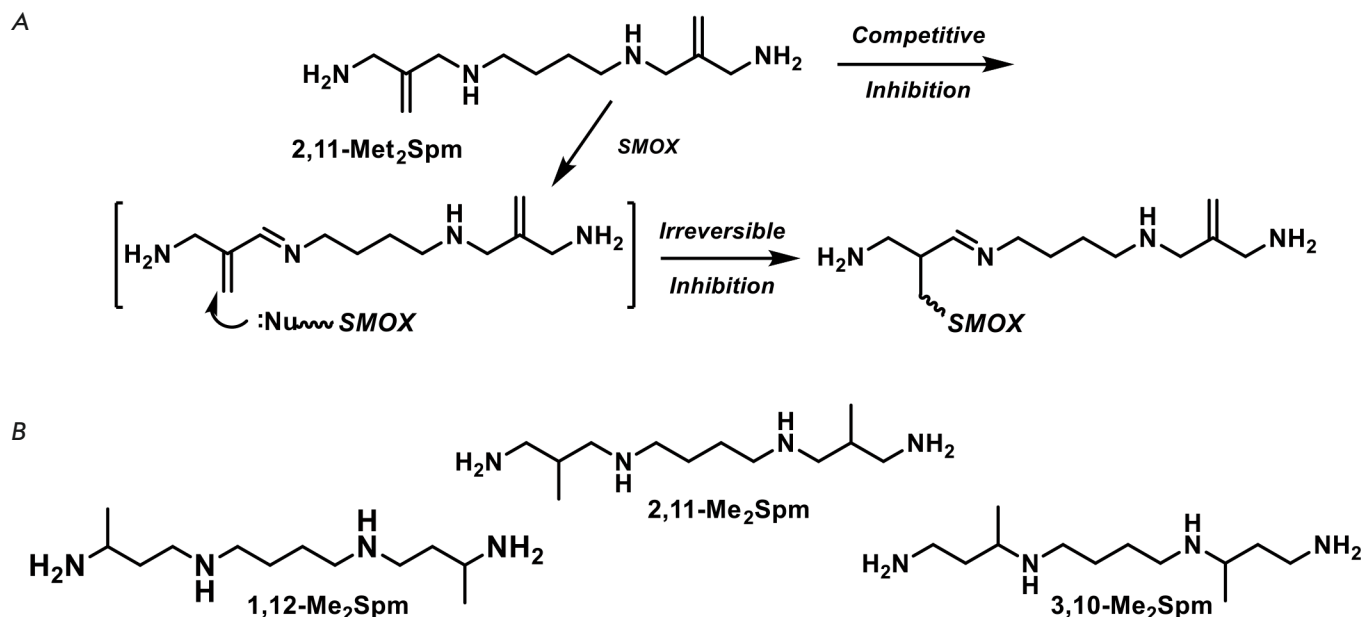


Fig. 2. (A) Possible mechanism of SMOX inhibition with 2,11-Met₂-Spm. (B) Structures of bis-methylated Spm analogues: 1,12-Me₂-Spm, 2,11-Me₂-Spm and 3,10-Me₂-Spm

EXPERIMENTAL

Materials

1,12-Diamino-2,11-bis(methylidene)-4,9-diazadodecane tetrahydrochloride (2,11-Met₂-Spm) was synthesized essentially as described in [15] starting from 2-chloromethyl-3-chloropropene-1 (Aldrich), which was reacted with potassium phthalimide to give 1-phthalimido-2-methylidene-3-chloropropane, which was used to alkylate bis-*N*¹,*N*⁴-2-nitrophenylsulfonyl-1,4-diaminobutane. Subsequent removal of protecting groups resulted in 2,11-Met₂-Spm in a good overall yield.

Protein expression and purification

The bacterial expression vector pET15b carrying the gene coding for the human SMOX protein was used to transform and express SMOX in *E. coli* BL21(DE3) competent cells using Luria Broth (LB) media supplemented with carbenicillin (100 µg/mL), 20 mg/L riboflavin and induced with 0.1 mM IPTG overnight at 18°C. The cells were lysed in a buffer containing 50 mM Na₂HPO₄/NaH₂PO₄ (pH 8.0), 150 mM NaCl, 10 mM imidazole, 10% glycerol, and 1% Triton X-100. Flavin adenine dinucleotide (FAD) was added at 250 µM with protease inhibitor (1 mM phenylmethylsulfonyl fluoride) and 7 µL β-mercaptoethanol per 10 mL lysis buffer. The lysate was centrifuged at 12,000 rpm for 30 min at 4°C, and the supernatant was applied to a Ni-NTA column. The column was pre-equilibrated with lysis buffer, and the protein was eluted in a gradient in buf-

fer containing 50 mM Na₂HPO₄/NaH₂PO₄ (pH 8.0), 150 mM NaCl, and imidazole ranging from 50 to 250 mM. To remove the polyhistidine tag, the protein was subjected to thrombin cleavage (25 U) and dialyzed with 10K MWCO snakeskin into buffer containing 100 mM Tris-HCl (pH 7.5) and 50 mM NaCl (with BME) overnight at 4°C. The resulting protein solution was then subjected to Source15Q anion exchange to remove impurities.

SMOX activity assay and enzyme inhibition studies

SMOX activity was measured using a chemiluminescent enzyme-based assay detecting the formation of H₂O₂ in the presence of Spm as the substrate, as described earlier [16]. To measure the activity of 2,11-Met₂-Spm against SMOX, the enzyme (300 ng) in 0.083 M glycine buffer (pH 8.0) and the inhibitor (0–250 µM) were added to the luminol-HRP master mix and incubated at 37°C for 2 min. Spm was then added to the reaction mixture at a final concentration of 250 µM, vortexed for 3 s, and chemiluminescence was integrated over 40 s. Data were averaged and normalized to the blank reaction (no inhibitor) as % SMOX activity. Inactivated SMOX served as a negative control and was accounted for in the calculations.

RESULTS AND DISCUSSION

Design of a SMOX inhibitor of Spm origin

There is a set of different strategies to design suicide inhibitors of the enzymes of amino acid metabolism.

One strategy consists in using a substrate/product analogue with a properly positioned activated double bond(s); for example, the allene group in MDL72527, which obeys irreversible inhibition [10]. An activated double bond may be generated at one of the steps of the substrate-like transformation of the inhibitor, like in the case of pyridoxal-5'-phosphate (PLP)-dependent ornithine decarboxylase and its suicide inhibitor DFMO [17]. The subsequent addition of a nucleophile to the activated double bond results in irreversible inhibition, which is developed in time. A double bond may already exist in the structure of the amino acid analogue and become activated as a result of the interaction with the coenzyme, similar to the mechanisms involved with the interaction between α -vinylic amino acids and PLP-dependent enzymes [18]. Here, these considerations were transformed into 1,12-diamino-2,11-bis(methylidene)-4,9-diazadodecane tetrahydrochloride (2,11-Met₂-Spm) having a double bond in the beta position to the splitting C-N bond (Fig. 2A). The methylidene group may be activated as a result of the substrate-like transformation of 2,11-Met₂-Spm, leading to the formation of the intermediate Schiff base (Fig. 2A). The possibility of substrate-like transformations of 2,11-Met₂-Spm is evidenced by the known dependence of the substrate properties of bis-methylated Spm analogues in the SMOX reaction on the position of the methyl groups in the analogue structure. The ability of racemic 1,12-Me₂Spm, 2,11-Me₂Spm and 3,10-Me₂Spm (Fig. 2B) to serve as substrates for SMOX decreased as the methyl group was positioned closer to the secondary (N4) amino group, and for 3,10-Me₂Spm, kinetic parameters were impossible to determine [19]. This is likely because the methyl group at the third position of the Spm backbone may restrict the proton splitting at the C3 carbon atom and influence the formation of the Schiff base, a key intermediate of the SMOX reaction.

Enzyme inhibition studies

The experiments on the inhibition of SMOX with 2,11-Met₂-Spm were performed under standard assay conditions, preincubating the enzyme with the inhibitor for 2 min and starting the reaction with the addition of Spm: with 250 μ M of 2,11-Met₂-Spm added, the enzyme was inhibited by 72% (Fig. 3). If the inhibition is competitive, the affinity of 2,11-Met₂-Spm towards SMOX must be greater than that of Spm (Spm concentration in the substrate mixture was also 250 μ M, i.e. 14 K_m). High affinity of 2,11-Met₂-Spm for SMOX seems unlikely due to the high substrate specificity of the enzyme. Among twenty-nine closely related Spm analogues of tetra- and pentaamine nature, the best substrate was pentaamine 3433 (1,16-diami-

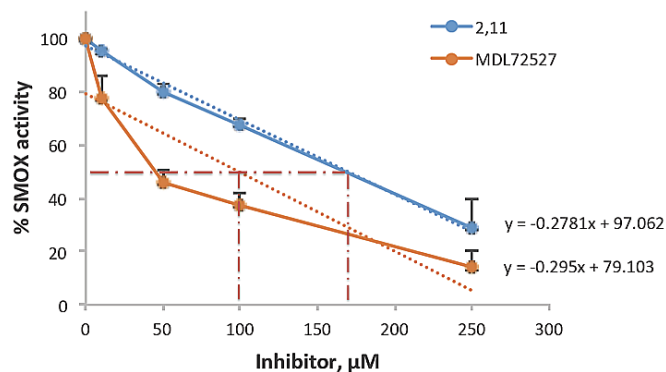


Fig. 3. Inhibition of SMOX with 2,11-Met₂-Spm (blue line) and MDL72527 (yellow line) as a positive control. Conditions: HRP-luminol (1 ng) in glycine buffer pH 8.0, enzyme and inhibitor (0–250 μ M) were incubated at 37°C for 2 min. Spm was then added at a final concentration of 250 μ M, and luminescence was integrated for 40 s. 2,11-Met₂-Spm and MDL72527 have IC₅₀ values of 169 and 100 μ M, respectively. Unlike 2,11-Met₂-Spm, the inhibition of purified SMOX by MDL72527 does not conform well to a linear transformation but it correlates well with the published IC₅₀ value of 90 μ M [14]. The R-squared values for 2,11-Met₂-Spm and MDL72527 are 0.992 and 0.7821, respectively. Data were collected from three independent experiments with standard deviations (SD)

no-4,8,13-triazahexadecane), with K_m of 1.3 μ M, i.e. 14 times better than Spm; among the rest, only pentaamine 3434 (1,17-diamino-4,9,13-triazaheptadecane) was as efficient as Spm [20]. However, if the inhibition of SMOX is irreversible, the affinity of the inhibitor towards the enzyme at the reversible stage may be poor, being consistent with the results observed when SMOX was preincubated with 2,11-Met₂-Spm at 100 μ M and the enzyme activity was inhibited only by 33% (Fig. 3). It is currently unclear how quickly inhibition develops in time and the 2 min preincubation time, typical for MDL72527, may be too short for 2,11-Met₂-Spm and SMOX because of the steric effect of the methylidene group in the β -position to the splitting C-N bond.

The activity of 2,11-Met₂-Spm towards SMOX (IC₅₀ = 169 μ M) was worse than that reported for MDL72527 (IC₅₀ = 90 μ M [14]), which is an irreversible PAOX inhibitor of a Put nature with reactive allene substituents. As a Spm derivative, it is likely that 2,11-Met₂-Spm will be less inhibitory of PAOX (natural substrates are N¹-Ac-Spd and less effective N¹-Ac-Spm) compared with SMOX. This is likely based on the comparison of the activity of the structurally similar *rac*-2,11-Me₂Spm (Fig. 2B) towards SMOX and PAOX. *Rac*-2,11-Me₂Spm was a comparatively poor substrate of SMOX, having a V_{max} of 124 pmol/min/ μ g protein and a K_m of 121 μ M, while the activity of PAOX

was inhibited for 60% only at the 500 μM concentration, when a fixed 50 μM concentration of the substrate N^1 -Ac-Spd was used in the PAOX assay [19].

Our results clearly show that it is possible to design a Spm analogue that inhibits the FAD-dependent SMOX, a key enzyme of polyamine catabolism. 2,11-Met₂-Spm has an IC₅₀ value of 166 μM towards SMOX. Although the precise mechanism of the inhibition, the specificity of 2,11-Met₂-Spm action, and the activity in cell culture are under investigation, the development of a selective inhibitor remains critical, not only as an experimental tool, but also as a potential therapeutic agent as SMOX is known to play a critical role in the development of multiple diseases, including cancer [5, 7, 8, 10].

FUNDING AND ACKNOWLEDGMENTS

Synthesis of the inhibitor was supported by the Russian Science Foundation grant 17-74-20049 (AMK and ARK). Inhibition studies were supported by the National Institutes of Health grants NCI R01CA204234 and RO1CA235863 (RAC). This work was supported by a research grant from the University of Pennsylvania Orphan Disease Center in partnership with the Snyder-Robinson Foundation MDBR-20-135-SRS (RAC, TMS). We would like to thank Dr. Michelle S. Miller and Puchong Thirawatananond for their help in designing the purification protocol of SMOX. ●

REFERENCES

1. Miller-Fleming L., Olin-Sandoval V., Campbell K., Ralser M. // *J. Mol. Biol.* 2015. V. 427. P. 3389–3406.
2. Pegg A.E. // *J. Biol. Chem.* 2016. V. 291. P. 14904–14912.
3. Michael A.J. // *Biochem. J.* 2016. V. 473. P. 2315–2329.
4. Ramani D., De Bandt J.P., Cynober L. // *Clin. Nut.* 2014. V. 33. P. 14–22.
5. Casero R.A., Murray Stewart T., Pegg A.E. // *Nature Rev. Cancer* 2018. V. 18. P. 681–695.
6. Gerner E.W., Bruckheimer E., Cohen A. // *J. Biol. Chem.* 2018. V. 293. P. 18770–18778.
7. Goodwin A., Jadallah S., Toubaji A., Lecksell K., Hicks J.L., Kowalski J., Bova G.S., De Marzo A.M., Netto G.J., Casero R.A. // *Prostate.* 2008. V. 68. P. 766–772.
8. Chaturved R., Asim M., Romero-Gallo J., Barry D.P., Hoge S., Sablet T., Delgado A.G., Wroblewski L.E., Piazuelo M.B., Yan F., et al. // *Gastroenterology.* 2011. V. 141. P. 1696–1708.
9. Goodwin A.C., Shields C.D., Wu S., Huso D.L., Wu X., Murray Stewart T., Rabizadeh S., Woster P.M., Sears C.L., Casero R.A. // *Proc. Natl. Acad. Sci. USA.* 2011. V. 108. P. 15354–15359.
10. Sierra J.C., Piazuelo M.B., Luis P.B., Barry D.P., Allaman M.M., Asim M., Sebrell T.A., Finley J.L., Rose K.L., Hill S. et al. // *Oncogene.* 2020. V. 39. P. 4465–4474.
11. Bey P., Bolkenius F.N., Seiler N., Casara P. // *J. Med. Chem.* 1985. V. 28. P. 1–2.
12. Sun L., Yang J., Qin Y., Wang Y., Wu H., Zhou Y., Cao C. // *J. Enzyme Inhib. Med. Chem.* 2019. V. 34. P. 1140–1151.
13. Masuko T., Takao K., Samejima K., Shirahata A., Igarashi K., Casero Jr. R.A., Kizawaa Y., Sugita Y. // *Neurosci. Lett.* 2018. V. 672. P. 118–122.
14. Holshouser S., Dunworth M., Murray Stewart T., Peterson Y.K., Burger P., Kirkpatrick J., Chen H.-H., Casero Jr. R.A., Woster P.M. // *Med. Chem. Commun.* 2019. V. 10. P. 778–790.
15. Grigorenko N.A., Khomutov M.A., Simonian A.R., Kochetkov S.N., Khomutov A.R. // *Rus. J. Bioorg. Chem.* 2016. V. 42. P. 423–427.
16. Goodwin A.C., Murray Stewart T.R., Casero Jr. R.A. // *Methods Mol. Biol.* 2011. V. 720. P. 173–181.
17. Metcalf B.W., Bey P., Danzin C., Jung M.J., Casara P., Vevert J.P. // *J. Am. Chem. Soc.* 1978. V. 100. P. 2551–2553.
18. Berkowitz D.B., Charette B.D., Karukurichi K.R., McFadden J.M. // *Tetrahedron Asym.* 2006. V. 17. P. 869–882.
19. Khomutov M., Hyvönen M.T., Simonian A., Formanovsky A.A., Mikhura I.V., Chizhov A.O., Kochetkov S.N., Alhonen L., Vepsäläinen J., Keinänen T.A., Khomutov A.R. // *J. Med. Chem.* 2019. V. 62. P. 11335–11347.
20. Takao K., Shivahata A., Samejima K., Casero R.A., Igarashi K., Sugita Y. // *Biol. Pharm. Bull.* 2013. V. 36. P. 407–411.

GENERAL RULES

Acta Naturae publishes experimental articles and reviews, as well as articles on topical issues, short reviews, and reports on the subjects of basic and applied life sciences and biotechnology.

The journal *Acta Naturae* is on the list of the leading periodicals of the Higher Attestation Commission of the Russian Ministry of Education and Science. The journal *Acta Naturae* is indexed in PubMed, Web of Science, Scopus and RCSI databases.

The editors of *Acta Naturae* ask of the authors that they follow certain guidelines listed below. Articles which fail to conform to these guidelines will be rejected without review. The editors will not consider articles whose results have already been published or are being considered by other publications.

The maximum length of a review, together with tables and references, cannot exceed 60,000 characters with spaces (approximately 30 pages, A4 format, 1.5 spacing, Times New Roman font, size 12) and cannot contain more than 16 figures.

Experimental articles should not exceed 30,000 symbols (approximately 15 pages in A4 format, including tables and references). They should contain no more than ten figures.

A short report must include the study's rationale, experimental material, and conclusions. A short report should not exceed 12,000 symbols (8 pages in A4 format including no more than 12 references). It should contain no more than four figures.

The manuscript and all necessary files should be uploaded to www.actanaturae.ru:

- 1) text in Word 2003 for Windows format;
- 2) the figures in TIFF format;
- 3) the text of the article and figures in one pdf file;
- 4) the article's title, the names and initials of the authors, the full name of the organizations, the abstract, keywords, abbreviations, figure captions, and Russian references should be translated to English;
- 5) the cover letter stating that the submitted manuscript has not been published elsewhere and is not under consideration for publication;
- 6) the license agreement (the agreement form can be downloaded from the website www.actanaturae.ru).

MANUSCRIPT FORMATTING

The manuscript should be formatted in the following manner:

- Article title. Bold font. The title should not be too long or too short and must be informative. The title should not exceed 100 characters. It should reflect the major result, the essence, and uniqueness of the work, names and initials of the authors.
- The corresponding author, who will also be working with the proofs, should be marked with a footnote *.
- Full name of the scientific organization and its departmental affiliation. If there are two or more scientific organizations involved, they should be linked by digital superscripts with the authors' names. Abstract. The structure of the abstract should be

very clear and must reflect the following: it should introduce the reader to the main issue and describe the experimental approach, the possibility of practical use, and the possibility of further research in the field. The average length of an abstract is 20 lines (1,500 characters).

- Keywords (3 – 6). These should include the field of research, methods, experimental subject, and the specifics of the work. List of abbreviations.

• INTRODUCTION

• EXPERIMENTAL PROCEDURES

• RESULTS AND DISCUSSION

• CONCLUSION

The organizations that funded the work should be listed at the end of this section with grant numbers in parenthesis.

• REFERENCES

The in-text references should be in brackets, such as [1].

RECOMMENDATIONS ON THE TYPING AND FORMATTING OF THE TEXT

- We recommend the use of Microsoft Word 2003 for Windows text editing software.
- The Times New Roman font should be used. Standard font size is 12.
- The space between the lines is 1.5.
- Using more than one whole space between words is not recommended.
- We do not accept articles with automatic referencing; automatic word hyphenation; or automatic prohibition of hyphenation, listing, automatic indentation, etc.
- We recommend that tables be created using Word software options (Table → Insert Table) or MS Excel. Tables that were created manually (using lots of spaces without boxes) cannot be accepted.
- Initials and last names should always be separated by a whole space; for example, A. A. Ivanov.
- Throughout the text, all dates should appear in the “day.month.year” format, for example 02.05.1991, 26.12.1874, etc.
- There should be no periods after the title of the article, the authors' names, headings and subheadings, figure captions, units (s – second, g – gram, min – minute, h – hour, d – day, deg – degree).
- Periods should be used after footnotes (including those in tables), table comments, abstracts, and abbreviations (mon. – months, y. – years, m. temp. – melting temperature); however, they should not be used in subscripted indexes (T_m – melting temperature; $T_{p.t}$ – temperature of phase transition). One exception is mln – million, which should be used without a period.
- Decimal numbers should always contain a period and not a comma (0.25 and not 0,25).
- The hyphen (“-”) is surrounded by two whole spaces, while the “minus,” “interval,” or “chemical bond” symbols do not require a space.
- The only symbol used for multiplication is “×”; the “×” symbol can only be used if it has a number to its

right. The “·” symbol is used for denoting complex compounds in chemical formulas and also noncovalent complexes (such as DNA·RNA, etc.).

- Formulas must use the letter of the Latin and Greek alphabets.
- Latin genera and species' names should be in italics, while the taxa of higher orders should be in regular font.
- Gene names (except for yeast genes) should be italicized, while names of proteins should be in regular font.
- Names of nucleotides (A, T, G, C, U), amino acids (Arg, Ile, Val, etc.), and phosphonucleotides (ATP, AMP, etc.) should be written with Latin letters in regular font.
- Numeration of bases in nucleic acids and amino acid residues should not be hyphenated (T34, Ala89).
- When choosing units of measurement, SI units are to be used.
- Molecular mass should be in Daltons (Da, KDa, MDa).
- The number of nucleotide pairs should be abbreviated (bp, kbp).
- The number of amino acids should be abbreviated to aa.
- Biochemical terms, such as the names of enzymes, should conform to IUPAC standards.
- The number of term and name abbreviations in the text should be kept to a minimum.
- Repeating the same data in the text, tables, and graphs is not allowed.

GUIDENESS FOR ILLUSTRATIONS

- Figures should be supplied in separate files. Only TIFF is accepted.
- Figures should have a resolution of no less than 300 dpi for color and half-tone images and no less than 500 dpi.
- Files should not have any additional layers.

REVIEW AND PREPARATION OF THE MANUSCRIPT FOR PRINT AND PUBLICATION

Articles are published on a first-come, first-served basis. The members of the editorial board have the right to recommend the expedited publishing of articles which are deemed to be a priority and have received good reviews.

Articles which have been received by the editorial board are assessed by the board members and then sent for external review, if needed. The choice of reviewers is up to the editorial board. The manuscript is sent on to reviewers who are experts in this field of research, and the editorial board makes its decisions based on the reviews of these experts. The article may be accepted as is, sent back for improvements, or rejected.

The editorial board can decide to reject an article if it does not conform to the guidelines set above.

The return of an article to the authors for improvement does not mean that the article has been accepted

for publication. After the revised text has been received, a decision is made by the editorial board. The author must return the improved text, together with the responses to all comments. The date of acceptance is the day on which the final version of the article was received by the publisher.

A revised manuscript must be sent back to the publisher a week after the authors have received the comments; if not, the article is considered a resubmission.

E-mail is used at all the stages of communication between the author, editors, publishers, and reviewers, so it is of vital importance that the authors monitor the address that they list in the article and inform the publisher of any changes in due time.

After the layout for the relevant issue of the journal is ready, the publisher sends out PDF files to the authors for a final review.

Changes other than simple corrections in the text, figures, or tables are not allowed at the final review stage. If this is necessary, the issue is resolved by the editorial board.

FORMAT OF REFERENCES

The journal uses a numeric reference system, which means that references are denoted as numbers in the text (in brackets) which refer to the number in the reference list.

For books: the last name and initials of the author, full title of the book, location of publisher, publisher, year in which the work was published, and the volume or issue and the number of pages in the book.

For periodicals: the last name and initials of the author, title of the journal, year in which the work was published, volume, issue, first and last page of the article. Must specify the name of the first 10 authors. Ross M.T., Grafham D.V., Coffey A.J., Scherer S., McLay K., Muzny D., Platzer M., Howell G.R., Burrows C., Bird C.P., et al. // Nature. 2005. V. 434. № 7031. P. 325–337.

References to books which have Russian translations should be accompanied with references to the original material listing the required data.

References to doctoral thesis abstracts must include the last name and initials of the author, the title of the thesis, the location in which the work was performed, and the year of completion.

References to patents must include the last names and initials of the authors, the type of the patent document (the author's rights or patent), the patent number, the name of the country that issued the document, the international invention classification index, and the year of patent issue.

The list of references should be on a separate page. The tables should be on a separate page, and figure captions should also be on a separate page.

The following e-mail addresses can be used to contact the editorial staff: vera.knorre@gmail.com, actanaturae@gmail.com, tel.: (495) 727-38-60, (495) 930-87-07

ActaNaturae

RESEARCH ARTICLES

Fluorescence of cells after staining with various proteins. The mean values for the three experiments \pm mean error are given

Sample	Fluorescence intensity measured in the FL1 channel	
	SK-BR-3 cells	CHO cells
Unstained cells	3700 \pm 400	3700 \pm 900
+ β -LG-FITC	5700 \pm 600	3300 \pm 400
+ 4D5scFv-FITC	2.7 $\times 10^4 \pm 7 \times 10^3$	3200 \pm 500
+ 4D5scFv-miniSOG	2.3 $\times 10^4 \pm 3 \times 10^3$	4600 \pm 400
+ DARPin-miniSOG	1.71 $\times 10^4 \pm 1.6 \times 10^3$	3000 \pm 400

Hence, it has been demonstrated that the targeted recombinant proteins 4D5scFv-miniSOG and DARPin-miniSOG are capable of highly specific binding to the HER2/neu receptor on the surface of human breast adenocarcinoma SK-BR-3 cells.

It was revealed that receptor-mediated internalization of proteins did not take place after the DARPin-miniSOG and 4D5scFv-miniSOG proteins were bound to the receptor on the surface of SK-BR-3 cells at +4°C. However, the receptor-protein complex undergoes internalization at +37°C, as evidenced by the reduction in the fluorescence intensity Δ MFI (the difference between the average fluorescence intensities of stained and unstained cells) (Fig. 1). The DARPin-miniSOG recombinant protein as part of its complex with the receptor is internalized faster than 4D5scFv-miniSOG, since Δ MFI for DARPin-miniSOG decreases twofold as compared to its baseline during the first 10 min, while Δ MFI for 4D5scFv-miniSOG is 40 min. These findings are consistent with the published data: 4D5scFv-miniSOG has a higher cytotoxicity than DARPin-miniSOG [5, 6], because 4D5scFv-miniSOG resides on the membrane for a longer time. Since necrosis is the predominant death mechanism of cells irradiated in the presence of these phototoxins, membrane damage makes a crucial contribution to the toxicity of targeted proteins. However, the decline in the fluorescence intensity of miniSOG can be indicative of reactions involving chromophore, which is also expected to affect its efficiency as a phototoxin.

In order to elucidate the reasons for the decline in the fluorescence intensity and toxicity of miniSOG-based proteins observed during their internalization, we evaluated the effect of various factors on the fluorescent properties of miniSOG. A hypothesis has been put forward that quenching of DARPin-miniSOG

ActaNaturae

The EIMB Hydrogel Microarray Technology: Thirty Years Later



ZINC FINGER PROTEIN CG9890 – NEW COMPONENT OF ENY2-CONTAINING COMPLEXES OF DROSOPHILA
C. 110

IDENTIFICATION OF NOVEL INTERACTION PARTNERS OF AIF PROTEIN ON THE OUTER MITOCHONDRIAL MEMBRANE
C. 100

ActaNaturae

Journal “Acta Naturae” is a international journal on life sciences based in Moscow, Russia. Our goal is to present scientific work and discovery in molecular biology, biochemistry, biomedical disciplines and biotechnology. *Acta Naturae* is also a periodical for those who are curious in various aspects of biotechnological business, innovations in pharmaceutical areas, intellectual property protection and social consequences of scientific progress.

Being a totally unique publication in Russia, *Acta Naturae* will be useful to both representatives of fundamental research and experts in applied sciences.

Journal “Acta Naturae” is now available in open access in PubMed Central® and eLIBRARY.RU.

INFORMATION FOR AUTHORS:

if you want to publish in “Acta Naturae”, please contact us: actanaturae@gmail.com

